INFORMATION TO USERS

This manuscript has been reproduced from the microfilm master. UMI films the text directly from the original or copy submitted. Thus, some thesis and dissertation copies are in typewriter face, while others may be from any type of computer printer.

The quality of this reproduction is dependent upon the quality of the copy submitted. Broken or indistinct print, colored or poor quality illustrations and photographs, print bleedthrough, substandard margins, and improper alignment can adversely affect reproduction.

In the unlikely event that the author did not send UMI a complete manuscript and there are missing pages, these will be noted. Also, if unauthorized copyright material had to be removed, a note will indicate the deletion.

Oversize materials (e.g., maps, drawings, charts) are reproduced by sectioning the original, beginning at the upper left-hand corner and continuing from left to right in equal sections with small overlaps. Each original is also photographed in one exposure and is included in reduced form at the back of the book.

Photographs included in the original manuscript have been reproduced xerographically in this copy. Higher quality 6" x 9" black and white photographic prints are available for any photographs or illustrations appearing in this copy for an additional charge. Contact UMI directly to order.

UMI

A Bell & Howell Information Company
300 North Zeeb Road, Ann Arbor MI 48106-1346 USA
313/761-4700 800/521-0600

Micellar Electrokinetic Capillary Chromatography with Single & Double Alkyl Chain Cationic Surfactants

by

KANGMIN CHEN

A dissertation submitted to the Graduate Faculty in Chemistry in partial fulfillment of the requirements for the degree of Doctor of Philosophy.

The City University of New York

1997

This manuscript has been read and accepted by the Graduate Faculty in Chemistry in satisfaction of the dissertation requirement for the degree of Doctor of Philosophy.

3 July 97 — David C. Locke

Date **David C. Locke** **Chair of Examining Committee**

July 8, 1997 — Richard Pizer

Date **Richard Pizer** **Executive Officer**

Gary Mennitt

Gary Mennitt **Supervisory Committee**

Milton Rosen

Milton Rosen **Supervisory Committee**

The City University of New York

ABSTRACT

Micellar Electrokinetic Capillary Chromatography with Single and Double Alkyl Chain Cationic Surfactants

by

KANGMIN CHEN

Advisor: Professor David C. Locke

Micellar electrokinetic capillary chromatography (MECC) with single and double alkyl chain cationic surfactants was investigated in four different projects.

First, the separation of the eleven priority pollutant phenols was investigated with a cationic surfactant (C_{16}TAB) in MECC. The effects of buffer constituents, acetonitrile (ACN) additive, pH, ionic strength and surfactant concentration in the background electrolytes (BGEs) on retention behaviour were studied in detail. The most important factor in the separation was the amount of ACN in the BGEs.

Second, the interaction between charged and uncharged solutes and C_{16}TAB was investigated in MECC. For ionized acidic solutes, with increasing ionic strength of the BGE, the net mobilities increased and the capacity factors decreased; however, for cationic, uncharged and slightly ionized acidic solutes, the net mobilities and the capacity factors were almost

not affected. A fundamental theoretical and applied study of net mobility, capacity factor and distribution coefficient as a function of ionic strength in the BGEs was carried out.

Third, the use of a series of novel double alkyl chain (Gemini) cationic surfactants (Gemini-C8 to -C18) was evaluated in MECC. For comparison, the single chain surfactants (C_{12}TAB, C_{14}TAB, and C_{16}TAB) were examined as well. With increasing alkyl chains and concentration of each surfactant, the capacity factors increased linearly, but the net mobilities of both model solutes and the micelles changed differently and depended upon the surfactant concentrations. The best separation of the eleven priority pollutant phenols was achieved using Gemini-C12.

Last, two Gemini surfactants (Gemini-C12 and -C14) were synthesized and used in MECC for indicating purity and stability of dihydroergotoxine mesylates, therapeutic substances for the treatment of dysregulation of the circulatory system. For comparison, C_{14}TAB and C_{16}TAB were also utilized in MECC. Seventeen ergot alkaloids were well resolved in eight minutes using Gemini-C12 as the micelle-forming reagent; and Gemini-C14 provided better resolution for all the alkaloid isomers. These MECC separations could not be achieved using the single chain surfactants.

This dissertation is dedicated

to my lovely wife, Fengjie

Acknowledgments

At first, I would like to express my sincere gratitude to my advisor, Professor David C. Locke, for his encouragement and guidance through the course of this study and during the development of this dissertation. More than appreciation is extended to my other committee members, Professors Gary Mennitt and Milton Rosen, for their instruction and for serving on this dissertation examining committee.

I would like to acknowledge Drs. T. Maldacker, J. Lin and S. Asawasiripong (Novartis Pharmaceuticals Corp., East Hanover, NJ, USA) for their supporting this work.

I extend my appreciation to Dr. Li-dong Song for providing the Gemini surfactants in the preliminary screening study, and for many useful discussions about the Gemini surfactants.

I gratefully acknowledge the valuable discussion with Dr. Samuel Chang (Novartis Pharmaceuticals Corp.) regarding the interaction between the surfactant and the ergot alkaloids.

I want to thank Albemarle Corp. (Baton Rouge, LA, USA) for the donation of dodecyl-, tetradecyl and hexadecyl-N,N-dimethylamine.

Finally, I would like to express my appreciation to my family, my wife, my mother, my sisters and brothers-in-law, for their love, understanding, and support throughout my life.

TABLE OF CONTENTS

TABLE OF CONTENTS (cont'd)

TABLE OF CONTENTS (cont'd)

TABLE OF CONTENTS (cont'd)

TABLE OF CONTENTS (cont'd)

TABLE OF CONTENTS (cont'd)

List of Figures

List of Figures (cont'd)

Chapter. 3

List of Figures (cont'd)

List of Figures (cont'd)

Chapter. 4

List of Figures (cont'd)

List of Figures (cont'd)

List of Figures (cont'd)

Chapter. 5

List of Figures (cont'd)

List of Tables

Page

Chapter. 2

Chapter. 3

Chapter. 4

List of Tables (cont'd)

Chapter. 5

Chapter 1

Introduction

1. Background

Micellar electrokinetic capillary chromatography (MECC) is a mode of capillary electrophoresis (CE) involving electroosmosis, electrophoresis, and chromatography-like phase distribution (1, 2). Because of this characteristic, MECC has the great advantage over capillary zone electrophoresis (CZE) that it can separate mixtures containing both ionic and neutral solutes.

In MECC, surfactants are utilized as micelle-forming reagents - moving pseudostationary phases. Surfactants are molecules having polar head groups (cationic, anionic, non-ionic, and zwitterionic) and nonpolar tails (linear or branched alkyl chains with between eight and twenty carbons) (3). When the surfactant concentration is above the critical micelle concentration (CMC) (4), micelles are formed through the self-aggregation of surfactant molecules, i.e., the hydrocarbon tails orient towards the interior of the micelle as a result of the hydrophobic effect, and the polar head groups point outward. This unique amphiphilic structure provides the micelles with capability for hydrophobic and/or hydrophilic interactions for solutes. For example, one of the most important properties of

micelle is the ability to solublize solutes which are insoluble or only slightly soluble in water (5). The CMC value can be lowered by raising the ionic strength of the solution (6), increasing the alkyl chain length of the surfactants (7), and/or reducing solution temperature (decreasing thermal motion) (8). A surfactant of a low CMC value may be additionally useful in MECC because of avoiding possible Joule heat.

MECC is a two-phase chromatographic-like system. The BGE represents the primary phase, moving electroosmotically through the capillary; and the micelles represent the secondary phase, migrating through the capillary by a combination of electroosmotic flow (EOF) and micelle electrophoretic mobility. Usually, the micelle electrophoretic mobility direction is opposite to that of the EOF, but is of a smaller magnitude; thus, both phases are transported at different velocities toward a common end of the capillary. Meanwhile, solutes generally migrate at a rate between those of the EOF and the micelle. In addition, the flat velocity profile characteristic of the EOF results in narrow bands, thus high efficiency in MECC.

The type of surfactants has a major effect on the separation of solutes. The solute-micelle interaction can be either electrostatic or hydrophobic, or both, so for ionic solutes, the micellar head group and sign of the charge on the micellar head group are most important. The partitioning of neutral or ionic solutes

between the micelle and the aqueous phase is affected principally by the chain length of the surfactant hydrophobic moiety.

In the MECC system, the micelles are dynamic entities, i.e., the micelles constantly exchange with the monomers to form the new micelles. Microscopically, the micellar solution is heterogeneous. Therefore, the micellar aggregation numbers represent an average value (9). At low surfactant concentration, the dynamic exchange rate is low, the sizes and the shapes of micelles vary with time, which results in a range of the micelle electrophoretic mobilities. This phenomenon is called the micelle polydispersity. Only if the surfactant concentration is sufficiently high, the rate of micelle-monomer exchange is rapid, and the formation of the micelles is stable, which averages out the sizes and the shapes of the micelles to a mean constant value.

In a normal CE system, an electroosmotic flow (EOF) is from anode to cathode. However, an reversal of the EOF can occur if a cationic surfactant is introduced into the BGEs. As the cationic surfactant concentration (below CMC) increases, a dynamic bilayer phase will be gradually formed (10) in the fused silica capillary wall due to (i) an ionic interaction between the cationic head group of the surfactant and the anionic silanol group on the capillary wall, and (ii) a

hydrophobic interaction which binds the surfactant tails with each other, so the cationic head groups of the surfactants extend into the bulk solution (see Figure 1). In this way the charge reversal on the capillary wall is established as the net EOF slows down, and at high surfactant concentration becomes zero because of the neutralization of the charged surface. At still higher surfactant concentration, the surface charge reversal is built up until the net charge density on the capillary surface becomes positive because of the dynamic bilayer phase. The counter-ions building up near the surface to maintain charge balance are anions, which form a double-layer and create a potential difference known as the zeta (ζ) potential. Anions in the double-layer are attracted toward the positive electrode under the applied voltage, and drag the bulk solution in the capillary toward the anode. Thus is the EOF reversed. If the surfactant concentration is below CMC, no micelles will be formed, and only the EOF is reversed. This technique could be named reversed-polarity capillary zone electrophoresis (RP-CZE). However, if the surfactant concentration is above CMC, not only is the EOF reversed, but also the micelles are formed. This technique might be designated reversed-polarity micellar electrokinetic capillary chromatography (RP-MECC). For brevity, the name MECC is used rather than RP-MECC in this dissertation.

2. Significance of the Research

Although the majority of MECC separations have been performed with sodium dodecyl sulfate (SDS), CE separations utilizing cationic surfactants have been well documented in MECC, as well as in RP-CZE. Burton et al. (7) evaluated various surfactants in MECC, including sodium tetradecyl sulfate (STS), SDS, dodecyltrimethylammonium chloride (C_{12}TAC), cetyltrimethylammonium chloride (C_{16}TAC). Different selectivities were displayed for weakly acidic, weakly basic, polar, and nonpolar solutes. Separation of anionic polystyrene "nano-spheres" was demonstrated using cetyltrimethylammonium bromide (C_{16}TAB) (11). In that study, particle-capillary wall interactions were postulated to retain large particles to a higher degree. Kasper et al. (12) also exploited properties afforded by C_{16}TAB, including ion-pairing interactions, to efficiently separate linear DNA fragments. Selectivity was found to improve in the presence of urea (4 M). Liu et al. (13) demonstrated the separation of a series of angiotensin peptides consisting of seven to ten amino acid units in a buffer system containing dodecyltrimethylammonium bromide (C_{12}TAB). Selectivity was clearly shown to be superior when the concentration of C_{12}TAB was above its CMC value (14 mM), indicating that micellar interactions can play an important role in separations of charged components. Tetradecyltrimethylammonium brodide (C_{14}TAB) was used in

RP-CZE by Huang et al. (14) for the rapid separation of a series of low-molecular-mass carboxylic acids. Since electrophoresis and electroosmotic flow occurred in the same direction, analysis times were very short (< 3.5 min). Varghese et al. (15) applied C_{16}TAC in RP-CZE coupled with electrospray mass spectrometry to rapidly analyze picomole quantities of various cationic molecules including laser dyes, tripeptides, and larger bioactive peptides. Kaneta et al. (16) studied the migration behaviour of inorganic anions in CE using C_{16}TAC at concentrations below and above the CMC. The relationship between capacity factor and effective electrophoretic mobility was given at surfactant concentration above the CMC. Morin et al. (17) reported the use of C_{16}TAB in MECC for the separation of anionic and neutral glucosinolates. The elution order was that of solute hydrophobicity, while ion-pairing interactions also contributed to the migration of the anionic solutes. Khaledi et al. (18, 19) reported the use of phenomenological modes to describe the migration behaviour of ionic solutes in MECC with both anionic and cationic surfactants. The pH and the micellar concentration of the BGEs were taken into consideration in this fundamental study. Abubaker et al. (20) demonstrated the separation of six structurally similar, hydrophobic neutral steroids with 50 mM C_{12}TAB in the BGE.

In MECC using a cationic surfactant, a systematic investigation of the migration behaviour of the eleven priority

pollutant phenols has not been reported; also, the net mobility, capacity factor and distribution coefficient as a function of ionic strength in the BGE have not been fundamentally studied. In this work, these two aspects were investigated in detail.

Although there is a relatively wide range of commercially available surfactants, the range of MECC applicable surfactants is limited because of high CMC and/or low solubility in water (7). Therefore the introduction of new types of surfactants for MECC is of great interest and is expected to be useful in modulating selectivity. The Gemini (double alkyl chains) surfactants are one such kind of promising surfactant in MECC. For Gemini surfactants, the hydrophilicity is greatly enhanced due to the two ionic groups in the molecule, while the surface activity and micelle forming ability are greatly improved owing to the two hydrophobic groups in the molecule (21). The Gemini surfactants have much smaller CMCs and Kraft points (T_{kp}, the temperature at which the solubility is equal to the CMC) than the conventional single alkyl chain surfactants. These properties are expected to show different characteristics for the use in MECC. So far, only anionic Gemini surfactants have been reported in the MECC application. Tanaka et al. (22, 23) utilized three different double chain surfactants with two sulfonate groups as micelle-forming reagents in MECC. In comparison with the widely used SDS, these double chain surfactants exhibit remarkably different selectivities for the

substituted naphthalenes, and gave a wider migration time window.

However, cationic Gemini surfactants have not been evaluated and / or used in MECC. In this study, a series of novel Gemini cationic surfactants, with alkyl chains from C8 to C18, was investigated as micelle-forming reagents in MECC and applied to the separation of the eleven priority pollutant phenols, and to the separation of seventeen ergot alkaloids as an impurity profile for dihydroergoxine mesylates.

3. Objectives

The objective of this study was to investigate the migration behaviour of uncharged, anionic and cationic solutes in MECC with cationic surfactants; and to evaluate novel Gemini cationic surfactants as micelle-forming reagents in MECC. There are four major parts to this study: (i) study of the migration behaviour of the eleven priority pollutant phenols (chapters 2 and 4), (ii) study of the mechanism for the effect of ionic strength in the BGE on the migration behaviour of ionized acidic solutes (chapter 3), (iii) evaluation of a series of novel Gemini cationic surfactants in MECC and comparison with the single chain cationic surfactants (chapter 4), (iv) separation of seventeen ergot alkaloids in MECC with cationic surfactants (chapter 5).

Figure Caption:

Figure 1: Elimination and reversal of EOF using a cationic surfactant. (Ref. 24)

Figure 1

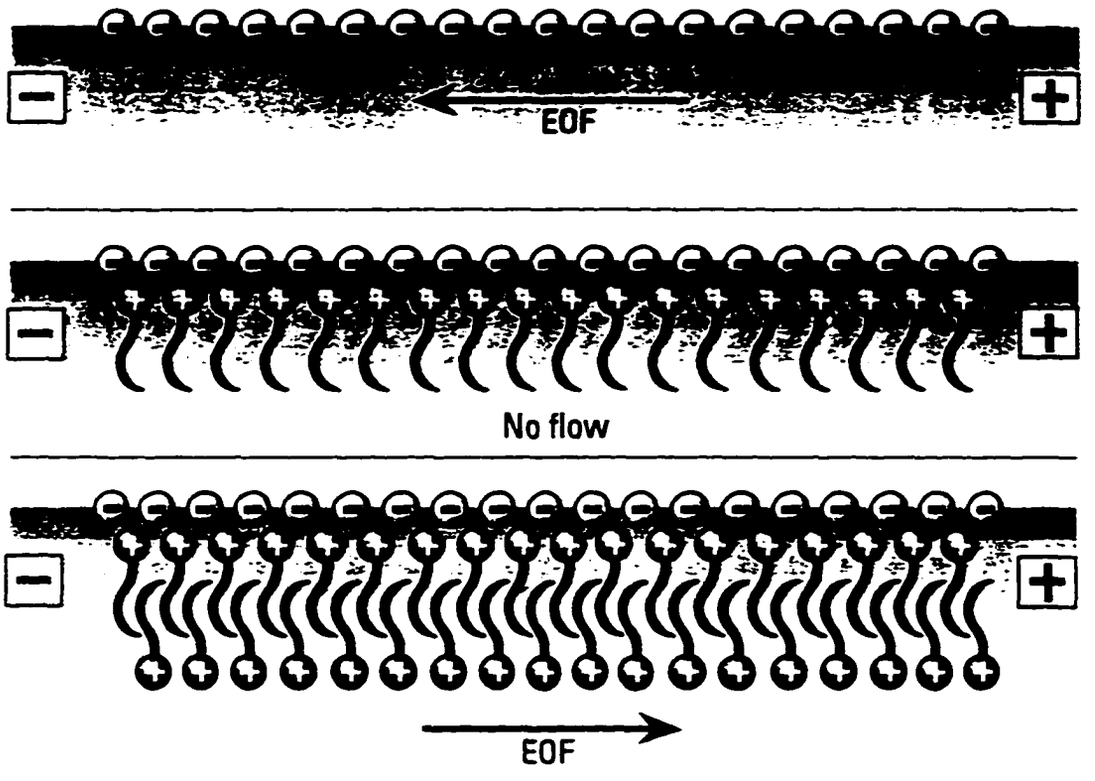

Chapter 2

Micellar Electrokinetic Capillary Chromatographic Separation of Eleven Priority Pollutant Phenols Using a Cationic Surfactant

Abstract

The separation of the eleven substituted phenols listed by the United States Environmental Protection Agency (USEPA) as priority pollutants was for the first time investigated using micellar electrokinetic capillary chromatography (MECC) with a cationic surfactant, cetyltrimethylammonium bromide (C_{16}TAB). The effects of the buffer constituents, acetonitrile, pH, surfactant concentration and ionic strength in the background electrolyte (BGE) on the retention behaviour of these eleven phenols was studied. It was found that addition of acetonitrile to the BGE was a very important factor to resolve these phenols. The optimum separation was achieved in approximately 10 minutes using a 50 μm I.D. x 30 cm effective length (37.5 cm total length) uncoated fused-silica capillary with a BGE consisting of 15 mM C_{16}TAB and 15% acetonitrile in 50 mM phosphate-10 mM acetate buffer (pH 4.2) at negative 13.5 kV potential. The %RSD of all the net mobilities on the five different occasions was less than 1.5%; and the mass limits of detection were of the order of 10^{-15} moles.

1. Introduction

Phenols are generated from diverse industries, including petroleum, pulp and paper, plastics, and pharmaceuticals. Phenols in drinking water subjected to the chlorination produce objectionable chlorinated products. The USEPA has included the eleven substituted phenols in the list of the priority pollutants (1) (see Table 1). Owing to their toxicity even at low concentrations, a variety of methodologies for the determination of eleven priority pollutant phenols have been developed, which include gas chromatography (GC) (2), and high-performance liquid chromatography (HPLC) (3, 4) with either reversed-phase isocratic or gradient elution. However, these methods are time-consuming. For example, phenols need to be preconcentrated and derivatized to enhance detectability and volatility prior to GC analysis.

Capillary zone electrophoresis (CZE) and micellar electrokinetic capillary chromatography (MECC) have already been demonstrated to give high resolution within a shorter time than conventional HPLC. In the past few years, CZE and MECC have been applied to the separation of these eleven priority pollutant phenols. Ong et al. (5) demonstrated the separation of the eleven priority phenols using MECC with sodium dodecyl sulfate (SDS). With a BGE containing 5 mM phosphate - 10 mM borate (pH 6.6) and 50 mM SDS in a 100 cm x 180 μm I.D.

capillary at 10 kV, satisfactory separation of the eleven priority phenols was obtained in *ca.* 45 minutes, with mass limits of detection (LODs) in the nanogram range. Chao and Whang (6) have separated these eleven phenols using CZE coupled with a laser-induced indirect fluorimetry detector. Using a 50 cm x 20 μm I.D. capillary at 9 kV and a BGE of 15 mM sodium borate (pH 9.9) containing 1 mM fluorescein, complete separation of the eleven compounds was achieved in less than 14 minutes providing LODs in the 10^{-6} - 10^{-7} M range. Li and Locke (7, 8) successfully resolved these compounds by normal CZE and nonionic micelle-modified CE. Using a 100 cm x 75 μm I.D. capillary at 22.5 kV with a 10 mM phosphate - 10 mM borate buffer (pH 9.8), these eleven phenols were completely separated in less than 15 minutes with concentration LODs in the 10^{-7} μg/mL range. With a 65 cm x 75 μm I.D. capillary at 20 kV and a BGE containing 12.5 mM phosphate-12.5 mM borate (pH 9.8) and 0.5% Tween 40 or 0.5% Brij 35 surfactant, better resolution was achieved compared to the same buffer without these nonionic surfactants. The analysis time was approximately 20 minutes for both nonionic micelle-modified CE separations.

Although a unique separation selectivity for these eleven phenols can be expected to be achieved by MECC using a cationic surfactant, there have been no any reports on the retention behaviours of these eleven priority pollutant phenols in MECC with a cationic surfactant. Considering the importance

of their determination, we studied the application of MECC with a cationic surfactant to resolve these eleven phenols. In this chapter, a systematic investigation of effects of buffer constituents, acetonitrile additive amount, pH, $C_{16}TAB$ concentration, and ionic strength in the BGE on the MECC separation of the eleven priority phenols is described.

2. Experimental

2.1 Apparatus

The MECC experiments were carried out with a Quanta 4000 CE system (Waters Chromatography, Milford, MA, USA). A fixed wavelength UV detector at 214 nm was employed in this study. The CE system was connected to a Waters/VAX 4000-50 data system through an LAC/E interface module, and Waters ExpertEase software (version 3.1) was used for data acquisition and processing. A Orion Model 290A pH meter was used to measure pH with a precision of ±0.01 unit.

Capillaries used were uncoated fused-silica capillary tubes obtained from Polymicro Technologies (Phoenix, AZ, USA) with 75 μm I.D. x 375 μm O.D., and 60 cm effective length and 67.5 cm total length; or 50 μm I.D. x 375 μm O.D., and 30 cm effective length and 37.5 cm total length.

2.2 Chemicals

All eleven phenols, listed in Table 1, were obtained from Aldrich (Milwaukee, WI, USA). They were dissolved in HPLC grade methanol to give a mixed stock sample solution at a concentration of approximately 2.5 mg/mL for phenol, 4-nitrophenol, 2,4-dinitrophenol, 2-methyl-4,6-dinitrophenol; approximately 5 mg/mL for 2-nitrophenol, 2-chlorophenol, 2,4-dimethylphenol, 4-chloro-3-methylphenol and 2,4-dichlorophenol; approximately 1.6 mg/mL for 2,4,6-trichlorophenol and pentachlorophenol.

Sodium citrate dihydrate, citric acid monohydrate, sodium acetate anhydrous and glacial acetic acid were obtained from Mallinckrodt Chemical (Paris, KY, USA); sodium tartrate dihydrate, tartaric acid, sodium phosphate monobasic anhydrous, sodium phosphate dibasic anhydrous and sodium tribasic dodecahydrate, 85% o-phosphoric acid and potassium hydroxide were obtained from Fisher Scientific (Fairlawn, NJ, USA); C_{16}TAB was obtained from Aldrich (Milwaukee, WI, USA); HPLC-grade methanol and acetonitrile were obtained from Burdick & Jackson (Muskegon, MI, USA). Millipore Milli-Q water was used to prepare stock buffer and stock surfactant solutions.

2.3 Procedure

The coating of new capillaries was removed by briefly placing the window area in a flame from a burner and then gently cleaning the burned material with a tissue dampened with methanol. New capillaries were conditioned by purging in order with 1 N potassium hydroxide solution, 0.1 N potassium hydroxide solution, degassed and filtered D.I. water, buffer without C_{16}TAB at a concentration three-fold higher than running buffer, and finally BGE, each for fifteen minutes.

A stock buffer solution was prepared by mixing equimolar solutions of an acid and its sodium salt and adjusting to the appropriate pH. Final BGEs were prepared by mixing stock buffer and surfactant solutions with acetonitrile at each appropriate concentration, which were then degassed and filtered through 0.45-μm syringe filters.

A test sample solution was prepared by twenty-fold dilution of the stock mixed sample solution in methanol with ten-fold diluted running buffer without C_{16}TAB. The sample solutions were injected in a gravity mode for 2 second. All experiments were performed at ambient temperature (approximately 25 °C). Negative voltages of 15 kV (for 75 μm I.D. x 60 cm effective length tubes) and 13.5 kV (for 50 μm I.D. x 30 cm effective length tubes), respectively, were applied.

3. Results and Discussion

In MECC by using cationic surfactant, a dynamic bilayer phase is formed on the fused silica surface (9) resulting from the ionic interaction between the cationic head group of the surfactant and the anionic silanol group on the capillary wall, and the hydrophobic interaction of the surfactant tails binding to each other. The cationic head groups of the surfactant extend into the bulk solution producing charge reversal on the capillary wall, and establishing a double layer with mobile anions of the BGE. Consequently, the EOF is directed toward the positive electrode and use of reversed-polarity in the instrument is necessary.

Because of its insolubility in aqueous solution, Sudan III is often used in MECC as a micelle marker. However, in this study it was found that pentachlorophenol (pK_a 4.5) co-eluted with Sudan III, indicating it is associated exclusively with the micelle phase. Because pentachlorophenol is one of the eleven priority pollutant phenols, and is easier to work with than Sudan III, it was used as the micelle marker. Methanol was used as the electroosmotic flow (EOF) marker. The capacity factor (k') in MECC is calculated by (10,11)

$$k' = \frac{\left(t_s - t_{EOF}\right)}{t_{EOF}\left(1 - \frac{t_s}{t_{mc}}\right)} \qquad (1)$$

where t_s, t_{EOF} and t_{mc} are the migration times (sec) of the solute, the EOF marker and the micelle, respectively. The capacity factor for pentachlorophenol was infinite. The net mobility (μ_{net}, cm^2/V-sec) is expressed as

$$\mu_{net} = \mu_{app} - \mu_{EOF} = \frac{lL}{Vt_s} - \frac{lL}{Vt_{EOF}} = \frac{lL}{V}\left(\frac{1}{t_s} - \frac{1}{t_{EOF}}\right) \qquad (2)$$

in which μ_{app} and μ_{EOF} are apparent mobility and EOF mobility (cm^2/V-sec); l and L are the length (cm) of the capillary from injection to detection and the total length (cm) of the capillary, respectively; and V is the applied voltage (V).

The net mobility reflects a combination of the electrophoretic mobilities of the solute itself and of the solute in the micelle. The amount of time spent by the solute in the micelle depends on the extent of solute partitioning between the micelles and the aqueous medium. In this study, the BGE pHs used were 3.5 and 4.2, respectively, the two dinitrophenols were partially ionized, whose electrophoretic mobilities were in the direction opposite to that of the cationic micelles, and the other phenols were neutral. So for all compounds, the greater the association with the micelle phase (higher k'), the smaller the net mobility. Because the EOF is in the direction opposite to that of the micelles, and is also larger, the net mobility has a value less than zero. Therefore, the separation in MECC depends upon the combination of charge/size ratios, and hydrophobic and ionic interactions of the solute with the

micelles. Thus BGE parameters such as buffer constituents, pH, ionic strength, organic additive, type and concentration of surfactant, and temperature influence the separations in MECC. The effect of varying some of these parameters on the migration behaviour of the eleven phenols was examined in detail.

3.1 Effect of the Buffer Constituents

Three different pH 3.5 buffers, citrate, tartrate and phosphate, were employed with 8 mM C_{16}TAB and 10% acetonitrile using a 75 μm I.D. x 60 cm effective length (67.5 cm total length) uncoated fused-silica capillary at negative 15 kV applied voltage.

As shown in Figures 1, 3 and 4, the order of migration of 2,4-dinitrophenol (pK_a 4.0) and 2-methyl-4,6-dinitrophenol (pK_a 4.7), were switched with increasing citrate concentration. Such changes in migration order were also observed with increasing tartrate concentration. However, as demonstrated in Figure 2 of the electropherograms at the same buffer concentration, the changes by the tartrate concentration were less than those by the citrate concentration; and the changes by the phosphate concentration were the smallest.

These changes in the migration time may be attributed to an ion-exchange competition between the two partially ionized dinitrophenols and the competing anions in the BGEs with the

cationic micellar head (the detailed mechanism is discussed in Chapter 3). At pH 3.5, the charges on the BGE anions decreased in the order citrate > tartrate > phosphate. Consequently, the degree of the ion-exchange competition decreases in the same order because of the decreasing coulombic interactions of the BGE anions with the cationic micellar head. Therefore, the phosphate BGE buffer was chosen because it gave the best separation of the eleven phenols.

An increase in the BGE buffer concentration decreased the EOF, as shown in Figure 5 using citrate as an example. As the EOF decreased, the migration time increased as seen in Figure 1. The influence of the ionic strength on the current is given in Figure 6. A linear relationship was found for citrate concentrations from 10 mM to 100 mM, indicating that there was no obvious Joule heat occurring with an increase in the citrate concentration in the BGEs.

3.2 Effect of Acetonitrile

A 50 μm I.D. x 30 cm effective length (37.5 cm total length) uncoated fused-silica capillary was used with a negative 13.5 kV voltage. The BGE consisted of 50 mM phosphate-10 mM acetate (pH 4.2) with 15 mM C_{16}TAB, and the acetonitrile additive amount in the BGEs was varied from 0% to 25% at 5% increments.

As in reversed phase HPLC, an organic solvent miscible with water can be utilized as a BGE additive to manipulate the separation in MECC. Unlike HPLC, however, a high concentration of organic solvent cannot be employed because of the breakdown of the micellar structure. Balchunas and Sepaniak (12) first reported the use of an organic solvent in MECC to improve the separation of highly hydrophobic compounds that eluted near or with the micelles. The interactions between the solutes and the micelles, i.e. the capacity factors, were decreased by addition of the organic solvent to the BGE. Furthermore, the presence of the organic solvent reduced the EOF through the decreased ζ potential, and consequently extended the migration window. As a result, the resolution of highly hydrophobic compounds could be greatly improved with the longer separation time.

As shown in Figures 7, 8 and 9, acetonitrile is an important factor in the separation of the eleven phenols. Without acetonitrile the five early-eluting compounds (phenol, 2-nitrophenol, 4-nitrophenol, 2-chlorophenol and 2,4-dimethylphenol) were well separated; but the later-eluting solutes (2,4,6-trichlorophenol, 2,4-dinitrophenol, and 2-methyl-4,6-dinitrophenol) exactly co-eluted with the micelle. However, the partitioning of the solutes between the micelle and the aqueous phase was dramatically reduced by adding acetonitrile, and the reduced EOF (as shown in Figure 10) increased the migration

window as demonstrated in Figure 7 of the electropherograms. As a result, the resolution and selectivity were significantly improved for the later-eluting phenols as given in Figures 11 and 12. However, when acetonitrile was increased over 20 %, the migration order of 2,4,6-trichlorophenol and 2,4-dinitrophenol was reversed, and the baseline separations for the five early-eluting compounds could not be maintained because the interactions between the phenols and the micelles were greatly reduced. The best separation was achieved with 15% acetonitrile.

3.3 Effect of pH

An uncoated fused-silica capillary with 50 μm I.D. and 30 cm effective length (37.5 cm total length) was employed under negative 13.5 kV applied voltage. BGEs consisted of 50 mM phosphate-10 mM acetate with 15 mM C_{16}TAB and 15% acetonitrile, at pH value from 3.7 to 11.5. Figures 13 and 14 demonstrate the dependence of both the capacity factors and the net mobilities on the BGE pH.

The variation of the EOF mobility with the pH changes is shown in Figure 15. With increasing pH, the fused silica surface became more negative because of the increased ionization of Si-OH groups enabling more C_{16}TAB monomers to be bound ionically to the surface, resulting in higher net positive charge density (13). As a result, for pH < 4.7, the EOF increased with

increasing pH. Although more Si-OH groups are ionized with further increases in pH, no more C_{16}TAB monomers can be bound to the fused-silica surface once a monolayer is formed. Consequently, the net positive surface charge density is reduced with further increasing pH, causing the EOF to be decreased after pH 4.7.

The pH is critical for the separation of ionizable solutes because it affects solute ionization and thus electrophoretic mobility, and alters the interaction with the micelle through the change in hydrophobicity and hydrophilicity. Consequently, capacity factors and net mobilities, selectivity and the efficiency are pH-dependent. At pH 3.7, except for the two dinitro compounds and pentachlorophenol which were partially ionized, all the others were neutral, and the separation of all eleven phenols could be achieved. However, the low BGE pH resulted in the smaller EOF, and thus longer analysis time, causing the broader band and lower efficiencies. As the BGE pH was increased from pH 3.7 to pH 6.5, the eleven phenols gradually became partially or totally ionized. Thus, except for 2-nitrophenol, the net mobilities of all the others were increased since their electrophoretic mobilities were in the EOF direction. For 2-nitrophenol (pK_a 7.23), an intra-molecular hydrogen bond can occur, reducing the polarity of the compound and thus increasing the hydrophobic interaction with the micelle. This causes a decrease in net mobility from pH 4.2

to pH 6.5, and a reversal of migration order of 4-nitrophenol and 2-chlorophenol. However, the high pH did not give separations with good resolution and efficiency as illustrated in Tables 2, 3 and 4. In addition, as expected, the migration order of the two dinitrophenols changed as the BGE pH was increased because of the increased dissociation and electrophoretic mobilities in the EOF direction. At pH 11.5 phenol (pK_a 9.89) was fully ionized and eluted before the EOF marker, meaning that phenol had a higher electrophoretic mobility and had no interaction with the micelles. Overall, use of pH 4.2 was preferred for the separation of the eleven phenols.

3.4 Effect of C_{16}TAB Concentration

This study was performed on a 50 μm I.D. x 30 cm effective length (37.5 cm total length) uncoated fused-silica capillary at negative 13.5 kV applied voltage. The BGE consisted of 50 mM phosphate-10 mM acetate at pH 4.2 with 15% acetonitrile; C_{16}TAB concentration in the BGE was changed from 5 mM to 25 mM at 5 mM increments. The results for this study are given in Figures 17 to 24.

The surfactant concentration affects the migration behaviour of the phenols because the phase ratio in the MECC system changes with surfactant concentration. Increased surfactant concentration results in a larger number of micelles, leading to more micellar partitioning, thus affecting selectivity. The

relationship between the capacity factor (k') and the surfactant concentration (C_{sf}) is approximated as follows (10)

$$k' = K \Phi_v (C_{sf} - CMC) \quad (3)$$

where K is the distribution coefficient and Φ_v is the partial specific volume of the micelle. It is obvious that the capacity factor increases linearly with increase in the surfactant concentration. As expected, the capacity factors of the eleven phenols were increased linearly with increasing surfactant concentration as shown in Figure 18. This reflects that the phenol distribution coefficients are almost constant regardless of the C_{16}TAB concentration, i.e., the partition isotherm is linear. As the micellar phase ratio increased by increasing the surfactant concentration, the net mobilities of the phenols decreased, as shown in Figure 19. However, the micelle net mobility was only increased slightly from 5 mM to 10 mM C_{16}TAB in the BGE, and was unchanged in high C_{16}TAB concentration.

As shown in Figure 17, the migration time of the micelle marker peak (pentachlorophenol) decreased with increasing surfactant concentration. However, at high surfactant concentrations, the migration time of the micelle peak was relatively unchanged. In MECC, the micelles are dynamic entities, i.e., the micelles constantly exchange with the monomers to form the new micelles. In this way, the size of a particular micelle varies with time; this phenomenon is called the micelle polydispersity

(14). Since the net mobility of the micelle changed only slightly, the micelle polydispersity was small. As a consequence, micelle polydispersity can not be attributed to the increased migration time of the micelle. On the other hand, the bilayer by the cationic surfactant is dynamic - the monomers on the surface dynamically exchange with monomers in the BGE; and it can be expected that the dynamic exchange at low surfactant concentration could be slower than that at high surfactant concentration. As a result, at the low surfactant concentrations, the net surface charge density could be less positive than that at the high surfactant concentrations, therefore the EOF could be small, causing the migration time of the micelle peak longer. However, at higher surfactant concentration, the exchange between the monomer on the surface and the monomer in the BGE reached stead state, so the EOF was no longer significantly affected by further increase in surfactant concentration. Thus the migration time of the micelles was almost unchanged. In addition, the surfactant concentration can affect the viscosity of the BGE, which also influences the EOF. However, first, the 5 mM C_{16}TAB concentration intervals would not be expected to produce a large difference in the viscosity of the BGEs. Second, the viscosity increases with increase in the surfactant concentration, which would reduce the EOF. Therefore, the change of the BGE viscosity with surfactant concentrations can not contribute to the increased EOF.

Furthermore, with increasing surfactant concentration the current could increase, causing an EOF increase. However, it was found that the current was changed only from ~ 32 μA to ~ 38 μA with increasing C_{16}TAB concentration from 5 mM to 25 mM. This small current increase within 50 μm I.D. capillary below 50 μA current would not produce undissipated Joule heat, hence could not cause increase in the EOF and reduction in the migration time of the micelle peak.

As shown in Figure 17, and Figures 22 to 24, for 2,4,6-trichlorophenol, 2,4-dinitrophenol, 2-methyl-4,6-dinitrophenol and pentachlorophenol, the higher the surfactant concentration, the more symmetrical and the narrower the peaks, and the higher the theoretical plate number. This can be attributed to the decreased micellar polydispersity with increasing surfactant concentration. At the surfactant concentration near the CMC (≤ 5 mM), a range of micellar mobilities exists even though the range is small, which causes the peaks of the later-eluting phenols to broaden. However, as shown in Figures 20 and 21, increase in the C_{16}TAB concentration beyond 20 mM resulted in a decrease in the resolution between 2,4,6-trichlorophenol and 2,4-dinitrophenol, and between 2,4-dinitrophenol and 2-methyl-4,6-dinitrophenol, as well as the selectivity between 2,4,6-trichlorophenol and 2,4-dinitrophenol. At concentration greater than 20 mM C_{16}TAB, the interactions between the micelles and the phenols were so strong that these compounds migrated close

to the micelles, causing the resolution, as well as the selectivity, to be reduced. As a consequence, C_{16}TAB concentration of 15 mM is the best choice.

3.5 Effect of Ionic Strength

A 50 μm I.D. and 30 cm effective length (37.5 cm total length) uncoated fused-silica capillary was applied at negative 13.5 kV voltage. The BGE consisted of 10 mM acetate at pH 4.2 with 15 mM C_{16}TAB and 15% acetonitrile; and phosphate buffer concentrations (pH 4.2) were 10 mM, 25 mM, 40 mM, 50 mM and 60 mM.

The capacity factors and the net mobilities as a function of ionic strength are plotted in Figures 25 and 26. For 2,4-dinitrophenol and 2-methyl-4,6-dinitrophenol, the capacity factors decreased and the net mobilities increased slightly with increasing phosphate concentration. This can be attributed to the ion-exchange effect discussed previously since at pH 4.2 these two dinitrophenols were ionized or partially ionized, and can interact ionically with the cationic micellar head in addition to the hydrophobic interactions. However, capacity factors and net mobilities were little affected for the other phenols since they were neutral at pH 4.2. The influence of ionic strength on the current is shown in Figure 27. A linear relationship was found with phosphate concentration from 10 mM to 60 mM, indicating that no obvious Joule heat was generated by the

increase in ionic strength. Moreover, as the ionic strength of the BGE was increased there was a decrease in the EOF. A linear decrease in EOF with log phosphate concentration is shown in Figure 28. As EOF decreases, migration time increases, and resolution between 2,4-dinitrophenol and 2-methyl-4,6-dinitrophenol improves as shown in Figure 29. However, as the phosphate concentration reached 60 mM, resolution and selectivity between 2,4,6-trichlorophenol and 2,4-dinitrophenol decreased as shown in Figures 29 and 30. The decrease in EOF with increasing BGE ionic strength is well documented (15, 16) and is attributed to a decrease in the zeta potential caused by compression of the electrical double-layer. Furthermore, the high ionic strength and subsequent high conductivity results in higher currents, and Joule heat. Therefore, use of 50 mM phosphate was preferable.

3.6 Optimized Separation Conditions

As discussed above, the optimized separation is achieved using a 30 cm effective length (37.5 cm total length) x 50 μm I.D. uncoated fused-silica capillary with a BGE containing 15 mM C_{16}TAB and 15% acetonitrile in 50 mM phosphate-10 mM acetate buffer (pH 4.2) under negative 13.5 kV applied voltage. (See the electropherogram in Figure 17).

3.7 Reproducibility of Net Mobility (μ_{net}) and Capacity Factor (k')

The advantage of working with net mobilities and capacity factors is that the effect of the irreproducible EOF is removed. Also the migration time of the micelle marker is not required to calculate the net mobility. Any uncertainty in the determination on the migration time of the micelle marker causes variation in the capacity factor. In Tables 5 and 6 are tabulated %RSDs of the net mobilities and the capacity factors for the phenols from five different measuremants. Obviously, %RSDs for net mobility were much smaller than those for capacity factor.

3.8 Limits of Detection

Mass limits of detection (MLOD) were calculated based on a signal to noise ratio of 3. The results are tabulated in Table 7.

4. Conclusions

For the first time we have demonstrated that excellent separation can be achieved for eleven priority pollutant phenols by MECC with a cationic surfactant.

Table 1

Eleven Priority Pollutant Phenols

No.	Compounds	pK_a	M.W.	Formulas
1	Phenol	9.89	94.11	C_6H_5OH
2	2-Nitrophenol	7.23	139.11	$C_6H_4(NO_2)OH$
3	4-Nitrophenol	7.15	139.11	$C_6H_4(NO_2)OH$
4	2-Chlorophenol	8.48	128.56	C_6H_4ClOH
5	2,4-Dimethylphenol	10.59	122.17	$(CH_3)_2C_6H_3OH$
6	4-Chloro-3-methylphenol	9.54	142.59	$ClC_6H_3(CH_3)OH$
7	2,4-Dichlorophenol	7.85	163.01	$C_6H_3Cl_2OH$
8	2,4,6-Trichlorophenol	7.42	197.46	$C_6H_2Cl_3OH$
9	2,4-Dinitrophenol	4.00	184.11	$C_6H_3(NO_2)_2OH$
10	2-Methyl-4,6-dinitrophenol	4.70	198.13	$C_6H_2(CH_3)(NO_2)_2OH$
11	Pentachlorophenol	4.50	266.35	C_6Cl_5OH

Table 2

Effect of Background Electrolyte pH on Resolution (R)

1) Resolution @ pH 4.2

Compound Pairs	Resolution
Phenol / 2-Nitrophenol	3.2
2-Nitrophenol / 4-Nitrophenol	5.3
4-Nitrophenol / 2-Chlorophenol	4.2
2-Chlorophenol / 2,4-Dimethylphenol	4.8
2,4-Dimethylphenol / 4-Chloro-3-Methylphenol	11.5
4-Chloro-3-Methylphenol / 2,4-Dichlorophenol	5.9
2,4-Dichlorophenol / 2,4,6-Trichlorophenol	9.1
2,4,6-Trichlorophenol / 2,4-Dinitrophenol	3.8
2,4-Dinitrophenol / 2-Methyl-4,6-Dinitrophenol	3.5
2-Methyl-4,6-Dinitrophenol / Pentachlorophenol	7.5

2) Resolution @ pH 9.5

Compound Pairs	Resolution
Phenol / 4-Nitrophenol	3.7
4-Nitrophenol / 2-Chlorophenol	3.1
2-Chlorophenol / 2-Nitrophenol	1.7
2-Nitrophenol / 2,4-Dimethylphenol	1.7
2,4-Dimethylphenol / 4-Chloro-3-Methylphenol	8.8
4-Chloro-3-Methylphenol / 2,4-Dinitrophenol	4.2
2,4-Dinitrophenol / 2,4-Dichlorophenol	1.8
2,4-Dichlorophenol / 2-Methyl-4,6-dinitrophenol	1.6
2-Methyl-4,6-Dinitrophenol / 2,4,6-Trichlorophenol	3.2
2,4,6-Trichlorophenol / Pentachlorophenol	2.2

Table 3

Effect of Background Electrolyte pH on Theoretical Plate Number (N)

	Theoretical Plate Number (N)	
Compounds	**pH 4.2**	**pH 9.5**
Phenol	65100	30400
2-Nitrophenol	69300	17300
4-Nitrophenol	37868	8900
2-Chlorophenol	46100	13100
2,4-Dimethylphenol	49500	40200
4-Chloro-3-Methylphenol	44900	29800
2,4-Dichlorophenol	46700	19700
2,4,6-Trichlorophenol	141800	30300
2,4-Dinitrophenol	50600	21900
2-Methyl-4,6-Dinitrophenol	68600	15900
Pentachlorophenol	84200	19000

Table 4

Effect of Background Electrolyte pH on Selectivity (*a*)

1) Selectivity @ pH 4.2

Compound Pairs	Selectivity
Phenol / 2-Nitrophenol	1.4
2-Nitrophenol / 4-Nitrophenol	1.6
4-Nitrophenol / 2-Chlorophenol	1.4
2-Chlorophenol / 2,4-Dimethylphenol	1.4
2,4-Dimethylphenol / 4-Chloro-3-Methylphenol	2.1
4-Chloro-3-Methylphenol / 2,4-Dichlorophenol	1.5
2,4-Dichlorophenol / 2,4,6-Trichlorophenol	1.9
2,4,6-Trichlorophenol / 2,4-Dinitrophenol	1.4
2,4-Dinitrophenol / 2-Methyl-4,6-Dinitrophenol	1.6

2) Selectivity @ pH 9.5

Compound Pairs	Selectivity
Phenol / 4-Nitrophenol	3.1
4-Nitrophenol / 2-Chlorophenol	2.2
2-Chlorophenol / 2-Nitrophenol	1.3
2-Nitrophenol / 2,4-Dimethylphenol	1.2
2,4-Dimethylphenol / 4-Chloro-3-Methylphenol	2.3
4-Chloro-3-Methylphenol / 2,4-Dinitrophenol	1.7
2,4-Dinitrophenol / 2,4-Dichlorophenol	1.3
2,4-Dichlorophenol / 2-Methyl-4,6-dinitrophenol	1.3
2-Methyl-4,6-Dinitrophenol / 2,4,6-Trichlorophenol	2.1

Table 5

Reproducibility of Net Mobilities (μ)

No.	Compounds	No. 1 Net μ	No. 2 Net μ	No. 3 Net μ	No. 4 Net μ	No. 5 Net μ	*Average Net μ*	SD	*%RSD*
1	Phenol	-7.683E-05	-7.668E-05	-7.712E-05	-7.782E-05	-7.943E-05	*-7.758E-05*	1.124E-06	*1.449*
2	2-Nitrophenol	-1.002E-04	-9.988E-05	-1.004E-04	-1.006E-04	-1.021E-04	*-1.006E-04*	8.775E-07	*0.872*
3	4-Nitrophenol	-1.371E-04	-1.366E-04	-1.374E-04	-1.380E-04	-1.411E-04	*-1.381E-04*	1.777E-06	*1.287*
4	2-Chlorophenol	-1.662E-04	-1.657E-04	-1.664E-04	-1.668E-04	-1.700E-04	*-1.670E-04*	1.736E-06	*1.039*
5	2,4-Dimethylphenol	-1.955E-04	-1.944E-04	-1.952E-04	-1.952E-04	-1.981E-04	*-1.957E-04*	1.428E-06	*0.730*
6	4-Chloro-3-Methylphenol	-2.566E-04	-2.546E-04	-2.550E-04	-2.543E-04	-2.570E-04	*-2.555E-04*	1.228E-06	*0.481*
7	2,4-Dichlorophenol	-2.840E-04	-2.813E-04	-2.818E-04	-2.802E-04	-2.825E-04	*-2.820E-04*	1.421E-06	*0.504*
8	2,4,6-Trichlorophenol	-3.145E-04	-3.108E-04	-3.112E-04	-3.081E-04	-3.096E-04	*-3.108E-04*	2.380E-06	*0.766*
9	2,4-Dinitrophenol	-3.253E-04	-3.211E-04	-3.216E-04	-3.185E-04	-3.196E-04	*-3.212E-04*	2.591E-06	*0.807*
10	2-Methyl-4,6-Dinitrophenol	-3.373E-04	-3.326E-04	-3.327E-04	-3.289E-04	-3.298E-04	*-3.322E-04*	3.263E-06	*0.982*
11	Pentachlorophenol	-3.581E-04	-3.521E-04	-3.524E-04	-3.472E-04	-3.474E-04	*-3.514E-04*	4.479E-06	*1.274*

Table 6

Reproducibility of Capacity Factors (k')

No.	*Compounds*	No. 1 k'	No. 2 k'	No. 3 k'	No. 4 k'	No. 5 k'	*Average* k'	SD	*%RSD*
1	Phenol	0.273	0.278	0.280	0.289	0.285	*0.281*	0.006	*2.172*
2	2-Nitrophenol	0.389	0.396	0.398	0.408	0.403	*0.399*	0.007	*1.828*
3	4-Nitrophenol	0.620	0.634	0.639	0.660	0.658	*0.642*	0.017	*2.615*
4	2-Chlorophenol	0.866	0.888	0.895	0.925	0.918	*0.898*	0.023	*2.610*
5	2,4-Dimethylphenol	1.202	1.233	1.241	1.284	1.272	*1.246*	0.033	*2.614*
6	4-Chloro-3-Methylphenol	2.527	2.610	2.616	2.739	2.704	*2.639*	0.084	*3.179*
7	2,4-Dichlorophenol	3.835	3.972	3.989	4.187	4.134	*4.023*	0.140	*3.474*
8	2,4,6-Trichlorophenol	7.213	7.521	7.550	7.881	7.745	*7.582*	0.254	*3.345*
9	2,4-Dinitrophenol	9.911	10.345	10.445	11.096	10.934	*10.546*	0.476	*4.516*
10	2-Methyl-4,6-Dinitrophenol	16.198	17.016	16.825	18.048	17.552	*17.128*	0.707	*4.125*

Table 7

Mass LODs of the Eleven Phenols by MECC with C_{16}TAB

No.	Compounds	Conc. (μg/mL)	Inj. Amt. (μg)	Signal (mAu)	LOD* (mol)
1	Phenol	123.58	4.20E-05	6.430	6.666E-15
2	2-Nitrophenol	126.93	4.32E-05	8.882	3.353E-15
3	4-Nitrophenol	251.25	8.54E-05	6.360	9.269E-15
4	2-Chlorophenol	255.13	8.67E-05	9.832	6.588E-15
5	2,4-Dimethylphenol	272.00	9.25E-05	8.887	8.177E-15
6	4-Chloro-3-Methylphenol	251.73	8.56E-05	6.626	8.696E-15
7	2,4-Dichlorophenol	252.85	8.60E-05	7.780	6.508E-15
8	2,4,6-Trichlorophenol	82.65	2.81E-05	8.168	1.673E-15
9	2,4-Dinitrophenol	123.50	4.20E-05	4.502	4.863E-15
10	2-Methyl-4,6-Dinitrophenol	123.13	4.19E-05	4.092	4.957E-15
11	Pentachlorophenol	86.88	2.95E-05	4.135	2.575E-15

* LOD is based on S / N = 3; and Noise level (mAu) = 0.032

Definitions: 1) Conc. (μg/mL): the concentrations of the eleven phenols;

2) Inj. Amt. (μg): the injected amounts of the eleven phenols on the capillary;

3) Signal (mAu): the peak heights for the eleven phenols in mAu;

4) LOD (mol): the mass limits of detection for the eleven phenols.

Figure Captions: (see Table 1 for the phenol identification)

Figure 1: Electropherograms of the eleven phenols at different citrate concentrations (pH 3.5) with 8 mM C_{16}TAB and 10% acetonitrile. (a) 10 mM, (b) 20 mM, (c) 40 mM, (d) 50 mM, (e) 60 mM, (f) 70 mM, (g) 90 mM, (h) 100 mM.

Figure 2: Electropherograms of the eleven phenols at three different buffers (pH 3.5) with 8 mM C_{16}TAB and 10% acetonitrile. (a) 80 mM citrate, (b) 80 mM tartrate, (c) 80 mM phosphate.

Figure 3: Effect of citrate concentration (with 8 mM C_{16}TAB and 10% acetonitrile, pH 3.5) on the capacity factors of the eleven phenols.

Figure 4: Effect of citrate concentration (with 8 mM C_{16}TAB and 10% acetonitrile, pH 3.5) on the net mobility of the eleven phenols.

Figure 5: Effect of log citrate concentration (with 8 mM C_{16}TAB and 10% acetonitrile, pH 3.5) on the electroosmotic mobility (linear relationship).

Figure 6: Effect of citrate concentrations (with 8 mM C_{16}TAB and 10% acetonitrile, pH 3.5) on the current (linear relationship).

Figure 7: Electropherograms of the eleven phenols at different acetonitrile concentrations using 50 mM phosphate - 10 mM acetate (pH 4.2) with 15 mM C_{16}TAB. (a) 0%, (b) 5%, (c) 10%, (d) 15%, (e) 20%, and (f) 25.

Figure 8: Effect of acetonitrile concentration on the capacity factor of the eleven phenols using 50 mM phosphate - 10 mM acetate (pH 4.2) with 15 mM C_{16}TAB.

Figure 9: Effect of acetonitrile concentration on the net mobility of the eleven phenols using 50 mM phosphate - 10 mM acetate (pH 4.2) with 15 mM C_{16}TAB.

Figure 10: Effect of acetonitrile concentration on the electroosmotic mobility using 50 mM phosphate-10 mM acetate (pH 4.2) with 15 mM C_{16}TAB.

Figure 11: Effect of acetonitrile concentration on the resolutions of the eleven phenols using 50 mM phosphate - 10 mM acetate (pH 4.2) with 15 mM C_{16}TAB.

Figure 12: Effect of acetonitrile concentration on the selectivities of the eleven phenols using 50 mM phosphate - 10 mM acetate (pH 4.2) with 15 mM C_{16}TAB.

Figure 13: Effect of pH of the background electrolyte on the capacity factors of the eleven phenols using 50 mM phosphate - 10 mM acetate with 15 mM C_{16}TAB and 15% acetonitrile.

Figure 14: Effect of pH of the background electrolyte on the net mobilities of the eleven phenols using 50 mM phosphate - 10 mM acetate with 15 mM C_{16}TAB and 15% acetonitrile.

Figure 15: Effect of pH of the background electrolyte on the electroosmotic mobility using 50 mM phosphate - 10 mM acetate with 15 mM C_{16}TAB and 15% acetonitrile.

Figure 16: Electropherograms of the eleven phenols at different pH of the background electrolyte using 50 mM phosphate - 10 mM acetate (pH 4.2) with 15 mM C_{16}TAB and 15% acetonitrile. (a) pH 4.2, (b) pH 9.5.

Figure 17: Electropherograms of the eleven phenols at different C_{16}TAB concentrations using 50 mM phosphate - 10 mM acetate (pH 4.2) with 15% acetonitrile.(a) 5 mM, (b) 10 mM, (c) 15 mM, (d) 20 mM, (e) 25 mM.

Figure 18: Effect of C_{16}TAB concentration on the capacity factors of the eleven phenols using 50 mM phosphate - 10 mM acetate (pH 4.2) with 15% acetonitrile.

Figure 19: Effect of C_{16}TAB concentration on net mobilities of the eleven phenols using 50 mM phosphate - 10 mM acetate (pH 4.2) with 15% acetonitrile.

Figure 20: Effect of C_{16}TAB concentration on the resolution of the eleven phenols using 50 mM phosphate - 10 mM acetate (pH 4.2) with 15% acetonitrile.

Figure 21: Effect of C_{16}TAB concentration on the selectivities for the eleven phenols using 50 mM phosphate - 10 mM acetate (pH 4.2) with 15% acetonitrile.

Figure 22: Effect of C_{16}TAB concentration on the theoretical plate numbers of the eleven phenols using 50 mM phosphate - 10 mM acetate (pH 4.2) with 15% acetonitrile.

Figure 23: Effect of C_{16}TAB concentration on the peak symmetries of the eleven phenols using 50 mM phosphate - 10 mM acetate (pH 4.2) with 15% acetonitrile.

Figure 24: Effect of C_{16}TAB concentration on the peak widths of the eleven phenols using 50 mM phosphate - 10 mM acetate (pH 4.2) with 15% acetonitrile.

Figure 25: Effect of phosphate concentrations (pH 4.2) on the capacity factor of the eleven phenols with 10 mM acetate, 15 mM C_{16}TAB and 15% acetonitrile.

Figure 26: Effect of phosphate concentration (pH 4.2) on the net mobilities of the eleven phenols with 10 mM acetate, 15 mM C_{16}TAB and 15% acetonitrile.

Figure 27: Effect of the phosphate concentration (pH 4.2) on the current with 10 mM acetate, 15 mM C_{16}TAB and 15% acetonitrile.

Figure 28: Effect of log phosphate concentration (pH 4.2) on the electroosmotic mobility with 10 mM acetate, 15 mM C_{16}TAB and 15% acetonitrile.

Figure 29: Effect of the phosphate concentration (pH 4.2) on the resolutions of the eleven phenols with 10 mM acetate, 15 mM C_{16}TAB and 15% acetonitrile.

Figure 30: Effect of the phosphate concentrations (pH 4.2) on the selectivities of the eleven phenols with 10 mM acetate, 15 mM C_{16}TAB and 15% acetonitrile.

Figure 1

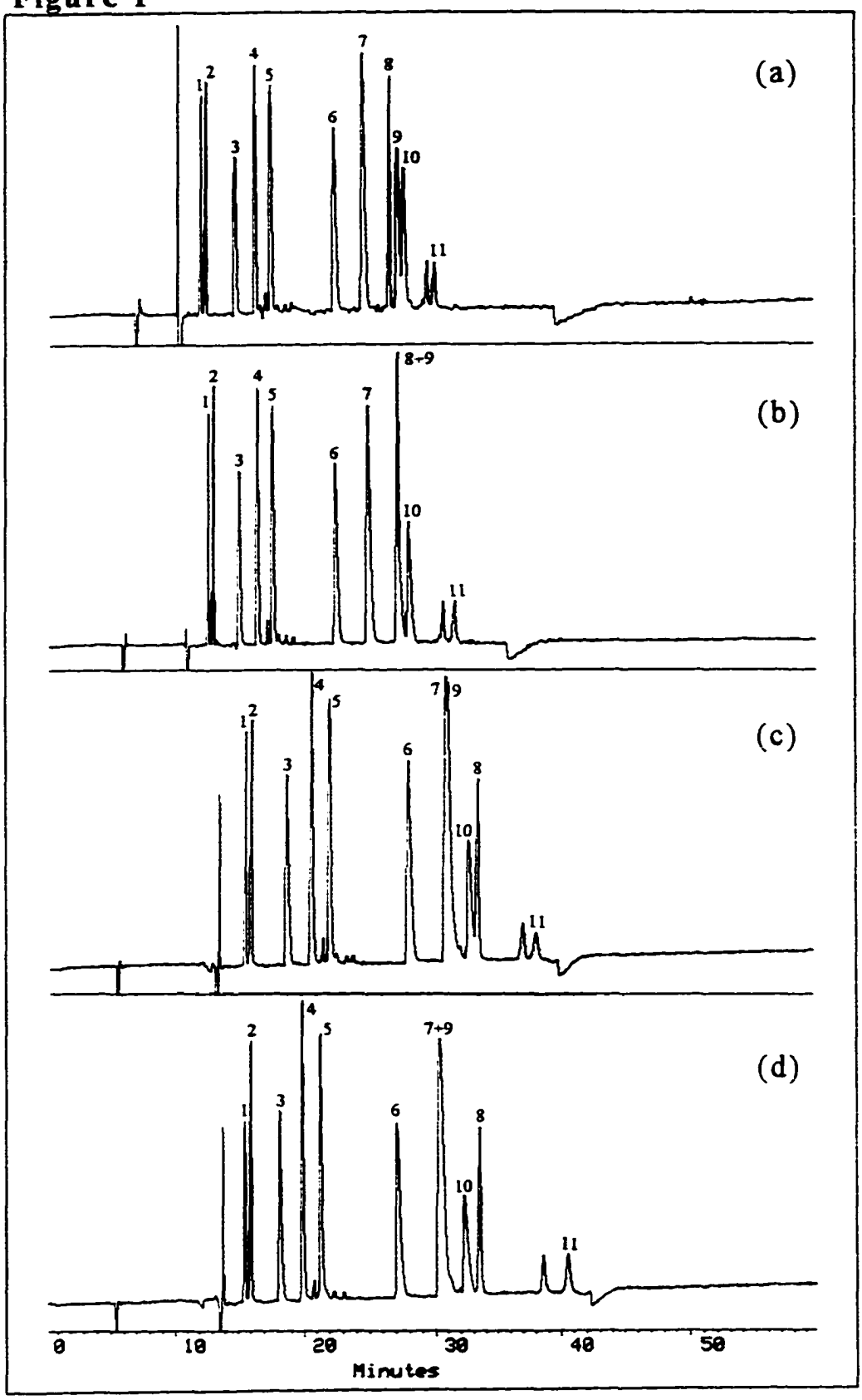

Figure 1 (continued)

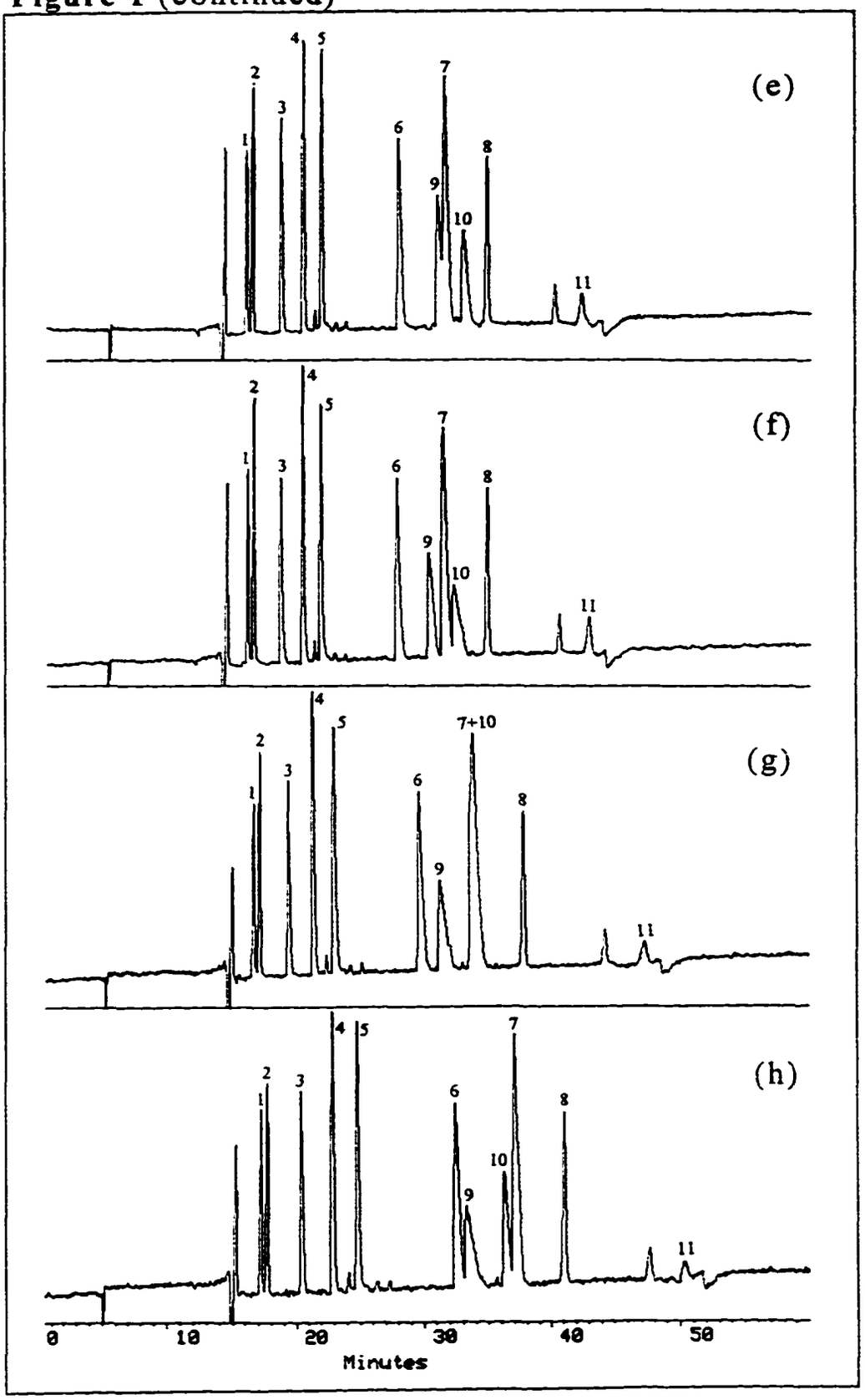

Figure 2

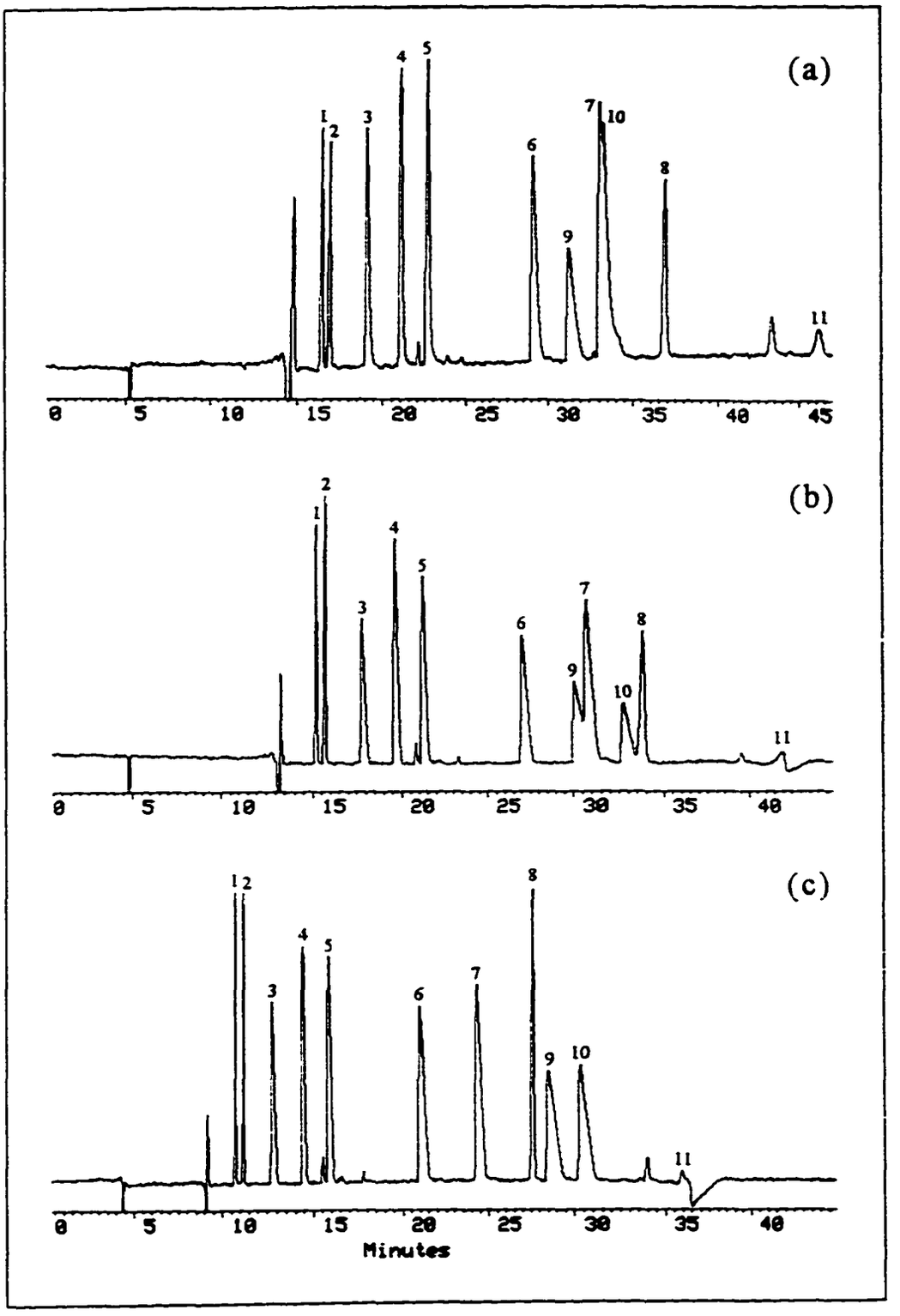

Figure 3

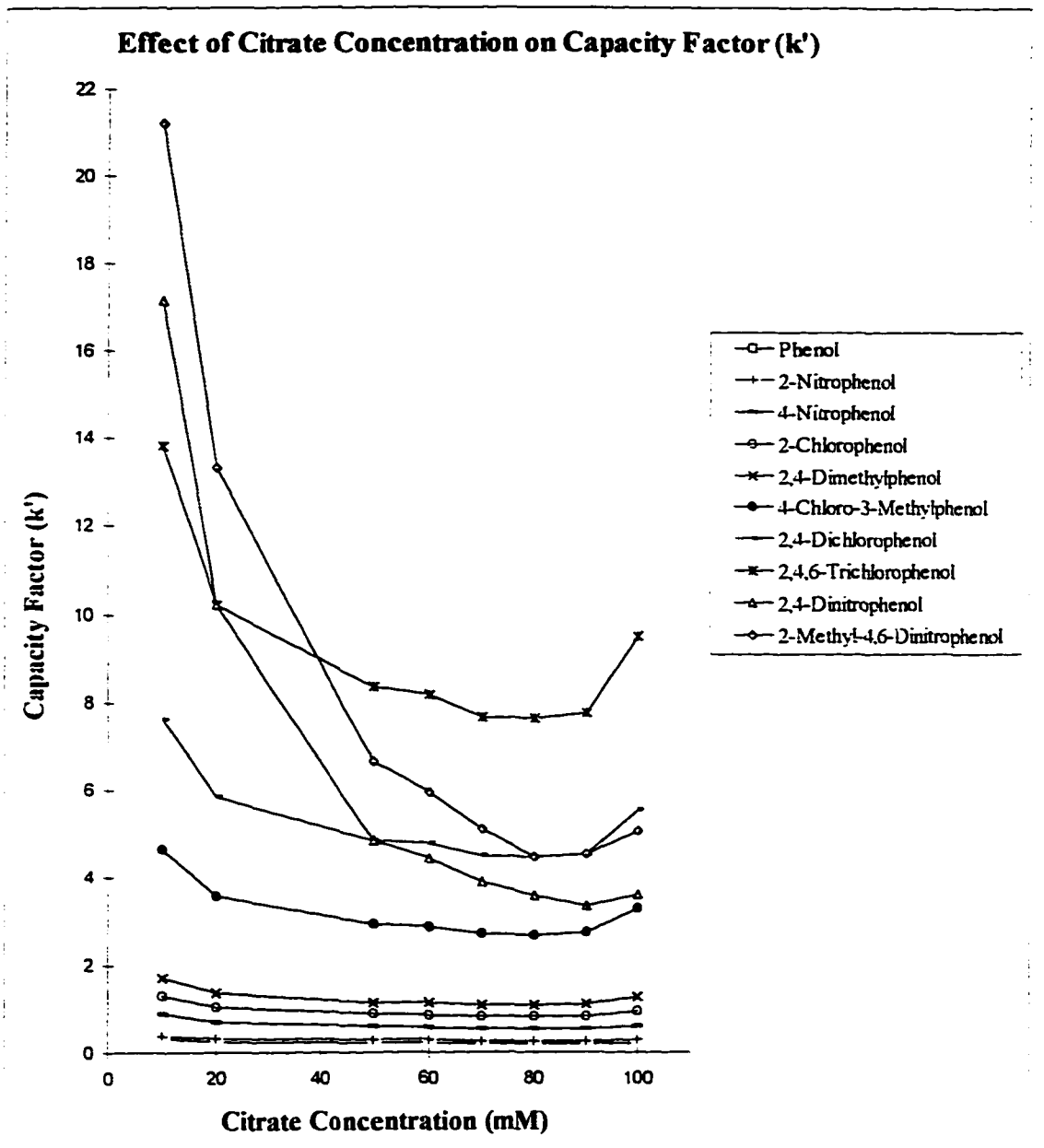

Figure 4

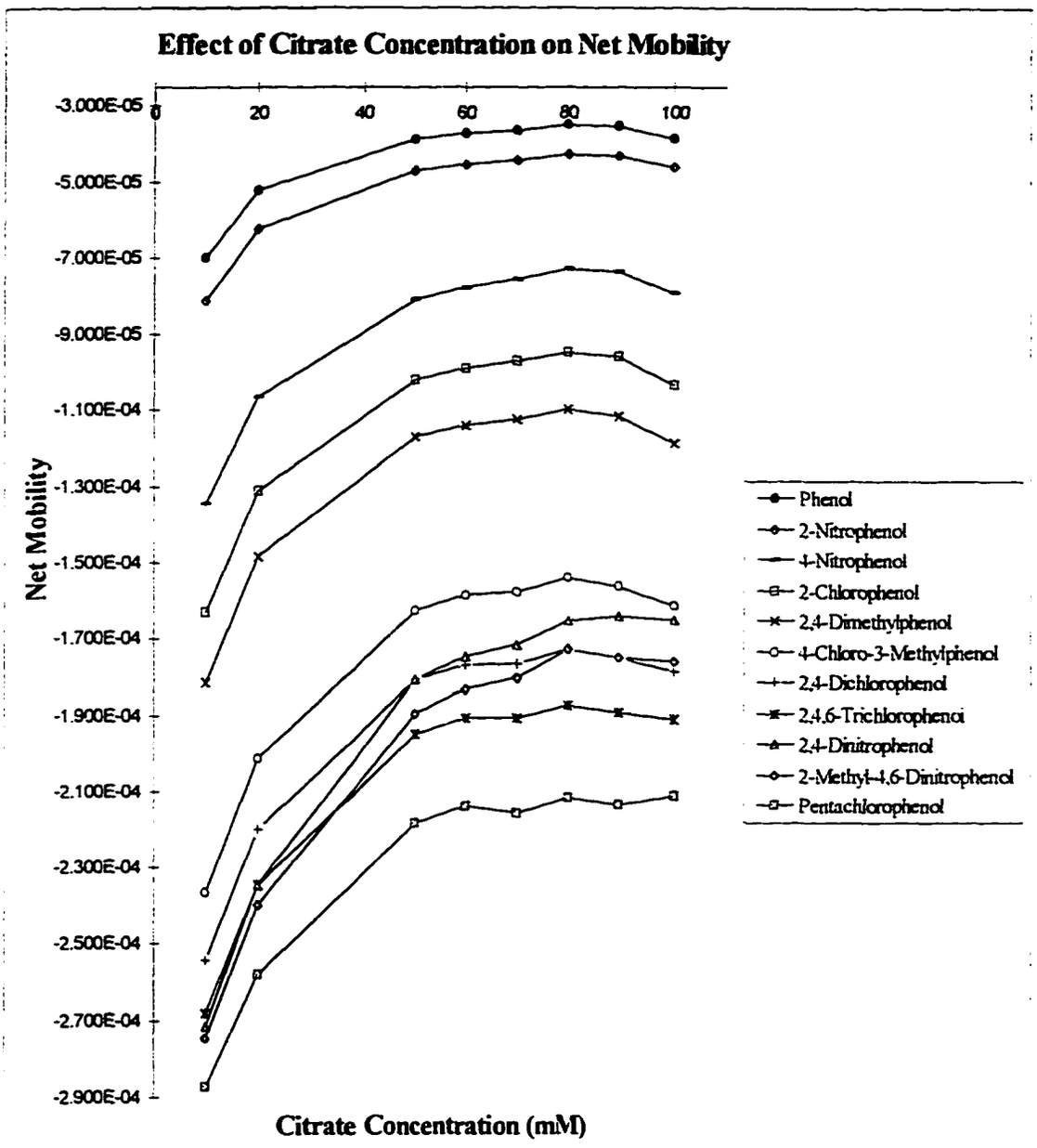

Figure 5

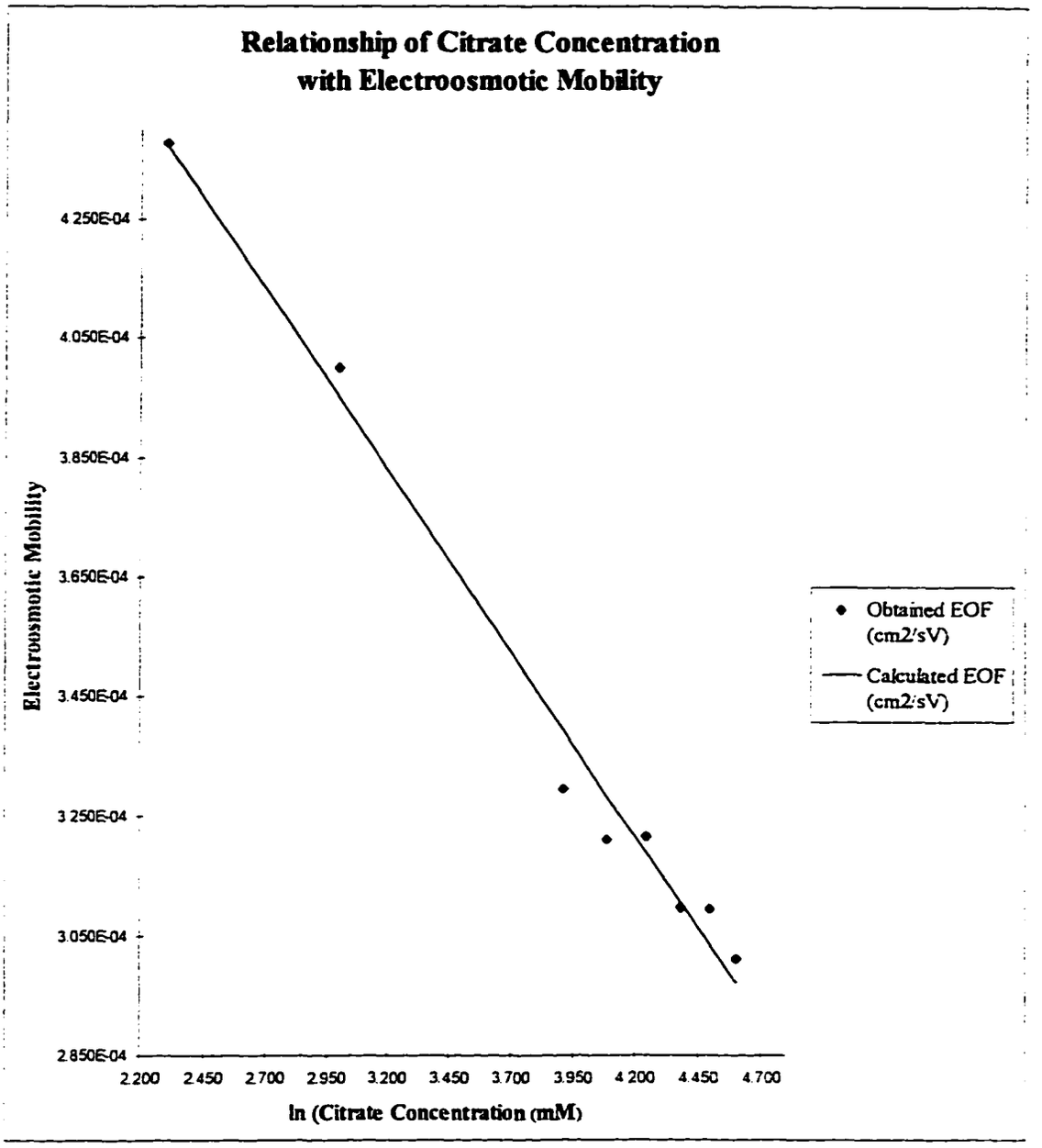

RSQ:	**0.987**
Slope:	**-6.080E-05**
Intercept:	**5.772E-04**

Figure 6

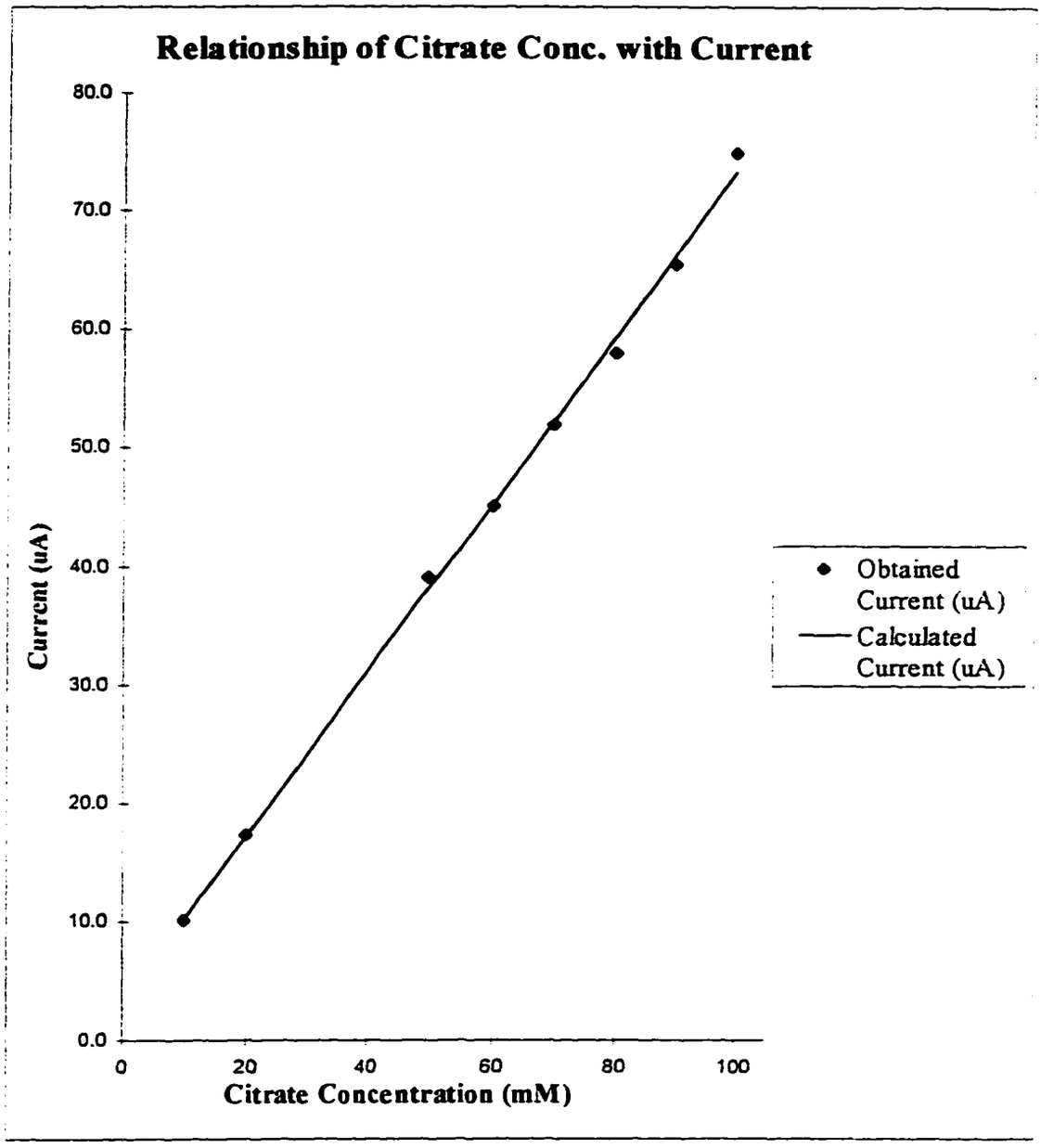

RSQ:	**0.999**
Slope:	**0.701**
Intercept:	**3.183**

Figure 7

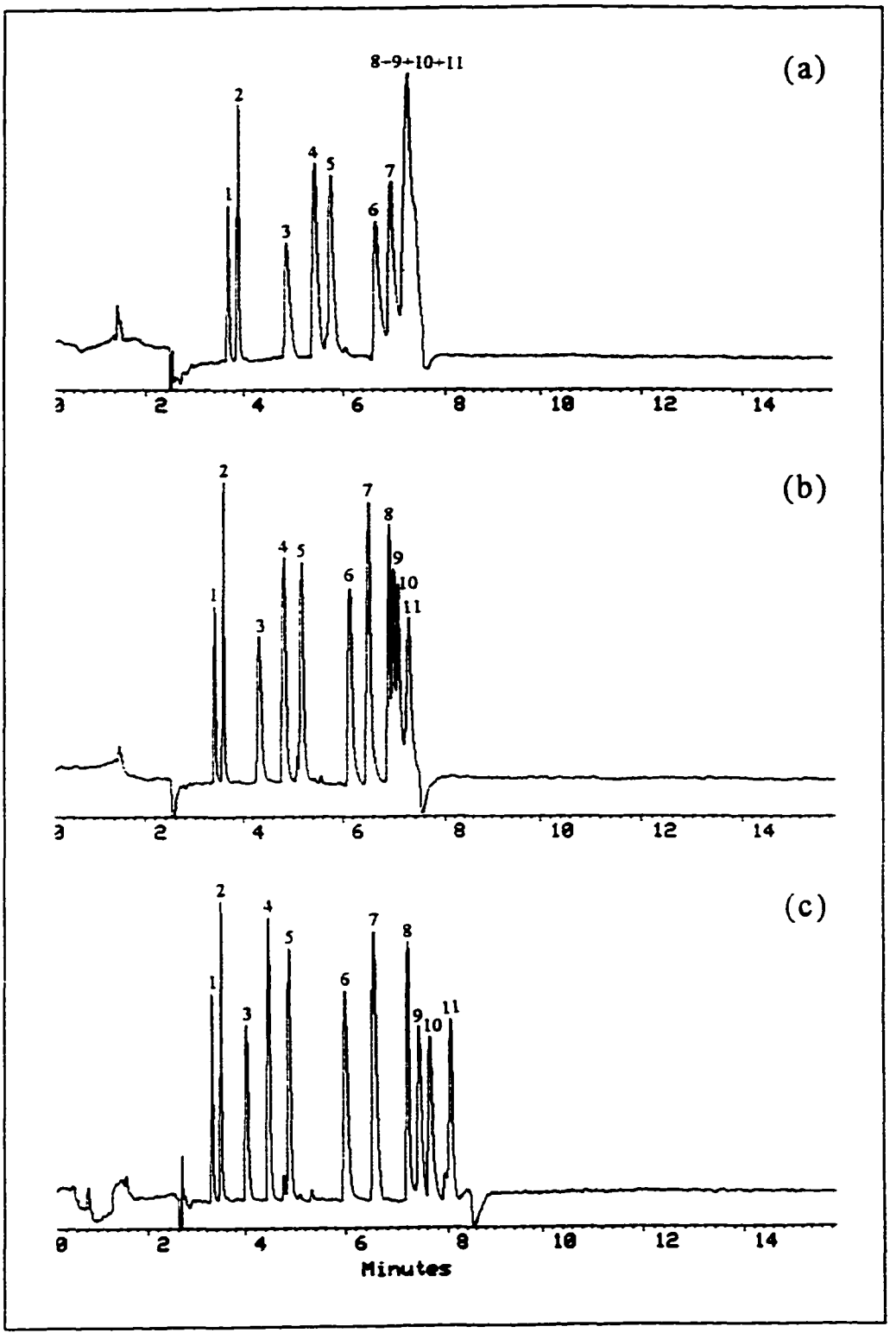

Figure 7 (continued)

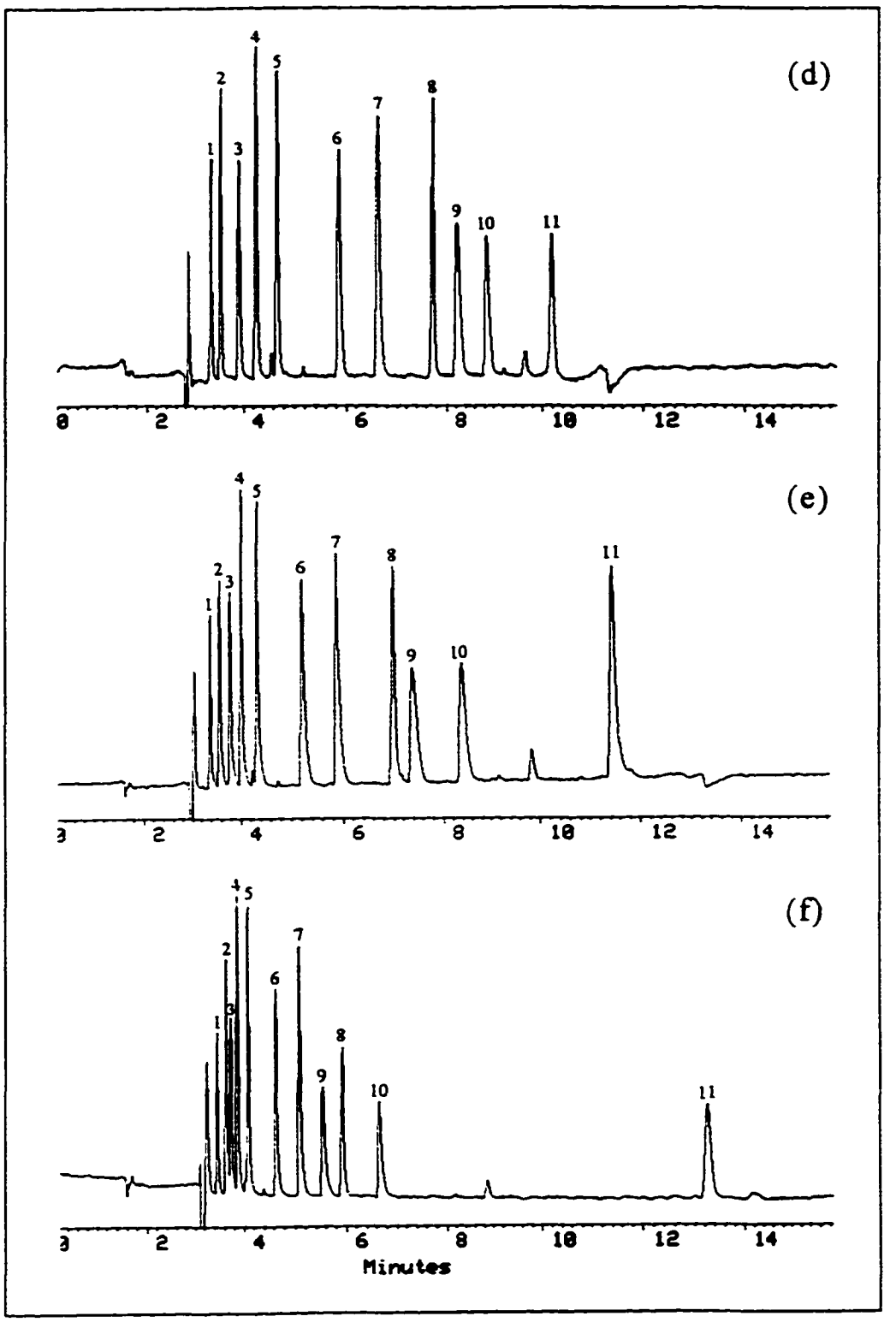

Figure 8

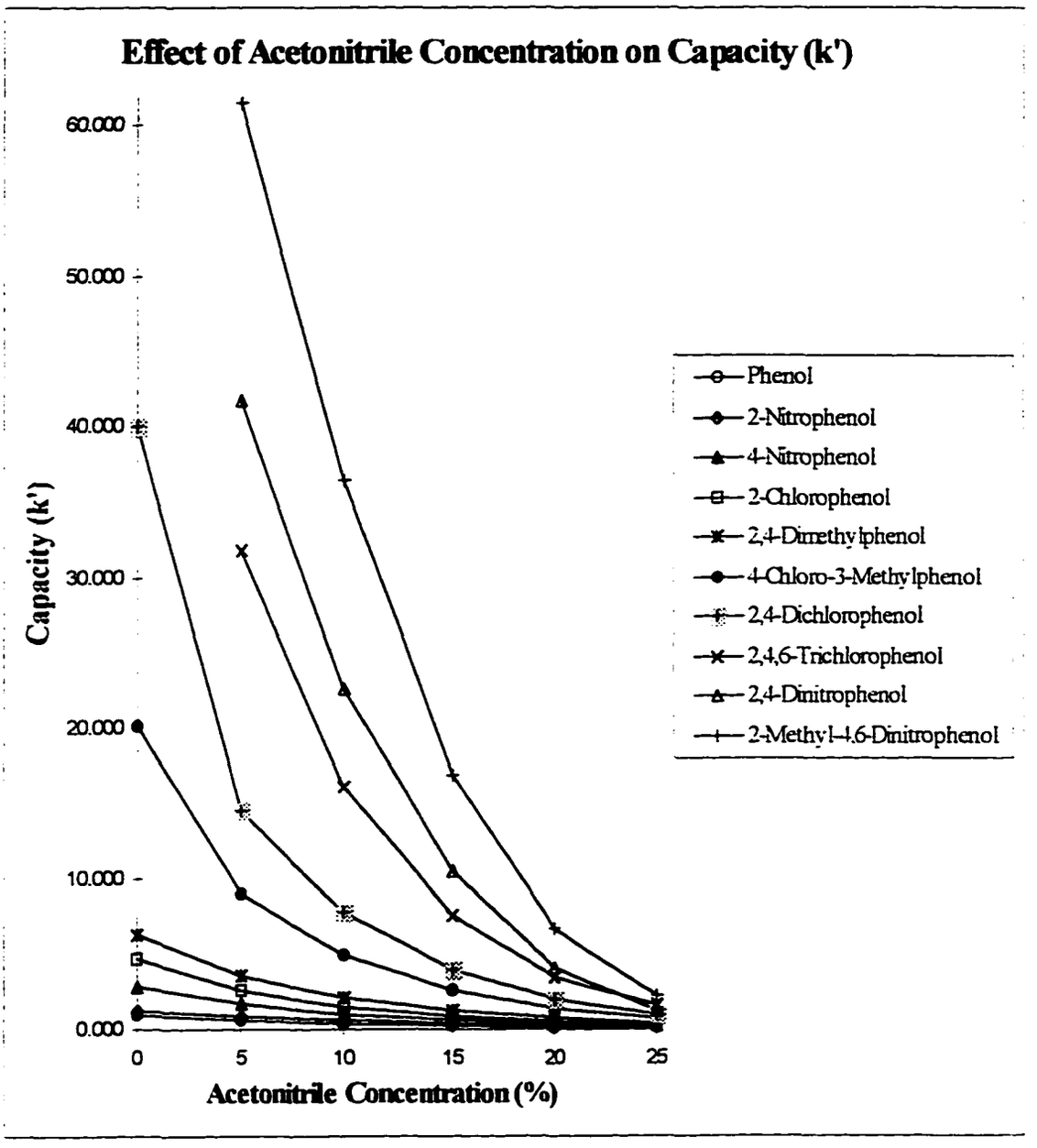

Figure 9

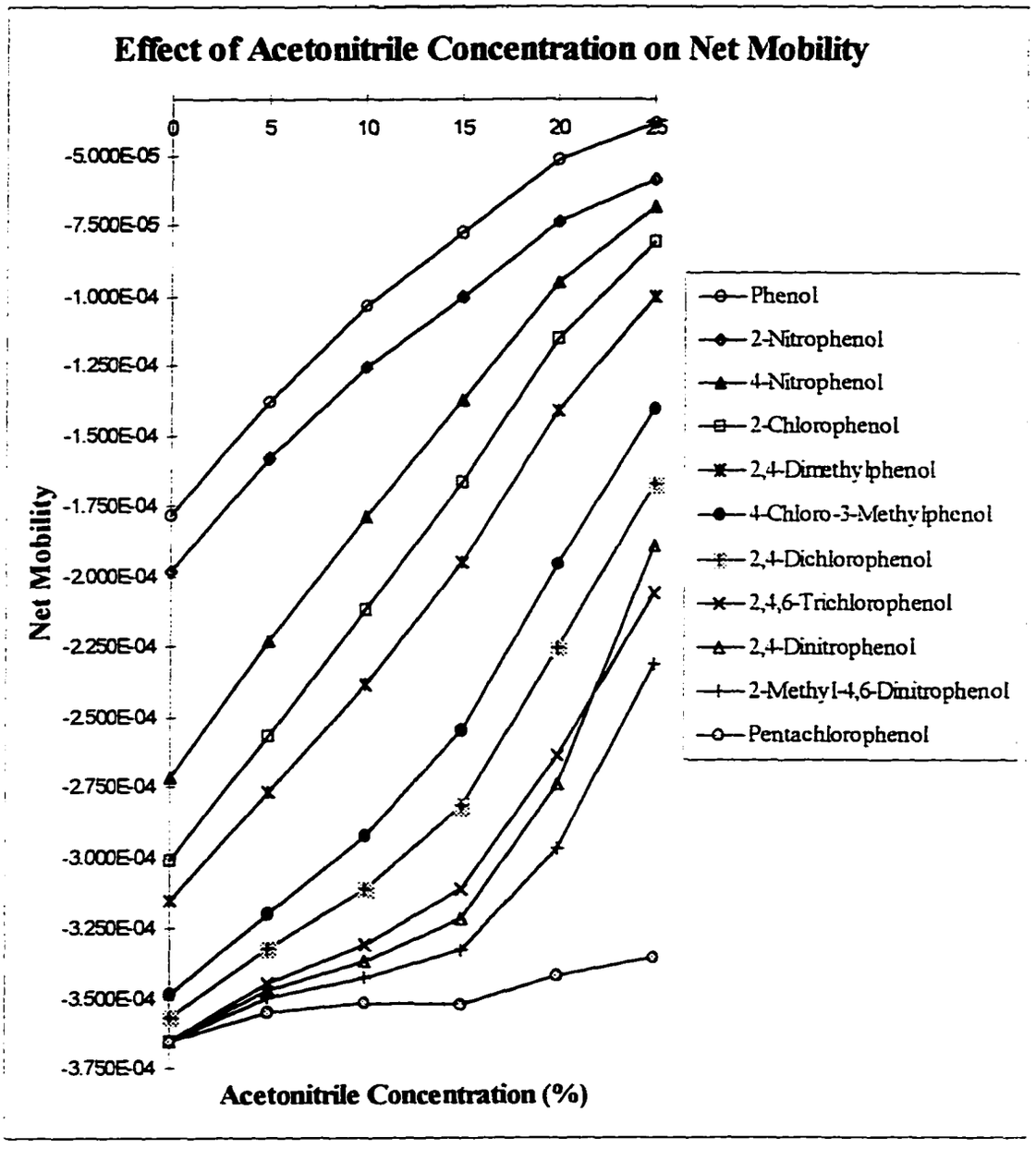

Figure 10

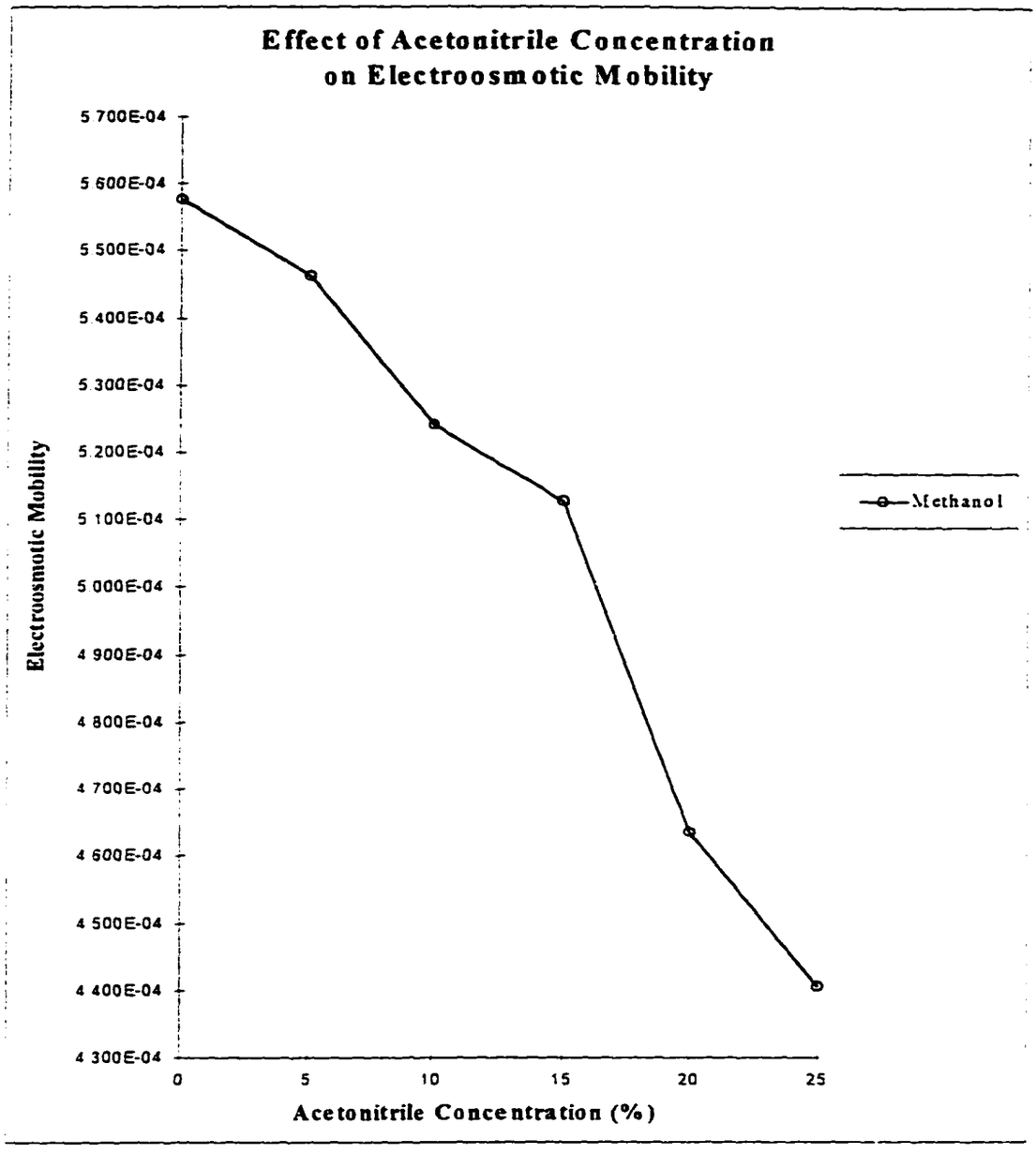

Figure 11

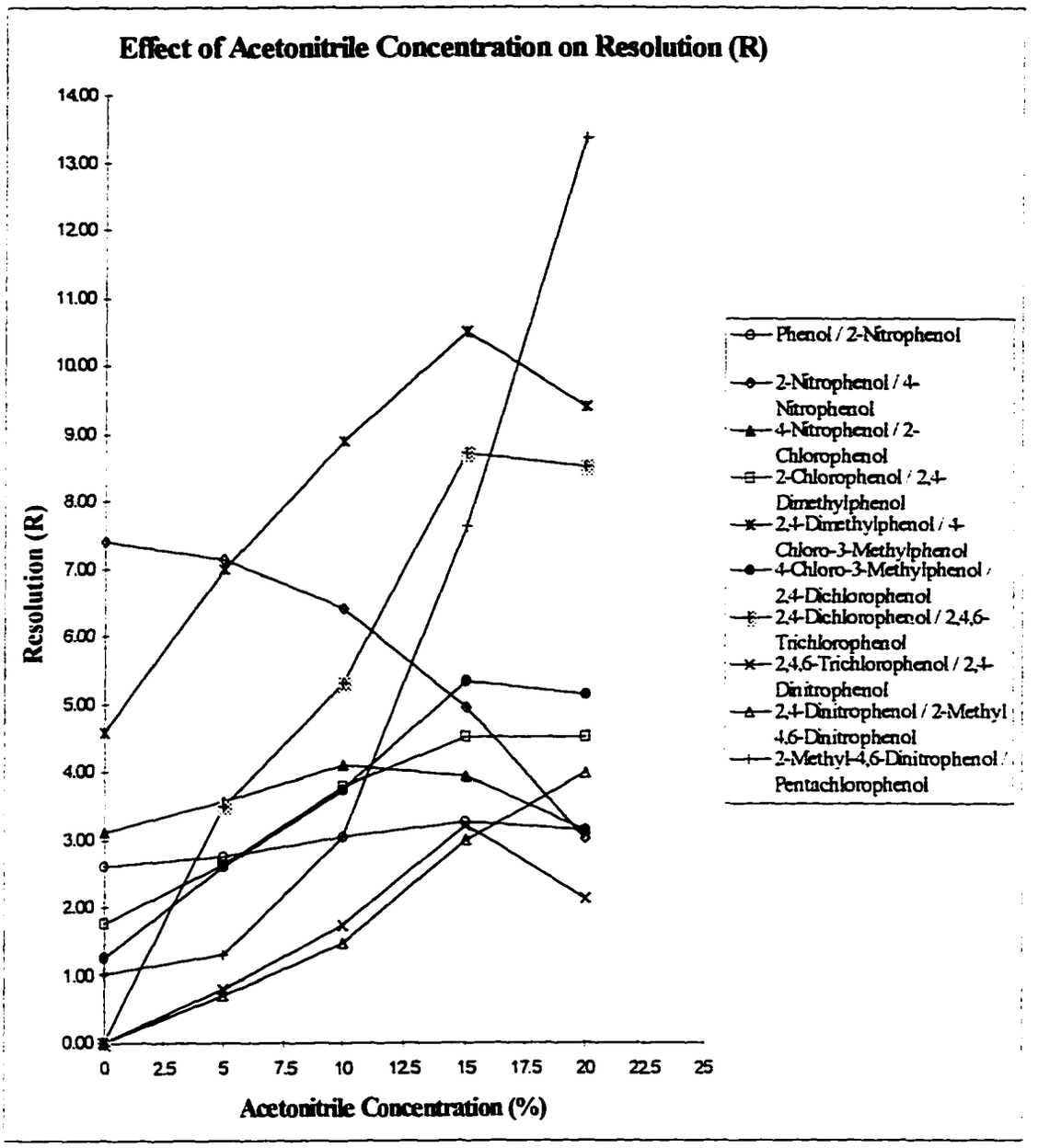

Figure 12

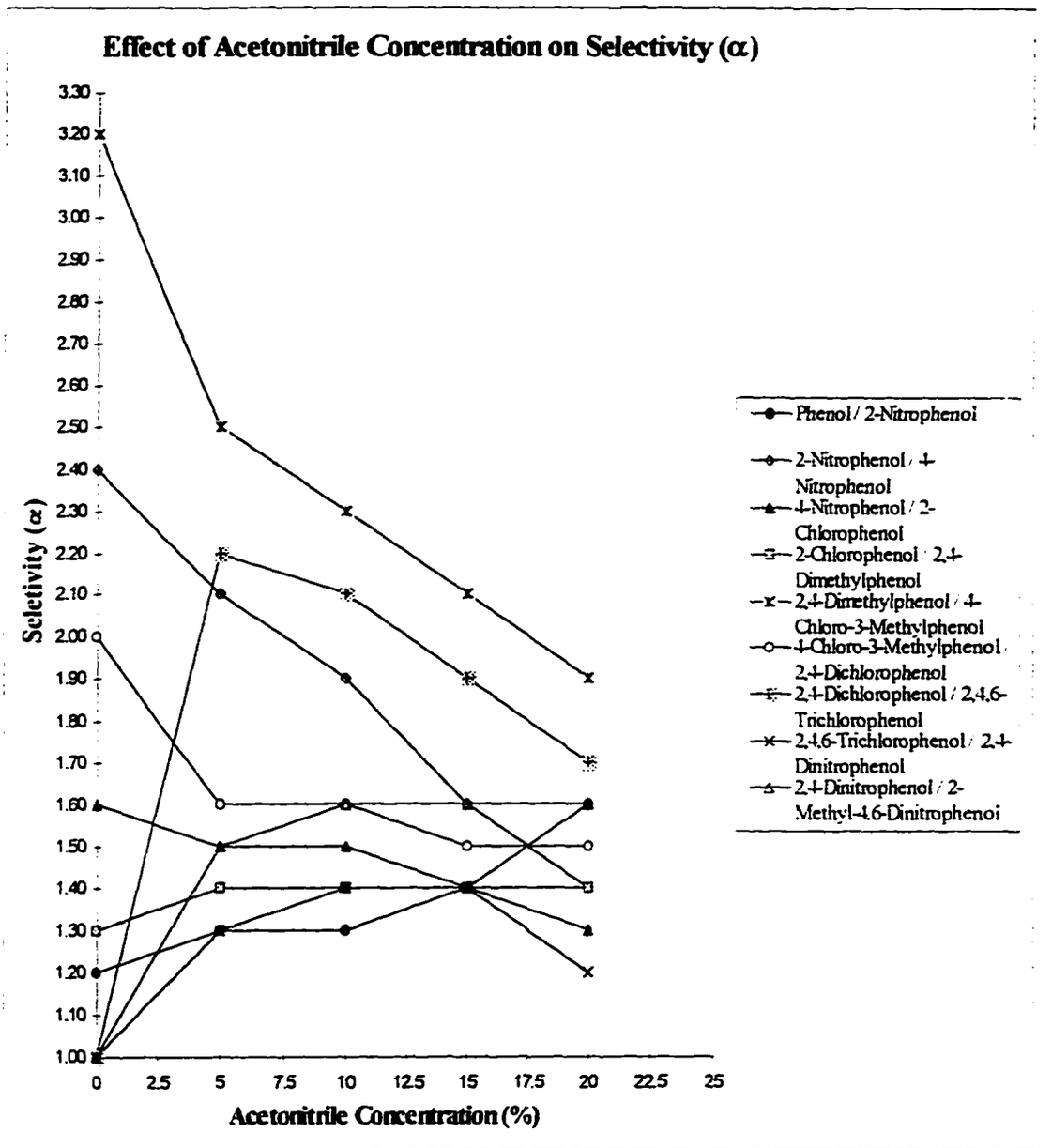

Figure 13

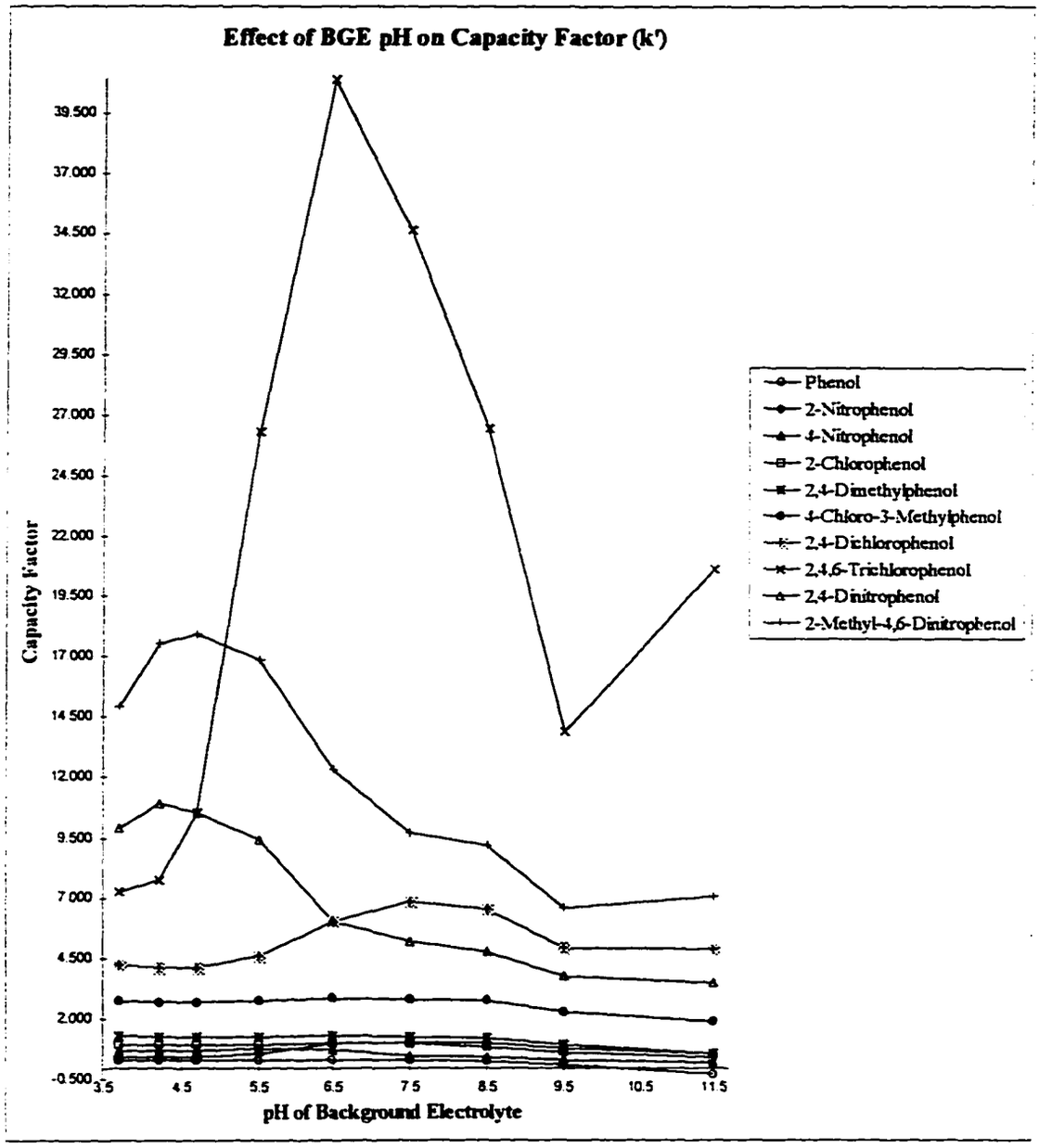

Figure 14

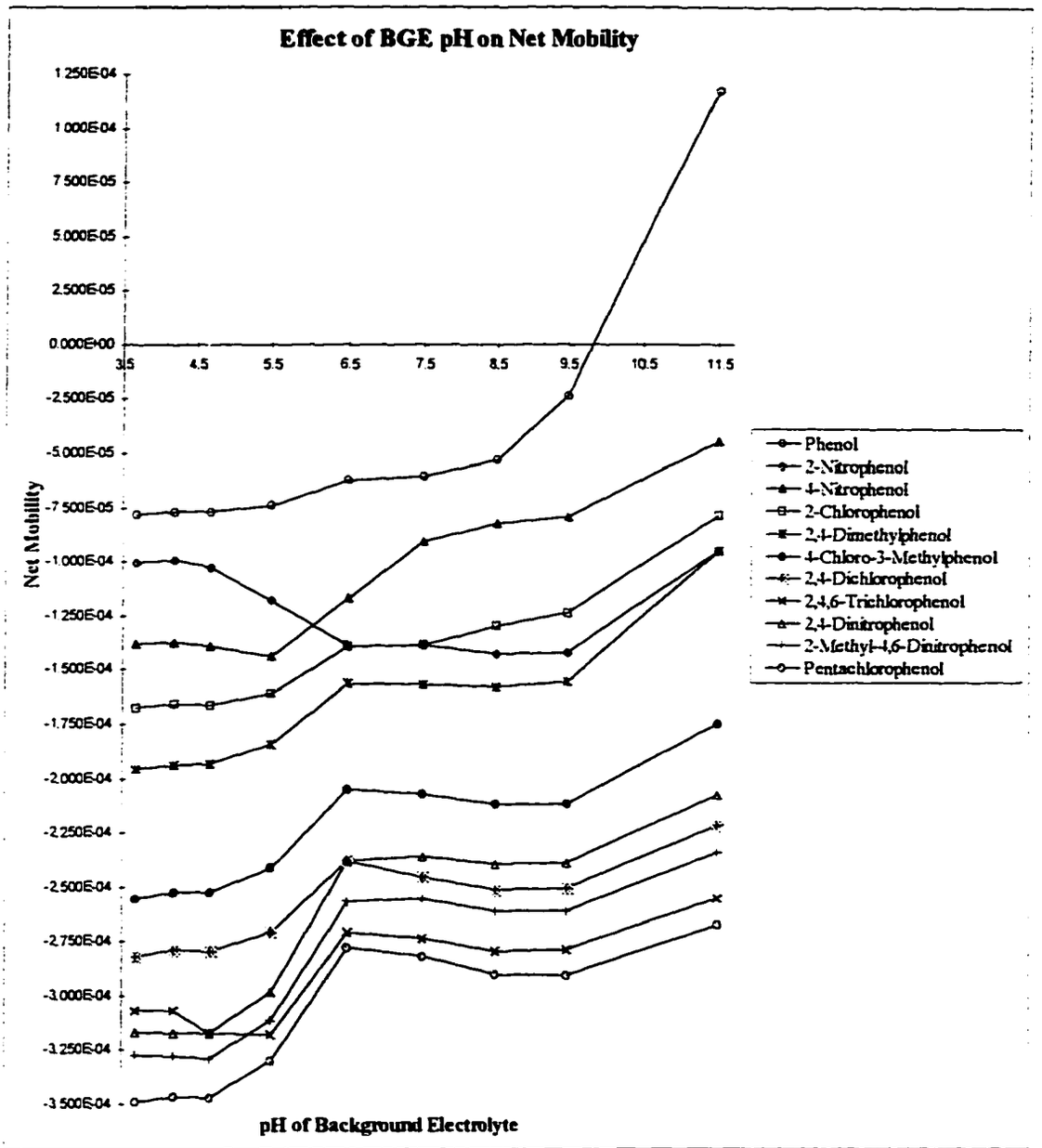

Figure 15

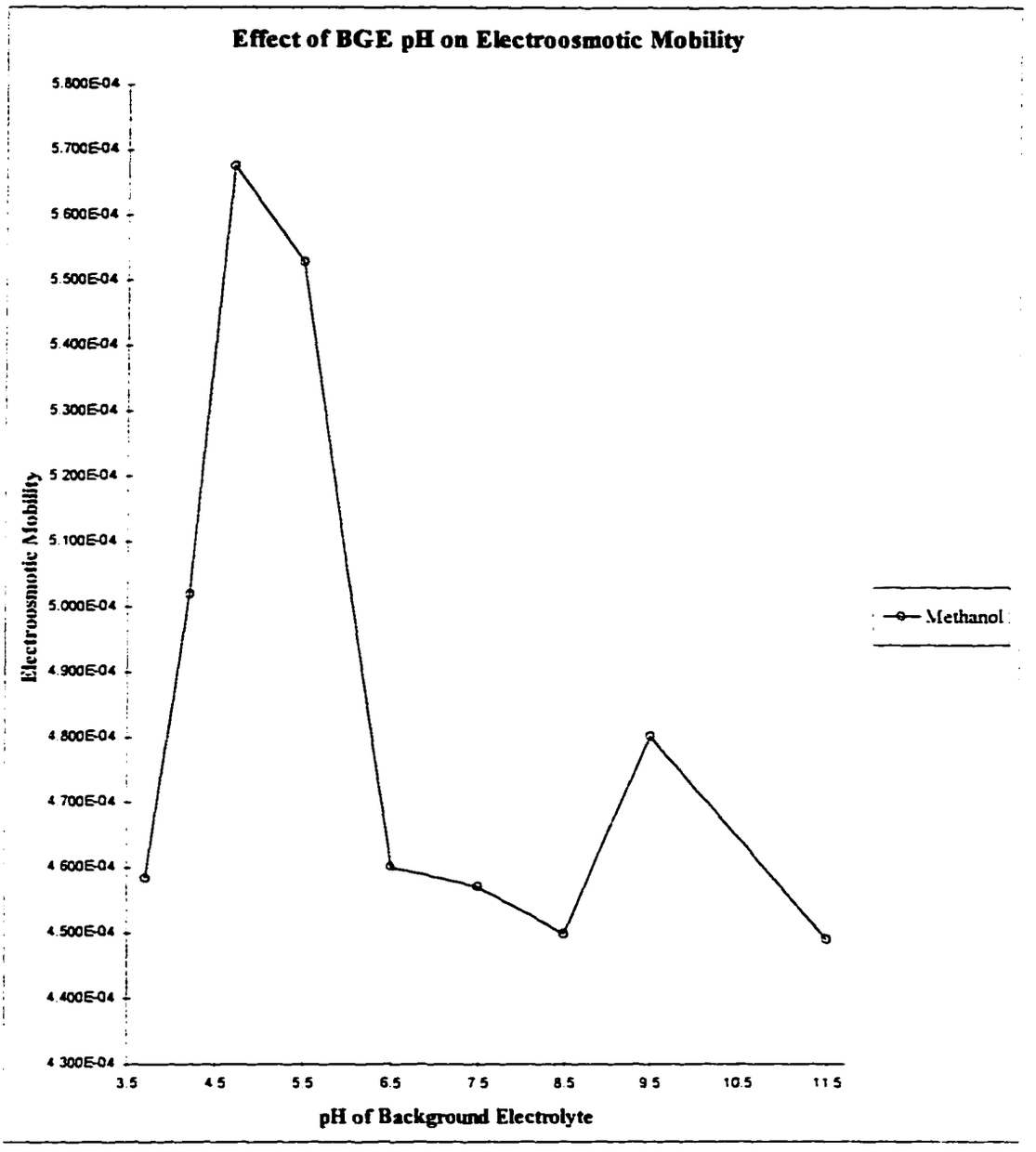

Figure 16

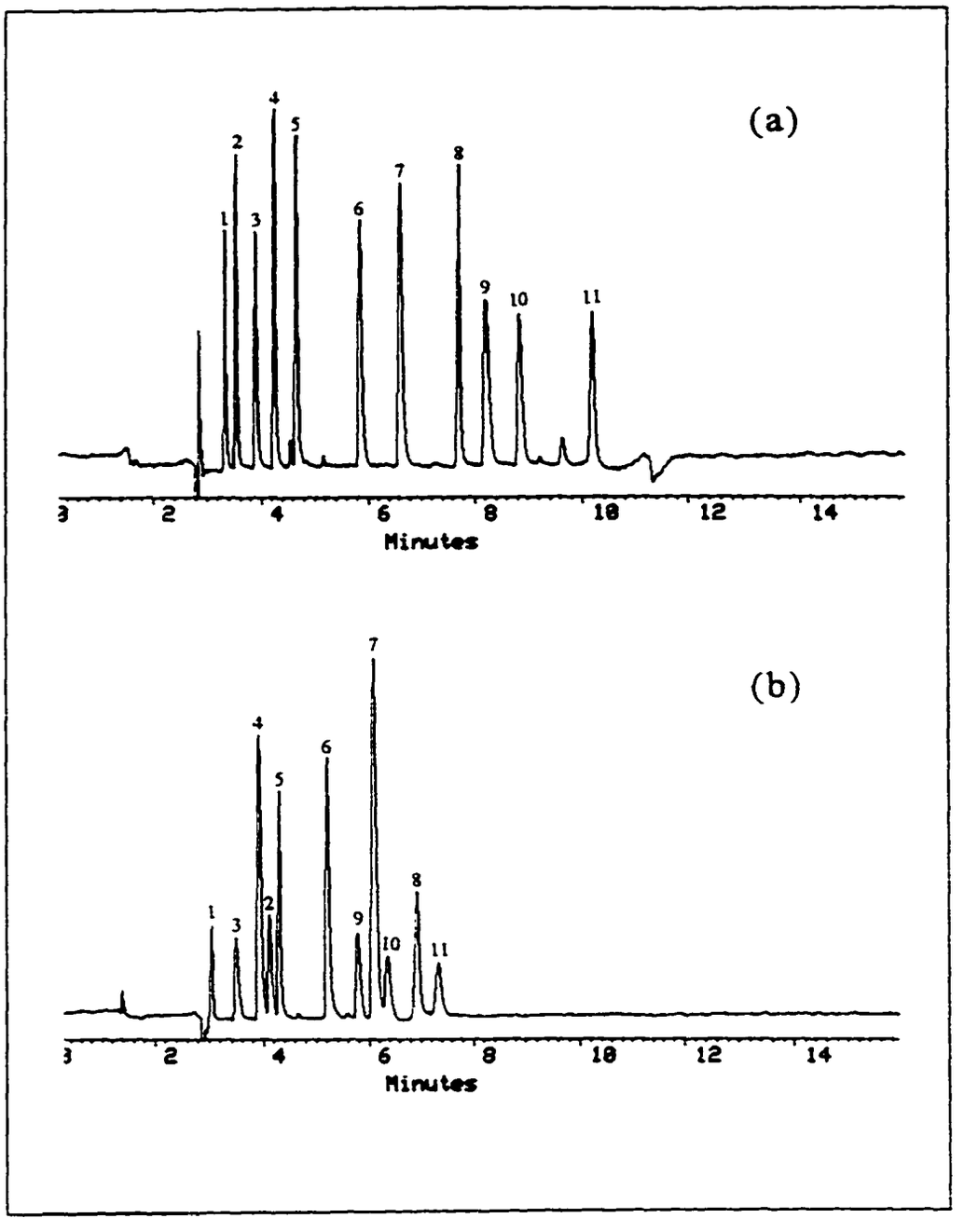

Figure 17

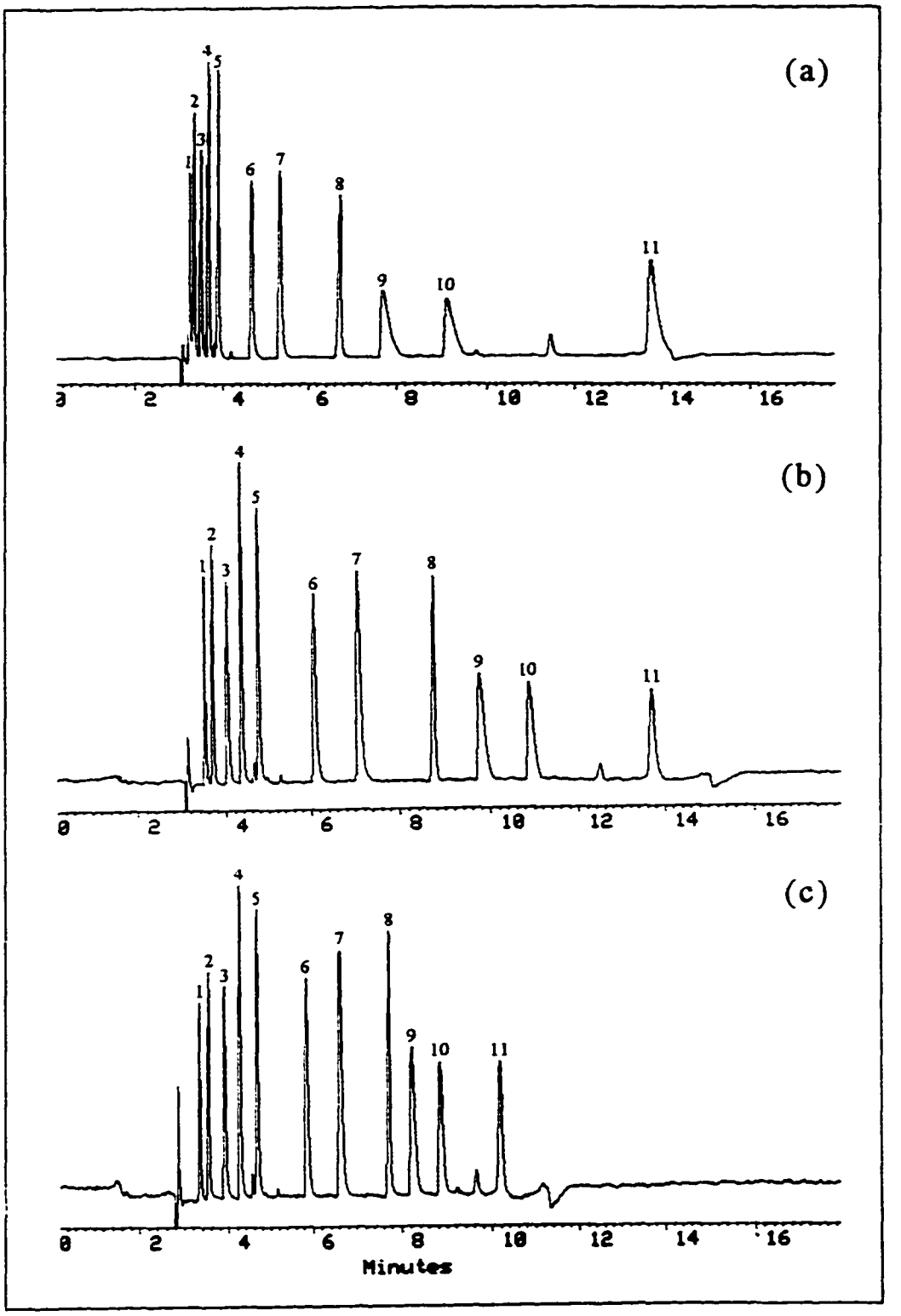

Figure 17 (continued)

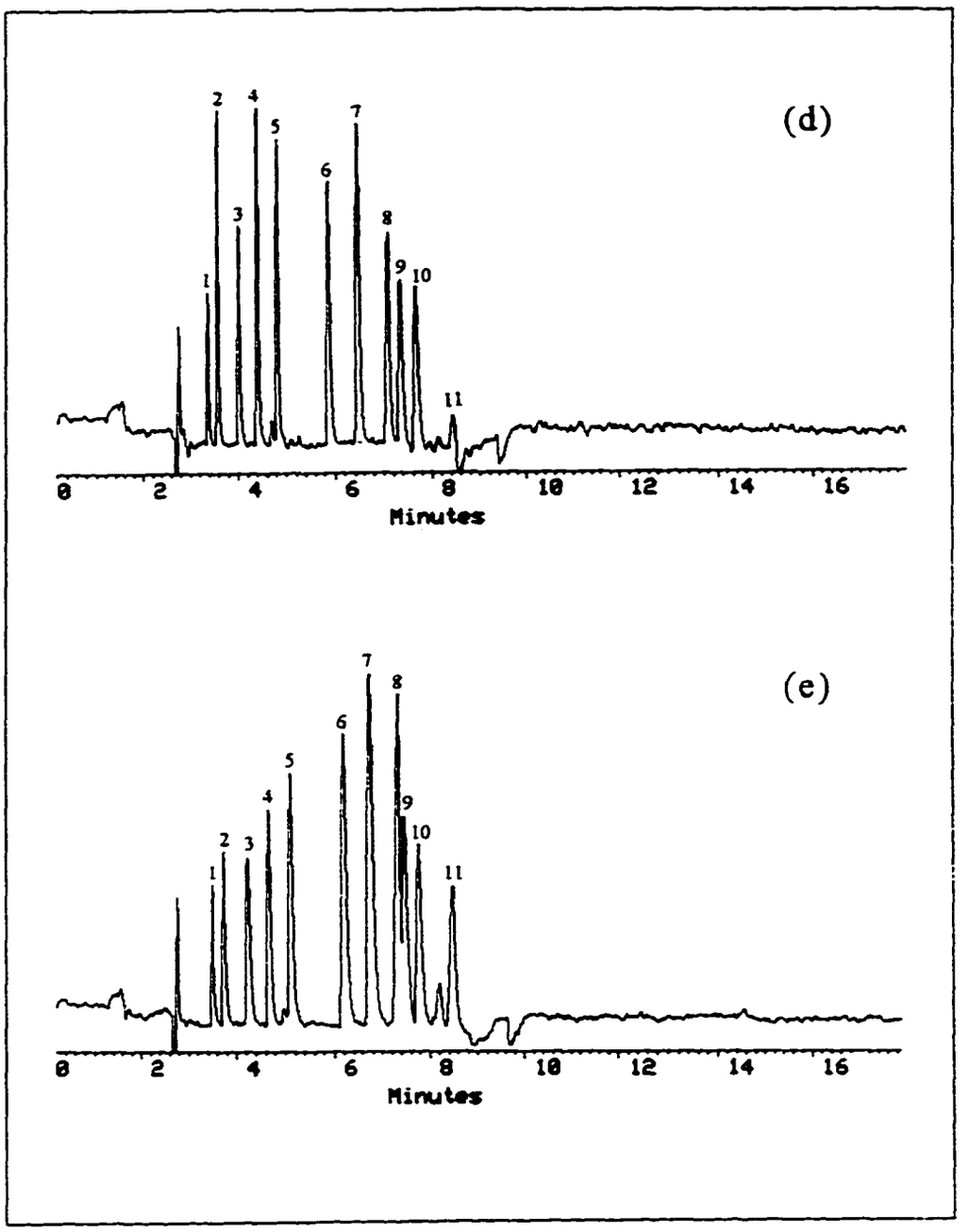

Figure 18

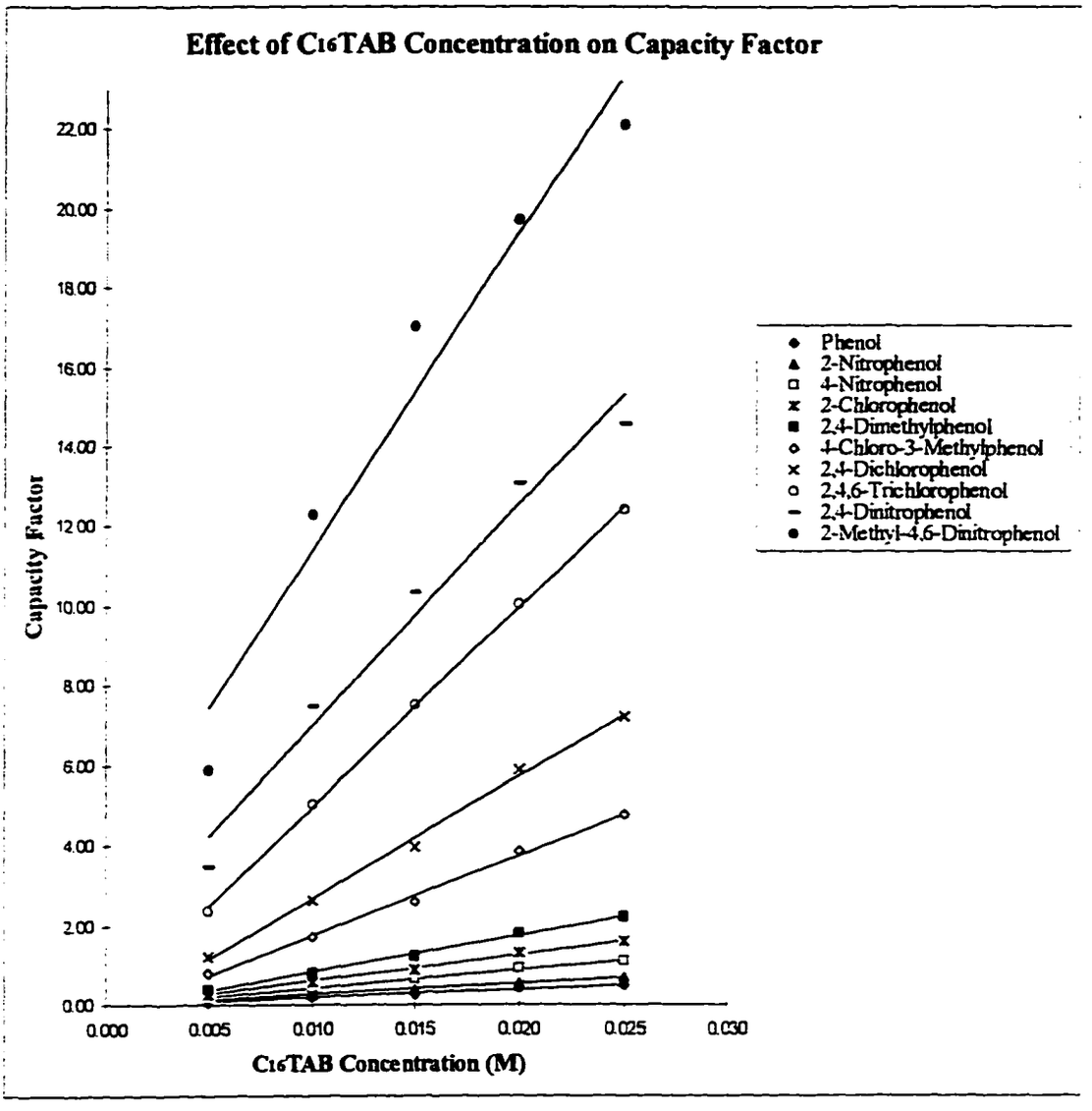

No.	Compounds	*RSQ*	*Slope*	*Intercept*
1	Phenol	0.998	20.91	-0.02
2	2-Nitrophenol	0.999	27.67	-0.01
3	4-Nitrophenol	0.998	46.52	-0.04
4	2-Chlorophenol	0.997	66.63	-0.07
5	2,4-Dimethylphenol	0.998	92.99	-0.11
6	4-Chloro-3-Methylphenol	0.997	200.81	-0.27
7	2,4-Dichlorophenol	0.997	304.79	-0.38
8	2,4,6-Trichlorophenol	1.000	500.11	-0.03
9	2,4-Dinitrophenol	0.974	552.89	1.48
10	2-Methyl-4,6-Dinitrophenol	0.955	795.30	3.45

Figure 19

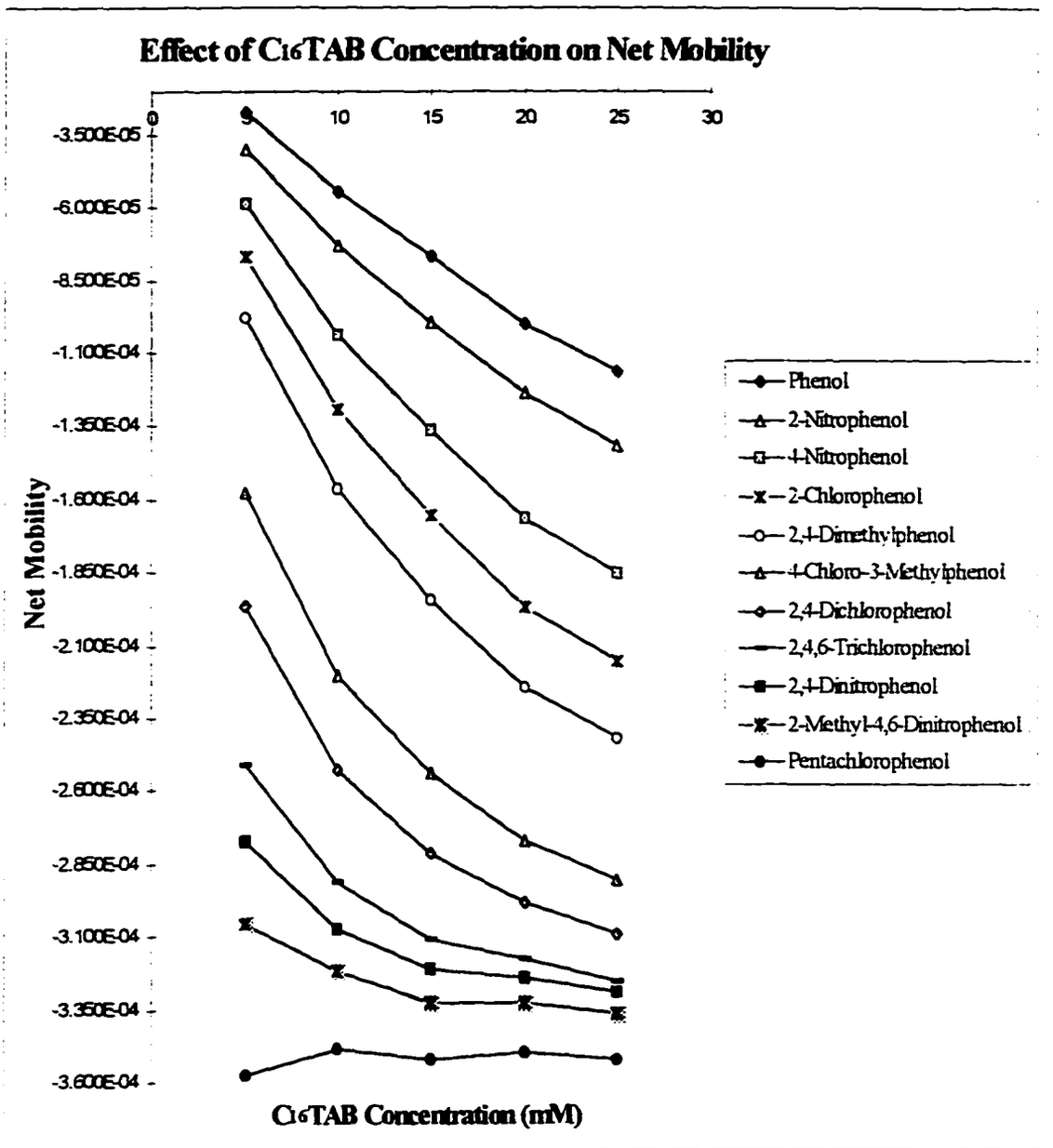

Figure 20

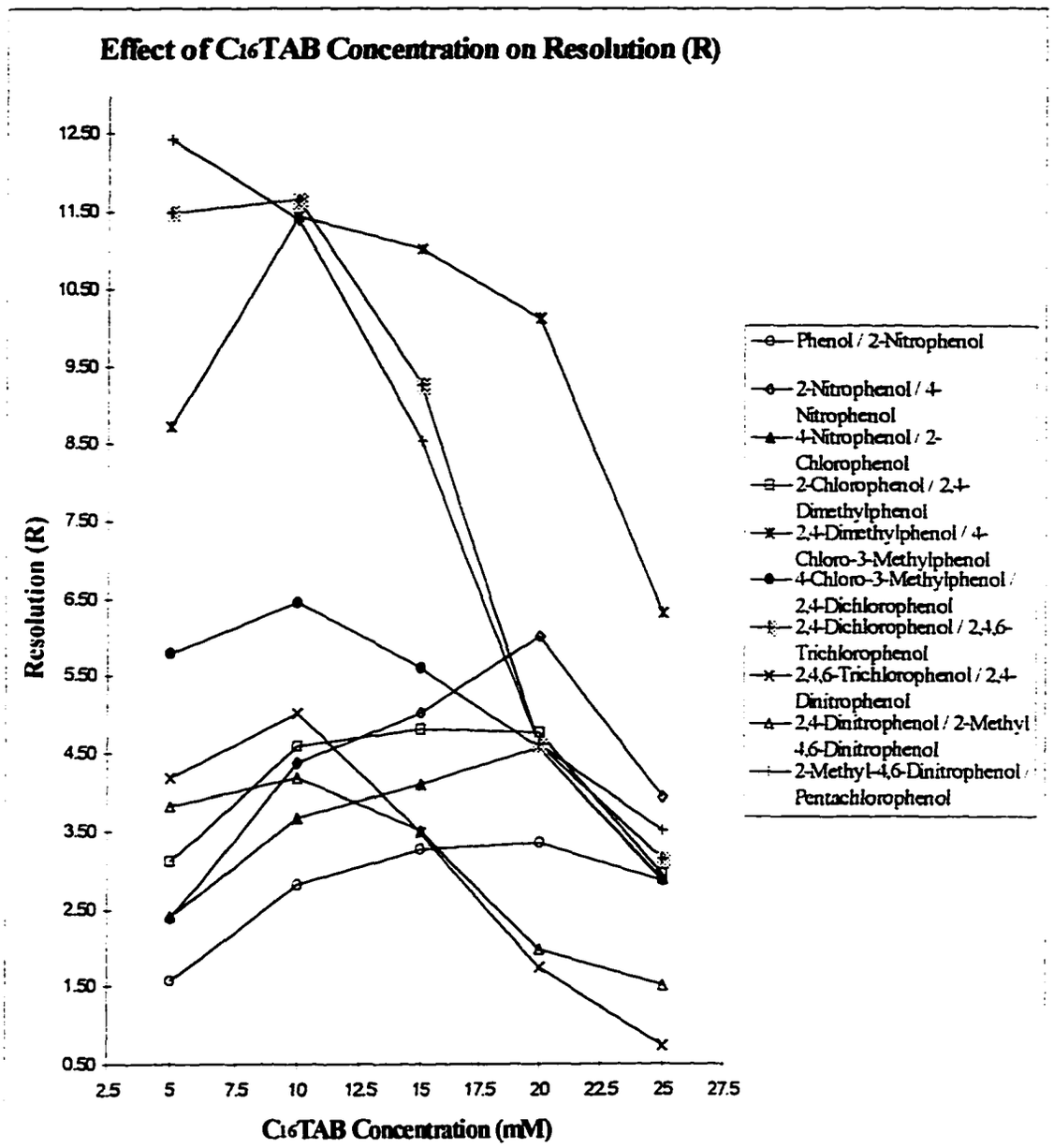

Figure 21

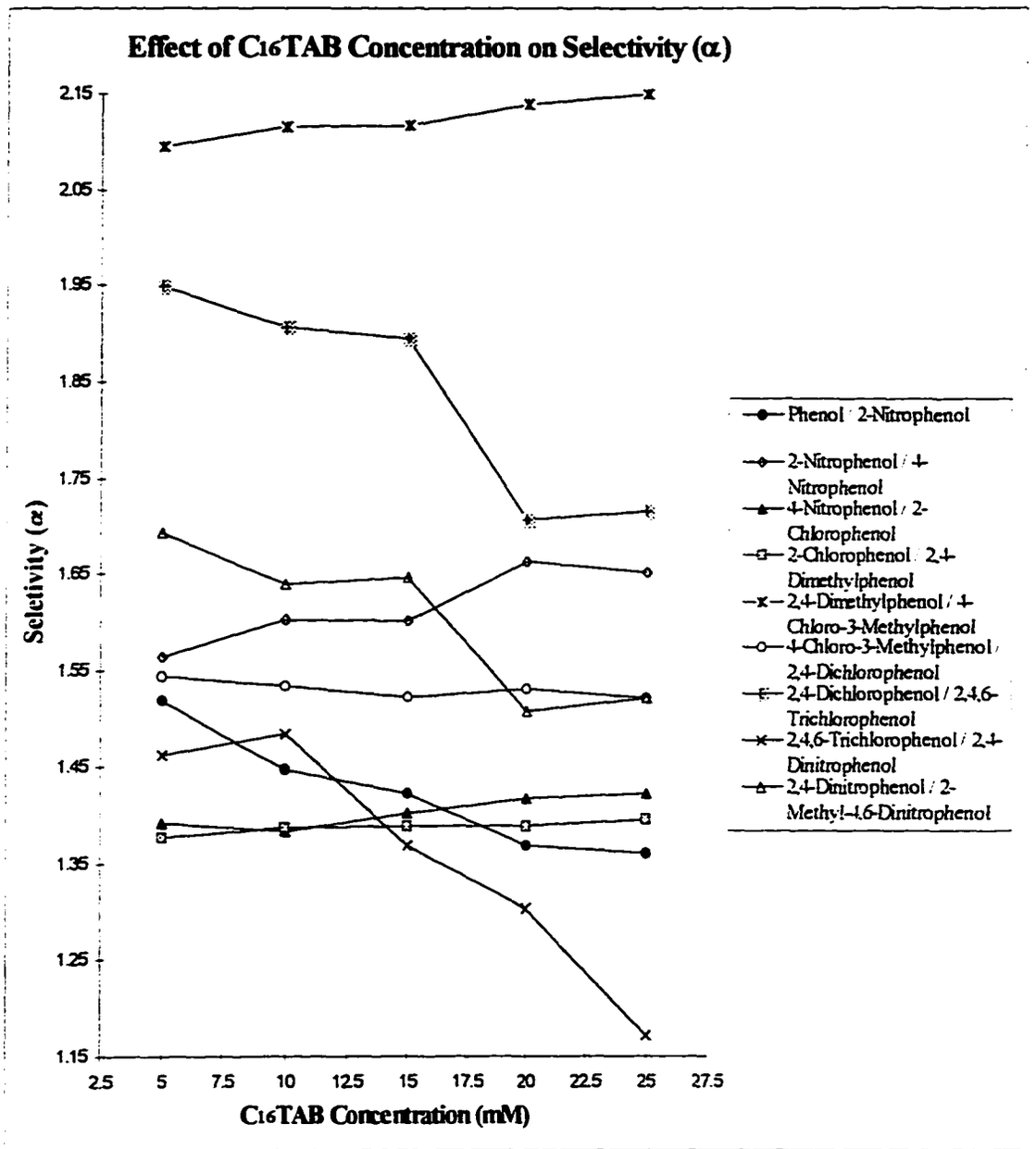

Figure 22

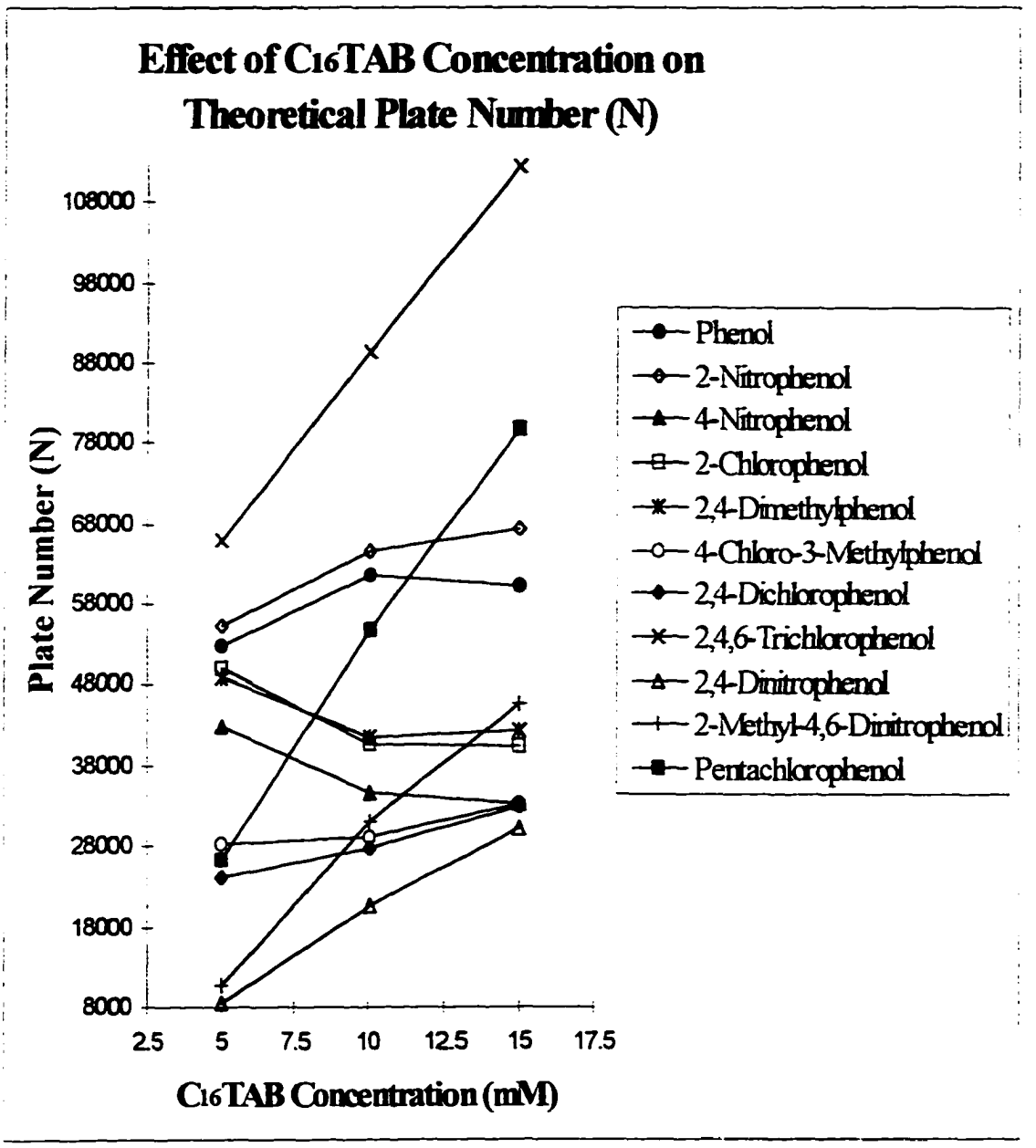

Figure 23

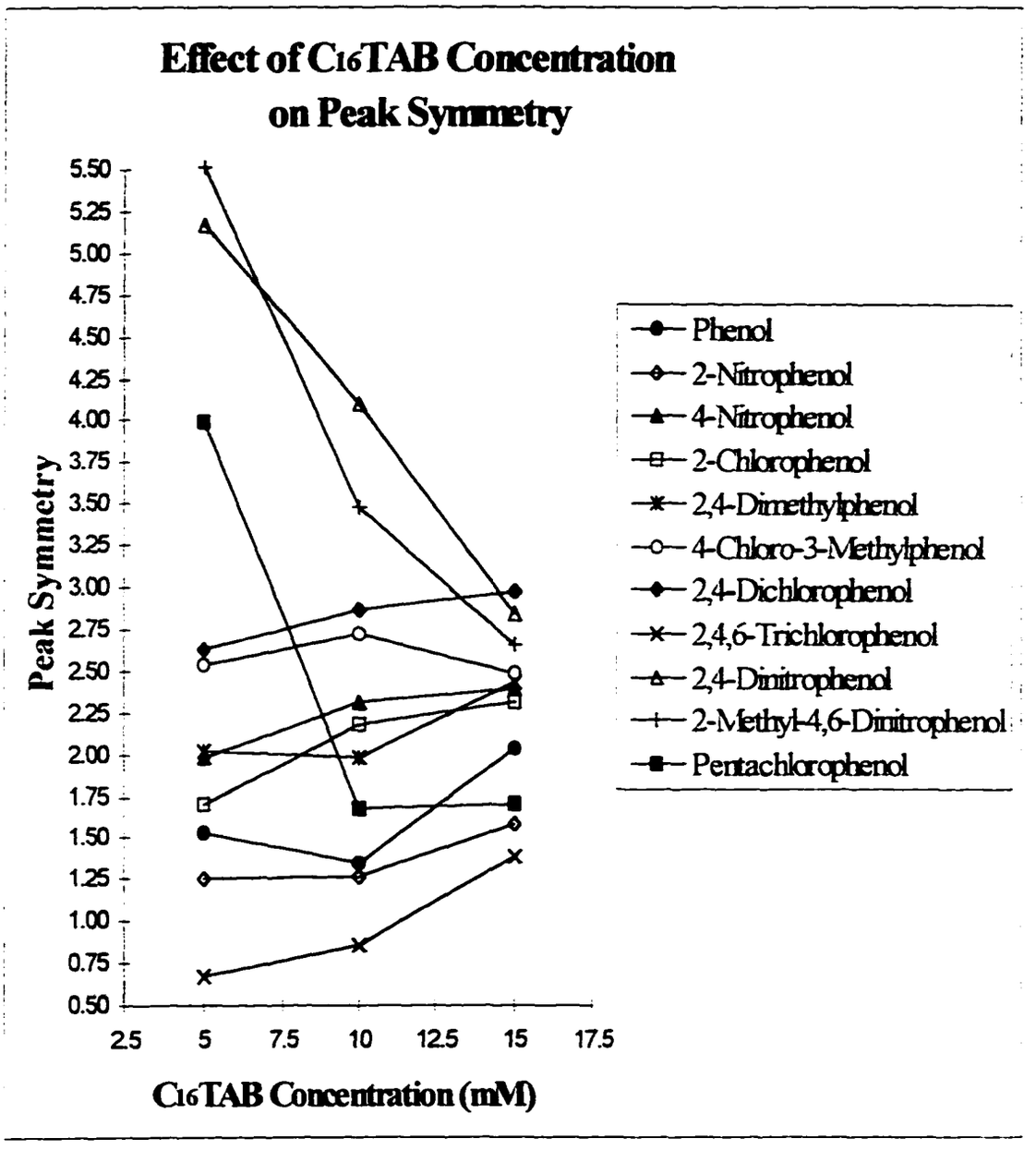

Figure 24

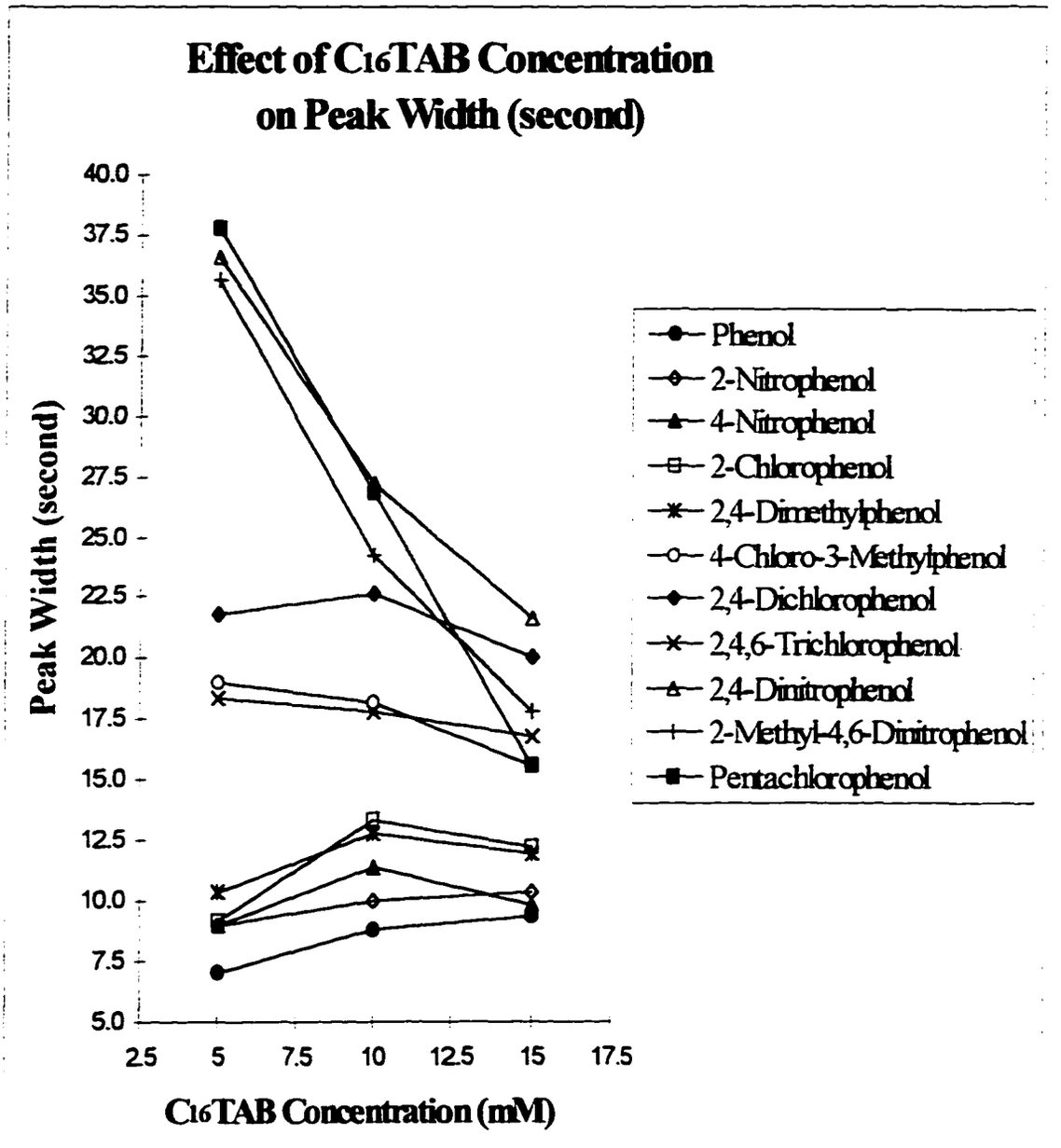

Figure 25

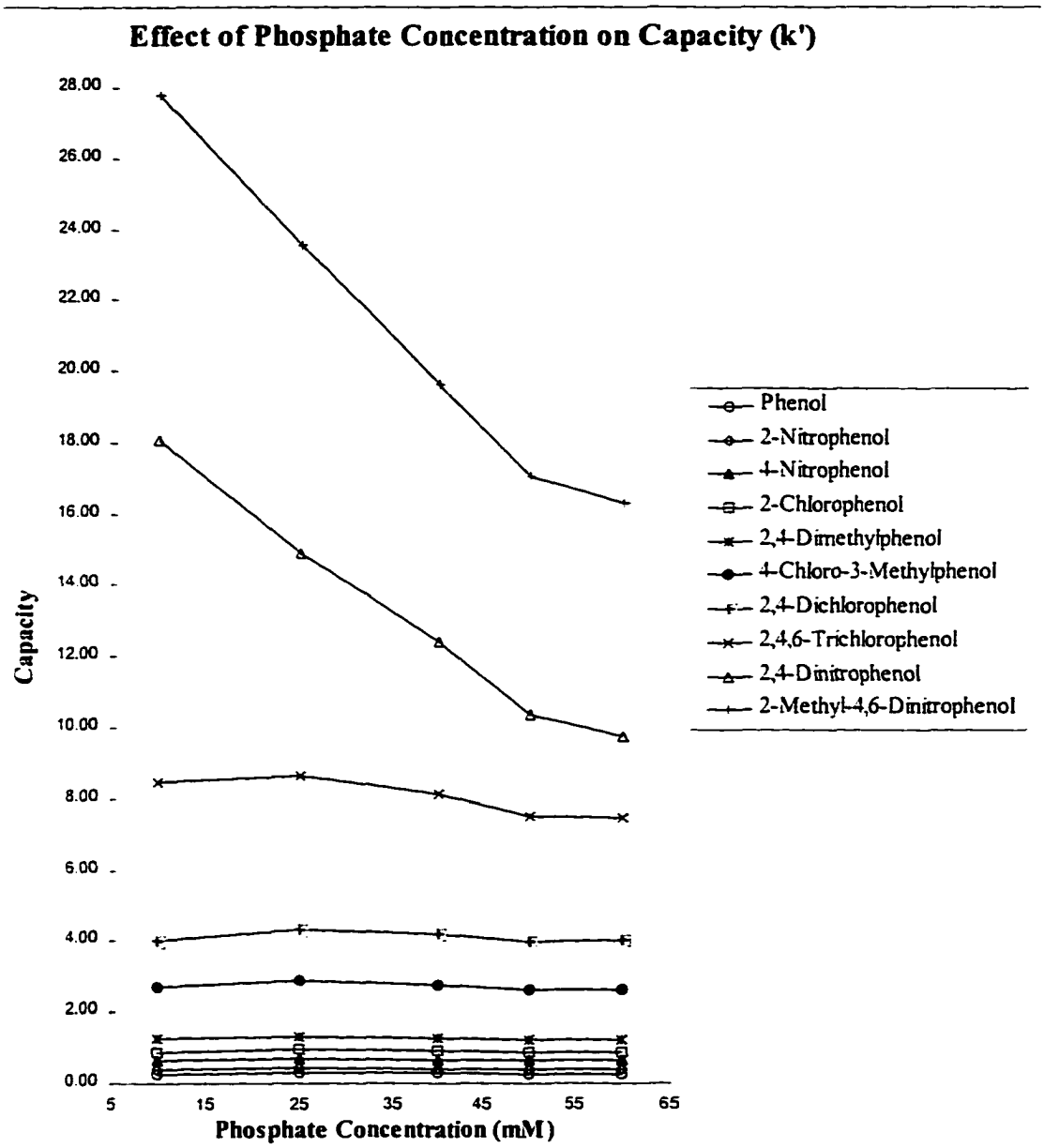

Figure 26

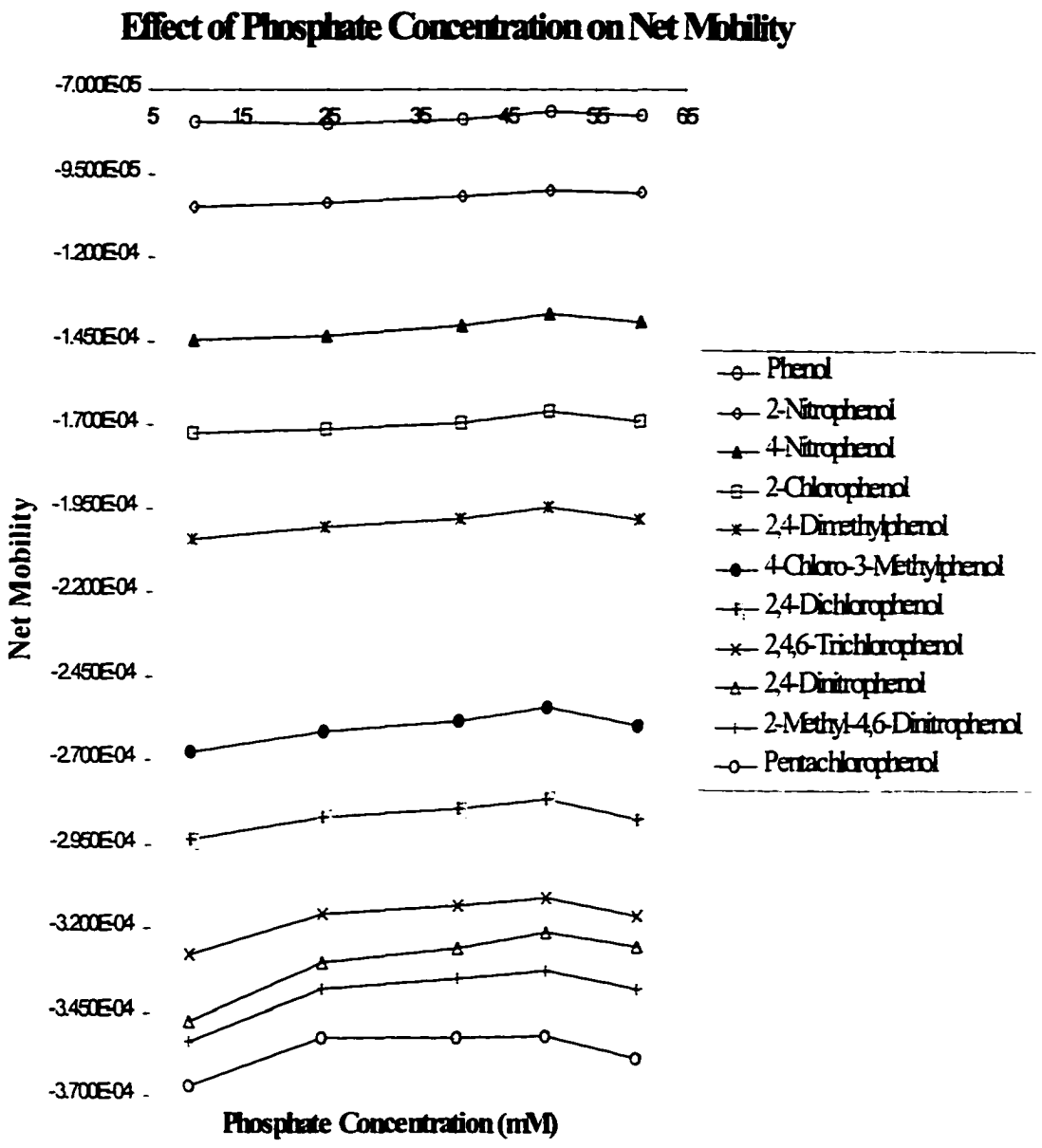

Figure 27

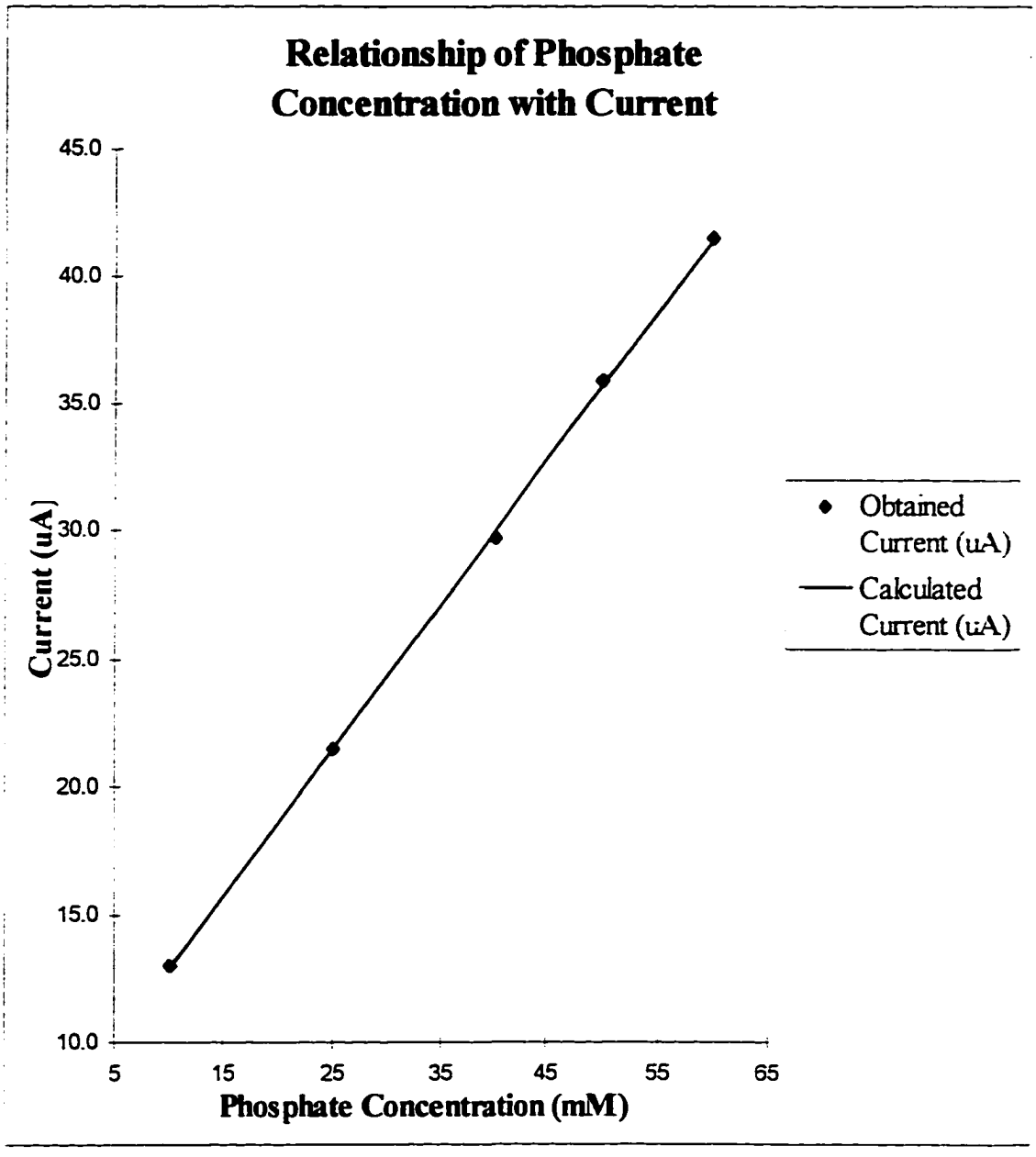

RSQ:	**0.9997**
Slope:	**0.570**
Intercept:	**7.214**

Figure 28

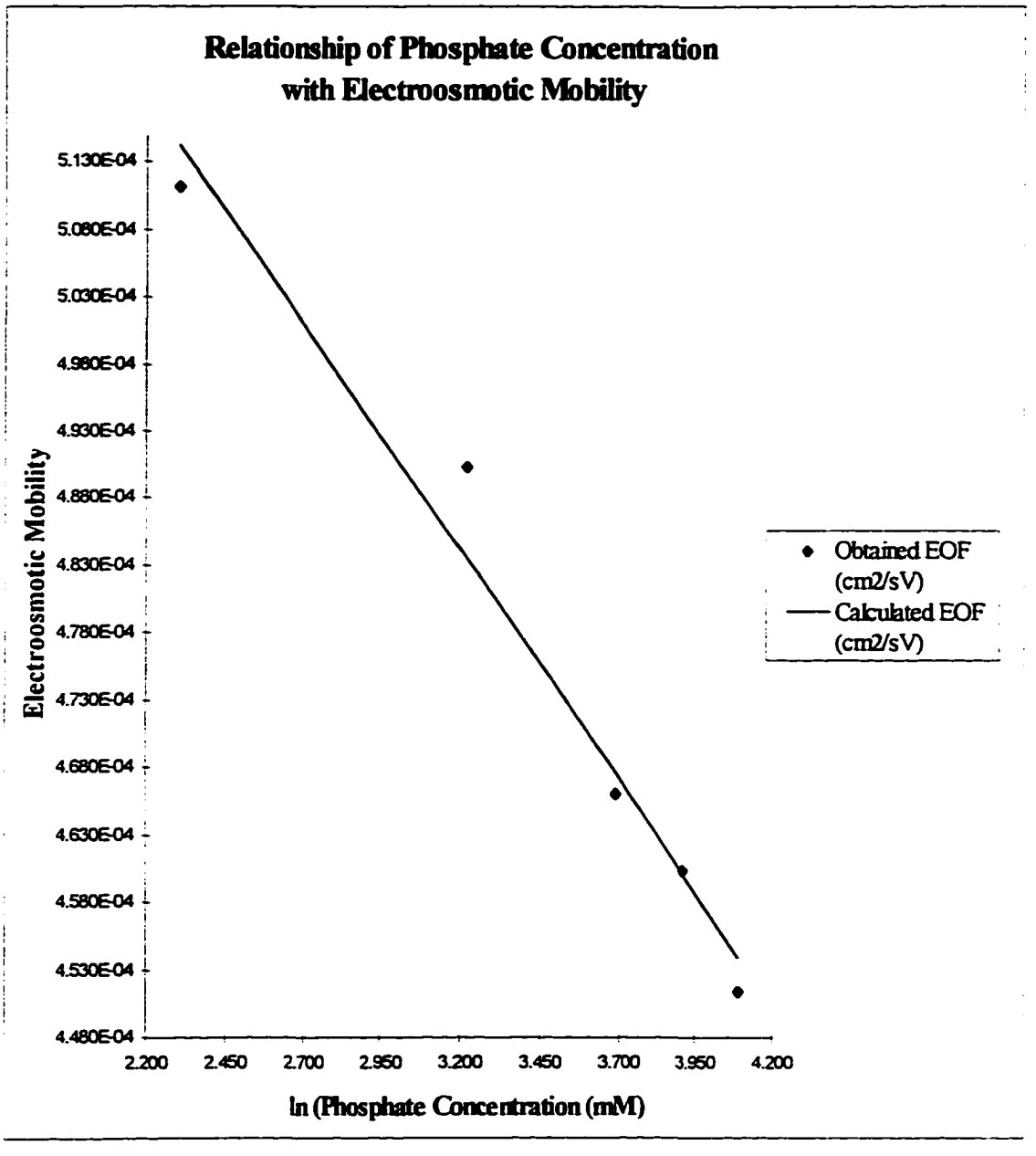

RSQ:	**0.973**
Slope:	**-3.363E-05**
Intercept:	**5.917E-04**

Figure 29

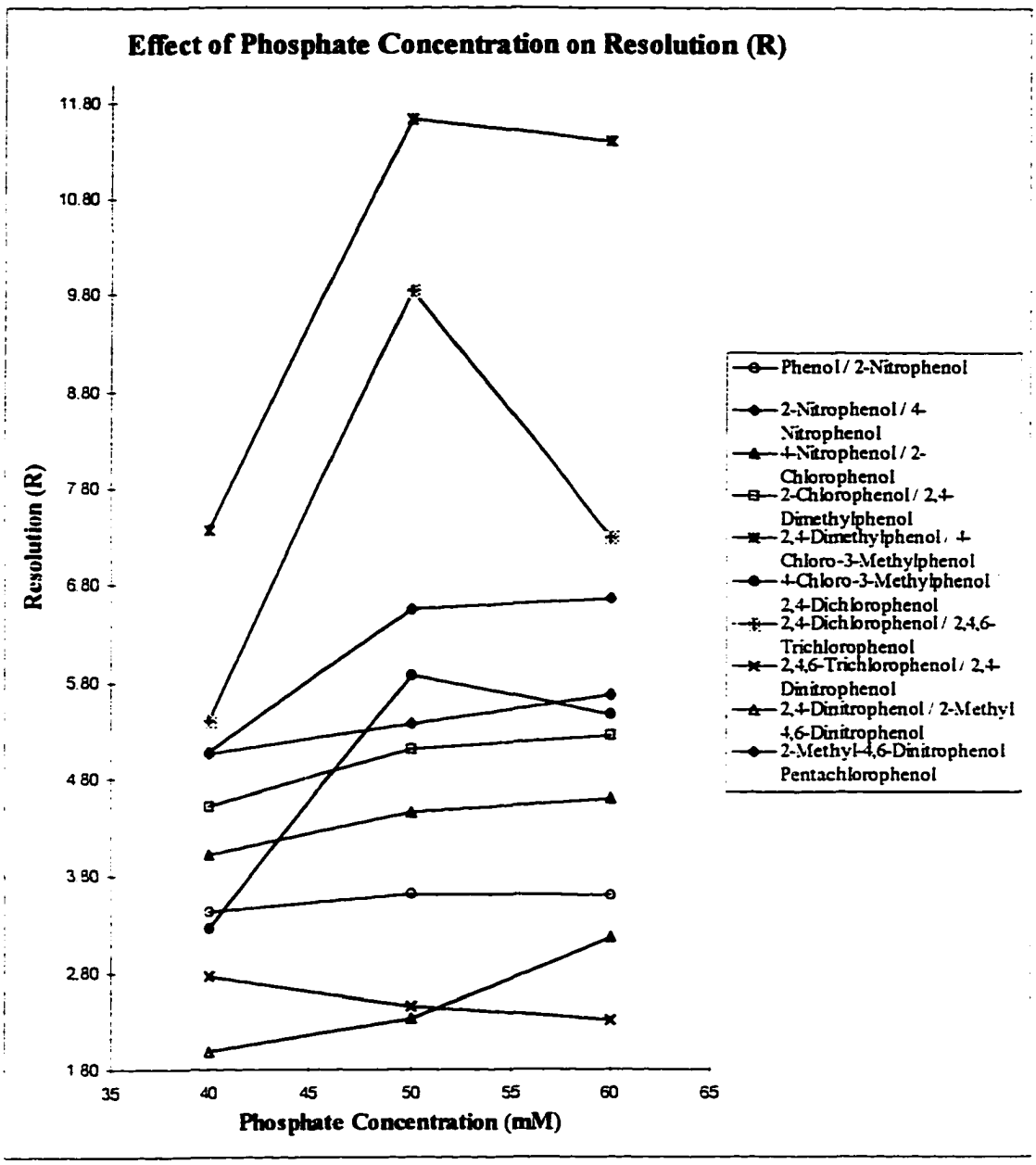

Figure 30

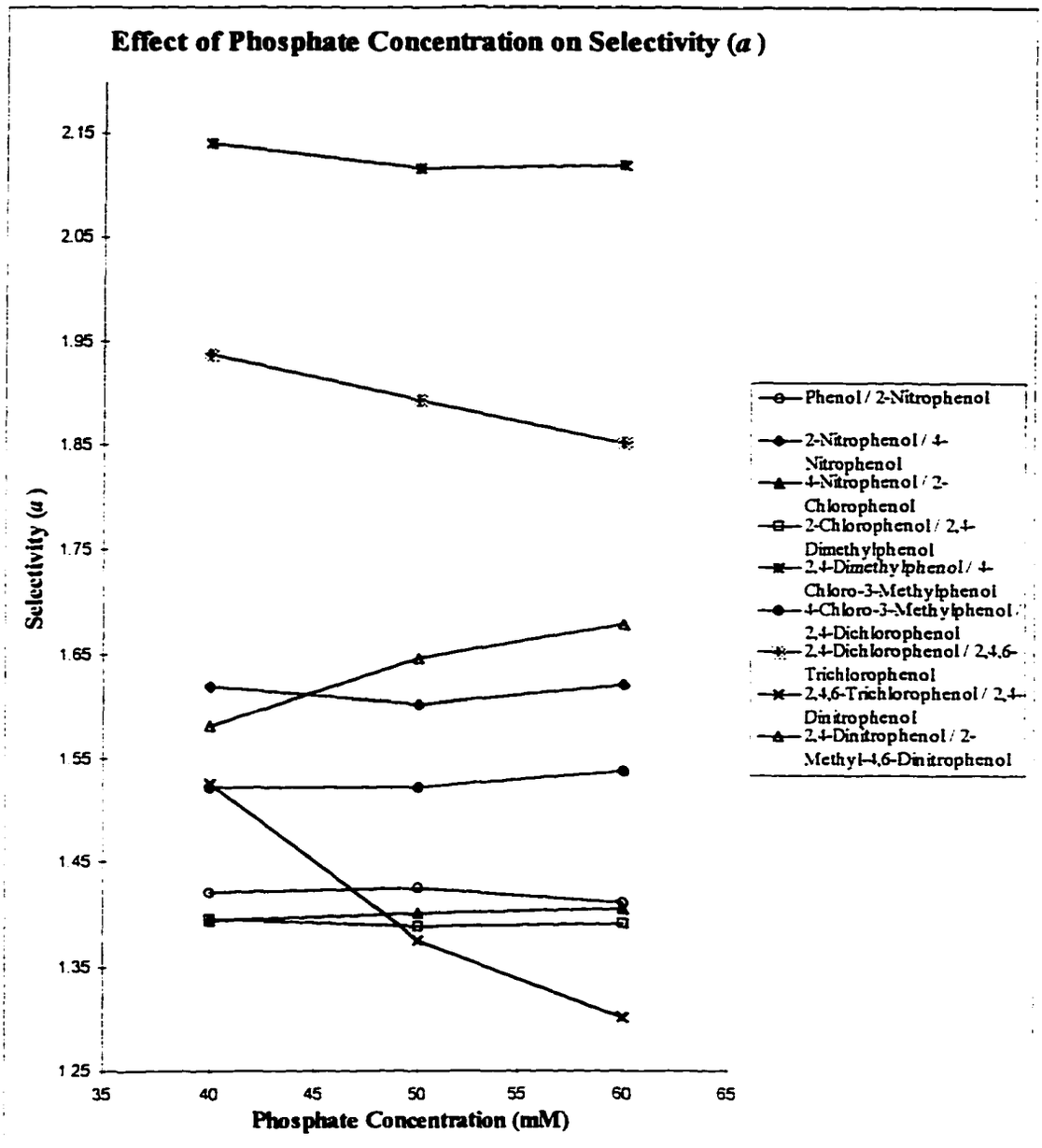

Chapter 3

Migration Behaviour of Charged & Uncharged Solutes in Micellar Electrokinetic Capillary Chromatography with a Cationic Surfactant

Abstract

The interactions between both charged and uncharged solutes and a cationic surfactant were investigated by micellar electrokinetic capillary chromatography (MECC). Cetyltrimethylammonium bromide (C_{16}TAB) was the cationic surfactant used. Increasing the ionic strength of the background electrolyte (BGE) increased the net mobilities of the ionized acidic solutes, but decreased their capacity factors. However, the net mobilities and the capacity factors of cationic, uncharged and slightly ionized acidic solutes were almost unaffected by the BGE ionic strength. In addition, an increase in the C_{16}TAB concentration in the BGE resulted in decrease in the net mobilities and increase in the capacity factors for all the solutes. But these changes were considerably larger for ionized acidic solutes than for cationic, uncharged and slightly ionized acidic solutes. A fundamental theoretical and applied study of net mobility, capacity factor and distribution coefficient as a function of ionic strength in the BGEs was carried out.

1. Introduction

Ionic solutes can interact hydrophobically with micelles that are neutral, or are either positively or negatively charged; but they can interact by attractive ionic forces only with micelles of the opposite charge. Investigation of the interaction between the ionic solute and a charged surfactant is best guided by a theory of the migration behaviour of ionic solutes in MECC. Ghowsi et al. (1) reported a theoretical study for the neutral solutes in MECC based on the electrochemical parameters. Terabe et al. (2, 3) investigated the migration behaviour of the ionic solutes in an anionic micellar solution, but only the capacity factors for the ionic solutes were reported. Kaneta and Taga (4) studied the migration behaviour of the inorganic anions in MECC using a cationic surfactant, but only a relationship between the capacity factor and the effective electrophoretic mobility was given for surfactant concentrations above the critical micellar concentration (CMC). Khaledi et al. (5, 6) reported phenomenological modes to describe the migration behaviour of the ionic solutes in MECC with both anionic and cationic micelles; however, only the pH and the surfactant concentration in the BGE were taken into consideration.

In this chapter, we present the relationships between the net mobility, the capacity factor, and the distribution coefficient and the ionic strength of the BGE. For both "totally" ionized acidic and neutral solutes, fundamental equations were derived

for the net mobility and the capacity factor as a simple, direct function of the ionic strength and the micelle concentration in the BGE. These equations agree qualitatively with the experimental results. An increase in the BGE ionic strength significantly increases the net mobilities, and dramatically decreases the capacity factors for the ionized acidic solutes; but the net mobilities and the capacity factors of the cationic, uncharged, and slightly ionized acidic solutes are little influenced. In addition, the distribution coefficient was studied as a function of the BGE ionic strength. The results reveal that the distribution coefficient decreased considerably for the ionized acidic solute, but was almost unaffected for the cationic, uncharged and slightly ionized acidic solutes with increasing the BGE ionic strength. For MECC using a cationic surfactant, the suitable pH range is 3 to 4.5 (7), therefore the surfactant concentration and the ionic strength of the BGE are two important experimental factors in the optimization strategy in order to achieve an adequate separation of complex mixtures.

2. Theoretical

2.1 Net Mobility as a Function of Ionic Strength and Micelle Concentration

The net mobility of an ionizable solute (μ_{net}) in MECC can be expressed as the weighted sum of the mobilities of various species of that solute:

$$\mu_{net} = (F_{S^-,MC} + F_{HS,MC} + F_{S^--mono,MC})\,\mu_{MC} + F_{S^-,AQ}\,\mu_{S^-,AQ} + F_{HS,AQ}\,\mu_{HS,AQ} + F_{S^--mono,AQ}\,\mu_{S^--mono,AQ} \quad (1)$$

where μ_{MC} is the mobility of the micellar phase; $\mu_{S^-,AQ}$ and $\mu_{HS,AQ}$ are the mobilities of the solute in the aqueous phase in the free acidic and neutral forms, respectively. $\mu_{S^--mono,AQ}$ is the mobility of an ion-pair of the acidic solute associated with the surfactant monomer. Since $\mu_{S^--mono,AQ}$ and $\mu_{HS,AQ}$ refer to neutral species with no electrophoretic mobility, they are equal to zero. The F values represent the mole fractions of solute in the micellar and aqueous phases in the free acidic or neutral forms, and the mole fractions of the acidic solute - C_{16}TAB monomer ion-pair in the micellar and aqueous phases. In this study, the total concentration of C_{16}TAB employed in the BGE was 15 mM while the C_{16}TAB monomer concentration in the BGE was approximately 1 mM (the same as the CMC). Therefore, the micelle concentration is much higher than the monomer concentration. As a result, the ion-pair formation of the acidic solute with the C_{16}TAB monomer is neglected. Then the net mobility of a solute (μ_{net}) can be written as:

$$\mu_{net} = (F_{S^-,MC} + F_{HS,MC})\,\mu_{MC} + F_{S^-,AQ}\,\mu_{S^-,AQ} \quad (2)$$

For a sake of simplicity, two cases are only considered: (i) the acidic solute is "totally" ionized and (ii) the solute is neutral.

2.1.1 Net mobility for totally ionized acidic solute

For the "totally" ionized acidic solute, the equation (2) can be simplified as:

$$\mu_{net} = F_{S^-,MC}\,\mu_{MC} + F_{S^-,AQ}\,\mu_{S^-,AQ} \quad (3)$$

in which $F_{S^-,MC}$ is given by

$$F_{S^-,AQ} = [S^-]_{AQ}/([S^-M^-]_{MC}+[S^-]_{AQ}) = 1/\{1+([S^-M^-]_{MC}/[S^-]_{AQ})\} \quad (4)$$

where $[S^-M^-]_{MC}$ and $[S^-]_{AQ}$ are the concentrations of an ionic solute in the micellar phase and the aqueous phase, respectively.

Since $$[S^-]_{AQ} + [M^-] \Leftrightarrow [S^-M^-]_{MC} \quad (5)$$

and $$[S^-M^-]_{MC} + [E^-]_{AQ} \Leftrightarrow [S^-]_{AQ} + [E^-M^-]_{MC} \quad (6)$$

in which $[M^-]$ is the micelle concentration, and $[E^-]_{AQ}$ and $[E^-M^-]_{MC}$ are the concentrations of anions (competing ions) in the aqueous phase and the micellar phase, respectively. By replacing $[S^-M^-]_{MC}/[S^-]_{AQ}$ with $[E^-M^-]_{MC}/K_{IE}[E^-]_{AQ}$, $F_{S^-,AQ}$ becomes:

$$F_{S^-,AQ} = 1 / \{1 + ([E^-M^-]_{MC} / K_{IE}[E^-]_{AQ})\} \quad (7)$$

where K_{IE} is an ion exchange constant between the anionic solute and the anions in the BGE with the head of $C_{16}TAB$ micelle. $F_{S^-,MC}$ can be derived similarly. Substituting these equations into equation (3), we have:

$$\mu_{net}=\{([E^-M^-]_{MC}/K_{IE}[E^-]_{AQ})\mu_{MC}+\mu_{S^-,AQ}\}/\{1+([E^-M^-]_{MC}/K_{IE}[E^-]_{AQ})\} \quad (8)$$

Since $[E^-]_{AQ}$ is greater than $[E^-M^-]_{MC}$ ($[E^-M^-]_{MC}$ is limited by the micelle concentration), and/or if the ion exchange constant is high, then $\{1+([E^-M^-]_{MC} / K_{IE}[E^-]_{AQ})\} \rightarrow 1$, so that

$$\mu_{net} = ([E^-M^-]_{MC} / K_{IE}\,[E^-]_{AQ})\,\mu_{MC} + \mu_{S^-,AQ} \quad (9)$$

Since μ_{MC} is has a minus sign and $\mu_{S^-,AQ}$ has a plus sign, as the anion concentration ($[E^-]_{AQ}$) in the BGE is increased, and/or the ion exchange constant is very high, the first term in the equation (9) predominates, thus the solute net mobility μ_{net} will increase. In an extreme condition, i.e. using a very high concentration buffer, the first term in the equation (9) can be omitted so that the net mobility is the same as the electrophoretic mobility of the ionic solute itself.

For equation (4), replacing $[S^-M^+]_{MC}/[S^-]_{AQ}$ with $[M^-]K_{S^-,MA}$, $F_{S^-,AQ}$ can be written:

$$F_{S^-,AQ} = 1 / (1 + [M^-] K_{S^-,MA}) \qquad (10)$$

where $K_{S^-,MA}$ is the binding constant of the ionic solute with the micelle phase. Similarly, $F_{S^-,MC}$ can be derived. Substituting these equations into equation (3), we have:

$$\mu_{net}=\{([M^-]K_{S^-,MA}/(1+[M^-]K_{S^-,MA})\}\mu_{MC}+\{1/(1+[M^-]K_{S^-,MA})\}\mu_{S^-,AQ} \qquad (11)$$

Again μ_{MC} has a minus sign and $\mu_{S^-,AQ}$ has a plus sign, therefore if the micelle concentration ($[M^-]$) in the BGE is increased, and/or the binding constant is high, the second term in equation (11) will be decreased, thus reducing the solute net mobility. In an extreme condition, i.e. a very high micelle concentration, and/or a very high binding constant, $\{1/(1+[M^-]K_{S^-,MA})\}\rightarrow 0$, and $\{([M^-]K_{S^-,MA}/(1+[M^-]K_{S^-,MA})\}\rightarrow 1$, so that the net mobility of an ionic solute is the same as the electrophoretic mobility of the

micelle, because the solute is associated exclusively in the micelle phase.

2.1.2 Net mobility for neutral solute

For a neutral solute, equation (1) can be simplified to:

$$\mu_{net} = F_{HS,MC}\, \mu_{MC} \qquad (12)$$

where $F_{HS,MC}$ is given by

$$F_{HS,MC} = [HSM^-]_{MC} / ([HSM^-]_{MC} + [HS]_{AQ})$$
$$= ([HSM^-]_{MC}/[HS]_{AQ}) / (1 + [HSM^-]_{MC}/[HS]_{AQ}) \qquad (13)$$

in which $[HSM^-]_{MC}$ and $[HS]_{AQ}$ represent the concentrations of a neutral solute in the micellar phase and the aqueous phase. By replacing $[HSM^-]_{MC}/[HS]_{AQ}$ with $K_{HS,MA}[M^-]$, $F_{HS,MC}$ can be written as:

$$F_{HS,MC} = K_{HS,MA}\,[M^-] / (1 + K_{HS,MA}\,[M^-]) \qquad (14)$$

where $K_{HS,MA}$ is a binding constant of the neutral solute with the micelle. Substituting equation (14) into equation (12), we have:

$$\mu_{net} = \{K_{HS,MA}\,[M^-] / (1 + K_{HS,MA}\,[M^-])\}\, \mu_{MC} \qquad (15)$$

Therefore, the net mobility of a neutral solute is independent of the anion concentration in the BGE; however it depends on the binding constant and the micelle concentration. If these two parameters are high, meaning that the solute exists exclusively in the micelles, the net mobility of the solute will be the same as the electrophoretic mobility of the micelle.

2.2 Capacity Factor as a Function of Ionic Strength and Micelle Concentration

2.2.1 Capacity factor for totally ionized acidic solute

For a "totally" ionized acidic solute, the capacity factor (k') can be defined as follows:

$$k' = \nu\, [S^-M^-]_{MC} / [S^-]_{AQ} \qquad (16)$$

in which ν is the phase ratio. By replacing for $[S^-M^-]_{MC}/[S^-]_{AQ}$ with $[M^-]K_{S^-,MA}$, we have:

$$k' = \nu\, K_{S^-,MA}\, [M^-] \qquad (17)$$

Therefore if the micelle concentration ($[M^-]$) in the BGE is increased, and/or the binding constant is high, the capacity factor of the ionized acidic solute is increased.

In equation (16), by replacing $[S^-M^-]_{MC}/[S^-]_{AQ}$ with $[E^-M^-]_{MC}/K_{IE}[E^-]_{AQ}$, k' can be written as:

$$k' = \nu\, [E^-M^-]_{MC} / K_{IE}\, [E^-]_{AQ} \qquad (18)$$

In this way, as the anion concentration ($[E^-]_{AQ}$) is increased, and/or the ion exchange constant is high, the capacity factor of the ionized acidic solute is decreased.

2.2.2 Capacity factor for neutral solute

Similarly, the capacity factor (k') of a neutral solute is given by

$$k' = \nu\, [HSM^-]_{MC} / [HS]_{AQ} \qquad (19)$$

By replacing $[HSM^-]_{MC}/[HS]_{AQ}$ with $K_{HS,MA}[M^+]$, k' can be written as:

$$k' = \nu K_{HS,MA} [M^+] \quad (20)$$

Hence the capacity factor of the neutral solute will also increase with an increase in the micelle concentration, and/or with a high binding constant.

2.3 Distribution Coefficient as a Function of Ionic Strength

The capacity factor k' in MECC is related to the distribution coefficient K of a solute between the micellar and aqueous phases (8) as follows:

$$k' = K \Phi_v (C_{sf} - CMC) \quad (21)$$

or

$$\ln k' = \ln K + \ln[\Phi_v (C_{sf} - CMC)] \quad (22)$$

in which Φ_v is the partial specific volume of the micelle and C_{sf} is the surfactant concentration.

The temperature dependence of the distribution coefficient is given by the van't Hoff equation:

$$\ln K = - \Delta H^\circ / RT + \Delta S^\circ / R \quad (23)$$

where ΔH° is the enthalpy change associated with micelle solubilization or the transfer of the solute from the aqueous phase to the micelle, ΔS° is the corresponding entropy change, R is the gas constant, and T is the absolute temperature. By substituting equation (23) into equation (22), we have:

$$\ln k' = - \Delta H^\circ / RT + \Delta S^\circ / R + \ln[\Phi_v (C_{sf} - CMC)] \quad (24)$$

Logarithms of the capacity factor at different temperatures are plotted against the reciprocal temperature to give straight lines. The values of ΔH° and ΔS° can be calculated from the slope and the intercept, and thus the distribution coefficient (K) can be calculated at different temperature, since Φ_v is approximately 0.365 L/mole for C_{16}TAB at about 0.015 mole/L concentration (9); and the CMC is approximately 0.001 mole/L. The distribution coefficient (K) can also be investigated as a function of anion concentration by varying the anion concentrations and running each concentration at the different temperatures. From equation (22), it is suggested that the relationship between the anion concentration and the distribution coefficient should be similar to that with the capacity factor since the second term, $\ln[\Phi_v(C_{sf}\text{-CMC})]$, is a constant as long as the surfactant type and its concentration are known.

3. Experimental

3.1 Apparatus

MECC experiments were carried out with a Quanta 4000 CE system (Waters Chromatography, Division of Millipore, Milford, MA, USA), and a Beckman P/ACE 5010 CE system (Beckman, Palo Alto, CA, USA). The CE systems were equipped with a UV absorbance detector at 214 nm and connected to a Waters/VAX 4000-50 data system through an

LAC/E interface module. The Waters ExpertEase software (version 3.1) was applied for data acquisition and processing. A Orion Model 290A pH meter was used to measure pH with a precision of ±0.01 unit.

Capillaries used were uncoated fused-silica capillary tubes obtained from Polymicro Technologies (Phoenix, AZ, USA) with 50 μm I.D. x 375 μm O.D, 30 cm effective length and 37 cm total length.

3.2 Chemicals and Reagents

The test solutes in this study (see Table 1) contained acidic, basic, or electron-withdrawing functional groups, and were obtained from Aldrich (Milwaukee, WI, USA). They were dissolved in HPLC-grade methanol to give a mixed stock sample solution at a concentration of approximately 5 mg/mL for 2,4-dihydroxybenzoic acid and 2,4-dinitroaniline; approximately 7.5 mg/mL for 3,4-dihydroxybenzoic acid; and approximately 10 mg/mL for 2-nitrobenzoic acid, 1,3-dinitrobenzen, 4-nitrophenol, 2,4-dinitrobenzoic acid, 3,5-dinitro-o-toluic acid, salicylic acid and 3,5-dinitrobenzoic acid. Pentachlorophenol (used as a micelle marker) was obtained from Aldrich.

Sodium citrate dihydrate, citric acid monohydrate, sodium benzoate, sodium chloride, sodium acetate anhydrous and

glacial acetic acid were obtained from Mallinckrodt Chemical (Paris, KY, USA); sodium tartrate dihydrate, tartaric acid, sodium phosphate monobasic anhydrous, sodium phosphate dibasic anhydrous, 85% o-phosphoric acid, sodium sulfate, sodium bromide and potassium hydroxide were obtained from Fisher Scientific (Fairlawn, NJ, USA); C_{16}TAB was obtained from Aldrich; HPLC-grade methanol and acetonitrile were obtained from Burdick & Jackson (Muskegon, MI, USA). Millipore Milli-Q water was used to prepare stock buffer and stock surfactant solutions.

3.3 Procedure

The coating of new capillaries was removed by briefly placing the window area in a flame from a burner and then gently cleaning the burned material with a tissue dampened with methanol. The capillary was conditioned by purging in order with 1 N potassium hydroxide solution, 0.1 N potassium hydroxide solution, degassed and filtered D.I. water, buffer at three-fold higher concentration than running buffer without C_{16}TAB, and finally BGE, each for fifteen minutes.

A stock buffer solution was prepared by mixing equimolar solutions of an acid and its sodium salt and adjusting to the appropriate pH. A final BGE was prepared by mixing the stock solutions of buffer, salt and surfactant with acetonitrile

at each appropriate concentration, then degassed and filtered through a 0.45-μm syringe filter.

A test sample solution was prepared by twenty-fold dilution of the stock mixed sample solution in methanol by the ten-fold diluted running buffers without C_{16}TAB. The sample solution was injected in the hydrodynamic mode for 2 second. Except where temperature was specified, otherwise, the experiments were performed at approximately 25 °C, and at constant negative voltages of 13.5 kV.

4. Results and Discussion

4.1 Reversed-polarity Capillary Electrophoresis

The direction of electroosmotic flow (EOF) in capillary electrophoresis (CE) is normally towards the cathode in the aqueous solutions. However, with cationic surfactants in the BGE, the surfactant bilayers are absorbed to the capillary wall, and then the zeta potential is reversed (10). The EOF will be directed toward the positive electrode (towards the detector side) and the normal electrode polarity is reversed. If the surfactant concentration is below the CMC, no micelles will be formed, but the EOF will be reversed. This technique might be called reversed-polarity capillary electrophoresis (RP-CE).

The net mobility (μ_{net}, cm^2/V-sec) is expressed as

$$\mu_{net} = \mu_{app} - \mu_{EOF} = \frac{lL}{Vt_s} - \frac{lL}{Vt_{EOF}} = \frac{lL}{V}\left(\frac{1}{t_s} - \frac{1}{t_{EOF}}\right) \qquad (25)$$

where t_s and t_{EOF} are the migration time (sec) of the solutes and the EOF marker (methanol is the marker); μ_{app} and μ_{EOF} are the apparent and EOF mobilities (cm^2/V-sec); l and L are the length (cm) of the capillary from injection to detection and the total length (cm) of the capillary, respectively; and V is the applied voltage (V).

4.1.1 Effect of buffer concentration on net mobilities

Two different pH 3.7 buffers, citrate and phosphate, were employed with 0.5 mM C_{16}TAB and 15% acetonitrile in the RP-CE system. The concentration of each buffer was 10, 25, 50, 75 and 100 mM. The results are given in Figures 1 and 2. The net mobilities of salicylic and 3,5-dinitrobenzoic acids were slightly increased with increasing citrate concentration. However, in all the other cases, the net mobilities of the anionic solutes were not really influenced by increasing buffer concentration. In addition, the uncharged solutes (1,3-dinitrobenzen and 4-nitrophenol) and the cationic solute (2,4-dinitroaniline) migrated with the EOF marker.

4.1.2 Effect of salt concentration on net mobilities

Sodium bromide (NaBr) solutions at concentrations of 0, 10, 25 and 50 mM were employed with 10 mM citrate buffer

(pH 3.7), 0.5 mM C_{16}TAB and 15% acetonitrile in the RP-CE system. Similar to the effect of citrate concentration, with increasing the NaBr concentration, the net mobilities of salicylic and 3,5-dinitrobenzoic acids were slightly increased as shown in Figure 3. The net mobilities of all the other anionic solutes were almost unaffected.

4.2 Micellar Electrokinetic Capillary Chromatography

If the surfactant concentration is above the CMC, not only is the EOF reversed, but micelles will form. This technique might be called the reversed-polarity micellar electrokinetic capillary chromatography (RP-MECC). In RP-MECC, or MECC for brevity, pentachlorophenol and methanol can be used as the micelle and the EOF markers, respectively (7). The capacity factor (k') in MECC is defined as (8, 11)

$$k' = \frac{(t_s - t_{EOF})}{t_{EOF}\left(1 - \frac{t_s}{t_{mc}}\right)} \qquad (26)$$

in which t_{MC} is the migration time (sec) of the micelle. Equation (25) for the calculation of the net mobility (μ_{net}, $cm^2/V\text{-}sec$) in RP-CE can be applied to MECC as well.

4.2.1 Effect of buffer concentration on net mobilities and capacity factors

Five different pH 3.7 buffers, including citrate, tartrate, phosphate, formate and acetate, were employed with 15 mM

C_{16}TAB and 15% acetonitrile in the MECC system at 25 °C. BGE with citrate was run at 45 °C as well. The concentration of each buffer in the BGEs was 10, 25, 50, 75 and 100 mM. The dependence of the net mobilities and the capacity factors on the buffer concentrations are presented in Figures 4 to 15. For 3,4-dihydroxybenzoic acid (pK_a 4.48, slightly ionized), 1,3-dinitrobenzene and 4-nitrophenol (uncharged), and 2,4-dinitroaniline (cationic), the net mobilities and the capacity factors were not or very slightly affected with increasing the buffer concentrations. However, for all the ionized acidic solutes, 2-nitrobenzoic, 2,4-dihydroxybenzoic, 2,4-dinitrobenzoic, 3,5-dinitro-o-toluic, salicylic and 3,5-dinitrobenzoic acids, the net mobilities were significantly increased and the capacity factors were dramatically decreased with increasing the buffer concentrations (except for acetate). However, with increasing acetate concentration, the net mobilities were slightly increased and the capacity factors were slightly decreased. The changes of the net mobilities and capacity factors for the ionized acidic solutes were in the following order:

citrate > tartrate > phosphate > formate > acetate (27)

Some solutes migrated ahead of the EOF marker with increasing citrate or tartrate concentrations, meaning there were no interactions between the solutes and the C_{16}TAB micelles. These solutes included 2-nitrobenzoic acid (above

25 mM citrate or tartrate), 2,4-dihydroxybenzoic acid (above 75 mM citrate) and 2,4-dinitrobenzoic acid (at 100 mM citrate). For these solutes migrating ahead of the EOF marker, physically meaningless negative k' values were obtained from equation (26) as shown in Figures 5, 7 and 9. However, the trends in the k' changes with increasing the buffer concentration were still seen.

4.2.2 Effect of salt concentration on net mobilities and capacity factors

Four different salts, including sodium sulfate (Na_2SO_4), sodium benzoate (C_6H_5COONa), sodium bromide (NaBr) and sodium chloride (NaCl) were employed with 10 mM citrate buffer (pH 3.7), 15 mM $C_{16}TAB$ and 15% acetonitrile in the MECC system. The concentrations of each salt solution were 0, 15, 40 and 65 mM. The relationships of the net mobilities and the capacity factors with increasing salt concentrations are illustrated in Figures 16 to 23. The total concentrations (including 10 mM citrate) were used in the plots at 10, 25, 50 and 75 mM. Similar to the effect of increasing the buffer concentrations, with increasing the salt concentrations, the net mobilities and the capacity factors were slightly affected for 3,4-dihydroxy-benzoic acid, 1,3-dinitrobenzene, 4-nitro-phenol and 2,4-dinitroaniline. However, for all the ionized acidic solutes, the net mobilities were significantly increased and the capacity factors were dramatically. Some solutes, 2-

nitrobenzoic acid, 2,4-dihydroxybenzoic acid and 2,4-dinitrobenzoic acid (only when using Na_2SO_4), migrated ahead of the EOF marker with increasing salt concentrations. Similarly, negative *k'* values were calculated using equation (26). Changes in the net mobilities and capacity factors of the ionized acidic solutes with increasing salt concentrations were:

$$Na_2SO_4 > C_6H_5COONa > NaBr > NaCl \qquad (28)$$

4.2.3 Effect of C_{16}TAB concentration on net mobilities and capacity factors

C_{16}TAB at concentrations of 4, 7.5, 15 and 30 mM were employed with 50 mM citrate buffer (pH 3.7) and 15% acetonitrile in the MECC system. The relationship between capacity factors and surfactant concentration remained linear even including the negative *k'* values obtained from equation (26) as shown in Figures 24 and 25.

With increasing C_{16}TAB concentrations, the net mobilities dramatically decreased and the capacity factors significantly increased for the ionized acidic solutes. For 3,4-dihydroxy-benzoic acid, 1,3-dinitrobenzene, 4-nitrophenol and 2,4-dinitroaniline, although the net mobilities decreased and the capacity factors increased with increasing C_{16}TAB concentrations, these changes were much smaller than for those of the ionized acidic solutes. In addition, when the C_{16}TAB

concentration increased up to 30 mM, none of the ionized acidic solutes migrated ahead of the EOF marker. Thus the interactions were re-established between the micelles and these solutes.

4.2.4 Effect of ionic strength on the distribution coefficient

The distribution coefficient (K) of a solute between the C_{16}TAB micelle phase and the aqueous phase as a function of the ionic strength of the BGE was investigated with citrate at concentrations of 10, 25, 50, and 75 mM, and then at each concentration at the various temperatures from 20 °C to 45 °C. As predicted, a similar relationship between capacity factors and citrate concentration was found for the distribution coefficients, which were significantly decreased for the ionized acidic solutes, but were little affected for the cationic, uncharged and slightly ionized acidic solutes with increasing citrate concentrations, as given in Figures 26, 27 and 28.

4.3 Mechanism for Migration of the Ionized Acidic Solutes in MECC with a Cationic Surfactant

For an ionic solute in MECC, the net mobility is a combination of the electrophoretic mobility and the interactions (both the ionic and hydrophobic interactions) with the micelle. In the RP-MECC system, the electrophoretic mobility of the

anionic solute and the EOF mobility are in the same direction, opposite to the electrophoretic mobility of the micelle. Therefore, the net mobility of an anionic solute can be increased with an increase in its electrophoretic mobility, and/or a decrease in the interaction with the micelle.

In the RP-CE system, the electrophoretic mobility of an ionized acidic solute is in the EOF direction. As described in section 4.1, increase in the ionic strength of the BGE almost unaffected the electrophoretic mobility of the ionized acidic solute. It can be assumed that in the MECC system, the increase in the ionic strength would not affect the electrophoretic mobility of the anionic solute either. Therefore, with increasing ionic strength of the BGEs, the increase in the net mobility of the ionized acidic solute is probably due to the decreased interaction with the C_{16}TAB micelle. Furthermore, since the net mobilities of the cationic, uncharged and slightly ionized acidic solutes were little affected by increasing ionic strength in the MECC system, the hydrophobic interaction of the ionized acidic solute with the micelles can not account for the net mobility increase. Consequently, only the decrease in the ionic interaction between the ionized acidic solute and the C_{16}TAB micelle can contribute to the net mobility increase with increased ionic strength. The decreased ionic interaction between the ionized acidic solute and the micelle is the result of (i) ion-pairing of the ionized acidic solute with the positive-

charged C_{16}TAB micellar head, and (ii) ion-exchange between the ion-paired acidic solute and the competing ions (anions in the BGE). As a result, ionic interactions were reduced between the ionized acidic solute and the micellar phase, thus causing the ionized acidic solute to exist predominantly in the aqueous phase and to migrate mainly electrophoretically. Moreover, ionized acidic solutes, with higher ion-exchange constants and higher electrophoretic mobilities, can migrate ahead of the EOF marker as the ionic strength of the BGE increases, meaning that there is no interaction between the ionized acidic solute and the C_{16}TAB micelle. The equations (9) and (18) for the ionized acidic solutes in the section 2.1.1 describe very well the phenomena addressed here.

The degree of the ion-exchange depends on the charges of the ionized acidic solutes and the competing ions, pK_a's of both the ionized acidic solutes and the selected buffer acids, and the solvated size and the polarizability of the ionized acidic solutes and the competing ions. In ion exchange chromatography, the affinity order for the anions on the strong base anion-exchangers is (12):

$$\text{citrate} > SO_4^{2-} > Br^- > Cl^- > H_2PO_4^- > CH_3COO^- > HCOO^- \quad (29)$$

The same trend was observed in MECC with a cationic surfactant except the order of CH_3COO^- and $HCOO^-$. The pH of the BGE (3.7) was about the same unit as pK_a of formic acid

(3.75); but was about one unit lower than pK_a of acetic acid (4.75), therefore the carboxylic functional group in the acetate buffer was much less dissociated, and the ion-pair interaction with the ionized acidic solute was almost nonexistent. Consequently, ion-exchange in the acetate buffer could not really occur as shown in Figures 14 and 15.

In general, an increase in the charge on the anions in the BGE increases the degree of the ion-exchange through the increased coulombic interactions with the cationic micellar head as seen in the orders (26) and (27). In addition, pK_{a1} and pK_{a2} of tartaric acid are 2.93 and 4.23, respectively. One carboxylic functional group was ionized and the other one was partially ionized at pH 3.7, therefore the degree of the ion-exchange in the tartrate buffer was less than that in the buffer with SO_4^{2-}; but was larger than that in the phosphate buffer as seen in the order (26), because phosphate existed in the monobasic form ($H_2PO_4^-$) at pH 3.7. On the other hand, since pK_{a1}, pK_{a2} and pK_{a3} of citric acid are at 3.12, 4.76 and 6.40, respectively, only one of the three carboxylic function groups was actually ionized in the BGE at pH 3.7. Na_2SO_4 solution was added into 10 mM citrate buffer. Therefore it was difficult to compare directly the degree of the ion-exchange between citrate and SO_4^{2-} in this study. So was the direct comparison between tartrate and benzoate.

The degree of the ion-exchange increases with the degree of the polarizability of the anions in the BGEs. This can be seen by comparison of the results in Figures 10 to 13, and Figures 20 to 23 for the singly charged anions, i.e., $Br^- > Cl^- > H_2PO_4^- > COO^-$.

An increase in the $C_{16}TAB$ concentration in the BGE results in an increase of the phase ratio in the MECC system. As a result, the net mobility is decreased and the capacity factor is increased. These effects can be predicted from equations (11) and (17) for the ionized acidic solute, as well as from equations (15) and (20) for the neutral solute. Moreover, because of the ionic interaction with the $C_{16}TAB$ micelle in addition to the hydrophobic interaction, for the ionized acidic solute, the binding constant ($K_{S^-,MA}$) should be much greater than the binding constant ($K_{HS,MA}$) for the neutral solute. Therefore, it can be predicted from the equations that the changes in both the net mobility and the capacity factor of the ionized acidic solute should be much larger than those of the neutral solute.

5. Conclusions

In MECC with a cationic surfactant, a fundamental study was carried out for the first time of the net mobilities, the capacity factors and the distribution coefficients as a function of the ionic strength of the BGE. The equations derived agree

qualitative very well with the experimental results. For the cationic, uncharged and slightly ionized acidic solutes, the net mobilities, capacity factors and distribution coefficients were almost unaffected by the ionic strength of the BGEs. However, for the ionized acidic solutes, the net mobilities were significantly increased; the capacity factors and distribution coefficients were dramatically decreased because of the effects of ion-pair formation with the cationic micellar head and then ion-exchange with the competing anions in the BGE. Therefore, in the optimization strategy for MECC using a cationic surfactant, the ionic strength of the BGE was an important experimental factor in achieving an adequate separation of complex mixtures. The optimized separation was achieved in approximately 10 minutes by using a 30 cm effective length (37 cm total length) x 50 μm I.D. uncoated fused-silica capillary with a BGE containing 50 mM phosphate (pH 3.7), 15 mM C_{16}TAB and 15% acetonitrile as shown in the electropherogram, Figure 29.

Table 1

Compounds Studied for BGE Ionic Strength Effect

No	Compounds	pK_a	M.W.	Formulas
1	3,4-Dihydroxybenzoic Acid	4.48	154.12	$(HO)_2C_6H_3CO_2H$
2	2-Nitrobenzoic Acid	2.18	167.12	$(NO_2)C_6H_4CO_2H$
3	1,3-Dinitrobenzene	-	168.11	$C_6H_4(NO_2)_2$
4	4-Nitrophenol	7.15	139.11	$C_5H_4(NO_2)OH$
5	2,4-Dihydroxybenzoic Acid	3.29	154.12	$(HO)_2C_6H_3CO_2H$
6	2,4-Dinitroaniline	18.46	183.10	$(NO_2)_2C_6H_3(NH_2)$
7	2,4-Dinitrobenzoic Acid	1.43	212.12	$(NO_2)_2C_6H_3CO_2H$
8	3,5-Dinitro-o-toluic Acid	< 2.85	226.15	$(NO_2)_2C_5H_2(CH_3)CO_2H$
9	Salicylic Acid (2-Hydroxybenzoic Acid)	2.98	138.12	$(HO)C_5H_4CO_2H$
10	3,5-Dinitrobenzoic Acid	2.85	212.12	$(NO_2)_2C_5H_3CO_2H$
11	Pentachlorophenol (Micellar Marker)	4.50	266.35	C_5Cl_5OH

Figure Captions:

Figure 1: Effect of citrate concentration (pH 3.7) on the net mobility of anionic solutes in reversed-polarity capillary electrophoresis with 0.5 M C_{16}TAB and 15% acetonitrile.

Figure 2: Effect of phosphate concentration (pH 3.7) on the net mobility of anionic solutes in reversed-polarity capillary electrophoresis with 0.5 M C_{16}TAB and 15% acetonitrile.

Figure 3: Effect of NaBr concentration on the net mobility of anionic solutes in reversed-polarity capillary electrophoresis with 10 mM citrate buffer (pH 3.7), 0.5 M C_{16}TAB and 15% acetonitrile.

Figure 4: Effect of citrate concentration (pH 3.7) on the net mobility of solutes in MECC with 15 M C_{16}TAB and 15% acetonitrile.

Figure 5: Effect of citrate concentration (pH 3.7) on the capacity factor of solutes in MECC with 15 M C_{16}TAB and 15% acetonitrile.

Figure 6: Effect of citrate concentration (pH 3.7) on the net mobility of solutes in MECC with 15 M C_{16}TAB and 15% acetonitrile at 45 °C.

Figure 7: Effect of citrate concentration (pH 3.7) on the capacity factor of solutes in MECC with 15 M C_{16}TAB and 15% acetonitrile at 45 °C.

Figure 8: Effect of tartrate concentration (pH 3.7) on the net mobility of solutes in MECC with 15 M C_{16}TAB and 15% acetonitrile.

Figure 9: Effect of tartrate concentration (pH 3.7) on the capacity factor of solutes in MECC with 15 M C_{16}TAB and 15% acetonitrile.

Figure 10: Effect of phosphate concentration (pH 3.7) on the net mobility of solutes in MECC with 15 M C_{16}TAB and 15% acetonitrile.

Figure 11: Effect of phosphate concentration (pH 3.7) on the capacity factor of solutes in MECC with 15 M C_{16}TAB and 15% acetonitrile.

Figure 12: Effect of formate concentration (pH 3.7) on the net mobility of solutes in MECC with 15 M C_{16}TAB and 15% acetonitrile.

Figure 13: Effect of formate concentration (pH 3.7) on the capacity factor of solutes in MECC with 15 M C_{16}TAB and 15% acetonitrile.

Figure 14: Effect of acetate concentration (pH 3.7) on the net mobility of solutes in MECC with 15 M C_{16}TAB and 15% acetonitrile.

Figure 15: Effect of acetate concentration (pH 3.7) on the capacity factor of solutes in MECC with 15 M C_{16}TAB and 15% acetonitrile.

Figure 16: Effect of Na_2SO_4 concentration on the net mobility of solutes in MECC with 10 mM citrate (pH 3.7), 15 M C_{16}TAB and 15% acetonitrile.

Figure 17: Effect of Na_2SO_4 concentration on the capacity factor of solutes in MECC with 10 mM citrate (pH 3.7), 15 M C_{16}TAB and 15% acetonitrile.

Figure 18: Effect of Na benzoate concentration on the net mobility of solutes in MECC with 10 mM citrate (pH 3.7), 15 M C_{16}TAB and 15% acetonitrile.

Figure 19: Effect of Na benzoate concentration on the capacity factor of solutes in MECC with 10 mM citrate (pH 3.7), 15 M C_{16}TAB and 15% acetonitrile.

Figure 20: Effect of NaBr concentration on the net mobility of solutes in MECC with 10 mM citrate (pH 3.7), 15 M C_{16}TAB and 15% acetonitrile.

Figure 21: Effect of NaBr concentration on the capacity factor of solutes in MECC with 10 mM citrate (pH 3.7), 15 M C_{16}TAB and 15% acetonitrile.

Figure 22: Effect of NaCl concentration on the net mobility of solutes in MECC with 10 mM citrate (pH 3.7), 15 M C_{16}TAB and 15% acetonitrile.

Figure 23: Effect of NaCl concentration on the capacity factor of solutes in MECC with 10 mM citrate (pH 3.7), 15 M C_{16}TAB and 15% acetonitrile.

Figure 24: Effect of C_{16}TAB concentration on the net mobility of solutes in MECC with 50 mM citrate (pH 3.7) and 15% acetonitrile.

Figure 25: Effect of C_{16}TAB concentration on the capacity factor of solutes in MECC with 50 mM citrate (pH 3.7) and 15% acetonitrile.

Figure 26: Effect of citrate concentration (pH 3.7) on the distribution coefficient of solutes between the aqueous phase and the micellar phase in MECC with 15 mM C_{16}TAB and 15% acetonitrile at 20 °C.

Figure 27: Effect of citrate concentration (pH 3.7) on the distribution coefficient of solutes between the aqueous phase and the micellar phase in MECC with 15 mM C_{16}TAB and 15% acetonitrile at 30 °C.

Figure 28: Effect of citrate concentration (pH 3.7) on the distribution coefficient of solutes between the aqueous phase and the micellar phase in MECC with 15 mM C_{16}TAB and 15% acetonitrile at 40 °C.

Figure 29: Electropherogram of the studied solutes (see Table 1 for the identification of compounds) using a 30 cm effective length (37 cm total length) x 50 μm I.D. uncoated fused-silica capillary with a BGE containing 50 mM phosphate (pH 3.7), 15 mM C_{16}TAB and 15% acetonitrile under -13.5 kV.

Figure 1

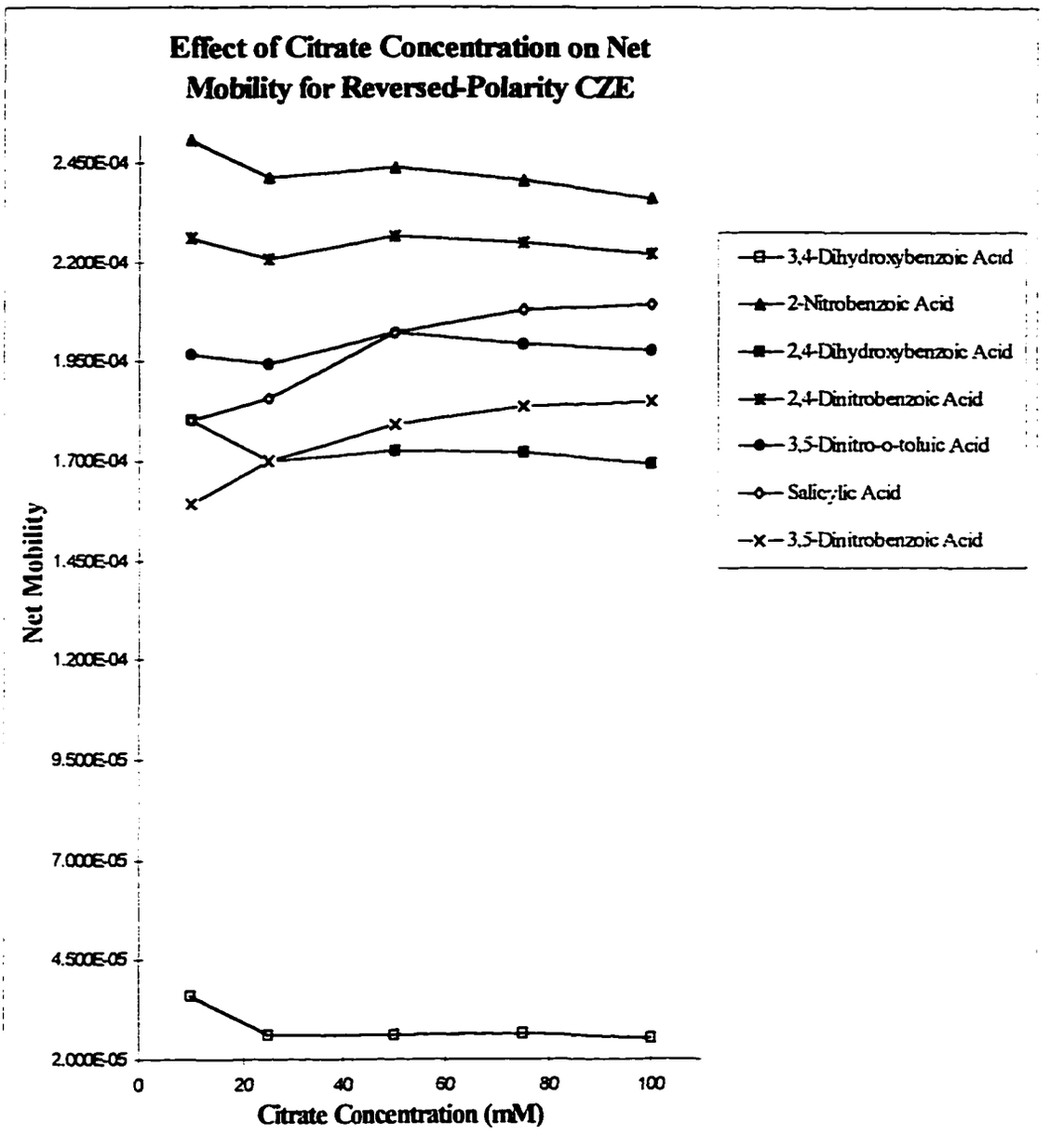

Figure 2

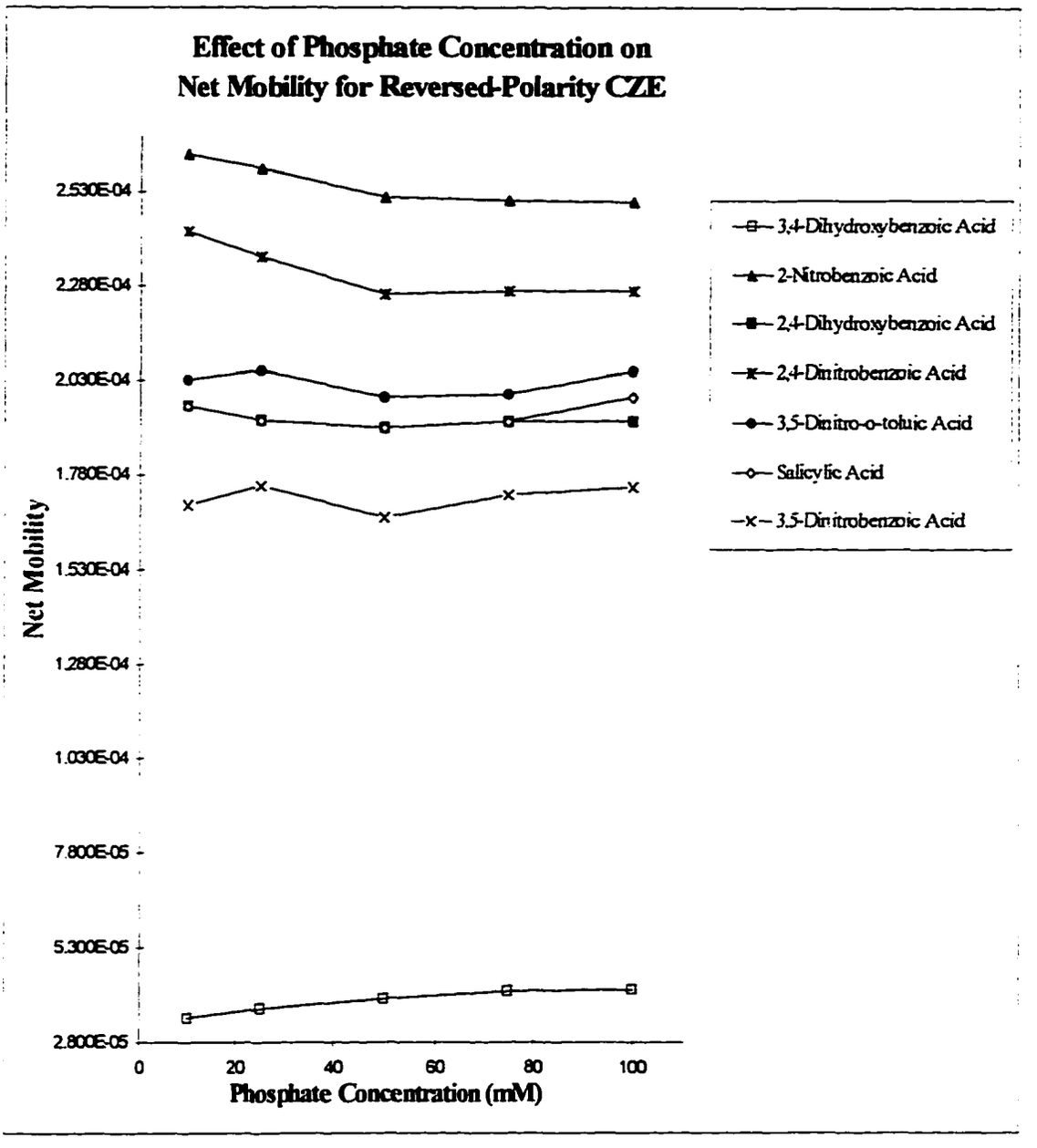

Figure 3

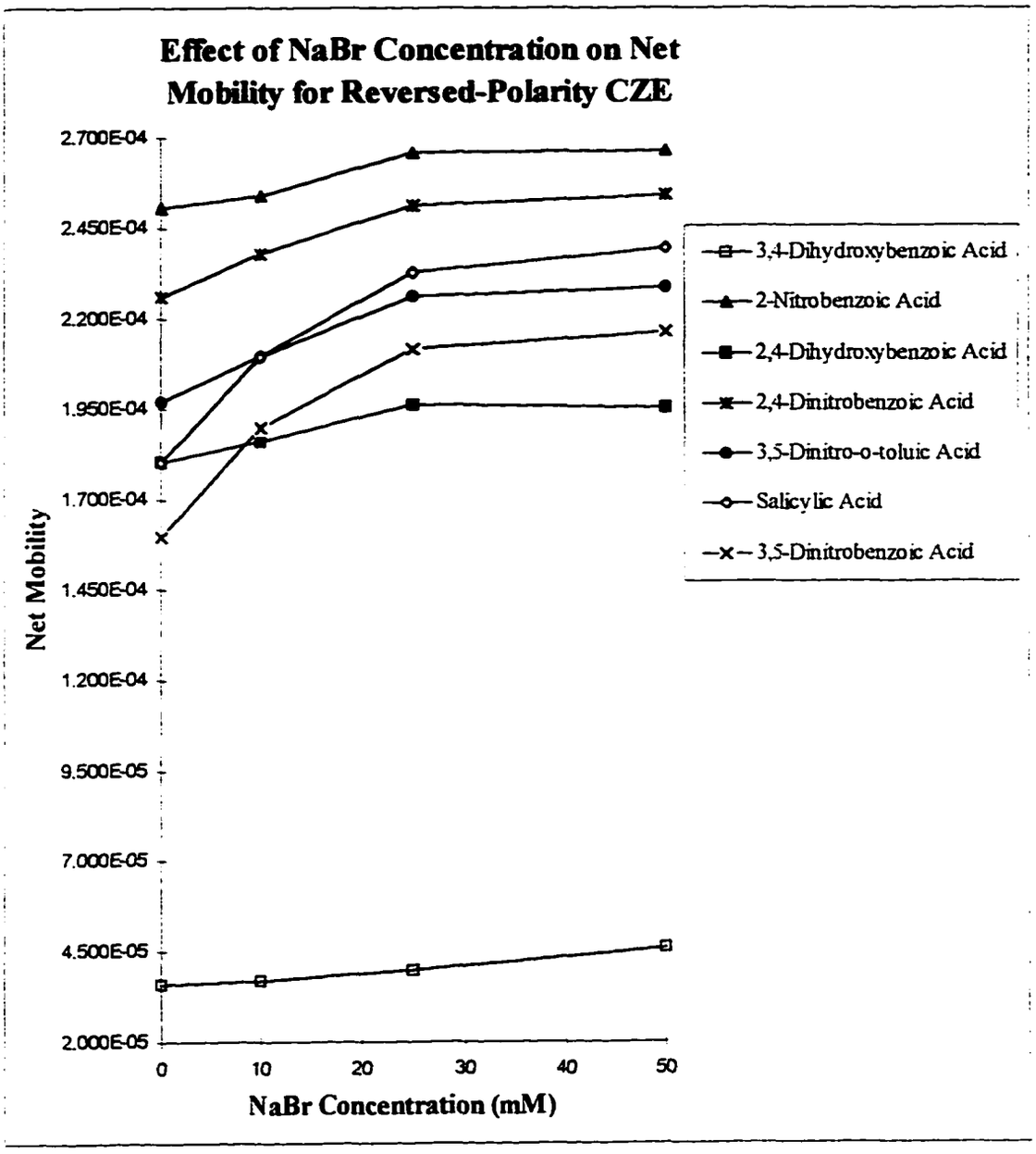

Figure 4

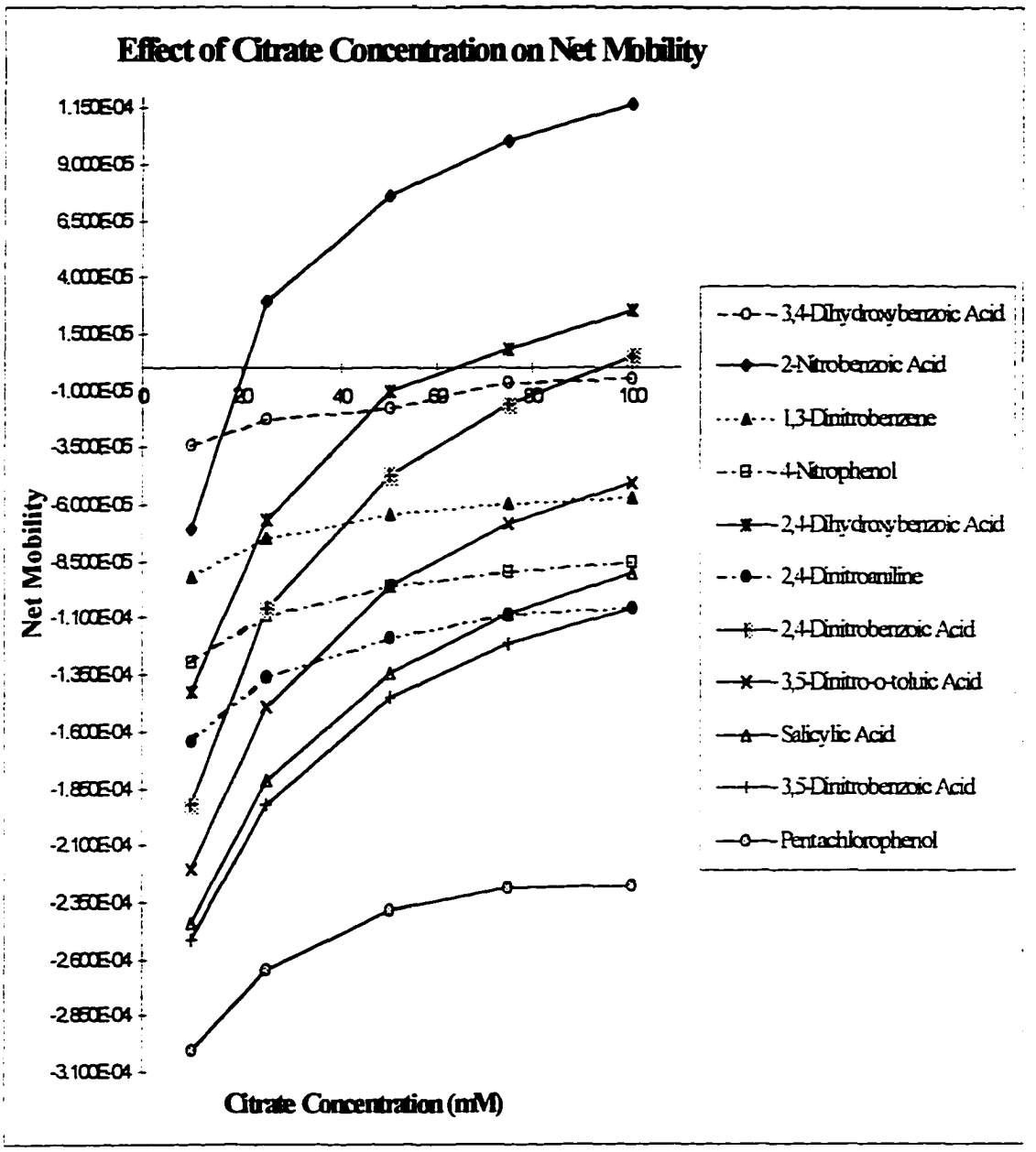

Figure 5

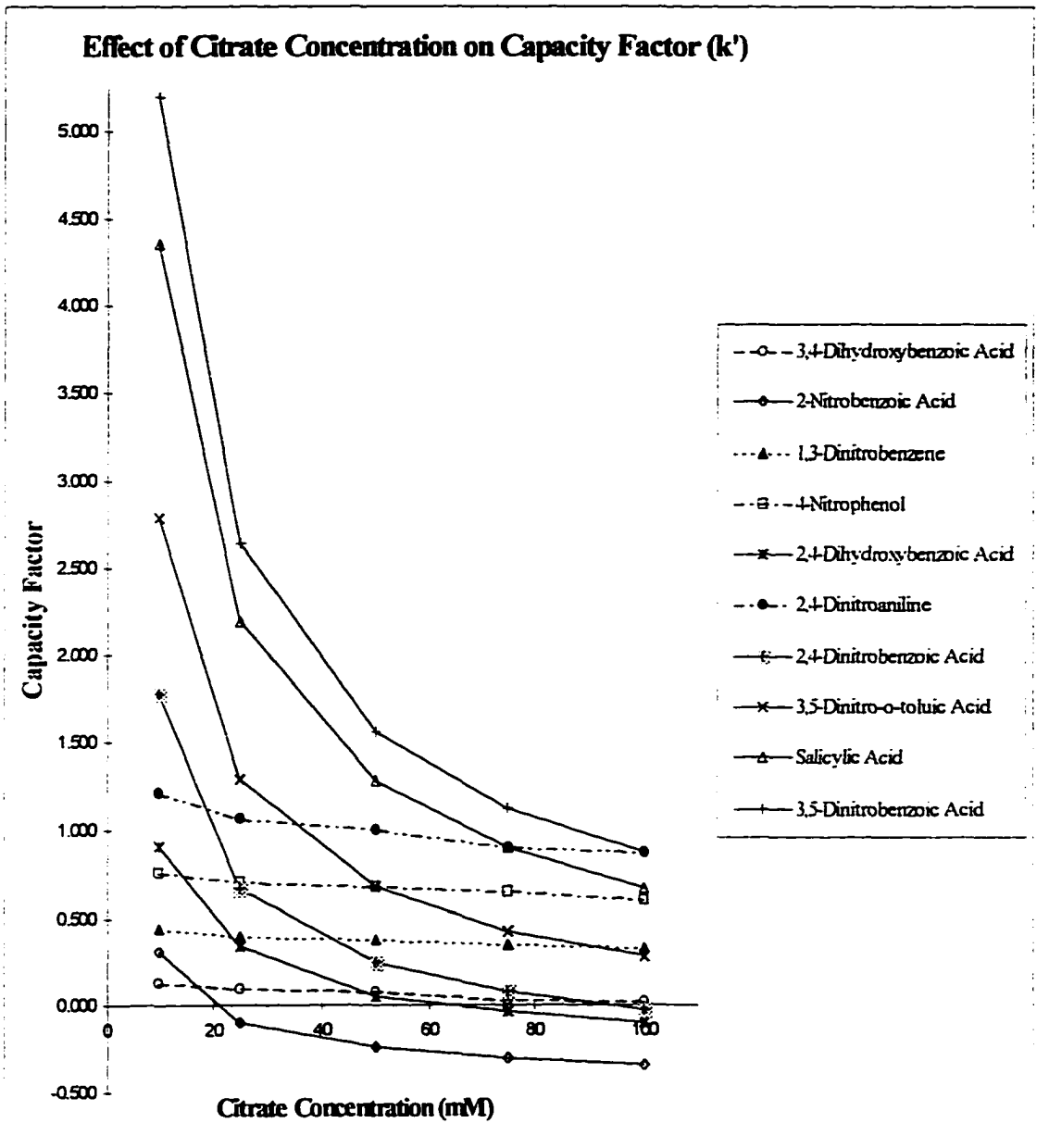

Figure 6

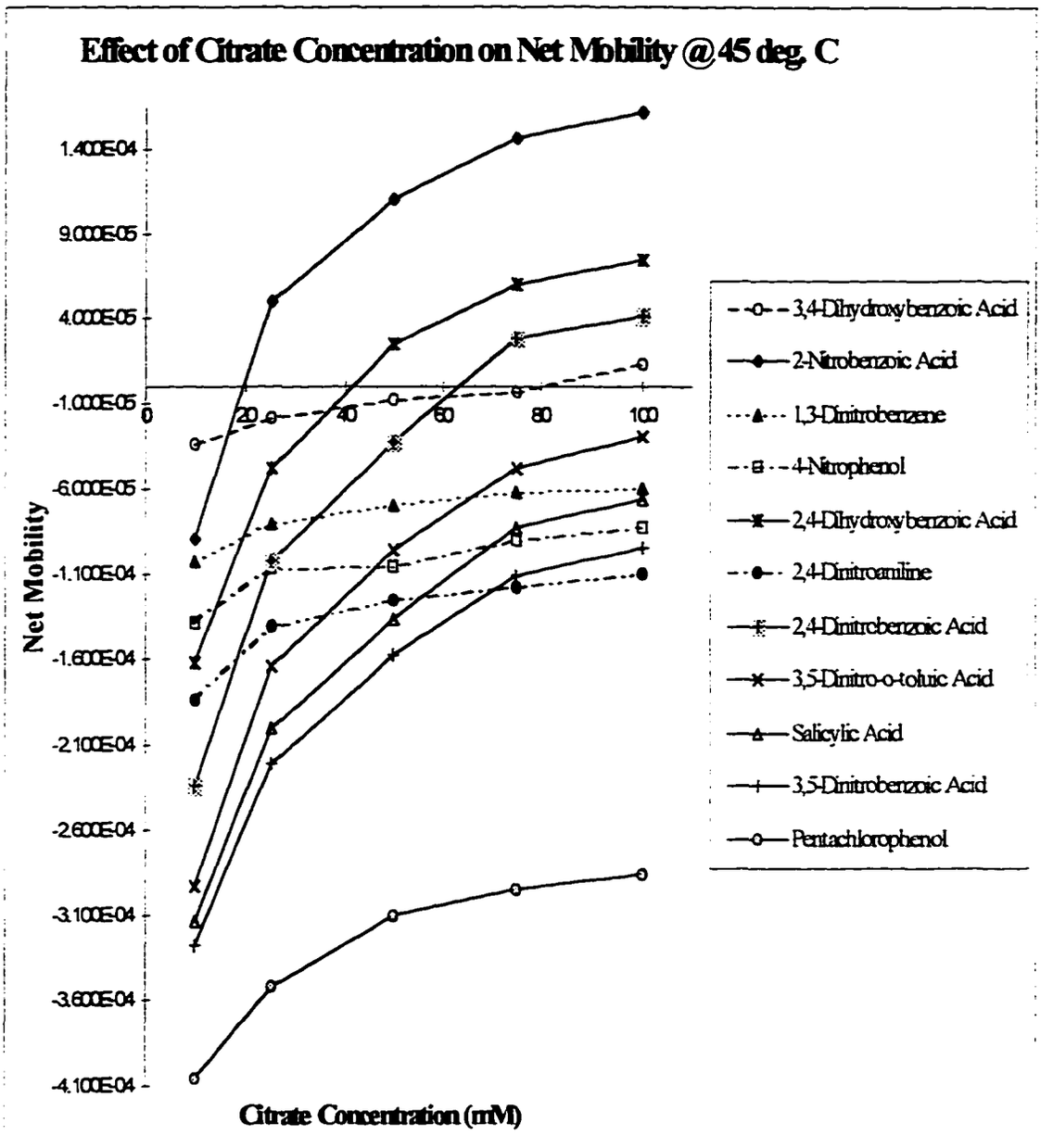

Figure 7

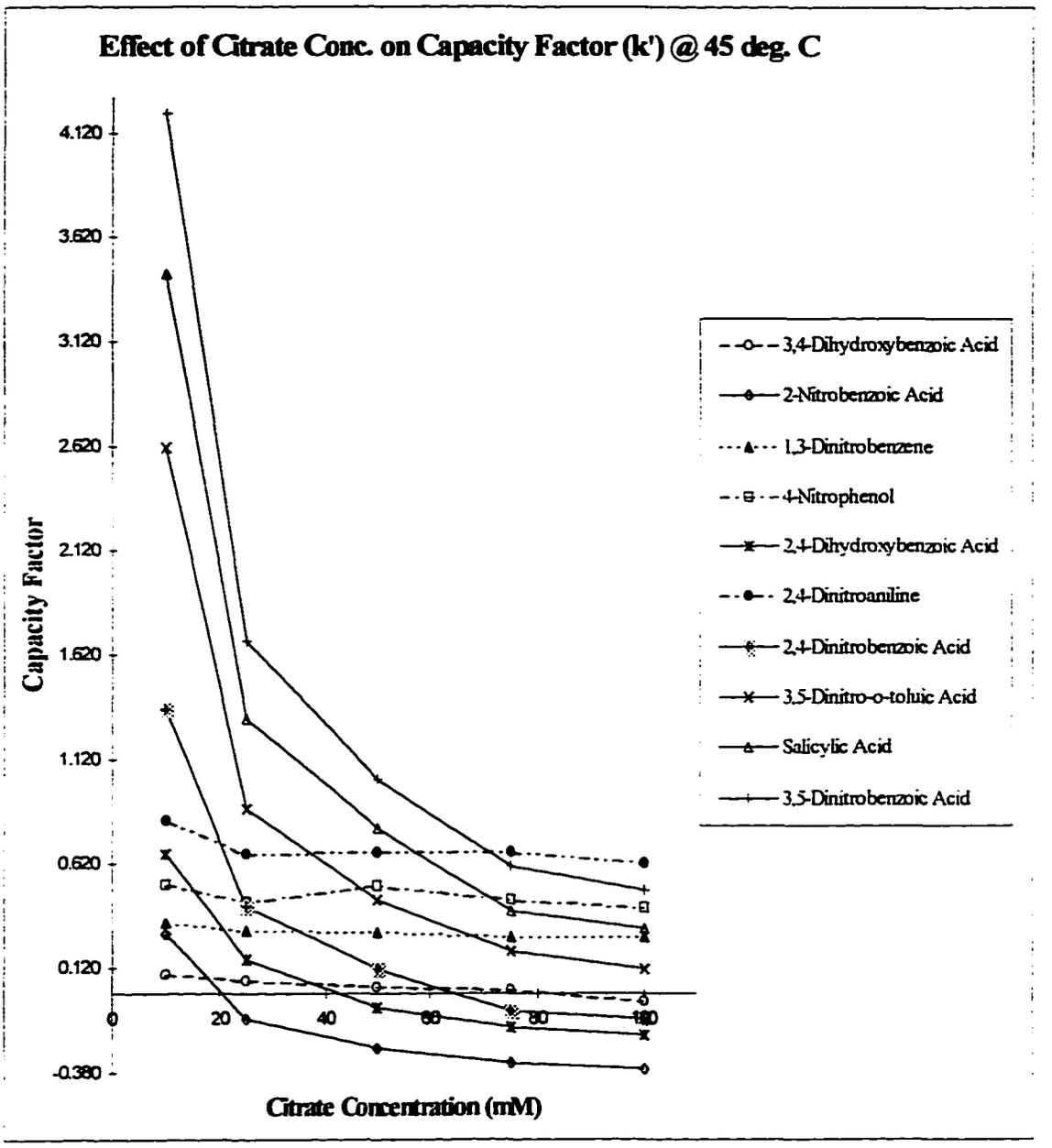

Figure 8

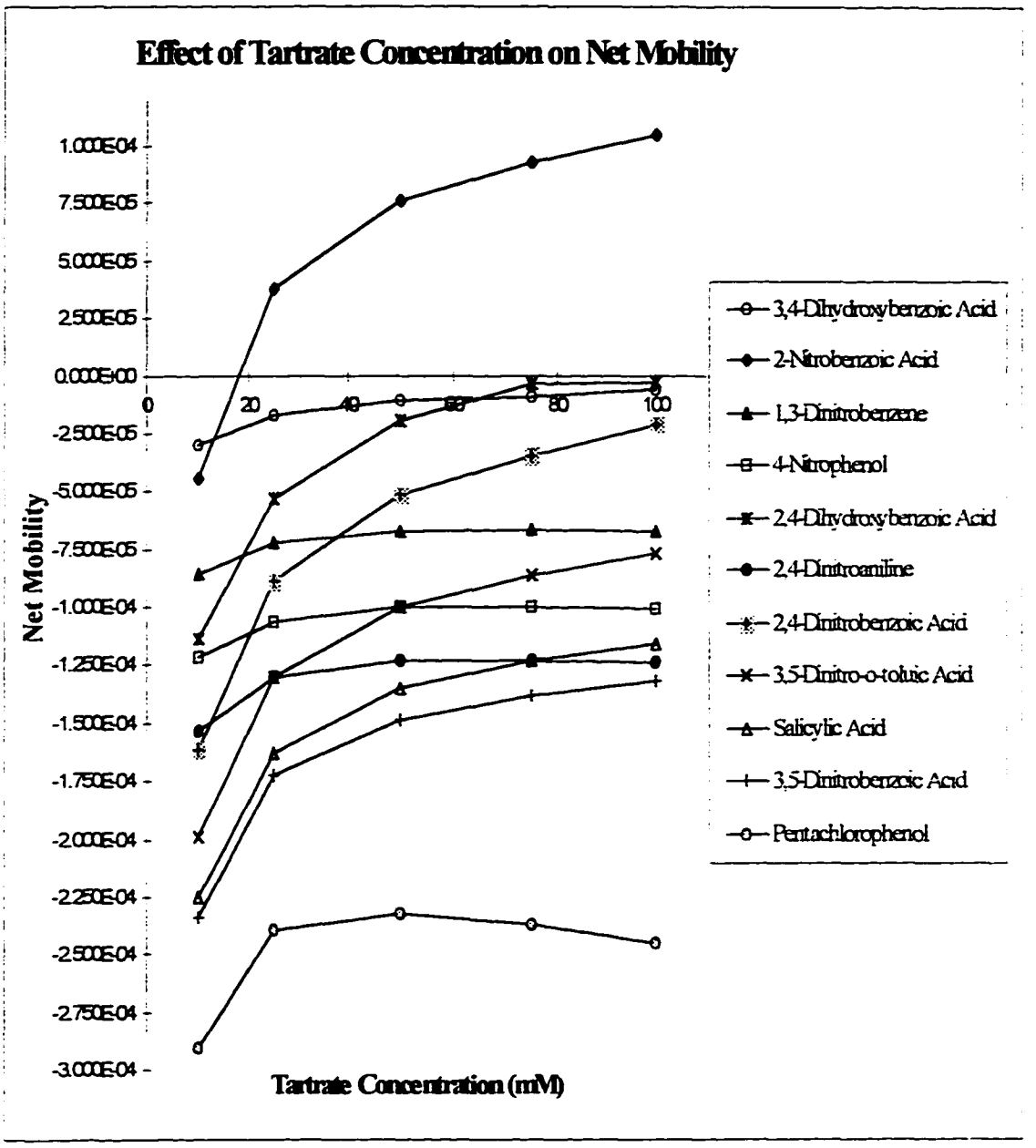

Figure 9

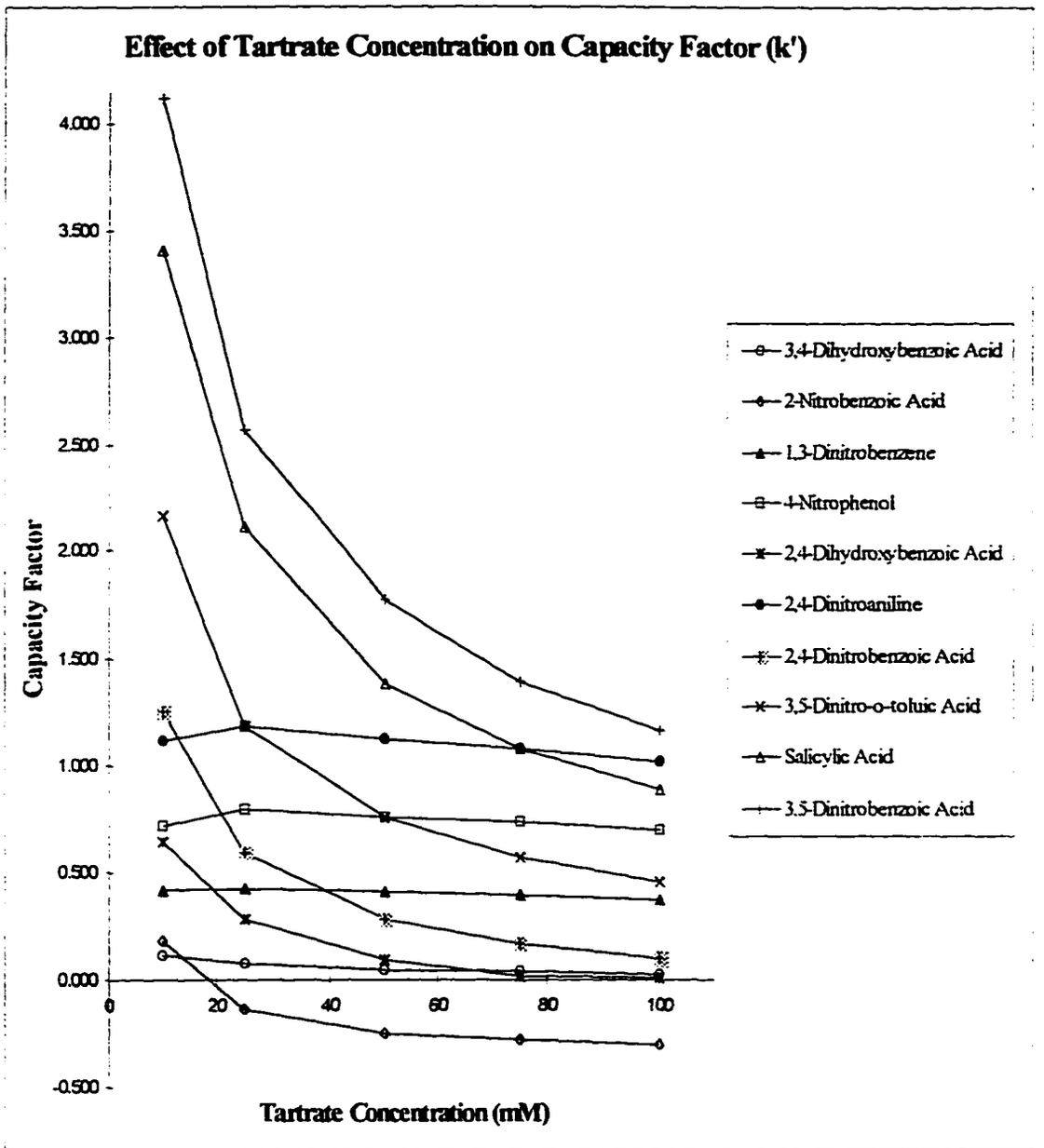

Figure 10

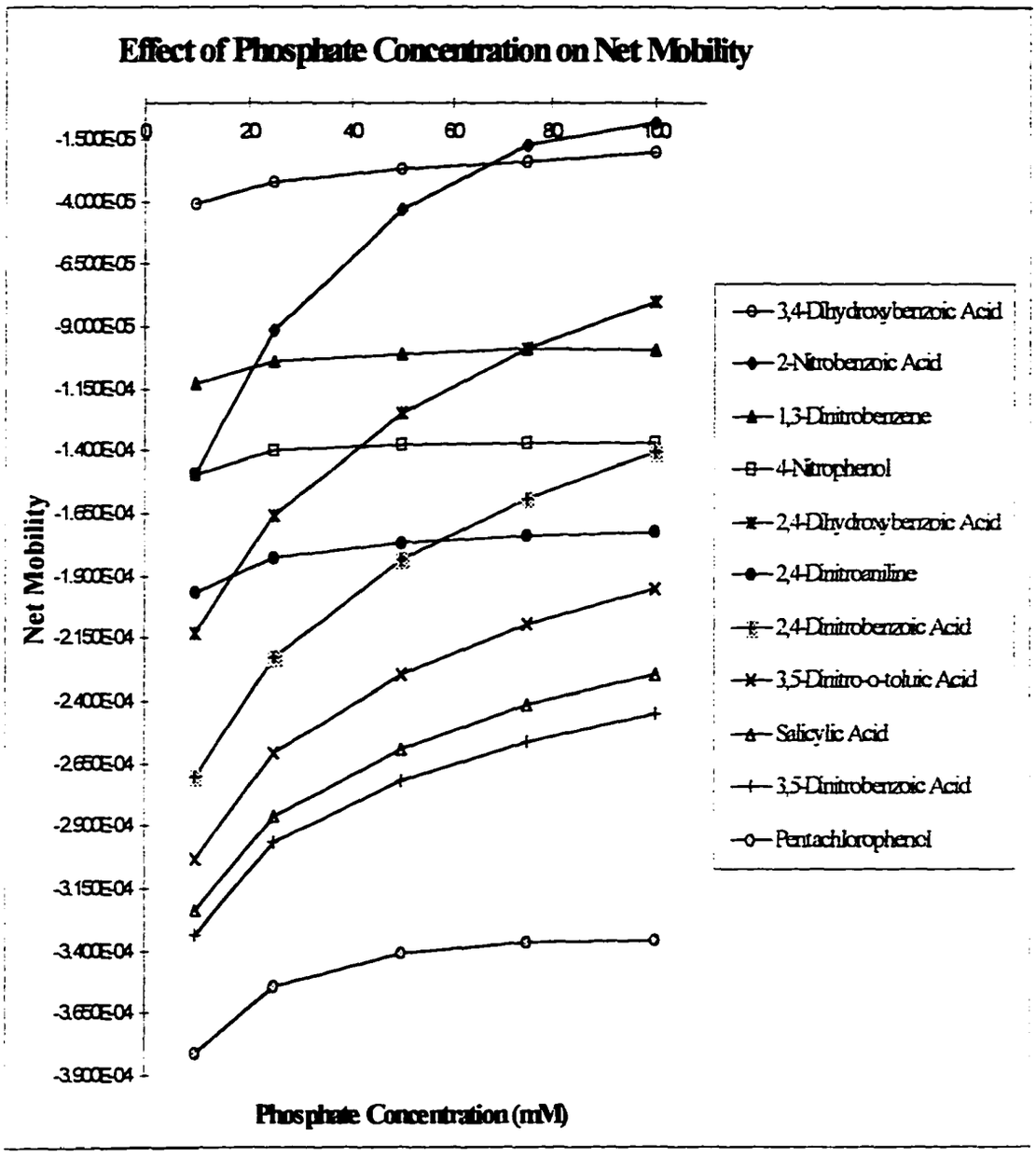

Figure 11

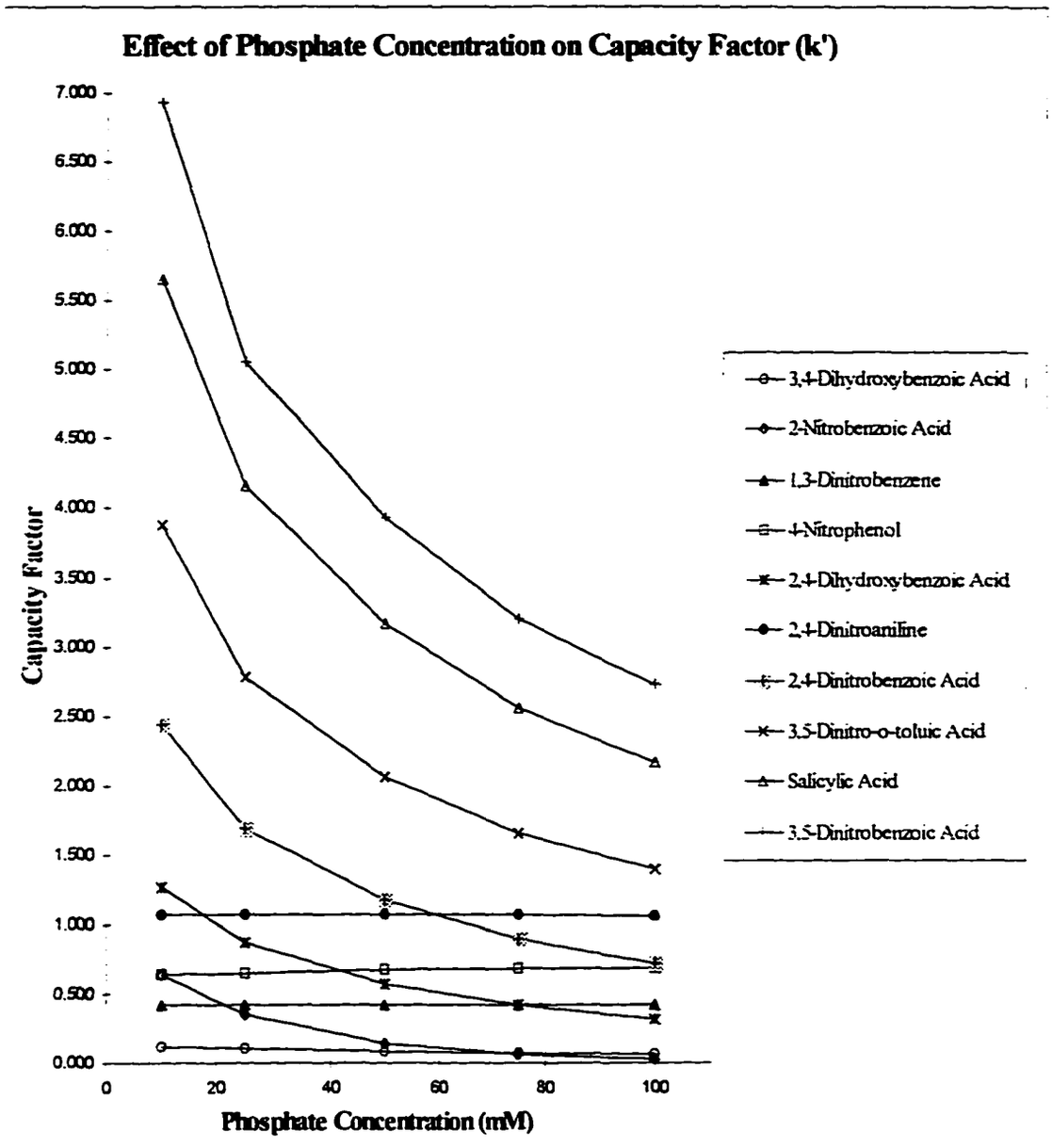

Figure 12

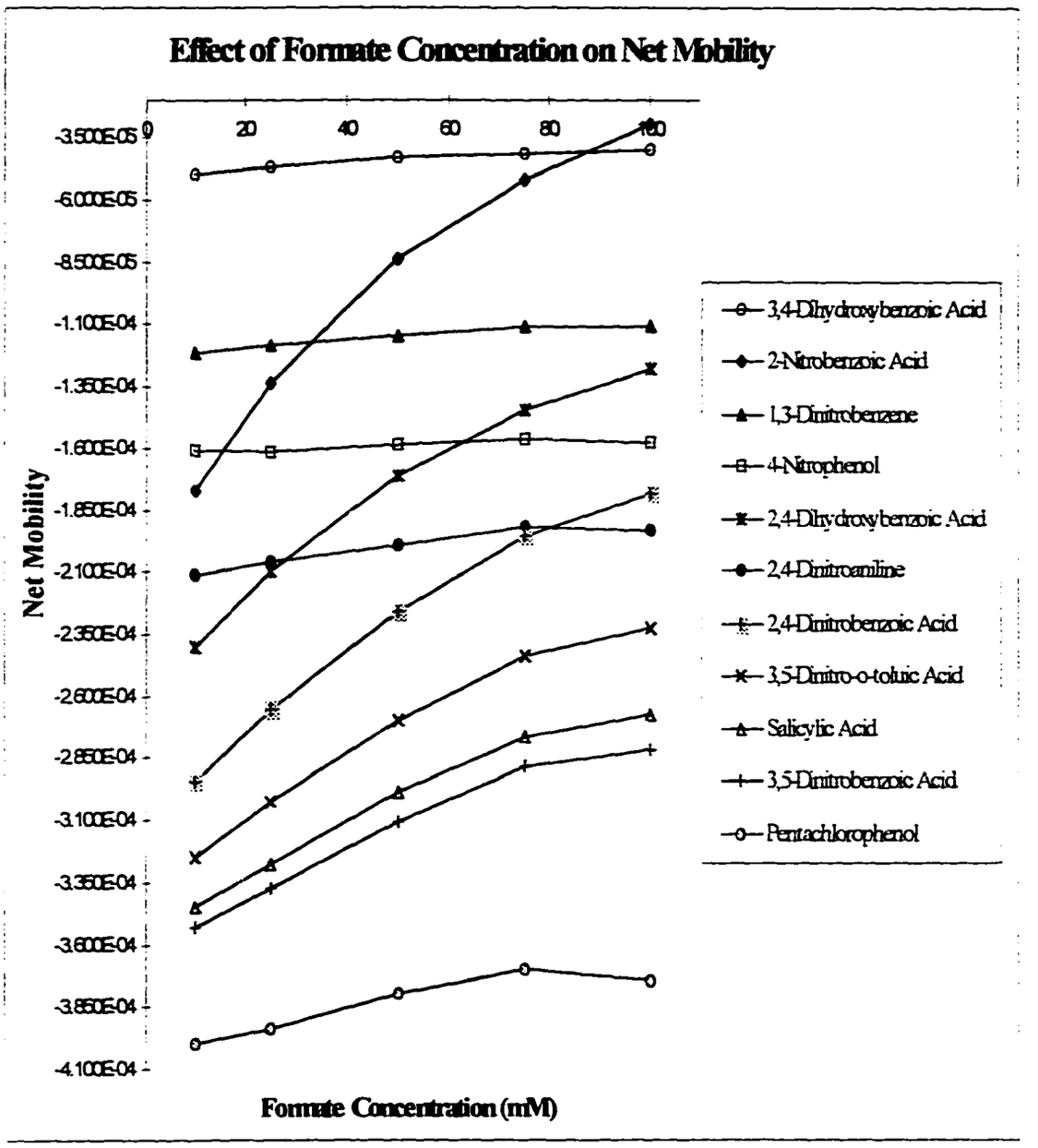

Figure 13

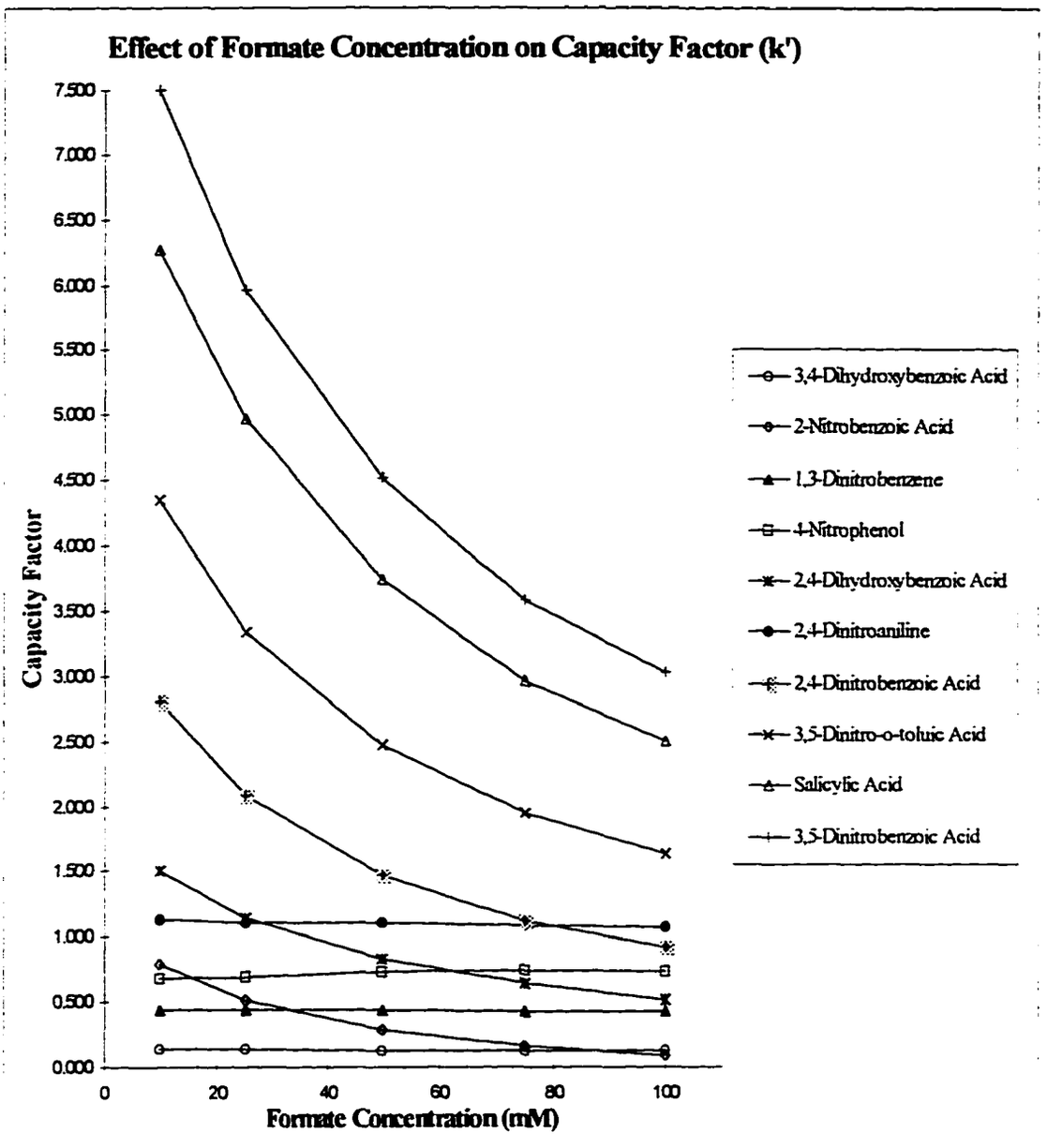

Figure 14

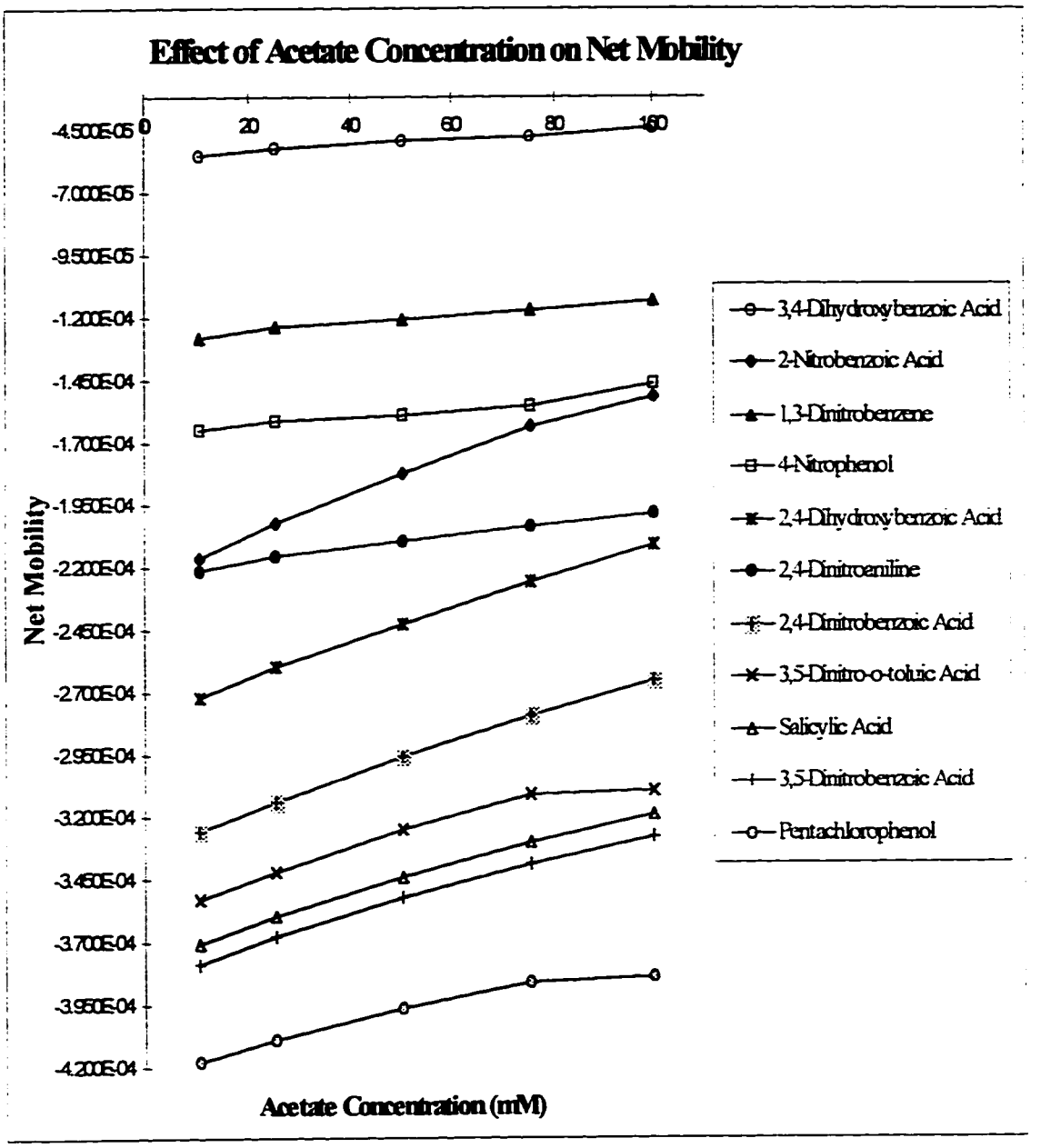

Figure 15

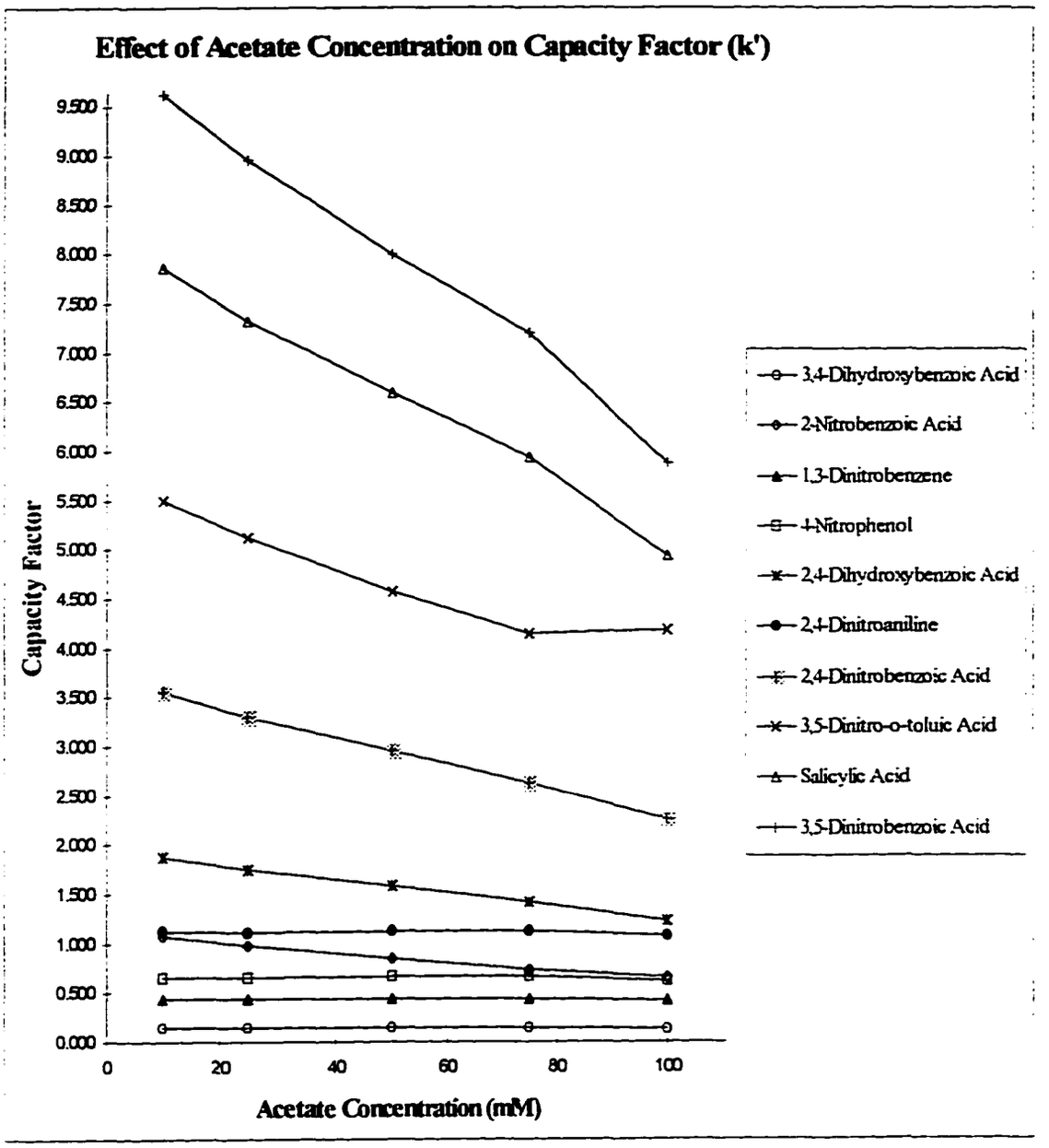

Figure 16

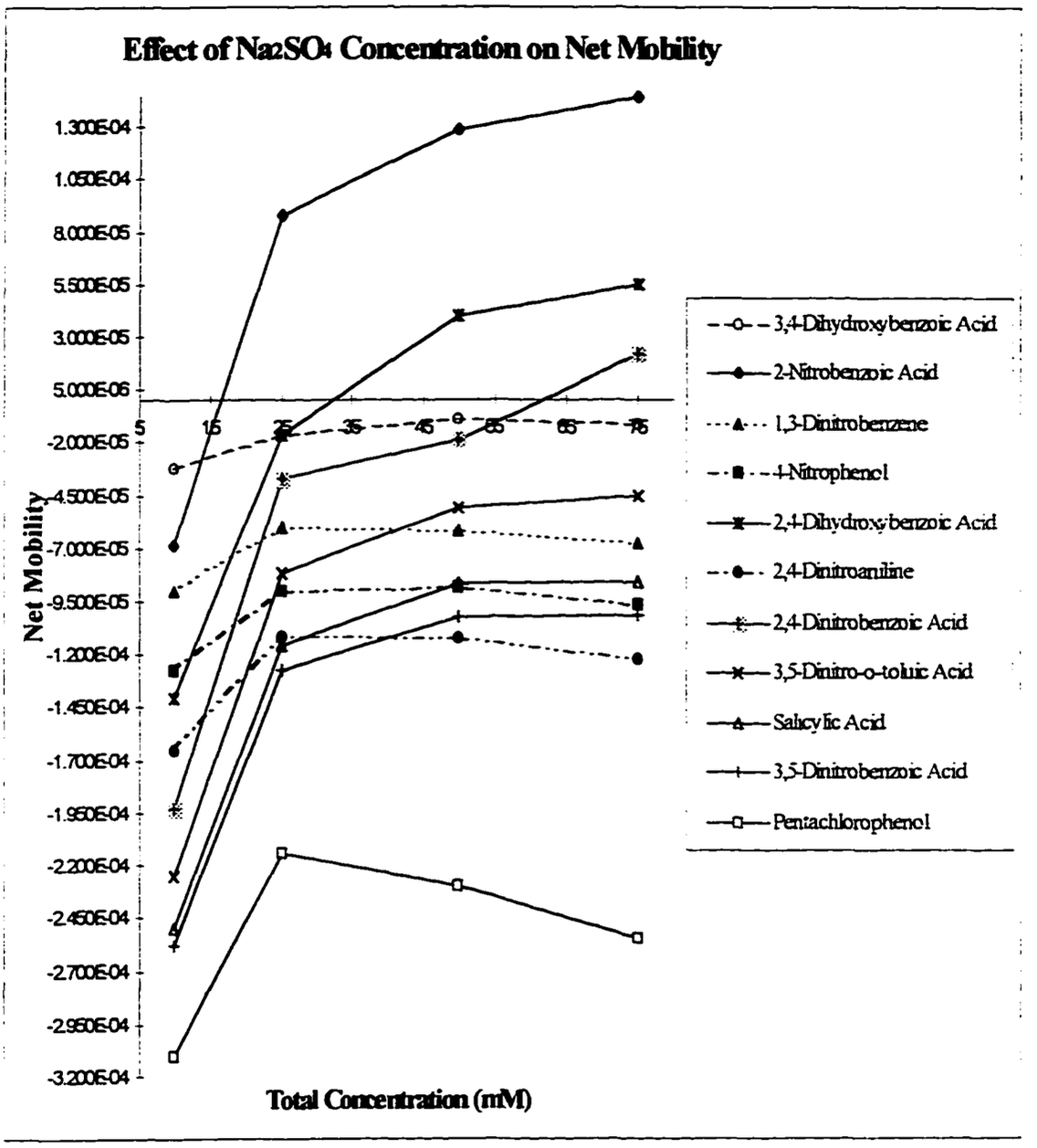

Figure 17

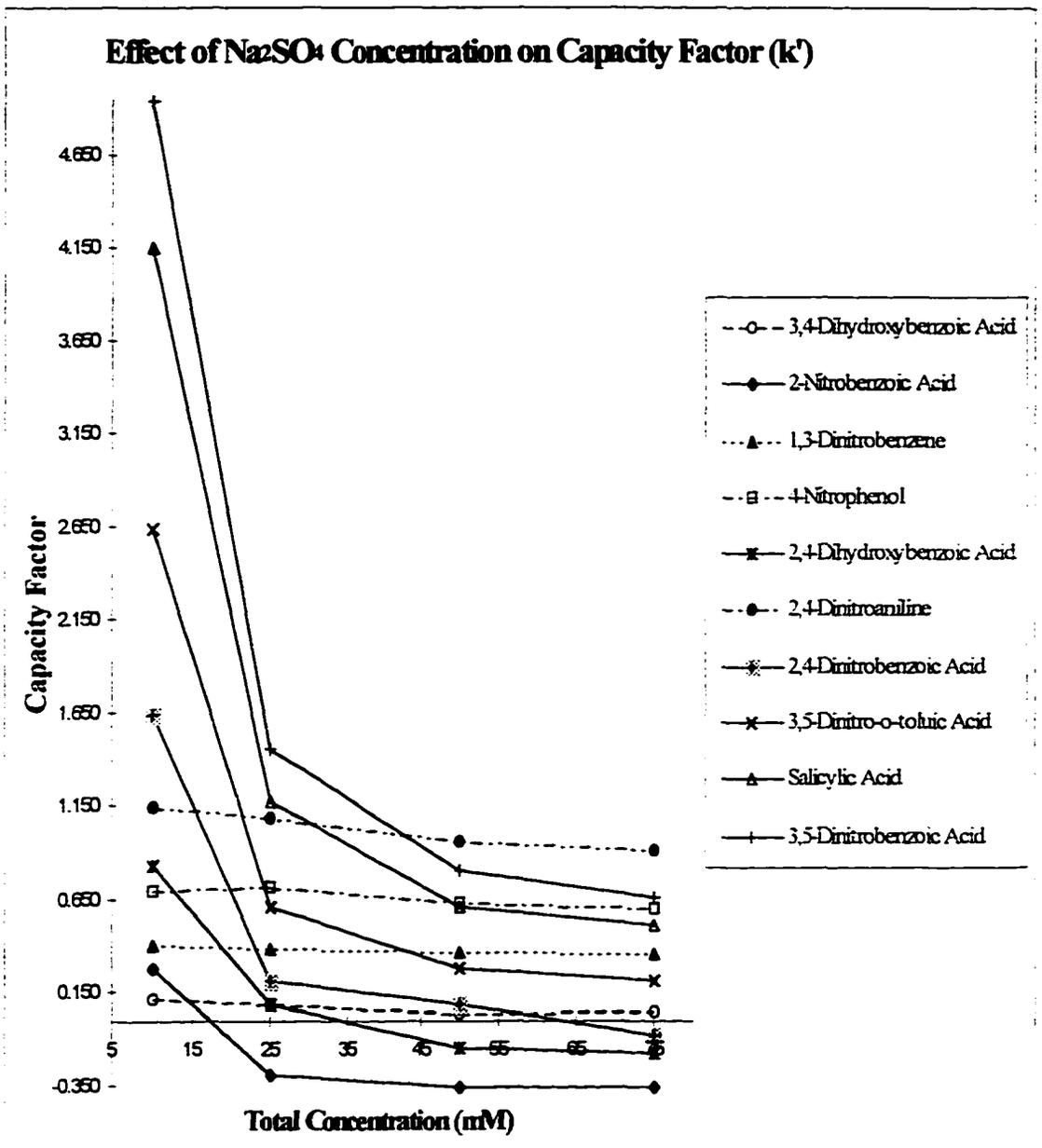

Figure 18

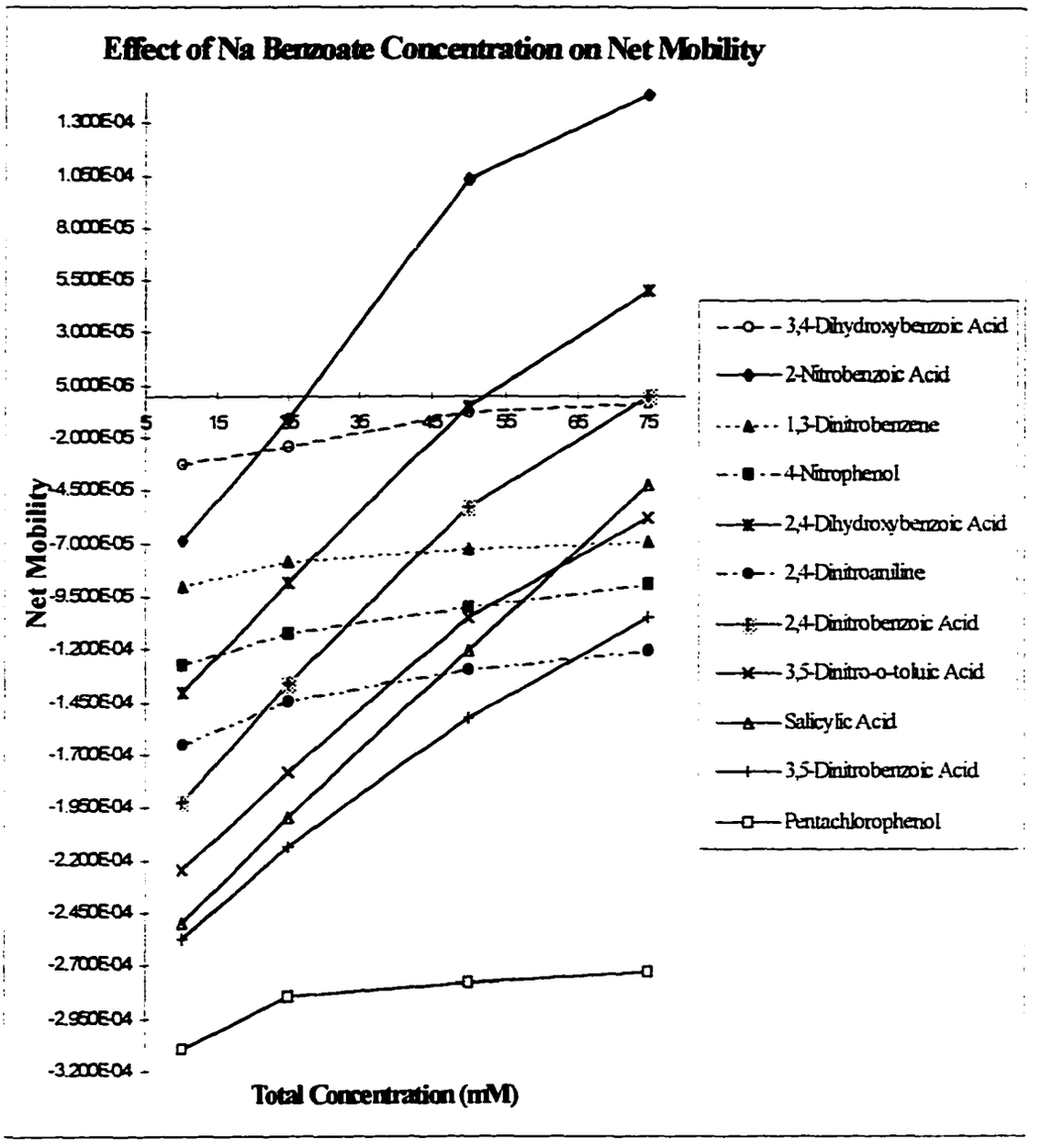

Figure 19

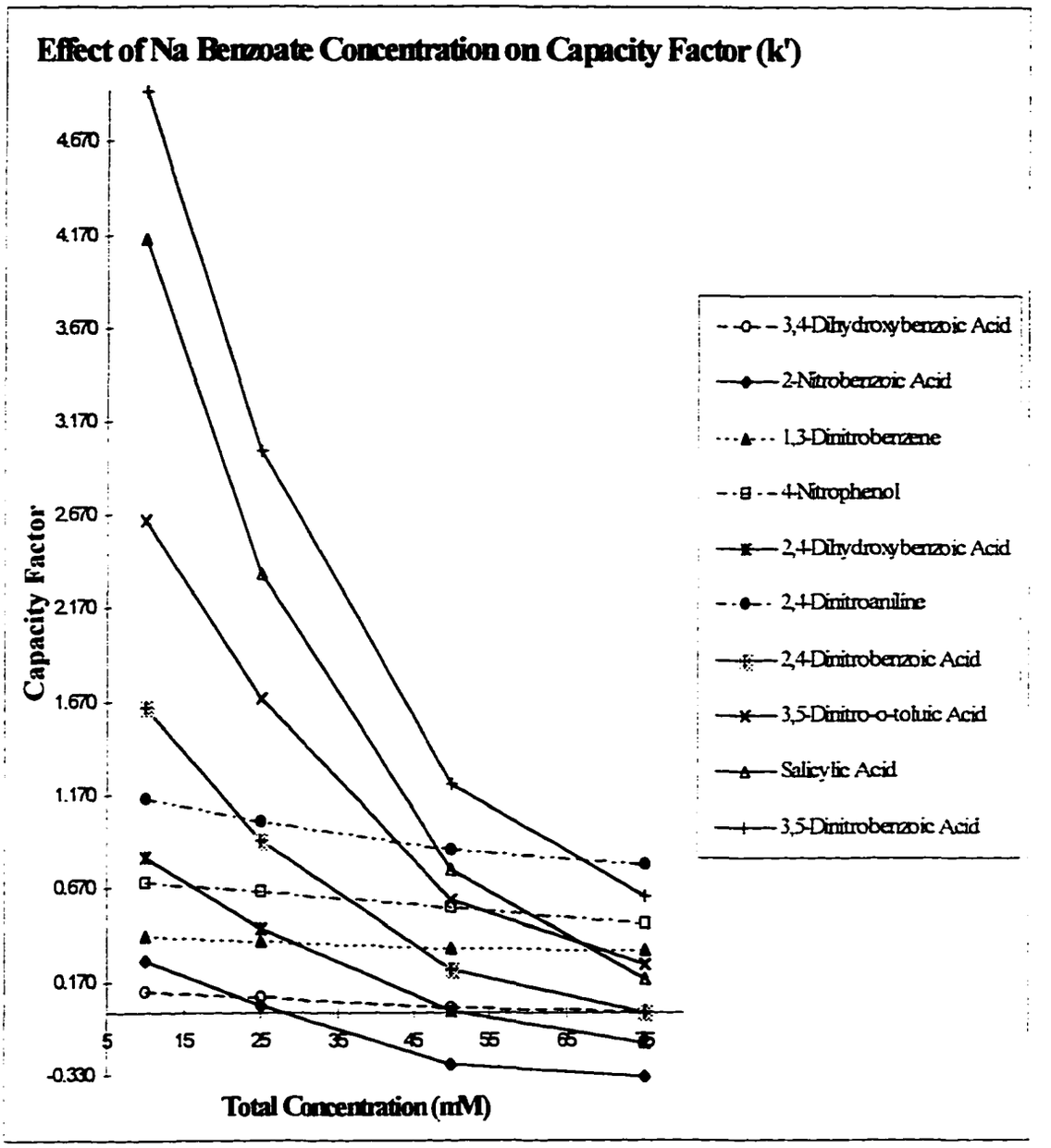

Figure 20

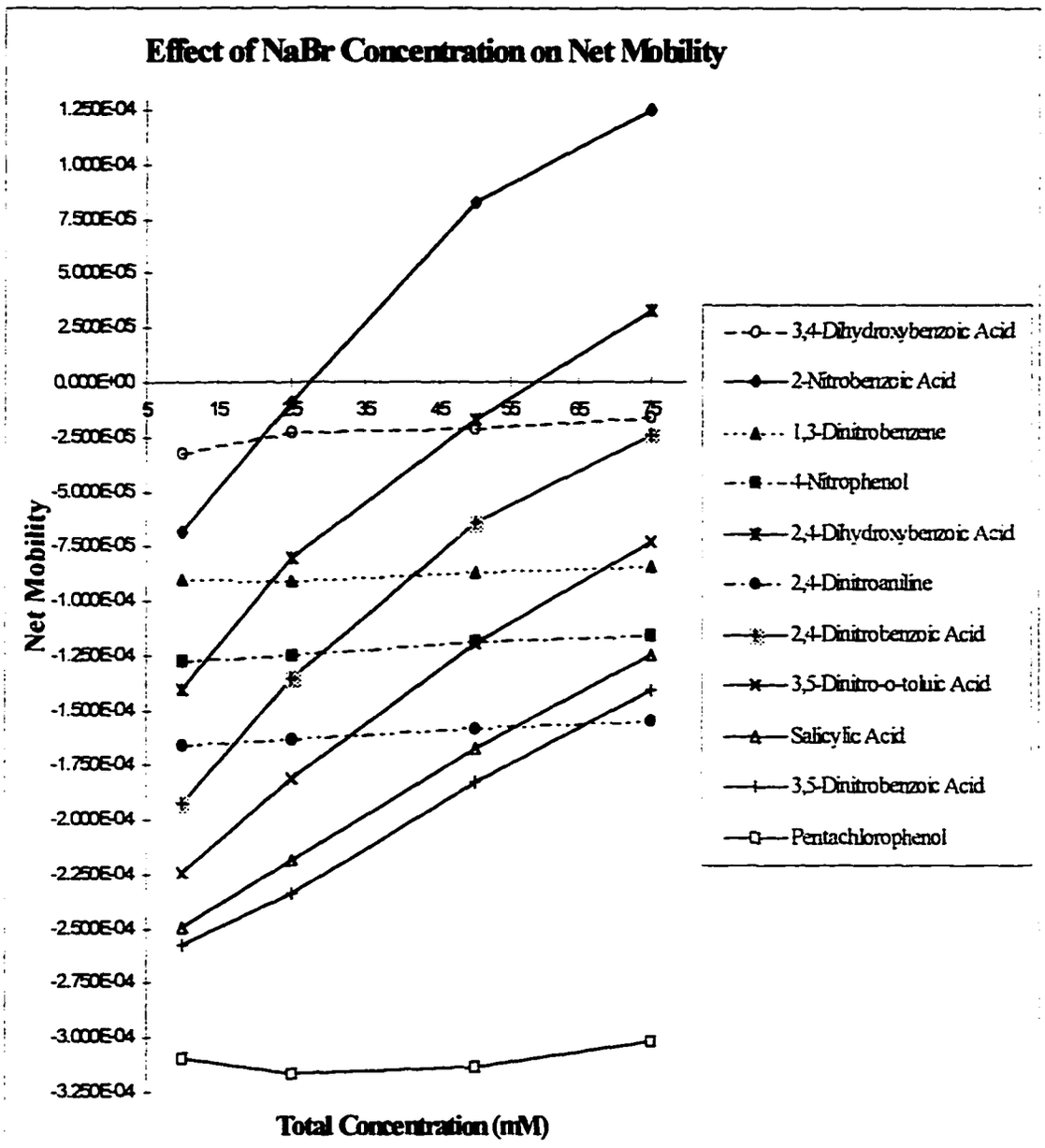

Figure 21

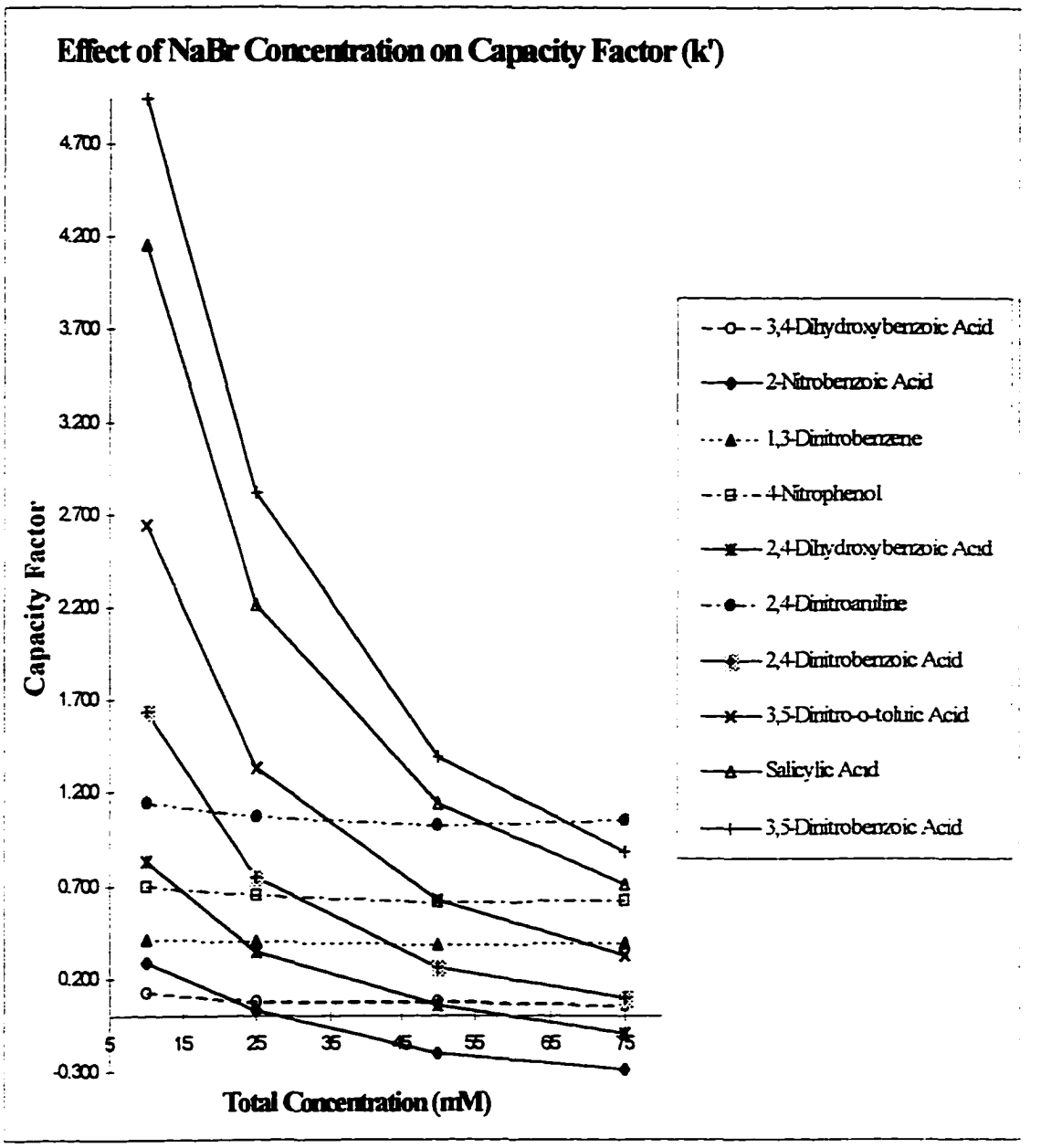

Figure 22

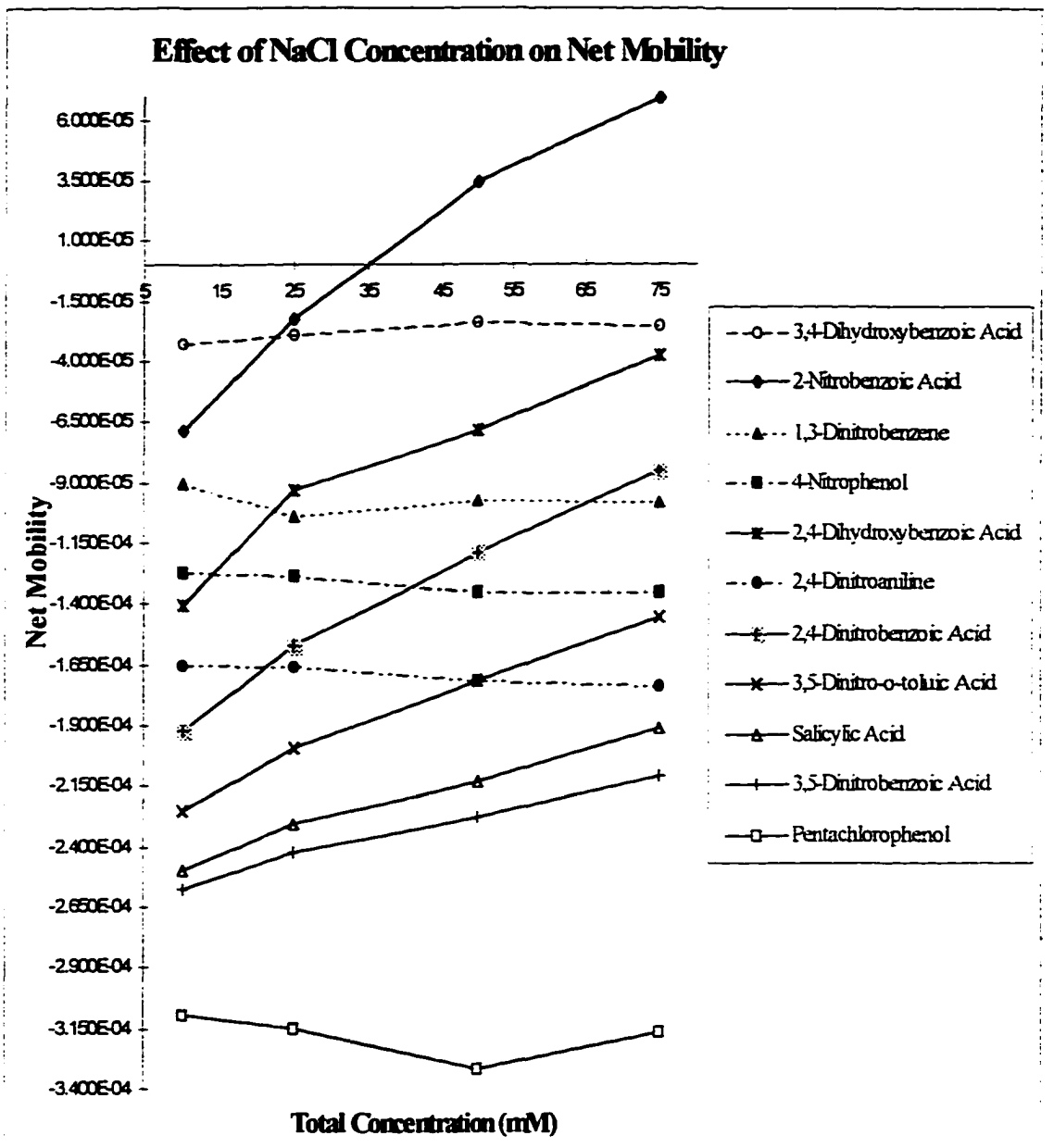

Figure 23

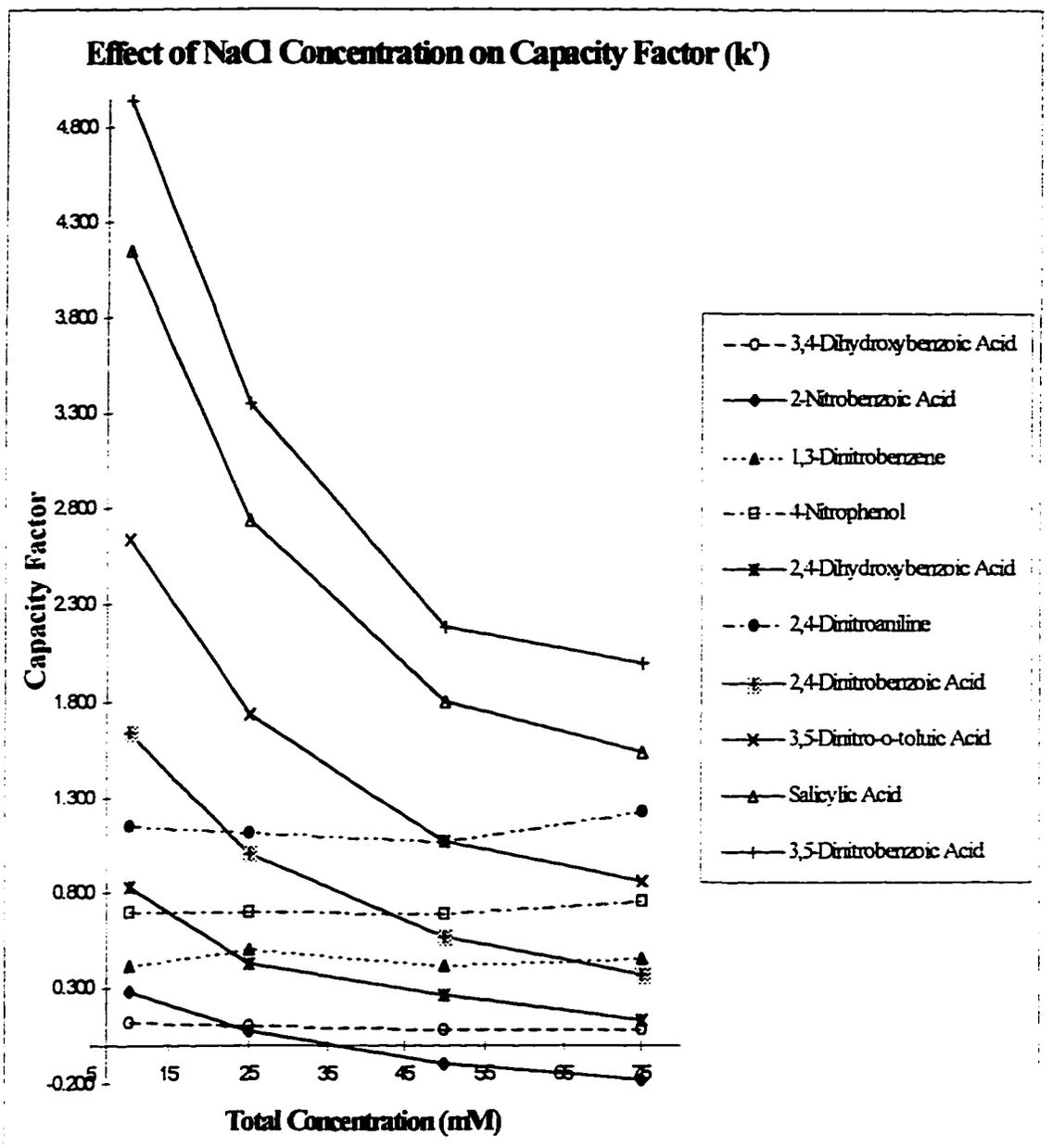

Figure 24

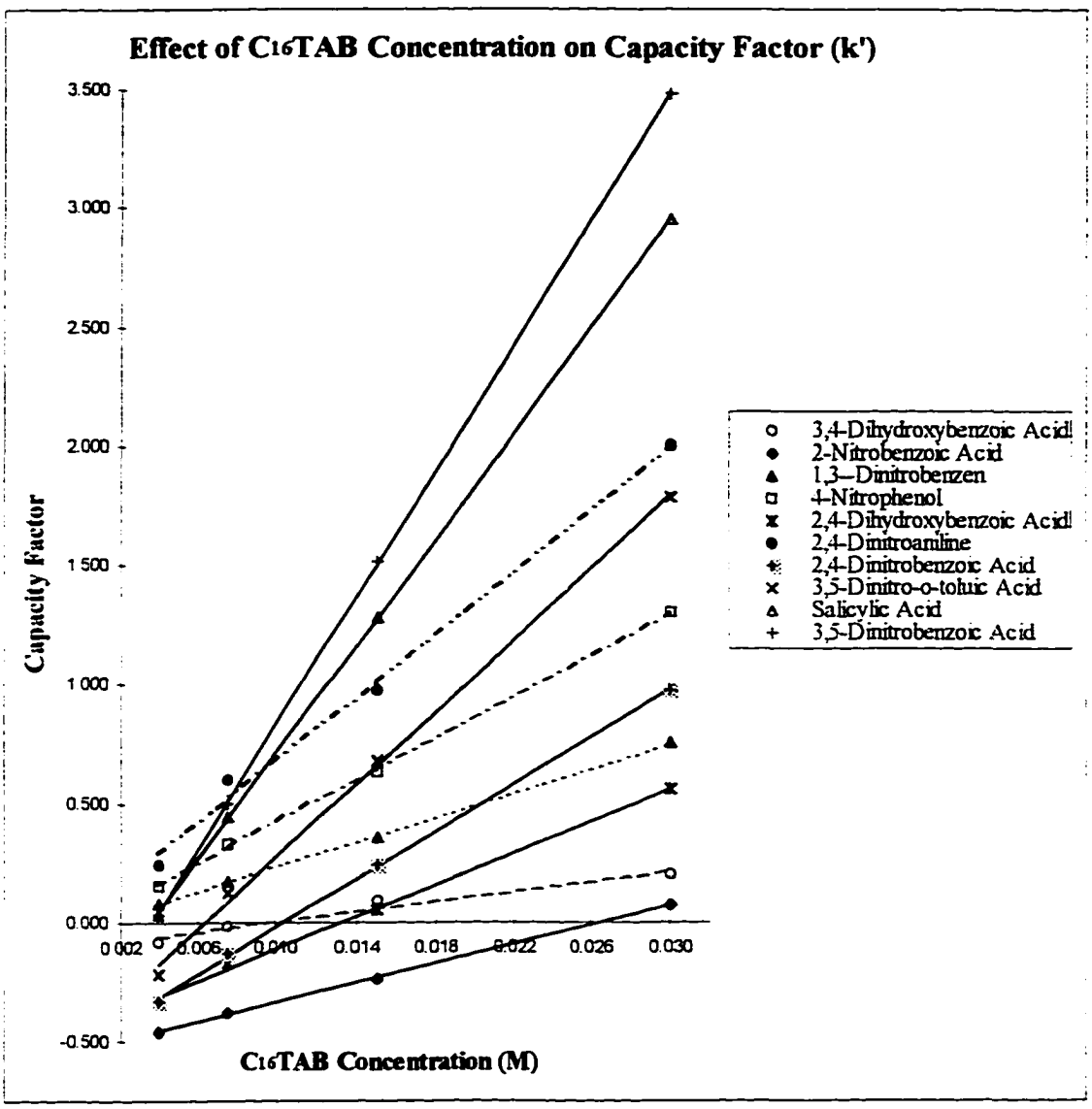

No.	Compounds	RSQ	Slope	Intercept
1	3,4-Dihydroxybenzoic Acid	0.957	10.488	-0.101
2	2-Nitrobenzoic Acid	0.999	20.234	-0.537
3	1,3-Dinitrobenzene	1.000	25.695	-0.022
4	4-Nitrophenol	0.999	43.787	-0.014
5	2,4-Dihydroxybenzoic Acid	0.997	33.383	-0.444
6	2,4-Dinitroaniline	0.994	65.787	0.024
7	2,4-Dinitrobenzoic Acid	0.999	49.821	-0.515
8	3,5-Dinitro-o-toluic Acid	0.999	75.820	-0.480
9	Salicylic Acid	1.000	111.825	-0.403
10	3,5-Dinitrobenzoic Acid	1.000	132.610	-0.492

Figure 25

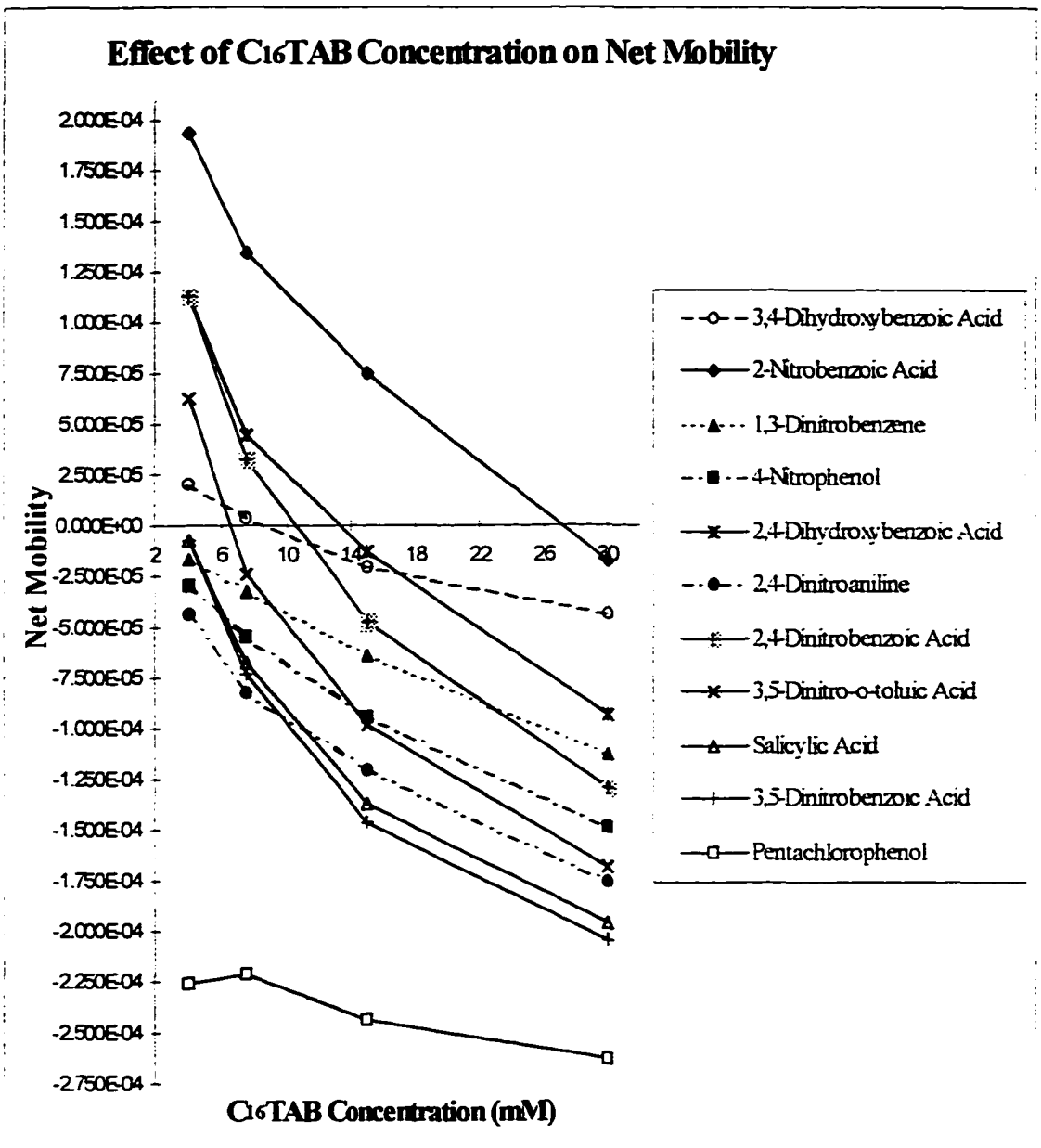

Figure 26

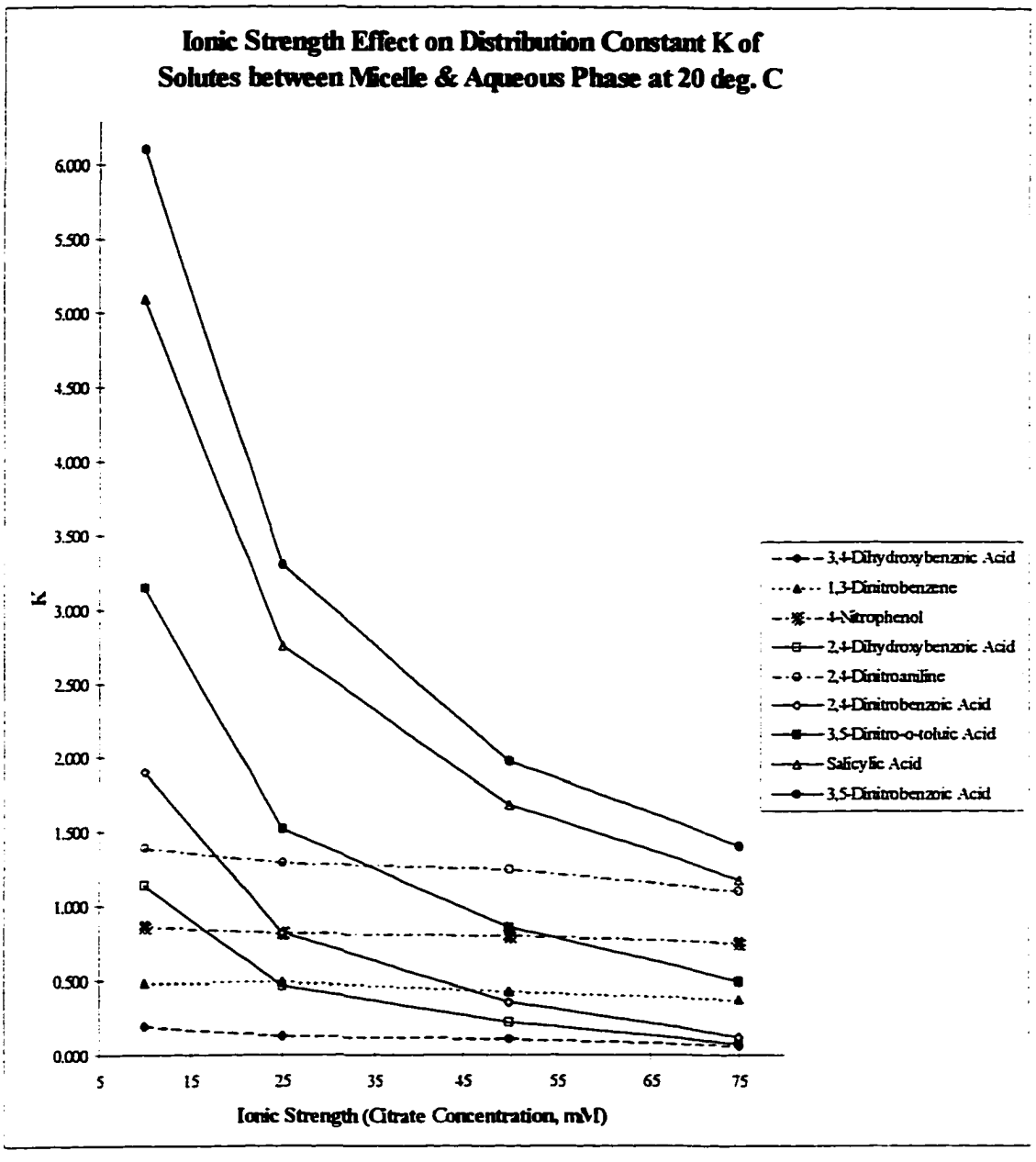

Figure 27

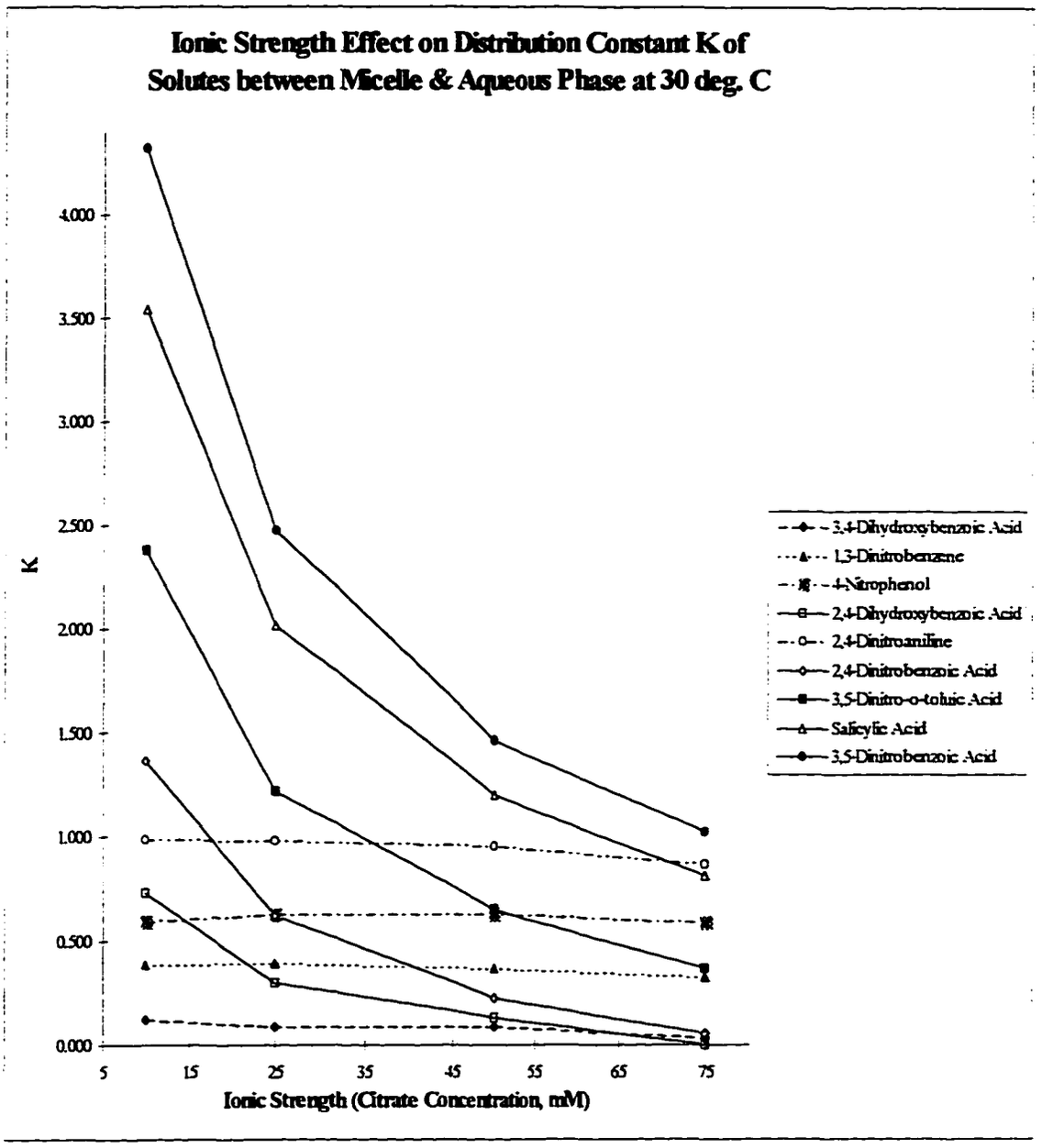

Figure 28

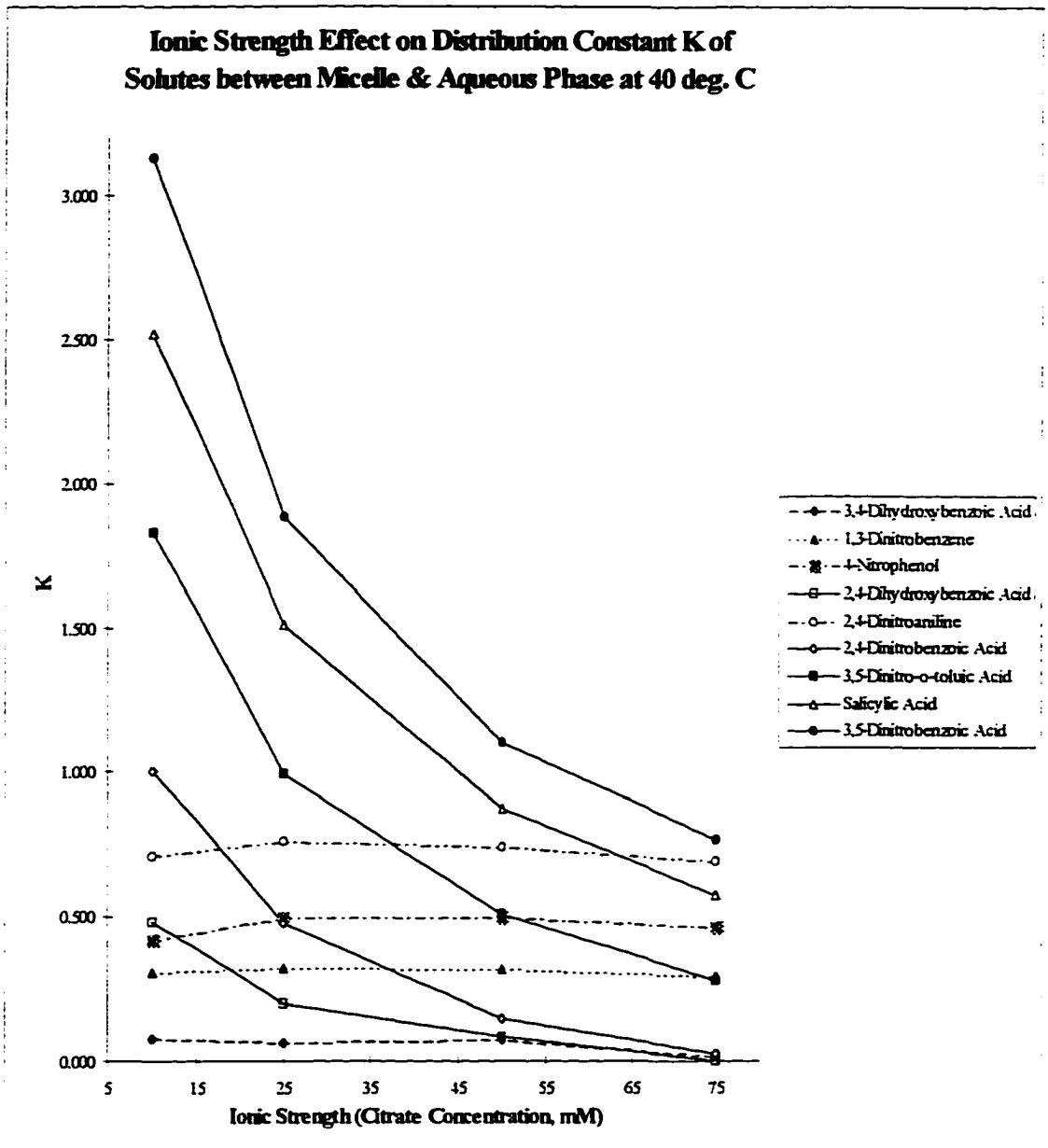

Figure 29

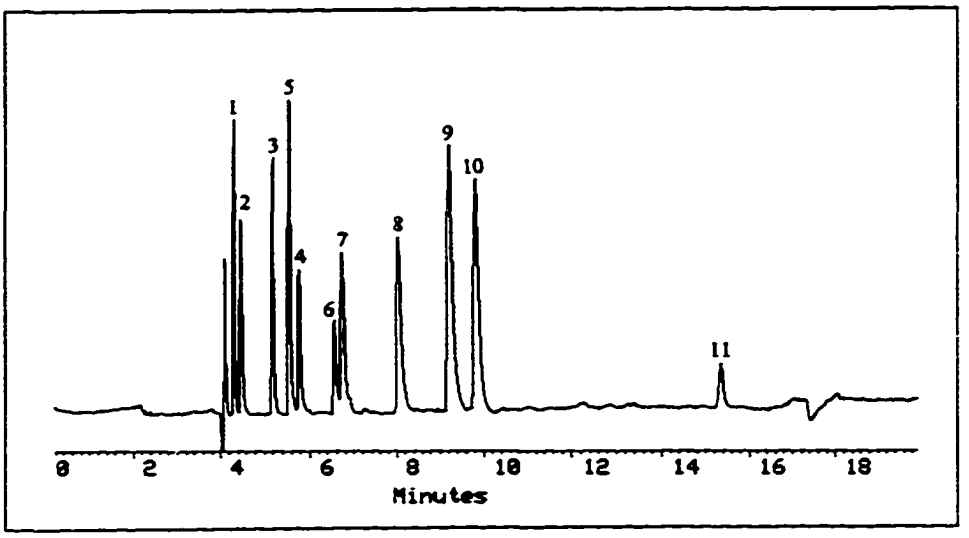

Chapter 4

Evaluation of Novel Gemini Cationic Surfactants in Micellar Electrokinetic Capillary Chromatography: Comparison of Single and Double Alkyl Chain Cationic Surfactants

Abstract

A series of novel Gemini (double alkyl chain) cationic surfactants (named Gemini-C8 to -C18) was for the first time evaluated in micellar electrokinetic capillary chromatography (MECC) of charged and uncharged model solutes. It was found Gemini-C12 and -C14 were useful in MECC. For comparison, the study was also carried out on the commercially available single alkyl chain cationic surfactants: alkyltrimethylammonium bromides. For both single and double chain surfactants, the capacity factors of the model solutes increased linearly with increase in the alkyl chain length and concentration of surfactant. However, with increasing alkyl chain length and concentration of the Gemini surfactants, the net mobilities of the model solutes and the micelles changed differently and depended upon the surfactant concentrations. Finally, an MECC application to the separation of the eleven priority pollutant phenols was investigated using the Gemini surfactants; the temperature effect especially was studied in detail.

1. Introduction

There is a wide range of commercially available surfactants, but the range of surfactants applicable to MECC is limited. Surfactants with alkyl chains of less than eight carbons (C8) do not generally form micelles (1), or do so only at high critical micelle concentrations (CMCs). Large surfactant concentrations can result in Joule heating problem in MECC. As the number of carbon atoms in the surfactant alkyl chain length increases, the CMC usually decreases. However, surfactants with an alkyl chain of more than sixteen carbons (C16) normally display limited solubility in water. In addition, surfactants with high UV absorbances are unsuitable for MECC because of high backgrounds with UV detector. Thus surfactants appropriate for particular separations by MECC have been tailor-made, especially for the separation of chiral compounds (2, 3), since surfactants with different molecule structures have different selectivities based on the type of interactions involved. In particular, the polar groups of the surfactant affect selectivity more significantly than the hydrophobic groups. In any event, introduction of new types of surfactants for MECC is of great interest and is expected to be useful in altering the selectivity. The Gemini (double alkyl chains) surfactants are one such kind of promising surfactant in MECC.

The Gemini surfactants possess two hydrophilic and two hydrophobic groups per molecule. The hydrophilicity is greatly increased because of the two ionic groups in the molecule, while their surface activity and micelle forming ability are greatly enhanced owing to the two hydrophobic groups in the molecule (4). These unique characteristics of the Gemini surfactants produce much smaller CMCs and Kraft points (T_{kp}, the temperature at which the solubility is equal to the CMC) than the conventional single alkyl chain surfactants. Consequently, the stability of the Gemini micelles in the presence of a relatively high organic content in the background electrolytes (BGEs) could be superior to that of the single chain micelles. The Gemini surfactants are therefore expected to show different characteristics for use in MECC.

To date, only anionic Gemini surfactants have been used in MECC. Tanaka et al. (5, 6) utilized three different double chain surfactants with two sulfonate groups as micelle-forming reagents in MECC. In comparison with the widely used sodium dodecyl sulphate (SDS), these double chain surfactants exhibit remarkably different selectivities for the substituted naphthalene and also gave a wider migration time window. The eight naphthalene derivatives were baseline- or nearly baseline-separated by BGEs with these double chain surfactants, whereas they were not completely resolved using SDS. Besides, the surfactant concentrations required were at most one order of

magnitude lower because of the low CMCs of the double chain surfactants.

In this study, a series of novel cationic Gemini surfactants, with alkyl chains from C8 to C18, was for the first time evaluated as micelle-forming reagents in MECC. The structures and some properties of these Gemini cationic surfactants are given in Figure 1 and Table 1, respectively. Cationic Gemini surfactants with alkyl chains from C12 to C16 were synthesized to provide sufficient surfactants for detailed study. Gemini-C12 and -C14 were successfully used as pseudostationary phases, micelle-forming reagents in MECC. For comparison with the Gemini surfactants, a series of single alkyl chain (C12 to C16) cationic surfactants were also studied. These surfactants include dodecyltrimethylammonium bromide (C_{12}TAB or DTAB), myristyltrimethylammonium bromide (C_{14}TAB or TTAB) and cetyltrimethyammonium bromide (C_{16}TAB or CTAB). The structures and some properties of these single alkyl chain cationic surfactants are also given in Figure 1 and Table 1, respectively.

For both single and double alkyl chain cationic surfactants, the capacity factors of the model solutes increased linearly with increase in the alkyl chain length from C12 to C16, and with increase in the concentration of each surfactant, indicating an increase in the hydrophobic and/or hydrophilic interaction with

the micelles. However, the dependence of the net mobilities on the alkyl chain length and the Gemini concentrations varied both for the different solutes and micelles. Only the net mobility of 1,3-dinitrobenzene almost decreased linearly with increasing alkyl chain length at the various surfactant concentrations. For all the other solutes and micelles, changes in the net mobilities with increasing alkyl chain length was related to the surfactant concentration.

An application of the Gemini surfactants for the separation of the eleven priority pollutant phenols was investigated. With no acetonitrile in the BGE, the effects of temperature, pH and surfactant concentration were studied. The BGE pH and temperature played critical roles in the separation of the eleven phenols without acetonitrile. The eleven phenols were baseline separated at 45 °C with a BGE consisted of 50 mM phosphate (pH 3.3) and 8 mM Gemini-C12. However, such a excellent separation could not be achieved using any of the other surfactants studied. In addition, the optimum separation conditions with acetonitrile in the BGE were further evaluated by varying the temperature with surfactant at different concentrations and 15% acetonitrile in 50 mM phosphate-10 mM acetate buffer (pH 4.2). Gemini-C12 provided the best separation at 35 °C in terms of efficiency, peak shape, baseline and run time.

2. Experimental

2.1 Apparatus

MECC experiments were carried out with a Beckman P/ACE 5010 CE system (Beckman Instruments, Palo Alto, CA, USA) equipped with a UV absorbance detector at 214 nm. The CE system was connected to a Waters/VAX 4000-50 data system through an LAC/E interface module. The Waters ExpertEase software (version 3.1) was used for data acquisition and processing. A Orion Model 290A pH meter with an precision of ±0.01 unit was used to measure pH.

The separation capillary was a uncoated fused silica capillary tube obtained from Polymicro Technologies (Phoenix, AZ, USA), with 50 μm I.D. x 375 μm O.D., and 30 cm effective length and approximately 37 cm total length.

2.2 Chemicals

The model solutes used in this study (see Table 2) contained acidic, basic, or electron-withdrawing functional groups, and were obtained from Aldrich (Milwaukee, WI, USA). They were dissolved in HPLC grade methanol to give a mixed stock solution at concentration about 2.5 mg/mL each. Pentachlorophenol was used as a micelle marker.

Sodium acetate anhydrous and glacial acetic acid were obtained from Mallinckrodt Chemicals (Paris, KY, USA); sodium phosphate monobasic, sodium phosphate dibasic, 85% o-phosphoric acid and potassium hydroxide were obtained from Fisher Scientific (Fairlawn, NJ, USA); C_{12}TAB, C_{14}TAB and C_{16}TAB surfactants were obtained from Aldrich; HPLC-grade methanol and acetonitrile were obtained from Burdick & Jackson (Muskegon, MI, USA). Millipore Milli-Q water was used to prepare stock buffer and surfactant solutions. Small quantities of the C8 to C18 Gemini cationic surfactants for the preliminary screening study were obtained from Surfactant Research Institute (Brooklyn College, CUNY, Brooklyn, NY, USA).

2.3 Synthesis of Gemini Cationic Surfactants

Gemini cationic surfactants with C12 to C16 alkyl chain length were synthesized according to the procedures of Rosen and Song (7) for a more complete study of their use in MECC. By reaction of 22.5 mL (30.0 g, 0.235 mole) 1,3-dichloro-2-propanol (Aldrich, Milwaukee, WI, USA) with 135.0 mL (105.0 g, 0.488 mole) dodecyl-, tetradecyl- and hexadecyl-N,N-dimethylamine (Albemarle, Baton Rouge, LA, USA) in 95% ethanol solvent under reflux for four hours. The remaining dimethylamine and ethanol were removed in a rotary evaporator under reduced pressure. The crude Gemini surfactants were

dissolved in a minimum amount of acetone and recrystallized from chloroform/acetone three times, and the solvent evaporated under vacuum to give a white solid powder.

The structures of the Gemini surfactants were confirmed using ^{1}H and ^{13}C nuclear magnetic resonance (NMR). Element analysis: (a) theory for Gemini-C12 monohydrate: C, 65.52; H, 12.32; N, 4.83; Cl, 12.36. Found: C, 64.81; H, 12.85; N, 4.82; Cl, 12.37; (b) theory for Gemini-C14 monohydrate: C, 66.74; H, 12.48; N, 4.45; Cl, 11.26. Found: C, 66.85; H, 13.06; N, 4.38; Cl, 11.24; (c) theory for Gemini-C16 monohydrate: C, 68.28; H, 12.64; N, 4.08; Cl, 10.34. Found: C, 68.15; H, 13.36; N, 4.04; Cl, 10.31. The purity of each Gemini surfactant was found to be more than 99% by HPLC analysis with a differential refractive index (RI) detector. For the HPLC analysis, a Waters μBondapak CN column (300 x 4 mm, 10 μm particle size) was used at 45 °C with a mobile phase containing 45% aqueous acetate buffer (pH 5.0) / 55% acetonitrile at 2.0 mL/min.

2.4 Procedure

The coating of new capillaries was removed by briefly placing the window area in a flame from a burner and then gently cleaning the burned material with a tissue dampened with methanol. New capillaries were conditioned by purging in order with 1 N potassium hydroxide solution, 0.1 N potassium hydroxide solution, degassed and filtered D.I. water, buffer

without surfactant at a concentration three times greater than running buffer, and finally BGE, each for fifteen minutes.

A stock buffer solution was prepared by mixing equimolar solutions of an acid and its sodium salt(s) and adjusting to the appropriate pH. A final BGE was prepared by mixing the stock buffer solution with the stock surfactant solution, and acetonitrile if necessary, at each appropriate concentration. The BGE was then degassed and filtered through a 0.45-μm syringe filter.

A model solute solution was prepared by 1 in 20 dilution of the stock mixed sample solution in methanol with ten-fold diluted running buffer with no surfactant solution. The model solute solution was injected in the hydrodynamic mode for 2 sec. Experiments were performed at constant negative voltage of 13.5 kV.

3. Results and Discussion

Sudan III is usually used as a micelle marker in MECC (8). However, in this study, it was found that pentachlorophenol (pK_a 4.5) exactly co-eluted with Sudan III, i.e. resided exclusively in the micelles. Because pentachlorophenol is easier to work with than Sudan III, it was used as the micelle marker. Methanol was the electroosmotic flow (EOF) marker. The

capacity factor (k') in MECC is determined experimentally from (9, 10)

$$k' = \frac{(t_s - t_{EOF})}{t_{EOF}\left(1 - \frac{t_s}{t_{mc}}\right)} \qquad (1)$$

where t_s, t_{EOF} and t_{mc} are the migration time (sec) of the solute, the EOF marker and the micelle. The net mobility (μ_{net}) is expressed as

$$\mu_{net} = \mu_{app} - \mu_{EOF} = \frac{lL}{Vt_s} - \frac{lL}{Vt_{EOF}} = \frac{lL}{V}\left(\frac{1}{t_s} - \frac{1}{t_{EOF}}\right) \qquad (2)$$

in which μ_{app} and μ_{EOF} are apparent mobility and EOF mobility (cm^2/V-sec); l and L are the length (cm) of the capillary from injection to detection and the total length (cm) of the capillary, respectively; and V is the applied voltage (V).

In MECC the net mobility results from the combination of the solute electrophoretic mobility and the solute partitioning between the micelles and the aqueous medium. Therefore, the separation depends upon a combination of the charge/size ratios and the hydrophobic and ionic interactions of the solutes with the micelles.

3.1 Minimum Concentrations of Gemini and Single Alkyl Chain Surfactants for the EOF Reversal

In a normal capillary electrophoresis (CE) system, an electroosmotic flow (EOF) is from anode to cathode. However,

a change in the EOF will be observed if a cationic surfactant is introduced into the BGE. As the cationic surfactant concentration (below the CMC) increases, a dynamic bilayer phase will be gradually formed (11) on the fused silica capillary wall because of (i) ionic attraction between the cationic head group of the surfactant and the anionic silanol group on the capillary wall, and (ii) hydrophobic interaction of the surfactant tails binding to each other. Thus the cationic head groups of the surfactant will extend into the bulk solution. In this way charge reversal on the capillary wall is gradually established. With increasing cationic surfactant concentration, the net EOF is initially slowed down as the surface is covered, passes through zero, and finally reverses direction as the bilayer formation is completed and the reverse double layer forms. As a result, reversed potential polarity capability in the CE instrument is necessary.

In this study, the concentrations at which the net EOF was approximately zero were approximately 0.1 mM for C_{16}TAB and 0.01 mM for Gemini-C12, respectively. EOF reversal was observed above these concentrations. The lower Gemini surfactant concentration for the polarity reversal results for two reasons. First, at the same molar concentration, there are twice as many cationic head groups for the Gemini surfactants compared to the single chain surfactants. Second, the Gemini surfactants are relatively more rigid than the single chain

surfactants, and the existence of 2-propanol connecting group between the two cationic heads for the Gemini surfactant molecules gives greater coverage of the capillary wall than that for the single chain surfactant molecules.

3.2 MECC Using Gemini Cationic Surfactants

For the Gemini surfactants with alkyl chain length ≤ C10, the migration windows were larger because of the smaller sizes and thus the higher electrophoretic mobilities of the micelles in the direction opposite the EOF. However, the solute capacities of the Gemini-C8 and -C10 micelles were too low to resolve the model solutes. Even at high surfactant concentrations, the solutes migrated close to the EOF marker. These low capacities are probably caused by the shorter alkyl chains and the higher CMCs. Therefore Gemini-C8 and -C10 are not useful for MECC. On the other hand, the low solubility of Gemini-C18 precludes its use in MECC. Similarly, Gemini-C16 can be used only at high temperature and / or with organic additives because of its limited solubility. In practice, Gemini-C16 can be used in MECC at 25 °C but to prevent precipitation, the run time must be short and the BGE must be heated to at least 50 °C before starting the run. Gemini-C12 and -C14 are the best choices of micelle-forming reagents in MECC.

3.2.1 Effect of the Gemini surfactant concentrations

The Gemini-C12 to -C16 surfactants were investigated in MECC. The BGE consisted of 50 mM phosphate (pH 3.7) with surfactant concentrations of 0.4, 1, 2, 4, 8, 16, and 20 mM, run at 25 °C and 40 °C. The experimental results are illustrated in Figures 2 to 18.

In MECC, the micelles are in a dynamic equilibrium with the monomeric surfactant molecules in solution. That the CMC values for Gemini-C12 to -C16 are very small (see Table 1) suggests that at same surfactant concentration, the micelle numbers in the BGEs for Gemini surfactants could be much larger than those for the single chain cationic surfactants. In addition, the extremely low CMCs of Gemini-C12 to -C16 reflect the greater stability of these micelles in comparison to the single chain surfactants.

Despite the low CMCs, separations cannot be successfully achieved without a surfactant concentration sufficient to produce enough micelles to provide the necessary solute capacity for resolution. Besides, even though separations were achieved at a surfactant concentration of 2 mM (already over hundred-fold higher than the CMC), the efficiency was so poor that the peaks were broad.

It is interesting that the net mobilities of the Gemini-C12 to -C16 micelles increased markedly by increasing surfactant concentration from 0.4 mM to 2 mM as shown in Figures 4, 6, 11, 13, 16 and 18. However for surfactant concentrations ≥ 4 mM, the net mobilities did not change with further increase in the surfactant concentration. As mentioned above, separation could be achieved at low surfactant concentration (≤ 2 mM), but the peak efficiencies were extremely low not only for the later-eluting solutes but also for the micelles. Efficiency was significantly improved by increasing both the temperature (from 25 °C to 40 °C) and the surfactant concentrations. The low efficiency at lower surfactant concentrations might be attributed to the micelle polydispersity.

Micelles are dynamic entities, i.e., the micelles constantly exchange monomers with the aqueous solution phase. In this way, the size of a particular micelle can vary somewhat with time. The micelle aggregation numbers represent an average value. The electrophoretic mobility of a particular micelle is determined by the micelle size, shape and charge, and subsequently by its specific aggregation number. At the low surfactant concentration, not only is the rate of dynamic exchange much lower than at high concentration, there are more "small" micelles present. As a result, at the low surfactant concentrations, the electrophoretic mobilities of the micelles were larger, but the net mobilities were smaller, and were

dramatically increased in the low surfactant concentration ranges. In addition, the existence of a range of micelle mobilities at low concentrations causes the peaks of the micelles and the later-eluting solutes to be very broad. However, as the Gemini surfactant concentrations became ≥ 4 mM, the formation of the micelles stabilized, i.e., the rate of micelle-monomer exchange was increased to a constant rate, the sizes, shapes, and charges of the micelles averaged out, and the micelle net mobilities became only slightly affected by increasing the surfactant concentration. As shown in Figures 2 and 9 of the electropherograms, as well as in Figures 7 and 8, high peak efficiencies for both micelles and the solutes are achieved by increasing the surfactant concentration. Furthermore, as shown in these figures improvement in the peak efficiency were obtained by increasing the temperature from 25 °C to 40 °C. High temperature increases the rate of micelle-monomer exchange and thus decreases the micelle polydispersity.

Surfactant concentration has a significant effect on the migration behaviour of the solutes because of its effect on the phase ratio. The relationship between the capacity factor (k') and the surfactant concentration (C_{sf}) can be approximated as follows (8)

$$k' = K \Phi_v (C_{sf} - CMC) \qquad (3)$$

in which K is the distribution coefficient and Φ_v is the partial specific volume of the micelle. As expected, the capacity factors of the model solutes increased linearly with increasing surfactant concentrations at both 25 °C and 40 °C. However, the capacity factors were lower at 40 °C than those at 25 °C owing to the higher solubilities of the solutes in the aqueous phase. Except for 2,4-dihydroxybenzoic acid with Gemini-C14 and -C16 at 25 °C, the net mobilities decreased with increasing surfactant concentrations as predicted. For 2,4-dihydroxy-benzoic acid (Figures 11 and 16), the stronger interactions with the cationic micelles (by both the hydrophobic and the electrostatic interactions) caused the net mobility to increase as the micelle net mobilities increased at the low surfactant concentration ranges ($\leq$ 4 mM).

The migration order (the same as the order numbers in Table 2) was not changed for the three Gemini surfactants at the different concentrations at pH 3.7. For uncharged 1,3-dinitro-benzene, the only interaction with the micelles is weak hydrophobic interaction causing it to migrate the fastest. For cationic 2,4-dinitroaniline, ionic repulsion between the base and the cationic micellar head caused the interaction with the micelles to be the lowest among the solutes. But since its electrophoretic mobility was opposite to the EOF direction, it migrated as the second solute. Neutral 2,4-dimethylphenol undergoes predominantly strong hydrophobic interactions with

the micelles, as well as possible hydrogen bonding with the 2-propanol group between the two micellar heads, and migrated as the third solute. For partially anionic 2,4-dihydroxybenzoic acid, besides the hydrophobic interaction with the micelles, there was strong electrostatic interaction with the cationic micellar head, so it migrated as the last solute. Finally, pentachlorophenol appeared as the micelle marker.

3.2.2 Effect of the alkyl chain length of the Gemini surfactants

The relationship between the capacity factors and the alkyl chain length (C12 to C16) of the Gemini surfactants are demonstrated in Figure 19. As predicted, the capacity factors of the model solutes increased linearly with alkyl chain length, indicating an increase in the hydrophobic phase ratio in the MECC systems.

However, the dependence of the net mobilities on the alkyl chain length was related to the surfactant concentrations. The results at both 25 °C and 40 °C are given in Figures 20 and 21.

At Gemini surfactant concentrations ≥ 4 mM, the net mobilities of the micelles increased with increasing alkyl chain length, reflecting the increased size of the micelles: the shorter the alkyl chain, the smaller the micelle size, the higher the electrophoretic mobility, and the smaller the net mobility.

However, at low surfactant concentrations, the net mobilities of the micelles decreased from Gemini-C12 to Gemini-C14, and then increased from Gemini-C14 to Gemini-C16. The reason causing this phenomenon has not yet been found.

In conventional chromatography the stationary phase is fixed, so the retention times of the hydrophobic solutes become longer with increasing the alkyl chain length of the stationary phase, especially for solutes that interact strongly. In MECC, however, the pseudostationary phase micelles move; the changes in the net mobilities of the strongly interacting solutes depend on the surfactant concentration because the micelle mobility changes as the surfactant concentration changes. For 1,3-dinitrobenzene, because the interaction with the micelles is weak, the net mobility decreased almost linearly with increasing alkyl chain length at the various surfactant concentrations. For 2,4-dimethylphenol and 2,4-dinitroaniline, the net mobilities generally decreased with increasing alkyl chain length. Such changes were large at low surfactant concentrations, but were small and even slight at the higher surfactant concentrations. For 2,4-dihydroxybenzoic acid, with increasing the alkyl chain length, the net mobility also decreased at the low surfactant concentrations, but slightly changed and even increased at higher surfactant concentrations. At the higher surfactant concentrations, the net mobility of the micelles increased with increasing the alkyl

chain length, and the interaction of 2,4-dihydroxybenzoic acid with the micelles was so strong that its net mobility was slightly changed and even increased with increasing the alkyl chain length. For 2,4-dimethylphenol and 2,4-dinitroaniline, the interaction with the micelles was also relatively strong, but less than that of 2,4-dihydroxybenzoic acid, and their net mobilities were only slightly affected by increasing the alkyl chain length.

3.3 MECC Using Single Alkyl Chain Cationic Surfactants

The single chain C12 to C16 cationic surfactants were investigated in order to compare with the Gemini cationic surfactants. The CMCs of single alkyl chain cationic surfactants are much higher than these of Gemini cationic surfactants as shown in Table 1. Although C_{12}TAB had the largest migration window, the highest CMC of C_{12}TAB somehow limited its application in MECC. Besides, compared to the other two single chain surfactants, the solute capacity of C_{12}TAB was much lower. The capacity of C_{16}TAB was the highest among the single chain surfactants studied, but the migration windows were the smallest. With an increase in the surfactant concentration, the efficiency was usually increased. However, at high C_{16}TAB concentration, the resolution was decreased because of the strong interaction between the micelle and the solutes. In terms of the capacity, efficiency,

resolution and migration window, the best separations were achieved using BGE with C_{14}TAB.

3.3.1 Effect of the single chain surfactant concentrations

The BGE consisted of 50 mM phosphate (pH 3.7) and each surfactant at different concentrations. The C_{12}TAB concentrations were 25, 30, 35, 40, and 50 mM, and temperature was at 25 °C; the C_{14}TAB concentrations were 4, 8, 16, 20, 25, and 30 mM, and the temperatures were at 25 °C and 40 °C; the C_{16}TAB concentrations were 1, 2, 4, 8, 16, 20, 25, and 30 mM, and the temperatures were at 25 °C and 40 °C. The experimental results are presented in Figures 22 to 36.

Similar to the effect of the Gemini surfactant concentrations, at the low concentration ranges for both C_{14}TAB and C_{16}TAB, the net mobilities remarkably increased with an increase in the surfactant concentrations due to the micelle polydispersity and the subsequent variations of the micelle mobilities. For C_{14}TAB concentrations $\geq$ 8 mM, and C_{16}TAB concentrations $\geq$ 4 mM, the micelle polydispersity was reduced, and the net mobilities no longer or slightly affected by increasing surfactant concentrations. As a result of reduced micelle polydispersity with increased surfactant concentration, the peak efficiency was dramatically improved as shown in electropherograms, as well as in Figures 30 and 31.

As discussed in the previous section for the Gemini surfactants, with increasing single chain surfactant concentrations the capacity factors of the model solutes increased linearly at 25 °C and 40 °C, and the capacity factors at 40 °C were lower than those at 25 °C because the interaction between the micelles and the solutes was reduced. Unlike Gemini-C14 and -C16 at 25 °C where the net mobility of 2,4-dihydroxybenzoic acid increased at low surfactant concentrations, with the single chain surfactants the net mobilities of all the model solutes decreased, even though the net mobilities of C_{14}TAB and C_{16}TAB micelles increased at low surfactant concentrations. This was the result of the lower solute capacities of the single chain surfactants compared to the Gemini surfactants.

The Gemini surfactants have two alkyl chains and two cationic heads, so the interactions of the solutes with the Gemini surfactants were much stronger than those with the single chain surfactants. Comparison between Figure 12 and Figure 26 shows the capacity factors at 40 °C for Gemini-C14 were even greater than those at 25 °C by C_{14}TAB. The solutes spent more time in the Gemini micelles than in the single chain micelles.

Unlike the Gemini surfactants where high efficiency could be obtained at 40 °C because of the reduced micelle polydispersity, the efficiency using the single chain surfactants

was only slightly or not improved by increasing temperature from 25 °C to 40 °C, as shown in Figures 30 and 31. The reason might be a combination effect of the temperature dependence of both CMCs and micelle numbers in the BGE, and the micelle polydispersity. The single chain surfactants have high CMCs in comparison to the Gemini surfactants. As the temperature increased, the CMCs could be much increased, resulting in larger amount of free monomers in the BGE, and subsequently thermal effects which reduced the peak efficiency because of a distorted pluglike flow profile (instead of the flat velocity profile characteristic of EOF). Besides, the increased CMCs result in the lower micelle numbers in the BGE at the same surfactant concentration, causing the low efficiency Furthermore, the micelle stability of the single chain surfactants could be lower than that of the Gemini surfactants. At elevated temperature, the breakdown of micelles could be even quicker than the enhanced dynamic exchange between the micelles and the monomers, which result in the reduced micelle numbers in the BGE, and consequently the lower efficiency. However, at the higher temperature the micelle polydispersity is reduced, which improves the efficiency. As a result of the combination of these two effects, the observed efficiency was slightly or not improved using the single chain surfactants in the BGE at the elevated temperature.

3.3.2 Effect of the alkyl chain length of the single chain surfactants

Similar to the Gemini surfactants, with the single chain surfactants the capacity factors of the solutes increased linearly with an increase in the surfactant alkyl chain length as shown in Figure 37, indicating an increase in the hydrophobic phase ratio.

The relationship between the net mobility and the alkyl chain length of the single chain surfactants is demonstrated in Figure 38. As predicted, the net mobilities of all the solutes decreased with increasing alkyl chain length at both 25 mM and 30 mM surfactant concentrations. However, the net mobilities of the micelles decreased from C12 to C14, and were almost unchanged from C14 to C16. For C_{12}TAB, the micelle concentration in BGE was the lowest among the applied single chain surfactants at the same surfactant concentrations because of the highest CMC. The surfactant concentrations at both 25 mM and 30 mM were less than twice of the CMC, therefore the micelle polydispersity for C_{12}TAB could occur, causing the sizes of C_{12}TAB micelles to be smaller, and hence to have higher electrophoretic mobility, which was in contrast to the observed high net mobility of C_{12}TAB micelle. Therefore the micelle polydispersity cannot be attributed to the high net mobility of C_{12}TAB micelle. By comparisons of the electropherograms

using C_{12}TAB (Figures 22) with using C_{14}TAB and C_{16}TAB (Figures 25 and 32), the migration order of partially anionic 2,4-dihydroxybenzoic acid switched. For 2,4-dihydroxybenzoic acid, besides the hydrophobic interaction with the micelles, there was electrostatic interaction with the cationic micellar head, so it was supposed to migrate as the last solute, which was found when using C_{14}TAB and C_{16}TAB, but was not observed as using C_{12}TAB, i.e. it migrated as the third solute ahead of neutral 2,4-dimethylphenol. This was implied that positive charges on the C_{12}TAB micelle head groups were somehow much less than those of the others, which resulted in low electrophoretic mobility, and hence high net mobility. Whereas, the CMCs of both C_{14}TAB and C_{16}TAB were relatively lower (see Table 1), and the difference between them was less than 3 mM. Besides, there are only two methylenes difference between C_{14}TAB and C_{16}TAB. Consequently, the micelle sizes of C_{14}TAB and C_{16}TAB could be similar to each other at both 25 mM and 30 mM surfactant concentrations, causing the net mobilities to be close to each other.

3.4 Applications of Gemini Surfactants in MECC for Separation of the Eleven Priority Pollutant Phenols

3.4.1 Separation without acetonitrile additive

3.4.1.1 Effect of temperature

The eleven priority pollutant phenols were investigated at different temperatures from 25 °C or 30 °C to 45 °C with BGE consisted of 50 mM phosphate (pH 3.3) and each surfactant at the different concentrations. The surfactants applied in this study were 8 mM Gemini-C12, -C14, and C_{16}TAB, and 20 mM C_{14}TAB. The results are shown in Figures 39 to 53.

As described in Chapter 2, at room temperature without acetonitrile additive, the interactions of 2,4,6-trichlorophenol, 2,4-dinitrophenol and 2-methyl-4,6-dinitrophenol with the C_{16}TAB micelle were so strong that these compounds migrated close to or with the micelle, and the separations of these compounds could not be achieved. However, the addition of acetonitrile reduced the interactions so that the excellent separations were achieved. In a manner similar to adding acetonitrile to weaken the strong interactions, an increase in the temperature also decreases strong interactions, and dramatically improves the separations, as shown in Figure 39. When the temperature reached 45 °C, all the eleven phenols were baseline-separated using 8 mM Gemini-C12 and 20 mM C_{14}TAB. However, they still were not well resolved using 8 mM

Gemini-C14 and 8 mM C_{16}TAB because of the strong hydrophobic interaction. Besides, although the eleven phenols can be separated using 20 mM C_{14}TAB at 45 °C, compared with the separation with 8 mM Gemini-C12, the surfactant concentration was two-fold higher; and the efficiency was much lower for the later-eluting solutes as shown in Figure 53. The reason of the low efficiency by the single chain surfactants was discussed earlier.

As the temperature was increased, the EOF mobilities almost linearly increased as predicted from the decrease in viscosity. However, the overall run time was not really decreased (see Figure 39) because the electrophoretic mobility of the micelle also increased with increasing temperature. Therefore, the migration window increased with temperature.

In this investigation without acetonitrile additive, the BGE pH was adjusted to 3.3, the eleven phenols were basically neutral, and the electrophoretic mobilities were zero. With increase in temperature the capacity factors linearly decreased because of the increased solubility of the solutes in the aqueous phase. On the other hand, the changes in the apparent mobilities of the solutes with temperature were related with the EOF and the interactions between the solutes and the micelles; and the changes in the net mobilities were only dependent of the interactions of the solutes with the micelles. For the weakly

interacting solutes, such as the five early-eluting solutes, because the interactions with the micelles were low, with increasing temperature the apparent mobilities considerably increased in a fashion dependent on the EOF increase. Whereas, the net mobilities almost unchanged (for phenol and 2-nitrophenol), or decreased slightly (for 4-nitrophenol) or medially (for 2-chlorophenol and 2,4-dimethylphenol). However, for the strongly interacting solutes (eluted later), with increasing temperature the changes in the apparent mobilities were unsignificant as a result of the combination of the increases in both the EOF and micelle electrophoretic mobilities; whereas, the net mobilities decreased dramatically due to the increase in the micelle electrophoretic mobilities.

The resolutions of the closely-eluted solutes were improved with increasing temperature (as shown in Figure 43), because the increases in solubility in the aqueous phase were different for the different solutes. Moreover, as tabulated in Table 3, with increasing the temperature, the theoretical plate numbers of the micelle peak increased slightly because of the decrease in micelle polydispersity; whereas, the theoretical plate numbers of the solute peaks decreased even if the micelle polydispersity was decreased. This was probably due to a thermal effect which could overcome the benefit from the reduced micelle polydispersity for the solutes, hence causing the band broadening.

3.4.1.2 Effect of BGE pH with Gemini-C12 at 45 °C

The BGE pH can significantly affect the separation of ionizable solutes. In this study, the BGE pH (containing 50 mM phosphate and 8 mM Gemini-C12) was studied at pH 2.9, 3.3, 3.7 and 4.2 at 45 °C. Except for two dinitrophenols (2,4-dinitrophenol and 2-methyl-4,6-dinitrophenol), which could be partially ionized at pH > 3.7, all the others were neutral solutes. As expected, the net mobilities were only slightly affected by changing the pH (see Figure 55). However the migration order of 2,4,6-trichlorophenol was exchanged with the two dinitrophenols for pH > 3.3, and all the other migration orders were unchanged. The separation could be achieved at both pH 2.9 and pH 3.3 as shown in Figures 54 and 55. But the low pH resulted in the low EOF, and thus the very long run time and the poor efficiency. As a result, the separation at the pH 3.3 was preferred.

3.4.1.3 Effect of Gemini-C12 concentration at 45 °C

The effect of the Gemini-C12 concentration on the separation of the eleven phenols at 45 °C was investigated. The BGEs consisted of 50 mM phosphate (pH 3.3) and the concentration of Gemini-C12 was 4, 8, 12, and 16 mM. The experimental results are illustrated in Figures 56 to 59.

As predicted, with increasing surfactant concentration, the capacity factors increased linearly and the net mobilities

decreased because the hydrophobic phase ratio was increased. Separation was achieved at 4 mM, 8 mM and 16 mM Gemini-C12. However, with increasing the surfactant concentration the two dinitrophenols eluted closer and closer, and finally at 16 mM, they migrated together. The resolution of the critical pairs are given in Figure 58. Obviously, the overall resolution at 8 mM Gemini-C12 was better than that at 12 mM Gemini-C12. Besides, the efficiency at 8 mM Gemini-C12 was much better than that at 4 mM Gemini-C12 as shown in Figure 59 because of the reduced micelle polydispersity. Hence 8 mM Gemini-C12 in the BGE was the best choice for the separation.

3.4.1.4 Optimum Separation without Acetonitrile Additive

As discussed above, it is obvious that optimum separation of the eleven phenols can be achieved in approximately eleven minutes in MECC without acetonitrile additive using 50 mM phosphate (pH 3.3) and 8 mM Gemini-C12 at 45 °C with a uncoated fused-silica capillary of 50 μm I.D. and 30 cm effective length (~ 37 cm total length) under a negative 13.5 kV voltage.

3.4.2 Separation with acetonitrile additive: temperature effect

The optimum separation of the eleven phenols at room temperature with a BGE containing 15 mM C_{16}TAB and 15%

acetonitrile in 50 mM phosphate-10 mM acetate (pH 4.2) was described in Chapter 2. The effect of temperature on this optimum separation was further evaluated at 25, 35 and 45 °C in this study. Here not only was 15 mM C_{16}TAB used, but also 15 mM Gemini-C12 and -C14, as well as 20 mM C_{14}TAB were applied in order to find which cationic surfactant was the most suitable for the separation of the eleven phenols at both room and elevated temperatures. The BGE consisted of 50 mM phosphate-10 mM acetate (pH 4.2) with 15% acetonitrile and each applied surfactant at different concentrations. The results are illustrated in Figures 60 to 75.

With increasing temperature the same phenomena occurred as discussed above for the BGE without acetonitrile additive: the EOF mobilities linearly increased because of the decrease in viscosity with increasing temperature. However, the electrophoretic mobility of the micelle increased with temperature as well and was opposite to the EOF direction, thus the overall run time was not significantly decreased, especially for the smaller sized micelles such as C_{14}TAB. As shown in Figures 68 and 70, the migration time and apparent mobility of the C_{14}TAB micelle was almost unaffected with increasing temperature because of the higher micelle electrophoretic mobility. In this way, the migration window was dramatically increased with temperature.

Again, the capacity factors decreased linearly with an increase in temperature because of the increased solubility of the solutes in the aqueous phase. In this investigation with acetonitrile additive, the BGE pH was adjusted to 4.2, at which only the two dinitrophenols were partially ionized and had the electrophoretic mobilities in the EOF direction; all the other phenols were neutral. Because the ionic and hydrophobic interactions of the two dinitrophenols with the micelles were strong, their electrophoretic mobilities were assumed to be negligible. Therefore, the changes in the apparent mobilities of the solutes with temperature were related both to the EOF and the interactions between the solutes and the micelles; and the changes in the net mobilities were mainly dependent of the interactions of the solutes with the micelles. In this study, even at higher surfactant concentrations (15 mM instead of 8 mM in the previous study) for Gemini-C12, -C14 and C_{16}TAB, because of the presence of acetonitrile, the interactions between the solutes and the micelles were reduced. Therefore the apparent mobilities of all the solutes (excluding pentachlorophenol as the micelle marker) were more dependent on the EOF and thus were all increased as the temperature was increased. Especially for the later-eluted solutes, such increases in the apparent mobilities with acetonitrile were larger than those without acetonitrile. Furthermore, unlike the phenomena described above using BGE without acetonitrile additive, in this study the

net mobilities of the medially interacting solutes, such as 4-chloro-3-methylphenol and 2,4-dichlorophenol, only slightly decreased with increasing temperature because the interaction with the micelles was decreased with acetonitrile. For all other solutes, however, the temperature effects on the net mobilities were similar with and without acetonitrile: the net mobilities of the weakly interacting solutes (the five early-eluting solutes) only little changed with increasing temperature; and the net mobilities of the strongly interacting solutes (the later-eluting phenols) decreased with increasing temperature, because of the increases in the micelle electrophoretic mobilities.

In addition, as shown in Table 4, the theoretical plate number of the micelle peak increased from 25 °C to 35 °C because of the decrease in the micelle polydispersity, and then decreased from 35 °C to 45 °C because of the large thermal effect. However, the theoretical plate numbers of the solute peaks were decreased with increasing the temperature owing to the thermal effect causing band broadening.

Finally, from the electropherograms as shown in Figures 60, 64, 68 and 72, as well as in Table 4, it can be concluded that the excellent separations with acetonitrile additive in the BGE can be achieved using Gemini-C12 no matter what temperatures; and the best separation was achieved at 35 °C in terms of overall efficiency, peak shape, baseline and run time.

4. Conclusions

A series of novel Gemini cationic surfactants (from Gemini-C8 to -C18) was for the first time evaluated as micelle-forming reagents in MECC. It was determined that both Gemini-C12 and -C14 were useful in MECC. Compared to the single chain cationic surfactants, the Gemini surfactants have much lower CMCs, and thus the stability of the micelles is superior. Among all the Gemini and single chain cationic surfactants evaluated in this study, Gemini-C12 was the most useful cationic surfactant in MECC. The excellent separation was achieved using Gemini-C12 in the BGE for both the model solutes and the eleven phenols at any temperatures, with or without acetonitrile. The novel Gemini-C12 probably can provide much more applications to MECC in the future.

Table 1

(a) Some Properties of Gemini Cationic Surfactants

Surfactants	M. W.	CMC * (mM)	
		25 °C	50 °C
Gemini-C8	443.6	9.55	10.7
Gemini-C10	499.7	0.398	0.631
Gemini-C12	555.8	9.55×10^{-3}	2.29×10^{-2}
Gemini-C14	611.9	1.00×10^{-2}	7.94
Gemini-C16	668.0	3.16×10^{-2}	6.92
Gemini-C18	724.1	N/A	N/A

* The data are from the reference 4.

(b) Some Properties of Single Chain Cationic Surfactants

Surfactants	M. W.	CMC*(mM)
C_{12}TAB	308.3	15.3
C_{14}TAB	336.4	3.6
C_{16}TAB	364.5	0.9

* The data are from reference 13.

Table 2

Model Solutes for Evaluation of Gemini and Single Chain Cationic Surfactants in MECC

No	Compounds	pKa	M. W.	Formulas
1	1,3-Dinitrobenzene	-	168.11	$C_6H_4(NO_2)_2$
2	2,4-Dinitroaniline	18.46	183.10	$(NO_2)_2C_6H_3(NH_2)$
3	2,4-Dimethylphenol	10.59	122.17	$(CH_3)_2C_6H_3OH$
4	2,4-Dihydroxybenzoic Acid	3.29	154.12	$(HO)_2C_6H_3CO_2H$
5	Pentachlorophenol*	4.50	266.35	C_6Cl_5OH

* Pentachlorophenol was taken as the micelle marker.

Table 3

Temperature Effect on Theoretical Plates using 8 mM Gemini-C12

No.	Compounds	*35 deg. C*	*45 deg. C*
1	Phenol	76160	53530
2	2-Nitrophenol	82460	61780
3	4-Nitrophenol	54750	51660
4	2-Chlorophenol	74850	56220
5	2,4-Dimethylphenol	68120	52010
6	4-Chloro-3-Methylphenol	88850	52870
7	2,4-Dichlorophenol	74460	51930
8	2,4,6-Trichlorophenol	94950	57220
9	2,4-Dinitrophenol	64360	49740
10	2-Methyl-4,6-Dinitrophenol	54980	42310
11	Pentachlorophenol	20950	22480

Table 4

Temperature Effect on Theoretical Plates using 15 mM Surfactants and 15% ACN

No.	Compounds	Gemini-C12			C_{16}TAB		
		25 deg. C	*35 deg. C*	*45 deg. C*	*25 deg. C*	*35 deg. C*	*45 deg. C*
1	Phenol	121800	100300	79000	115000	92810	76240
2	2-Nitrophenol	132700	108600	86730	120400	98440	81250
3	4-Nitrophenol	136100	116800	94890	110800	97220	83730
4	2-Chlorophenol	151400	129100	103200	131700	115600	96680
5	2,4-Dimethylphenol	161700	140100	109800	136500	122600	105500
6	4-Chloro-3-Methylphenol	165300	149700	122300	120800	113100	101800
7	2,4-Dichlorophenol	149500	143800	121200	120200	126700	108600
8	2,4,6-Trichlorophenol	139800	141800	121800	176100	186500	140300
9	2,4-Dinitrophenol	138500	134500	111200	125400	103900	84100
10	2-Methyl-4,6-Dinitrophenol	138500	143100	118600	160000	146400	108600
11	Pentachlorophenol	76840	85400	80670	65840	132806	114200

Figure Captions:

Figure 1: Structures of the Gemini and single alkyl chain cationic surfactants.

Figure 2: Electropherograms of the model solutes (see Table 1 for the identification of compounds) with BGEs containing 50 mM phosphate (pH 3.7) and different concentrations of Gemini-C12 at 25 °C and 40 °C, respectively.(a) 4 mM at 25 °C, (b) 4 mM at 40 °C, (c) 8 mM at 25 °C, (d) 8 mM at 40 °C, (e) 16 mM at 25 °C, (f) 16 mM at 40 °C, (g) 20 mM at 25 °C and (h) 20 mM at 40 °C.

Figure 3: Effect of Gemini-C12 concentration on the capacity factors of the model solutes with BGE containing 50 mM phosphate (pH 3.7) at 25 °C.

Figure 4: Effect of Gemini-C12 concentration on the net mobilities of the model solutes with BGE containing 50 mM phosphate (pH 3.7) at 25 °C.

Figure 5: Effect of Gemini-C12 concentrations on the capacity factors of the model solutes with BGE containing 50 mM phosphate (pH 3.7) at 40 °C.

Figure 6: Effect of Gemini-C12 concentration on the net mobilities of the model solutes with BGE containing 50 mM phosphate (pH 3.7) at 40 °C.

Figure 7: Effect of Gemini-C12 concentration on the theoretical plate numbers (N) of the model solutes with BGE containing 50 mM phosphate (pH 3.7) at 25 °C.

Figure 8: Effect of Gemini-C12 concentration on the theoretical plate numbers (N) of the model solutes with BGE containing 50 mM phosphate (pH 3.7) at 40 °C.

Figure 9: Electropherograms of the model solutes with BGE containing 50 mM phosphate (pH 3.7) and different concentrations of Gemini-C14 at 25 °C and 40 °C, respectively. (a) 4 mM at 25 °C, (b) 4 mM at 40 °C, (c) 8 mM at 25 °C, (d) 8 mM at 40 °C, (e) 16 mM at 25 °C, (f) 16 mM at 40 °C, (g) 20 mM at 25 °C and (h) 20 mM at 40 °C.

Figure 10: Effect of Gemini-C14 concentration on the capacity factors of the model solutes with BGE containing 50 mM phosphate (pH 3.7) at 25 °C.

Figure 11: Effect of Gemini-C14 concentration on the net mobilities of the model solutes with BGE containing 50 mM phosphate (pH 3.7) at 25 °C.

Figure 12: Effect of Gemini-C14 concentration on the capacity factors of the model solutes with BGE containing 50 mM phosphate (pH 3.7) at 40 °C.

Figure 13: Effect of Gemini-C14 concentration on the net mobilities of the model solutes with BGE containing 50 mM phosphate (pH 3.7) at 40 °C.

Figure 14: Electropherograms of the model solutes with BGE containing 50 mM phosphate (pH 3.7) and different concentrations of Gemini-C16 at 40 °C. (a) 2 mM, (b) 4 mM and (c) 8 mM.

Figure 15: Effect of Gemini-C16 concentration on the capacity factors of the model solutes with BGE containing 50 mM phosphate (pH 3.7) at 25 °C.

Figure 16: Effect of Gemini-C16 concentration on the net mobilities of the model solutes with BGE containing 50 mM phosphate (pH 3.7) at 25 °C.

Figure 17: Effect of Gemini-C16 concentration on the capacity factors of the model solutes with BGE containing 50 mM phosphate (pH 3.7) at 40 °C.

Figure 18: Effect of Gemini-C16 concentration on the net mobilities of the model solutes with BGE containing 50 mM phosphate (pH 3.7) at 40 °C.

Figure 19: Effect of the alkyl chain length of Gemini cationic surfactants on the capacity factors of the model solutes with BGE containing 50 mM phosphate (pH 3.7) at 40 °C. (a) C_{sf} = 0.4 mM, (b) C_{sf} = 1 mM, (c) C_{sf} = 2 mM, (d) C_{sf} = 4 mM, (e) C_{sf} = 8 mM and (f) C_{sf} = 16 mM.

Figure 20: Effect of the alkyl chain length of Gemini cationic surfactants on the net mobilities of the model solutes with BGE containing 50 mM phosphate (pH 3.7) at 40 °C. (a) C_{sf} = 0.4 mM, (b) C_{sf} = 1 mM, (c) C_{sf} = 2 mM, (d) C_{sf} = 4 mM, (e) C_{sf} = 8 mM, (f) C_{sf} = 16 mM and (g) C_{sf} = 20 mM.

Figure 21: Effect of the alkyl chain length of Gemini cationic surfactants on the net mobilities of the model solutes with BGE containing 50 mM phosphate (pH 3.7) at 25 °C. (a) C_{sf} = 0.4 mM, (b) C_{sf} = 1 mM, (c) C_{sf} = 2 mM, (d) C_{sf} = 4 mM, (e) C_{sf} = 8 mM, (f) C_{sf} = 16 mM and (g) C_{sf} = 20 mM.

Figure 22: Electropherogram of the model solutes with a BGE containing 50 mM phosphate (pH 3.7) and 35 mM C_{12}TAB at 25 °C.

Figure 23: Effect of C_{12}TAB concentration on the capacity factors of the model solutes with BGE containing 50 mM phosphate (pH 3.7) at 25 °C.

Figure 24: Effect of $C_{12}TAB$ concentration on the net mobilities of the model solutes with BGE containing 50 mM phosphate (pH 3.7) at 25 °C.

Figure 25: Electropherograms of the model solutes with BGE containing 50 mM phosphate (pH 3.7) and different concentrations of $C_{14}TAB$ at 25 °C. (a) 4 mM, (b) 8 mM, (c) 16 mM, (d) 20 mM, (e) 25 mM and (f) 30 mM.

Figure 26: Effect of $C_{14}TAB$ concentration on the capacity factors of the model solutes with BGE containing 50 mM phosphate (pH 3.7) at 25 °C.

Figure 27: Effect of $C_{14}TAB$ concentration on the net mobilities of the model solutes with BGE containing 50 mM phosphate (pH 3.7) at 25 °C.

Figure 28: Effect of $C_{14}TAB$ concentration on the capacity factors of the model solutes with BGE containing 50 mM phosphate (pH 3.7) at 40 °C.

Figure 29: Effect of $C_{14}TAB$ concentration on the net mobilities of the model solutes with BGE containing 50 mM phosphate (pH 3.7) at 40 °C.

Figure 30: Effect of C_{14}TAB concentration on the theoretical plate numbers (N) of the model solutes with BGE containing 50 mM phosphate (pH 3.7) at 25 °C.

Figure 31: Effect of C_{14}TAB concentration on the theoretical plate numbers (N) of the model solutes with BGE containing 50 mM phosphate (pH 3.7) at 40 °C.

Figure 32: Electropherograms of the model solutes with BGE containing 50 mM phosphate (pH 3.7) and different concentrations of C_{16}TAB at 25 °C. (a) 4 mM, (b) 8 mM, (c) 16 mM, (d) 20 mM, (e) 25 mM and (f) 30 mM.

Figure 33: Effect of C_{16}TAB concentration on the capacity factors of the model solutes with BGE containing 50 mM phosphate (pH 3.7) at 25 °C.

Figure 34: Effect of C_{16}TAB concentration on the net mobilities of the model solutes with BGE containing 50 mM phosphate (pH 3.7) at 25 °C.

Figure 35: Effect of C_{16}TAB concentration on the capacity factors of the model solutes with BGE containing 50 mM phosphate (pH 3.7) at 40 °C.

Figure 36: Effect of $C_{16}TAB$ concentration on the net mobilities of the model solutes with BGE containing 50 mM phosphate (pH 3.7) at 40 °C.

Figure 37: Effect of the alkyl chain length of the single chain cationic surfactants on the capacity factors of the model solutes with BGE containing 50 mM phosphate (pH 3.7) at 25 °C. (a) C_{sf} = 25 mM and (b) C_{sf} = 30 mM.

Figure 38: Effect of the alkyl chain length of Gemini cationic surfactants on the net mobilities of the model solutes with BGE containing 50 mM phosphate (pH 3.7) at 25 °C. (a) C_{sf} = 25 mM and (b) C_{sf} = 30 mM.

Figure 39: Electropherograms of the eleven phenols with a BGE containing 50 mM phosphate (pH 3.3) and 8 mM Gemini-C12 at different temperatures. (a) 30 °C, (b) 35 °C, (c) 40 °C and (d) 45 °C.

Figure 40: Effect of the temperature on the capacity factors of the eleven phenols with a BGE containing 50 mM phosphate (pH 3.3) and 8 mM Gemini-C12.

Figure 41: Effect of the temperature on the apparent mobilities of the eleven phenols with a BGE containing 50 mM phosphate (pH 3.3) and 8 mM Gemini-C12.

Figure 42: Effect of the temperature on the net mobilities of the eleven phenols with a BGE containing 50 mM phosphate (pH 3.3) and 8 mM Gemini-C12.

Figure 43: Effect of the temperature on the resolutions of the critical pairs of the phenols with a BGE containing 50 mM phosphate (pH 3.3) and 8 mM Gemini-C12.

Figure 44: Effect of the temperature on the capacity factors of the eleven phenols with a BGE containing 50 mM phosphate (pH 3.3) and 8 mM Gemini-C14.

Figure 45: Effect of the temperature on the apparent mobilities of the eleven phenols with a BGE containing 50 mM phosphate (pH 3.3) and 8 mM Gemini-C14.

Figure 46: Effect of the temperature on the net mobilities of the eleven phenols with a BGE containing 50 mM phosphate (pH 3.3) and 8 mM Gemini-C14.

Figure 47: Effect of the temperature on the capacity factors of the eleven phenols with a BGE containing 50 mM phosphate (pH 3.3) and 20 mM C_{14}TAB.

Figure 48: Effect of the temperature on the apparent mobilities of the eleven phenols with a BGE containing 50 mM phosphate (pH 3.3) and 20 mM C_{14}TAB.

Figure 49: Effect of the temperature on the net mobilities of the eleven phenols with a BGE containing 50 mM phosphate (pH 3.3) and 20 mM C_{14}TAB.

Figure 50: Effect of the temperature on the capacity factors of the eleven phenols with a BGE containing 50 mM phosphate (pH 3.3) and 8 mM C_{16}TAB.

Figure 51: Effect of the temperature on the apparent mobilities of the eleven phenols with a BGE containing 50 mM phosphate (pH 3.3) and 8 mM C_{16}TAB.

Figure 52: Effect of the temperature on the net mobilities of the eleven phenols with a BGE containing 50 mM phosphate (pH 3.3) and 8 mM C_{16}TAB.

Figure 53: Effect of the surfactant on the theoretical plate numbers of the later-eluting phenols between 8 mM Gemini-C12 and 20 mM C_{14}TAB in 50 mM phosphate (pH 3.3) at 45 °C.

Figure 54: Effect of the BGE pH on the capacity factors of the eleven phenols with BGE containing 50 mM phosphate (pH 3.3) and 8 mM Gemini-C12 at 45 °C.

Figure 55: Effect of the BGE pH on the net mobilities of the eleven phenols with BGE containing 50 mM phosphate (pH 3.3) and 8 mM Gemini-C12 at 45 °C.

Figure 56: Effect of the Gemini-C12 concentration on the capacity factors of the eleven phenols with BGE containing 50 mM phosphate (pH 3.3) at 45 °C.

Figure 57: Effect of the Gemini-C12 concentration on the net mobilities of the eleven phenols with BGE containing 50 mM phosphate (pH 3.3) at 45 °C.

Figure 58: Effect of the Gemini-C12 concentration on the resolution of the critical pairs of the phenols with BGE containing 50 mM phosphate (pH 3.3) at 45 °C.

Figure 59: Effect of the Gemini-C12 concentration on the theoretical plate numbers of the later-eluting phenols with BGE containing 50 mM phosphate (pH 3.3) at 45 °C.

Figure 60: Electropherograms of the eleven phenols with a BGE containing 50 mM phosphate-10 mM acetate (pH 4.2), 15 mM Gemini-C12 and 15% acetonitrile at different temperatures. (a) 25 °C, (b) 35 °C and (c) 45 °C.

Figure 61: Effect of the temperature on the capacity factors of the eleven phenols with a BGE containing 50 mM phosphate-10 mM acetate (pH 4.2), 15 mM Gemini-C12 and 15% acetonitrile.

Figure 62: Effect of the temperature on the apparent mobilities of the eleven phenols with a BGE containing 50 mM phosphate-10 mM acetate (pH 4.2), 15 mM Gemini-C12 and 15% acetonitrile.

Figure 63: Effect of the temperature on the net mobilities of the eleven phenols with a BGE containing 50 mM phosphate-10 mM acetate (pH 4.2), 15 mM Gemini-C12 and 15% acetonitrile.

Figure 64: Electropherograms of the eleven phenols with a BGE containing 50 mM phosphate-10 mM acetate (pH 4.2), 15 mM Gemini-C14 and 15% acetonitrile at different temperatures. (a) 25 °C, (b) 35 °C and (c) 45 °C.

Figure 65: Effect of the temperature on the capacity factors of the eleven phenols with a BGE containing 50 mM phosphate-10 mM acetate (pH 4.2), 15 mM Gemini-C14 and 15% acetonitrile.

Figure 66: Effect of the temperature on the apparent mobilities of the eleven phenols with a BGE containing 50 mM phosphate-10 mM acetate (pH 4.2), 15 mM Gemini-C14 and 15% acetonitrile.

Figure 67: Effect of the temperature on the net mobilities of the eleven phenols with a BGE containing 50 mM phosphate-10 mM acetate (pH 4.2), 15 mM Gemini-C14 and 15% acetonitrile.

Figure 68: Electropherograms of the eleven phenols with a BGE containing 50 mM phosphate-10 mM acetate (pH 4.2), 20 mM C_{14}TAB and 15% acetonitrile at different temperatures. (a) 25 °C, (b) 35 °C and (c) 45 °C.

Figure 69: Effect of the temperature on the capacity factors of the eleven phenols with a BGE containing 50 mM phosphate-10 mM acetate (pH 4.2), 20 mM C_{14}TAB and 15% acetonitrile.

Figure 70: Effect of the temperature on the apparent mobilities of the eleven phenols with a BGE containing 50 mM phosphate-10 mM acetate (pH 4.2), 20 mM C_{14}TAB and 15% acetonitrile.

Figure 71: Effect of the temperature on the net mobilities of the eleven phenols with a BGE containing 50 mM phosphate-10 mM acetate (pH 4.2), 20 mM C_{14}TAB and 15% acetonitrile.

Figure 72: Electropherograms of the eleven phenols with a BGE containing 50 mM phosphate-10 mM acetate (pH 4.2), 15 mM C_{16}TAB and 15% acetonitrile at different temperatures. (a) 25 °C, (b) 35 °C and (c) 45 °C.

Figure 73: Effect of the temperature on the capacity factors of the eleven phenols with a BGE containing 50 mM phosphate-10 mM acetate (pH 4.2), 15 mM C_{16}TAB and 15% acetonitrile.

Figure 74: Effect of the temperature on the apparent mobilities of the eleven phenols with a BGE containing 50 mM phosphate-10 mM acetate (pH 4.2), 15 mM C_{16}TAB and 15% acetonitrile.

Figure 75: Effect of the temperature on the net mobilities of the eleven phenols with a BGE containing 50 mM phosphate-10 mM acetate (pH 4.2), 15 mM C_{16}TAB and 15% acetonitrile.

Figure 1

(a) The Structures of the Gemini Cationic Surfactants

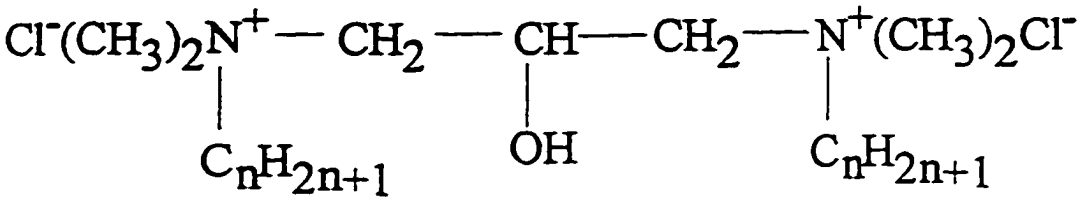

n = 8, 10, 12, 14, 16, and 18

(b) The Structures of the Single Chain Cationic Surfactants

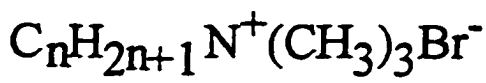

n = 12, 14, and 16

Figure 2

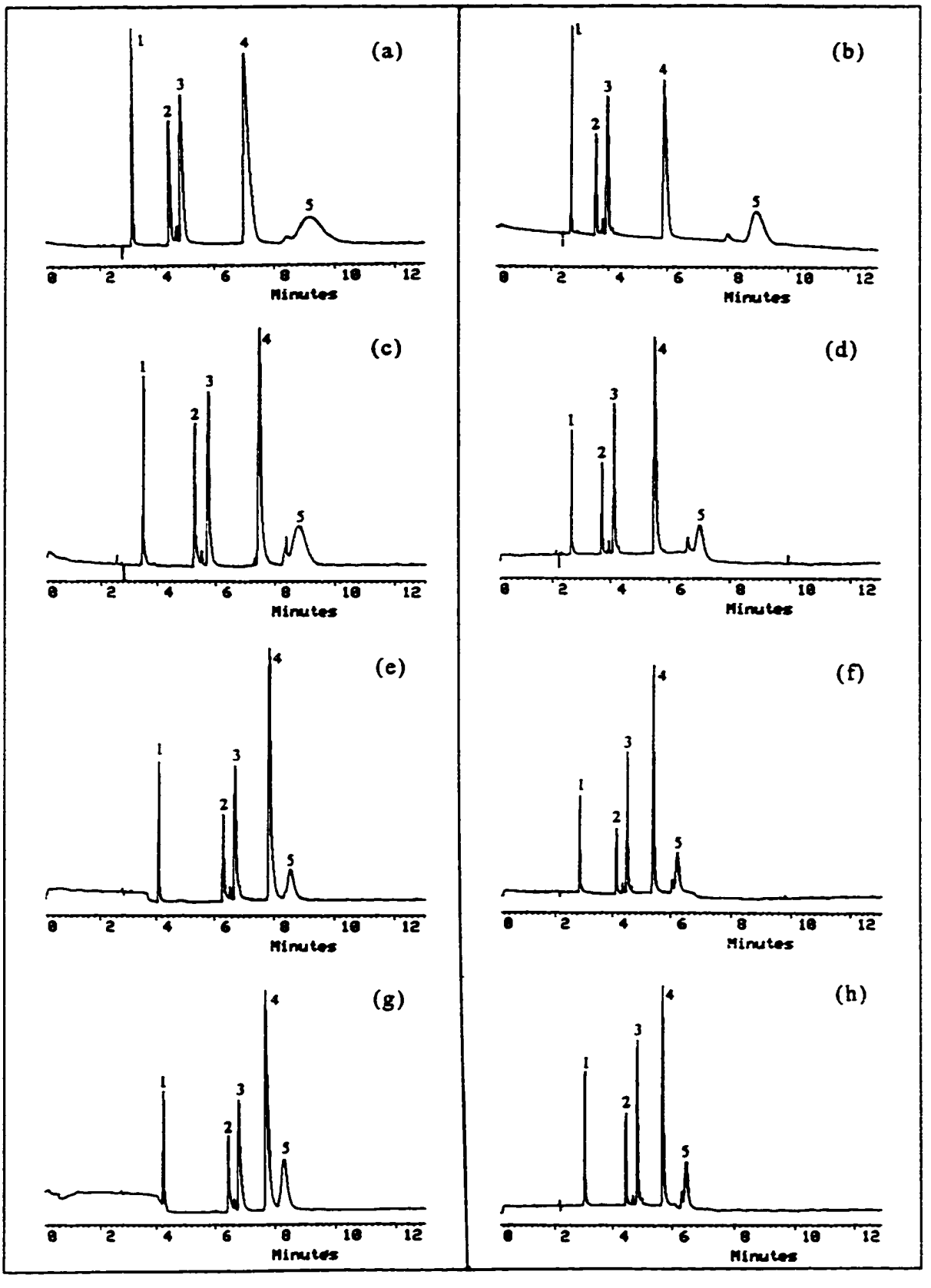

Figure 3

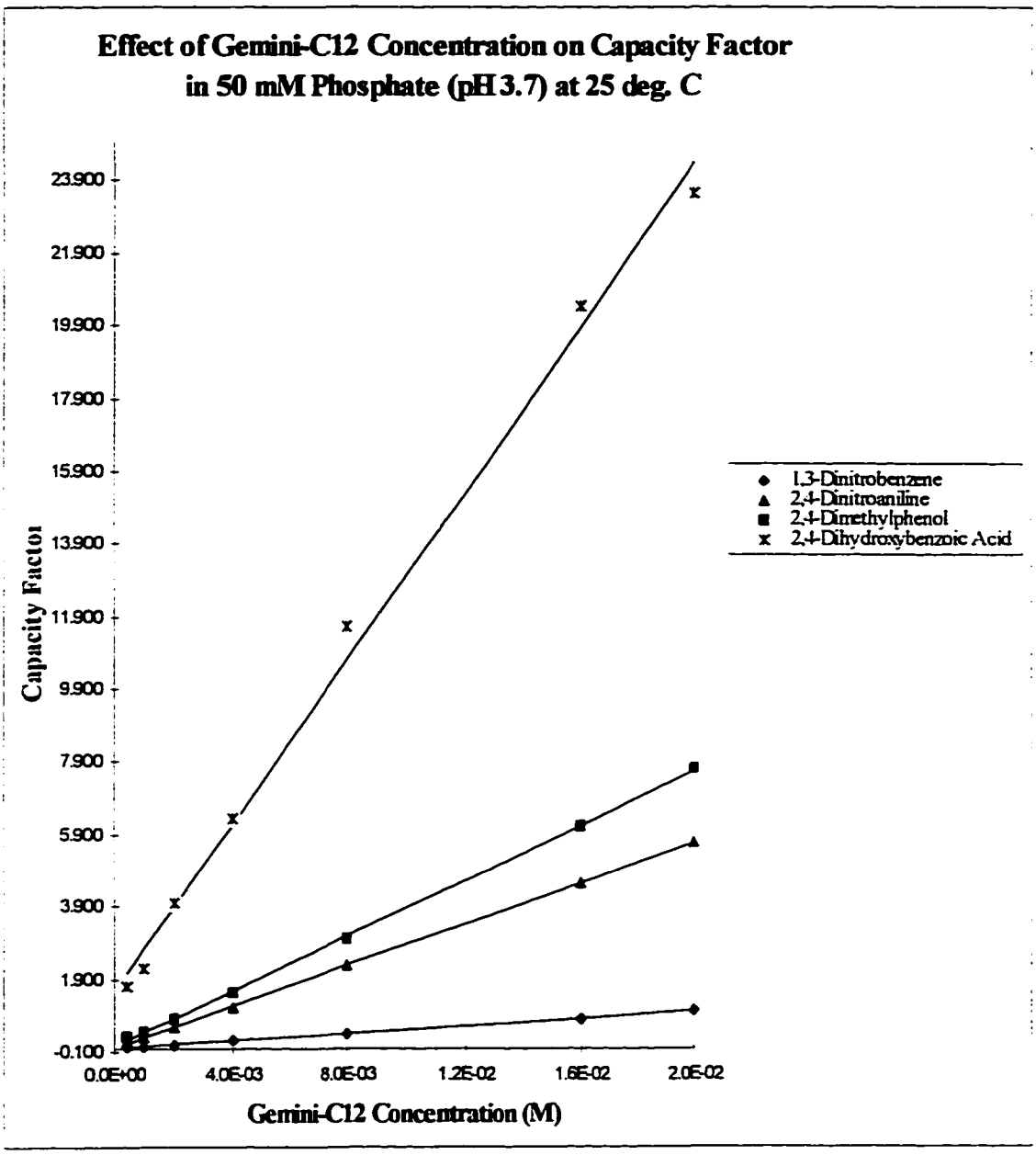

No.	Compounds	*RSQ*	*Slope*	*Intercept*
1	1,3-Dinitrobenzene	1.000	50.924	0.002
2	2,4-Dinitroaniline	1.000	283.199	0.019
3	2,4-Dimethylphenol	1.000	378.950	0.065
4	2,4-Dihydroxybenzoic Acid	0.995	1137.389	1.623

Figure 4

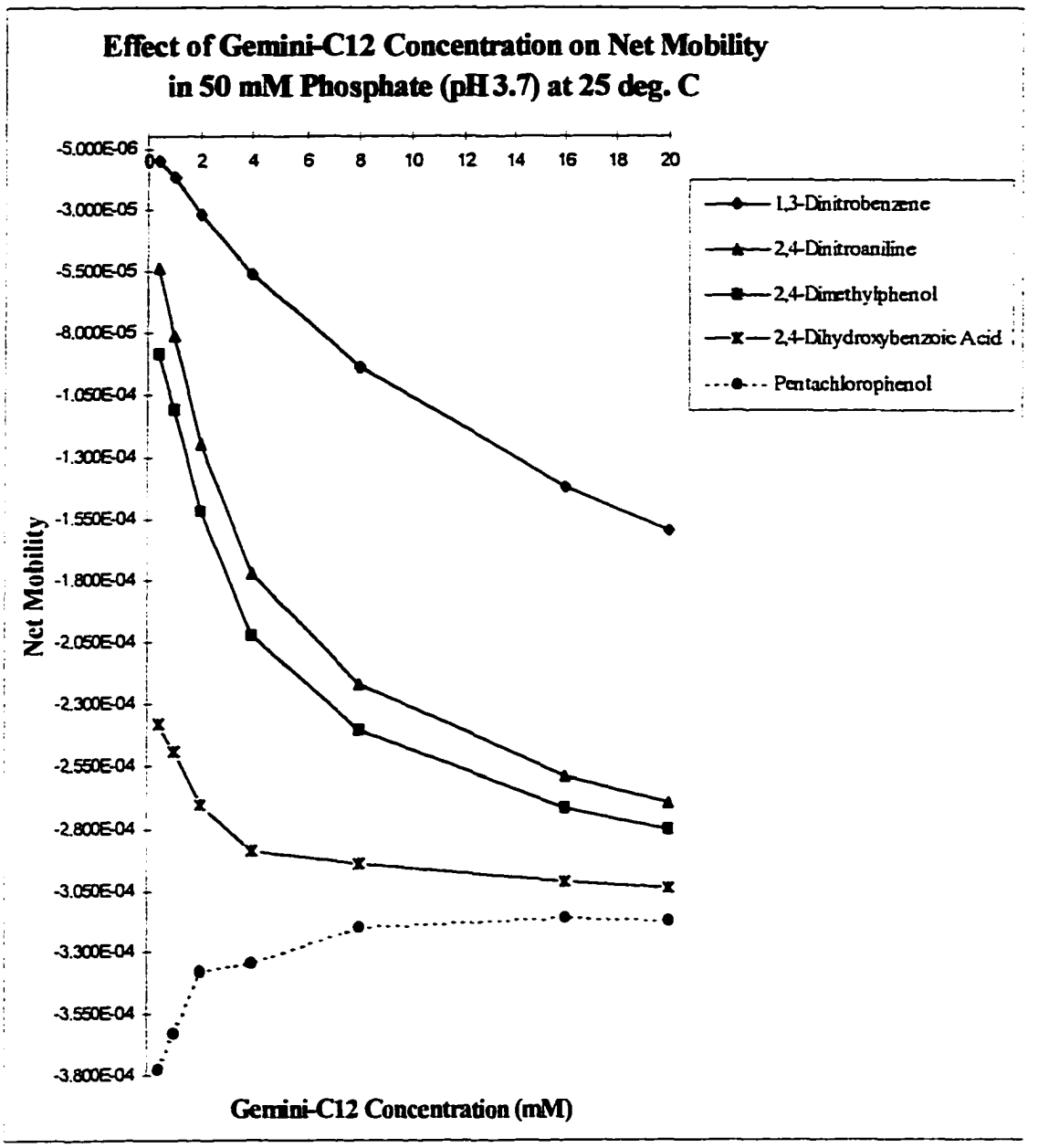

Figure 5

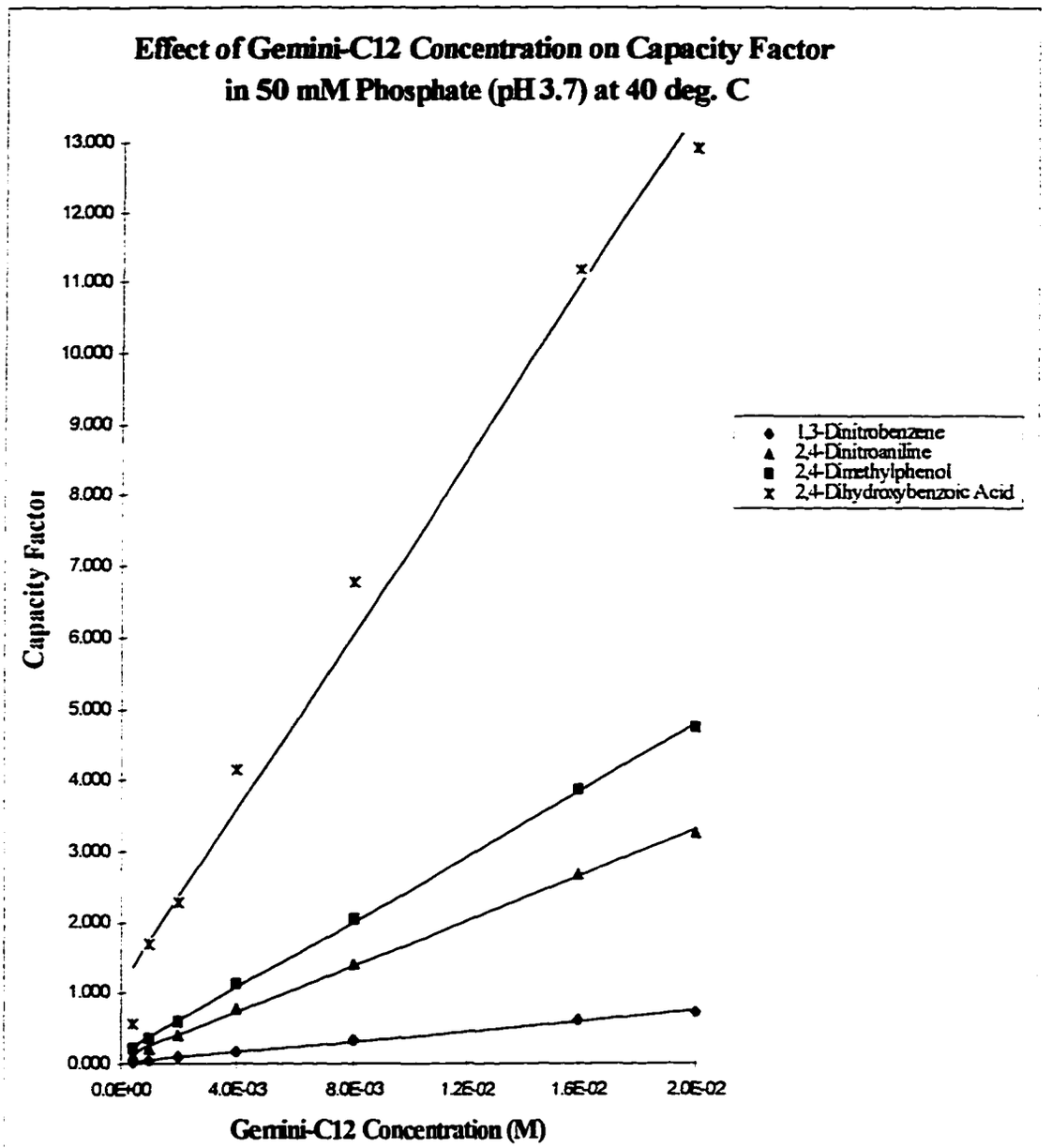

No.	Compounds	*RSQ*	*Slope*	*Intercept*
1	1,3-Dinitrobenzene	0.999	36.259	0.015
2	2,4-Dinitroaniline	0.999	160.619	0.086
3	2,4-Dimethylphenol	1.000	231.632	0.139
4	2,4-Dihydroxybenzoic Acid	0.987	615.678	1.123

Figure 6

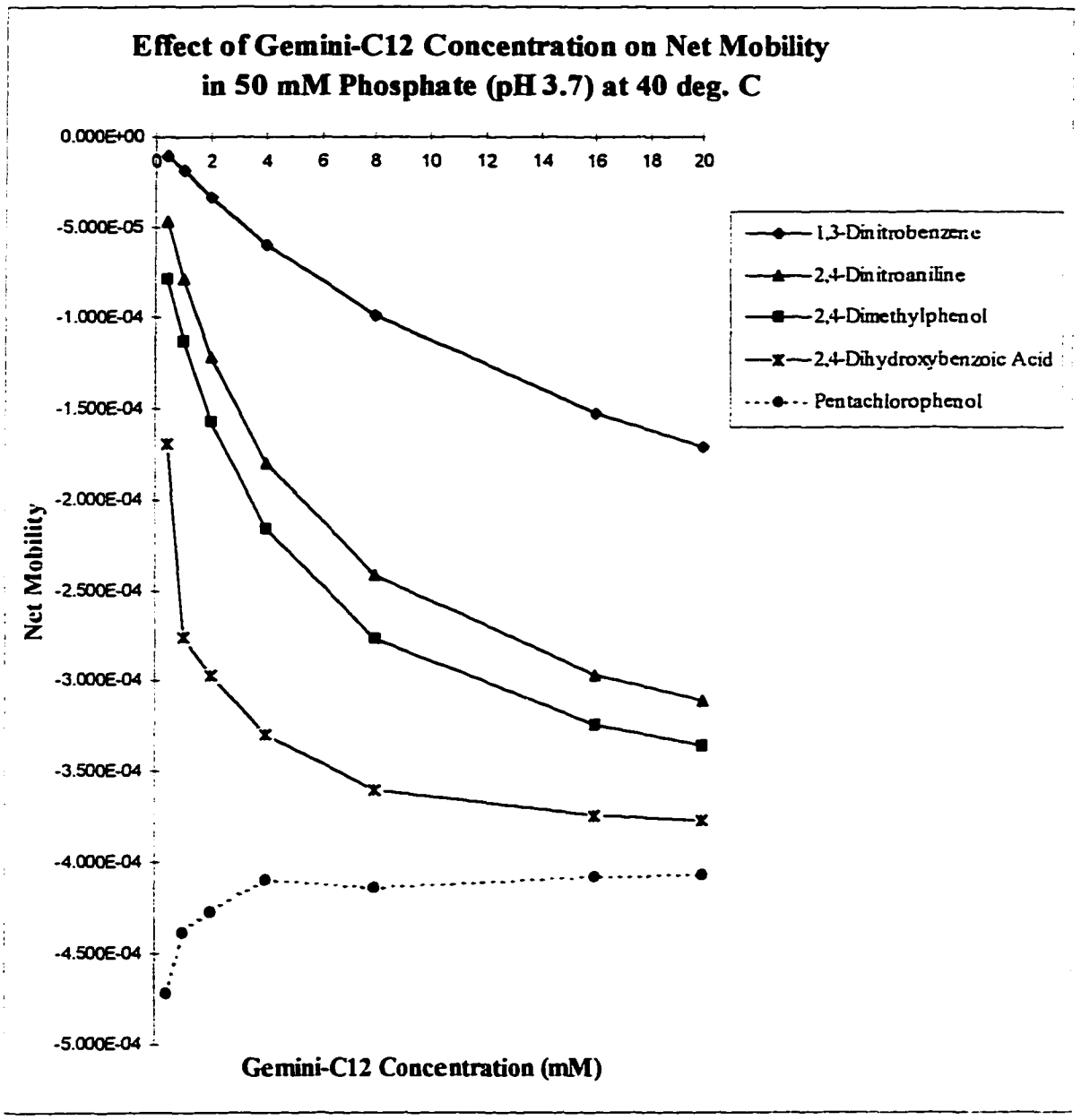

Figure 7

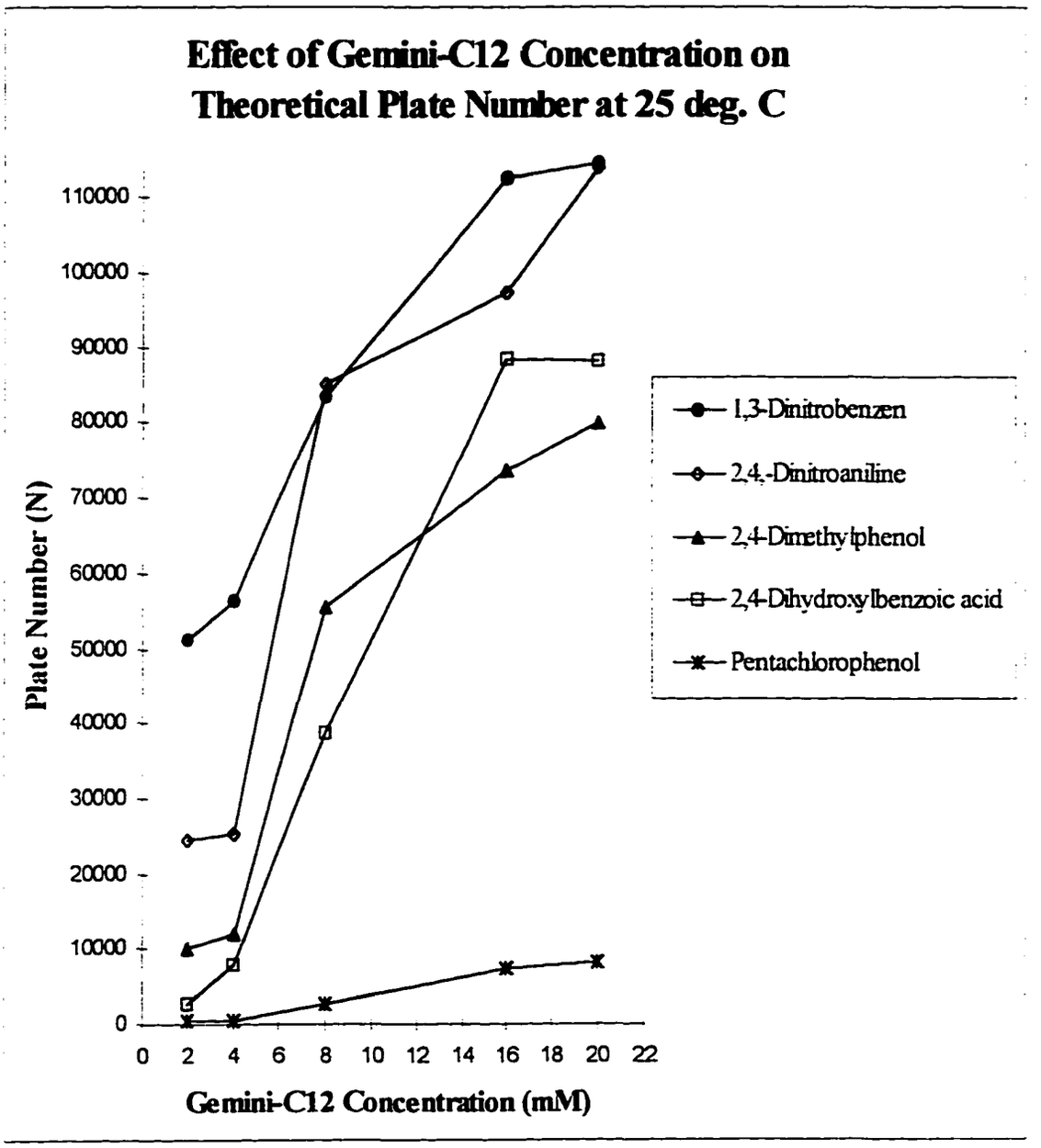

Figure 8

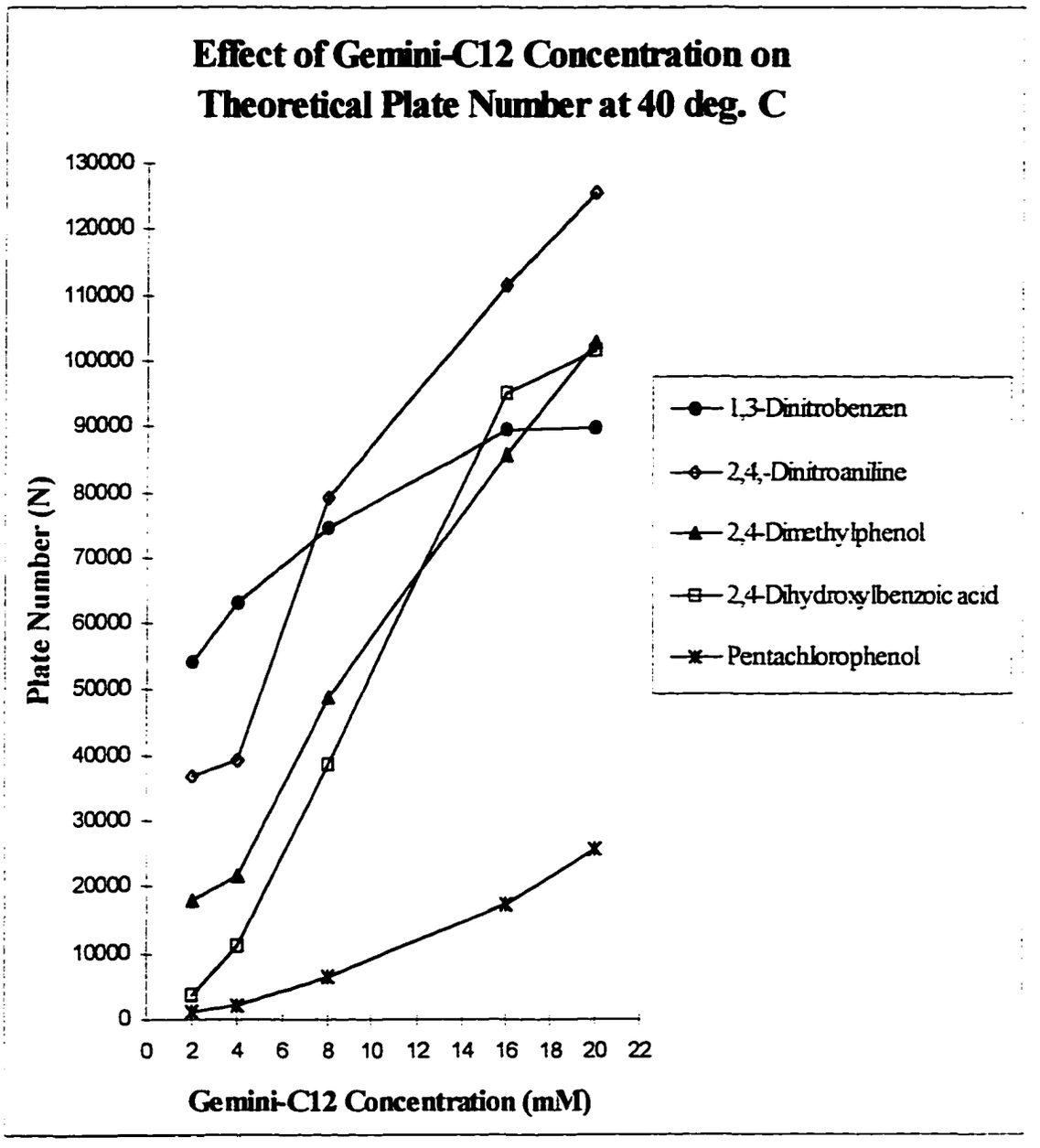

Figure 9

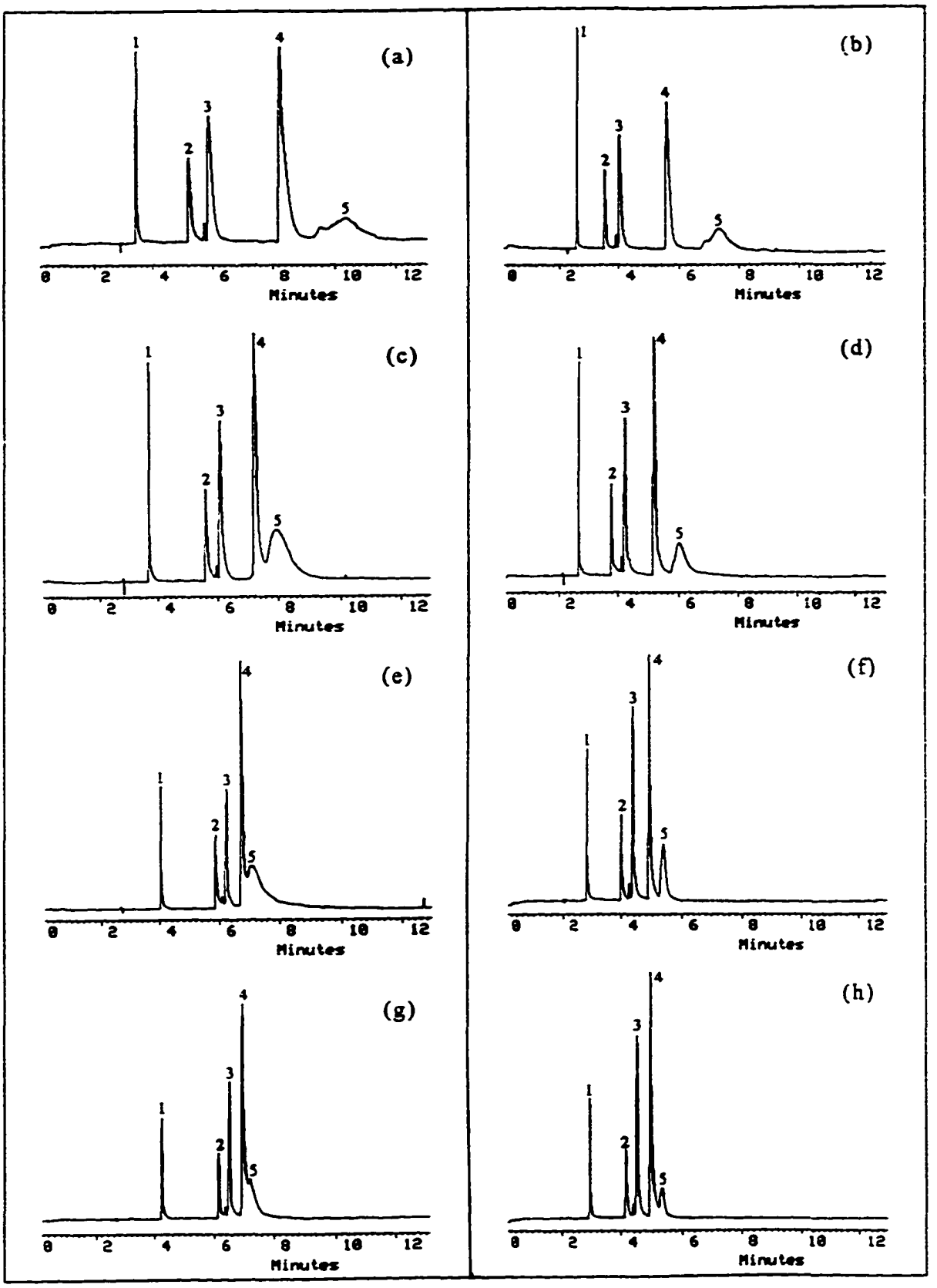

Figure 10

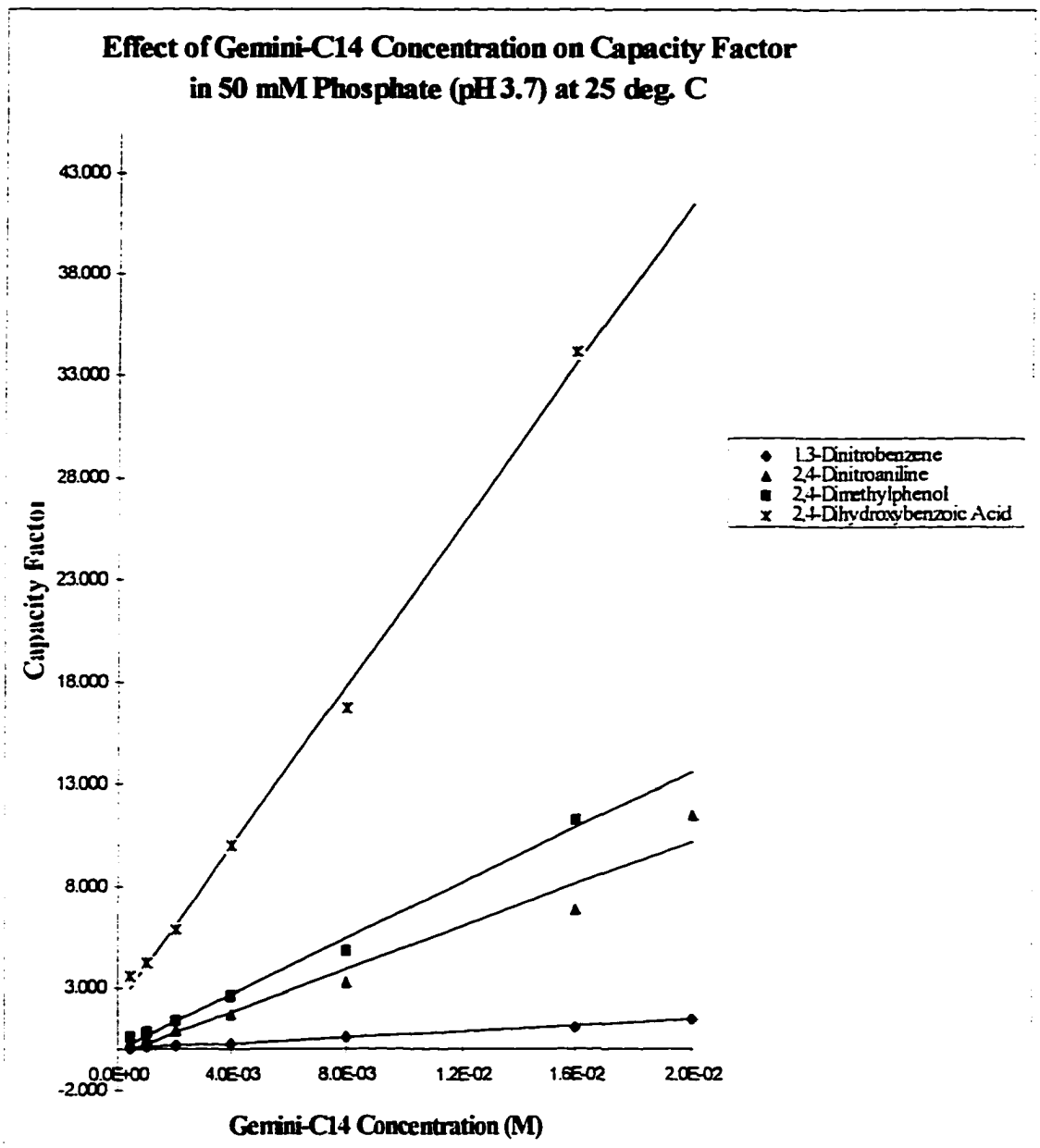

No.	Compounds	*RSQ*	*Slope*	*Intercept*
1	1,3-Dinitrobenzene	0.998	72.110	0.004
2	2,4-Dinitroaniline	0.961	521.497	-0.239
3	2,4-Dimethylphenol	0.993	678.170	0.026
4	2,4-Dihydroxybenzoic Acid	0.997	1962.895	2.156

Figure 11

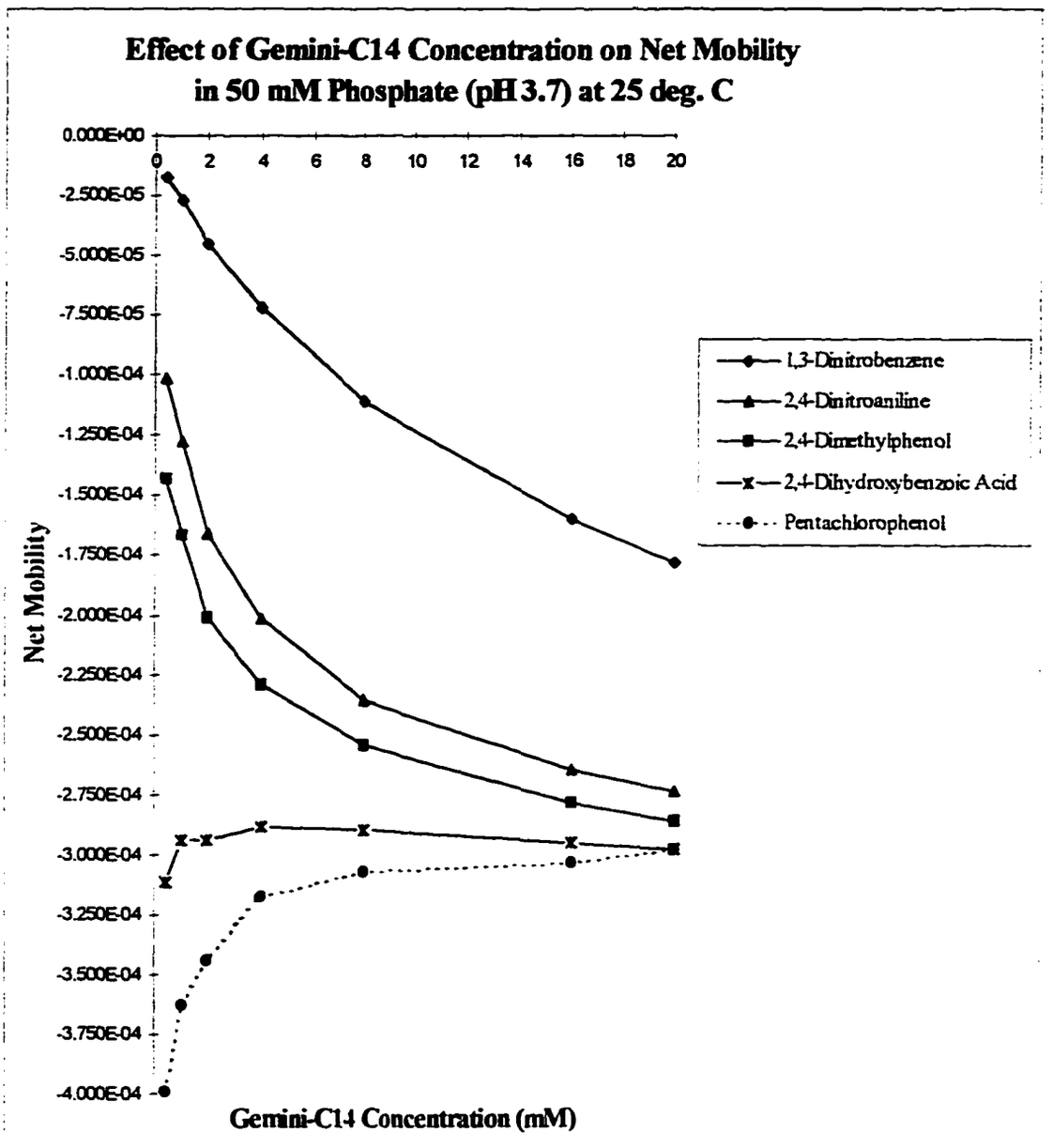

Figure 12

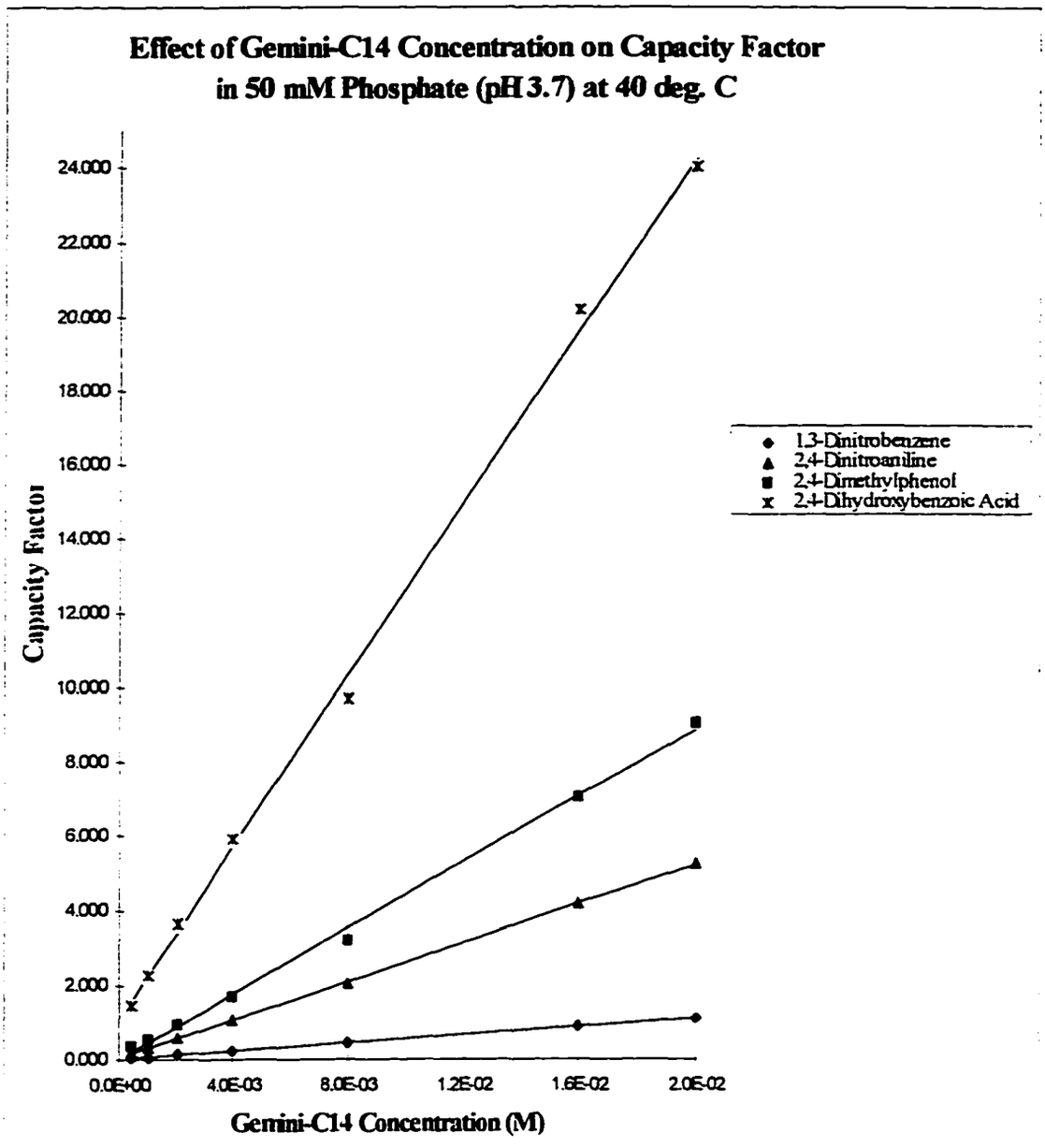

No.	Compounds	*RSQ*	*Slope*	*Intercept*
1	1,3-Dinitrobenzene	1.000	54.038	0.008
2	2,4-Dinitroaniline	1.000	256.779	0.054
3	2,4-Dimethylphenol	0.997	440.248	0.015
4	2,4-Dihydroxybenzoic Acid	0.998	1156.155	1.088

Figure 13

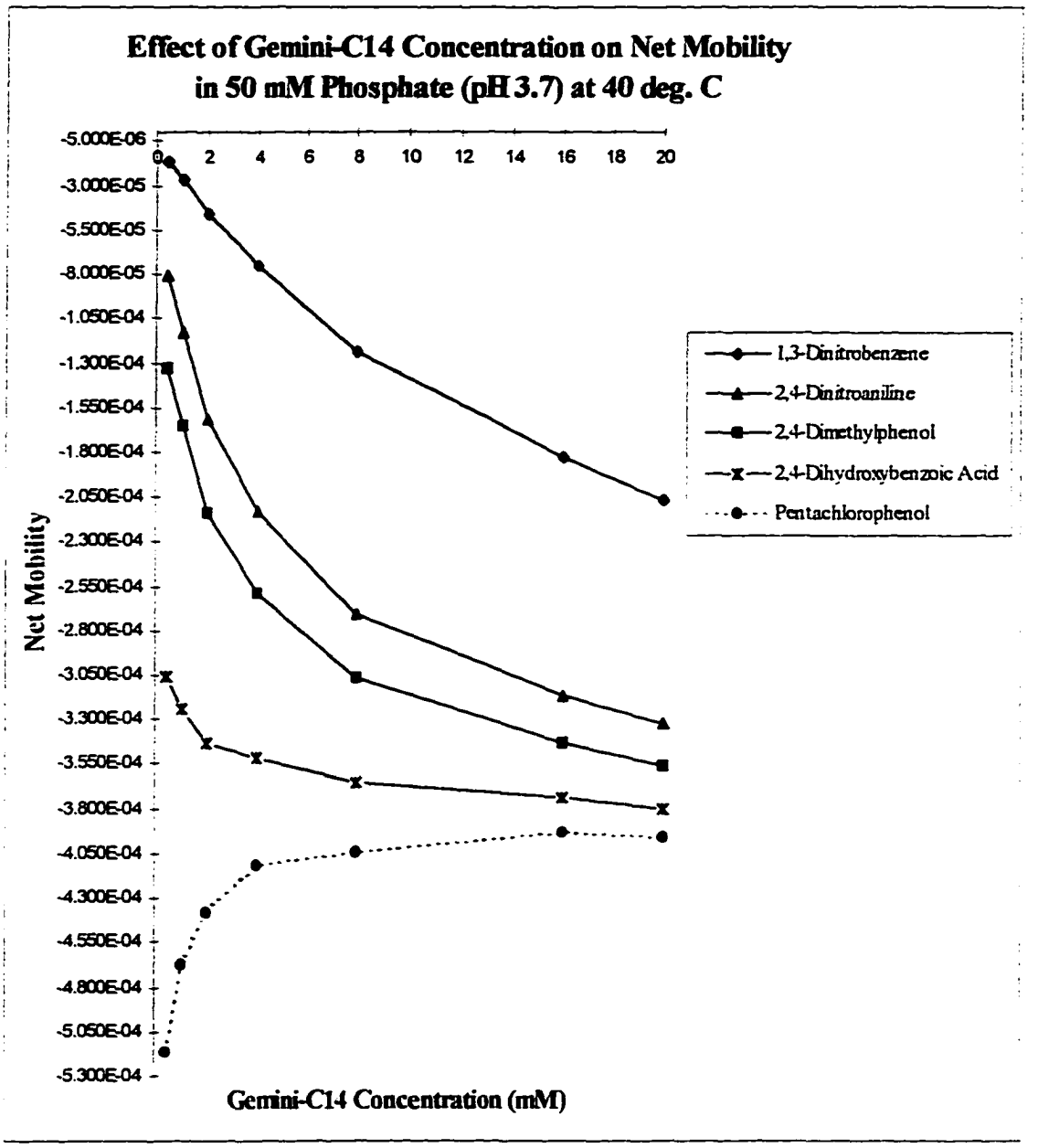

Figure 14

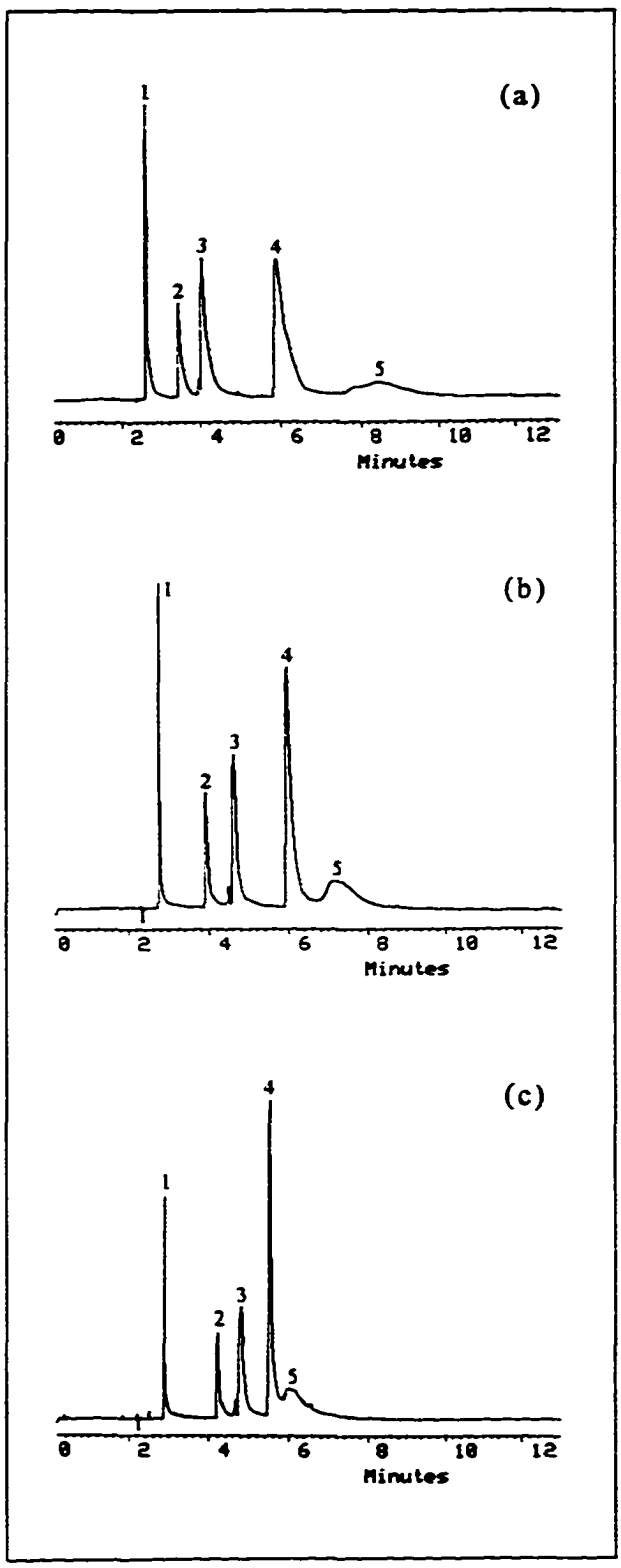

Figure 15

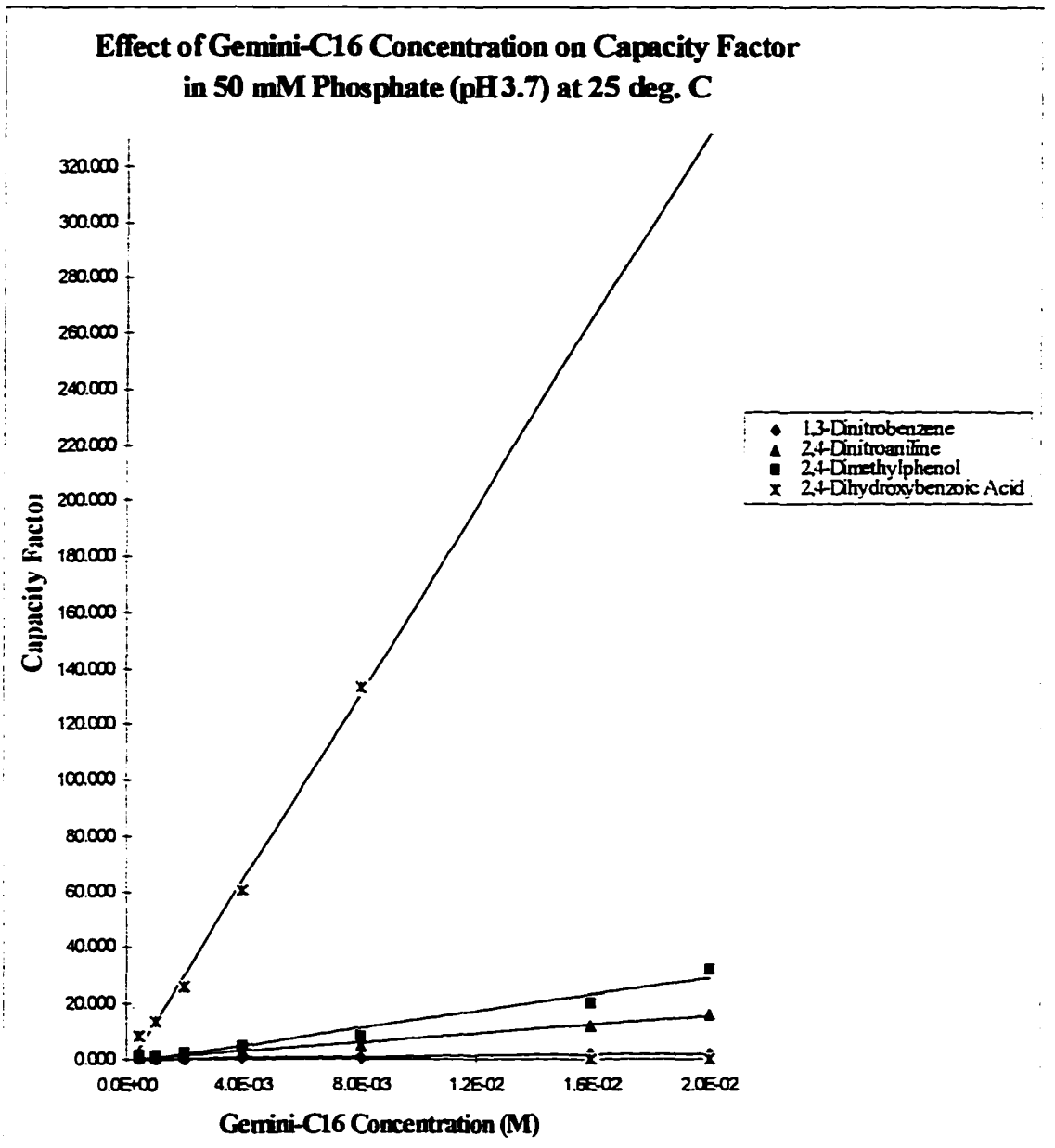

No.	Compounds	*RSQ*	*Slope*	*Intercept*
1	1,3-Dinitrobenzene	0.995	96.346	0.003
2	2,4-Dinitroaniline	0.991	786.064	-0.318
3	2,4-Dimethylphenol	0.967	1497.888	-0.970
4	2,4-Dihydroxybenzoic Acid	0.994	16745.488	-3.221

Figure 16

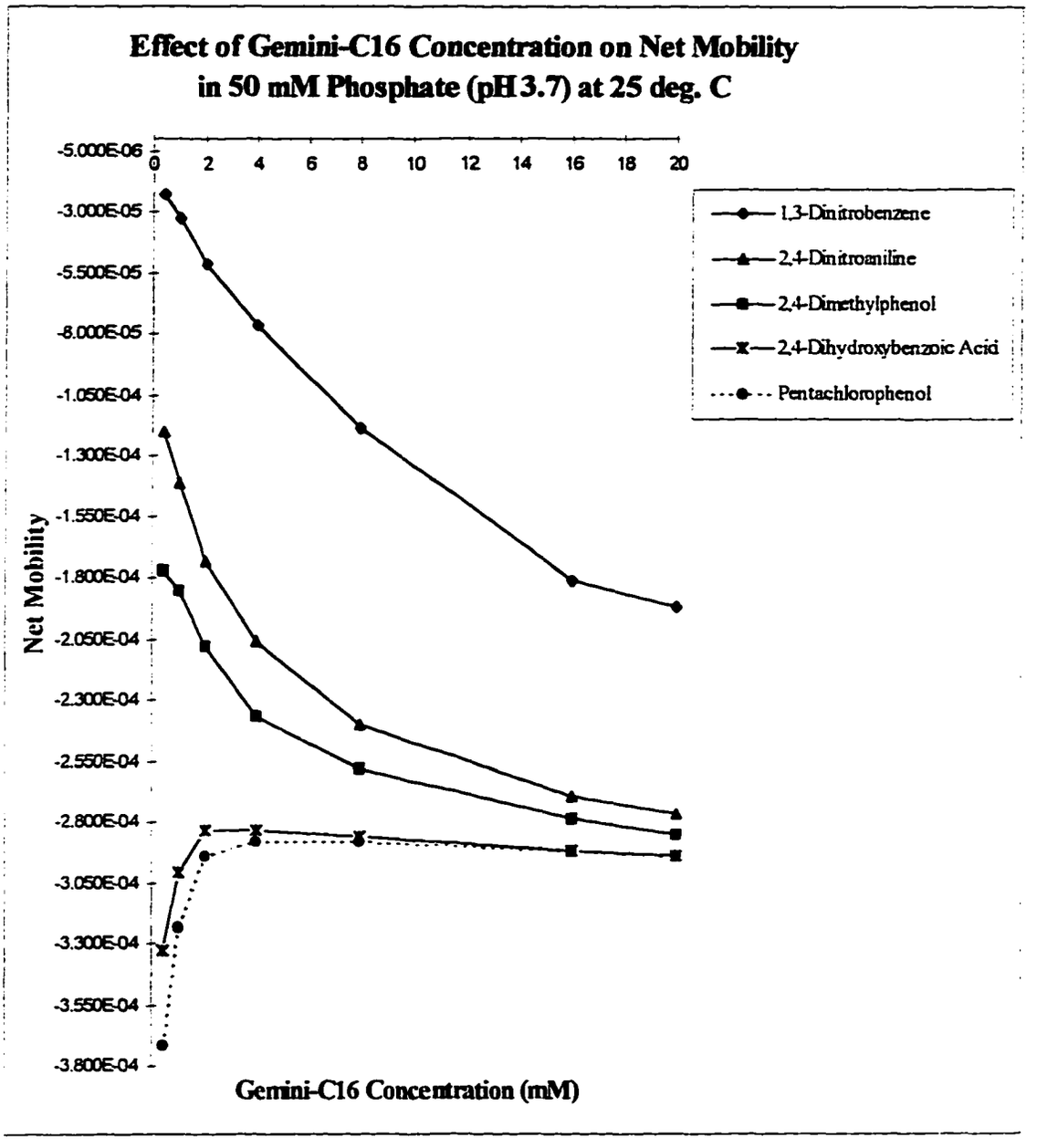

Figure 17

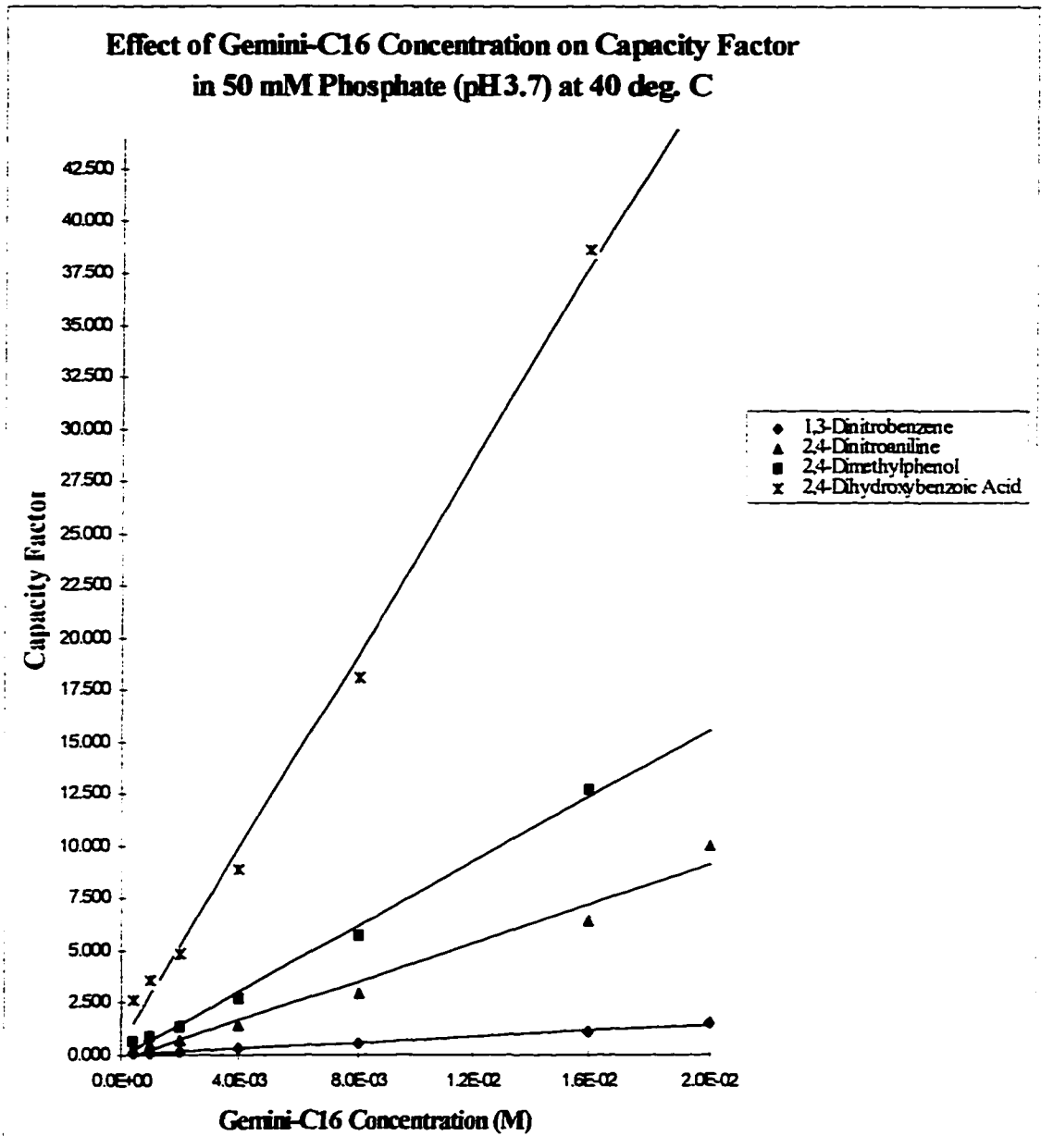

No.	Compounds	*RSQ*	*Slope*	*Intercept*
1	1,3-Dinitrobenzene	0.998	72.776	0.002
2	2,4-Dinitroaniline	0.975	467.860	-0.244
3	2,4-Dimethylphenol	0.994	781.955	-0.105
4	2,4-Dihydroxybenzoic Acid	0.995	2323.093	0.614

Figure 18

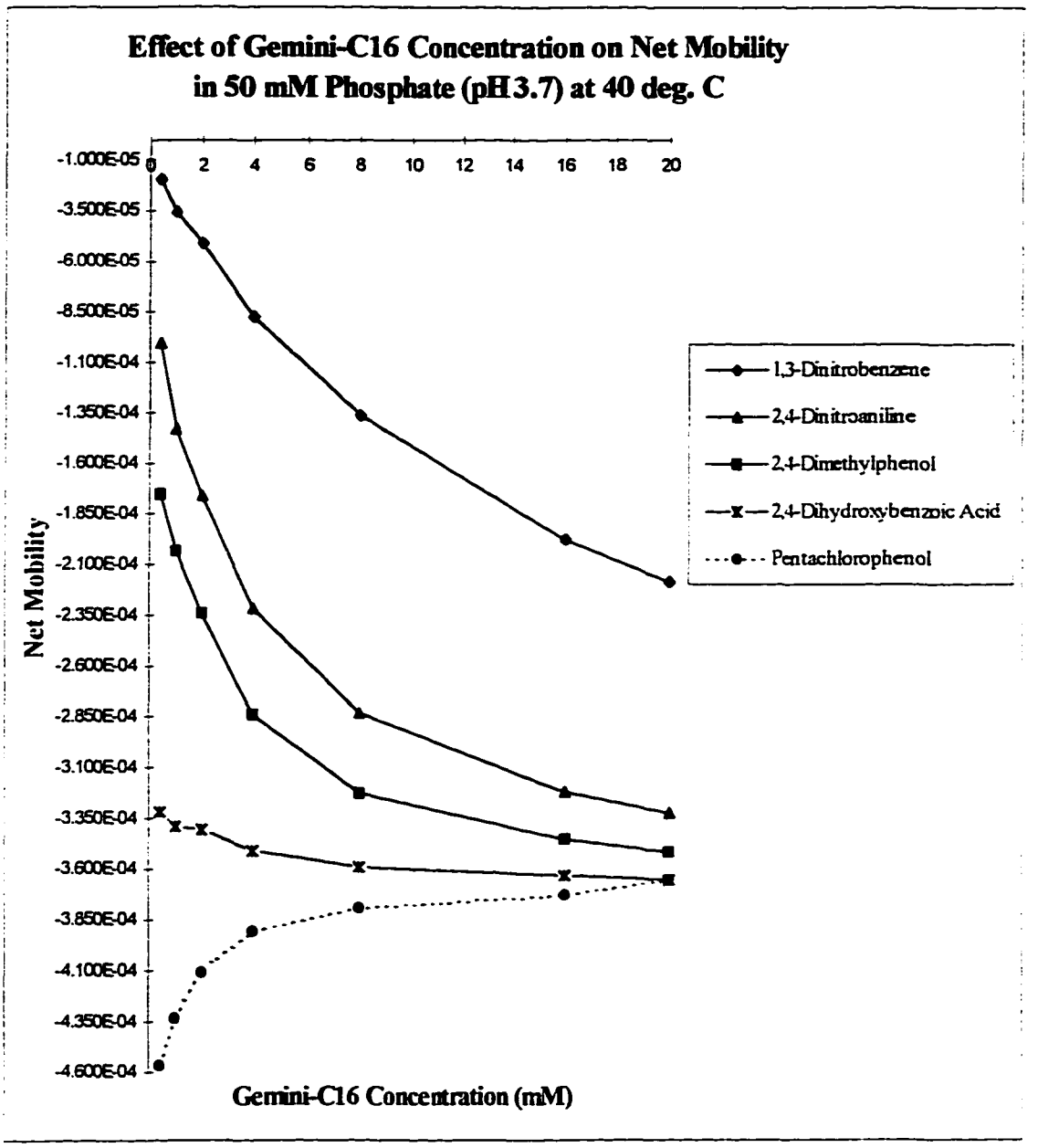

Figure 19 (a)

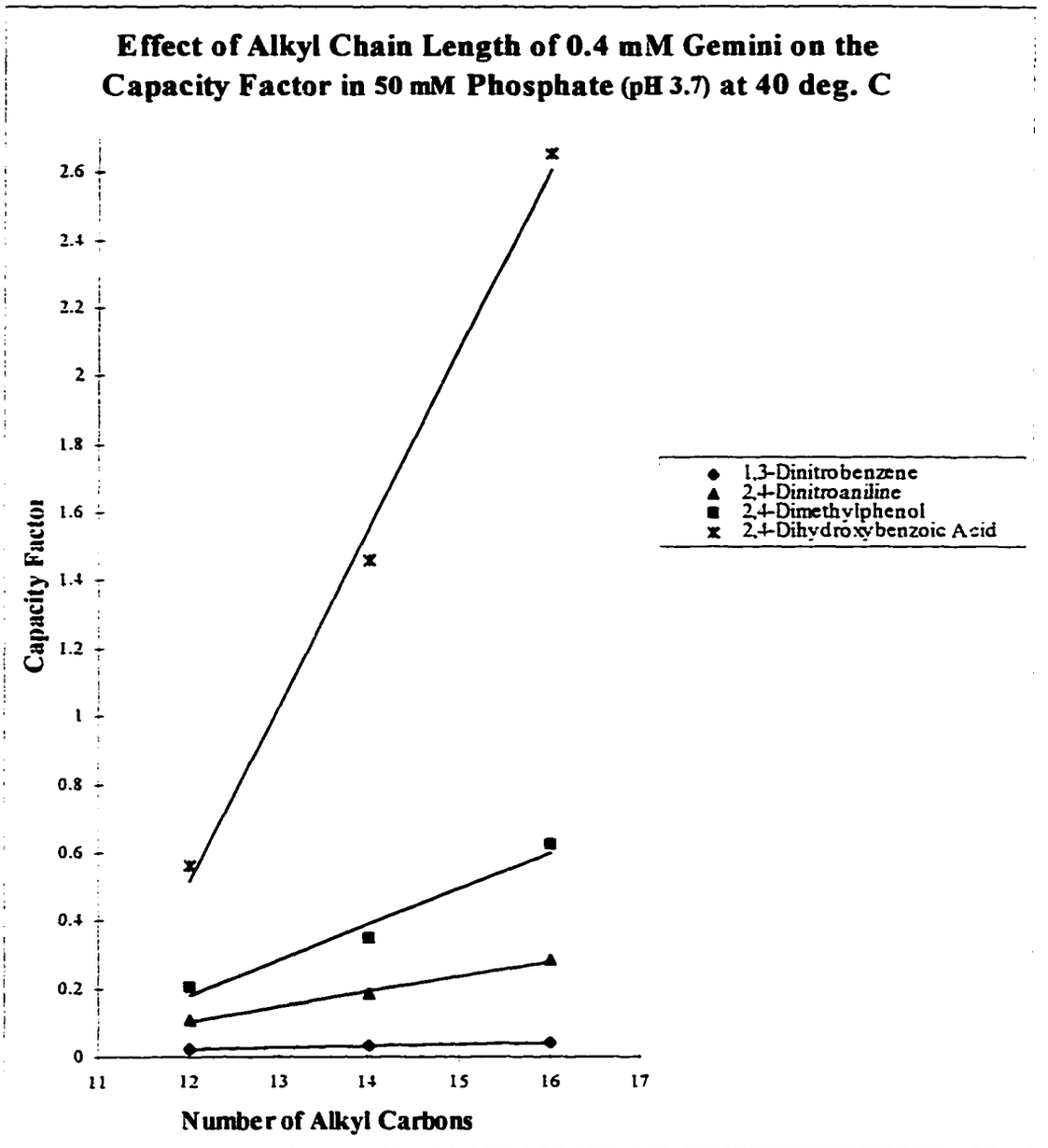

Compounds	*RSQ*
1,3-Dinitrobenzene	0.998
2,4-Dinitroaniline	0.996
2,4-Dimethylphenol	0.969
2,4-Dihydroxybenzoic Acid	0.993

Figure 19 (b)

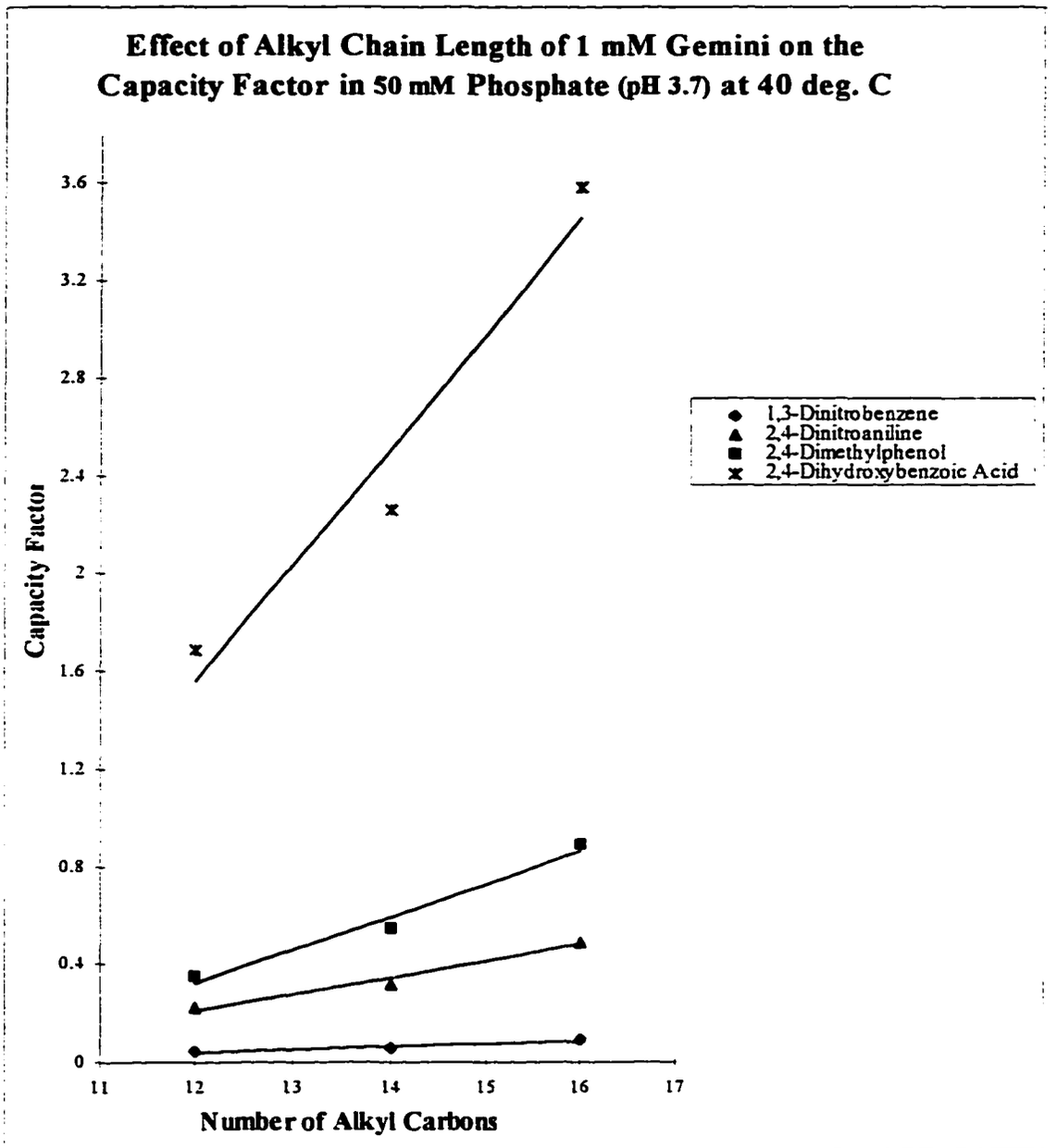

Compounds	*RSQ*
1,3-Dinitrobenzene	0.968
2,4-Dinitroaniline	0.976
2,4-Dimethylphenol	0.977
2,4-Dihydroxybenzoic Acid	0.950

Figure 19 (c)

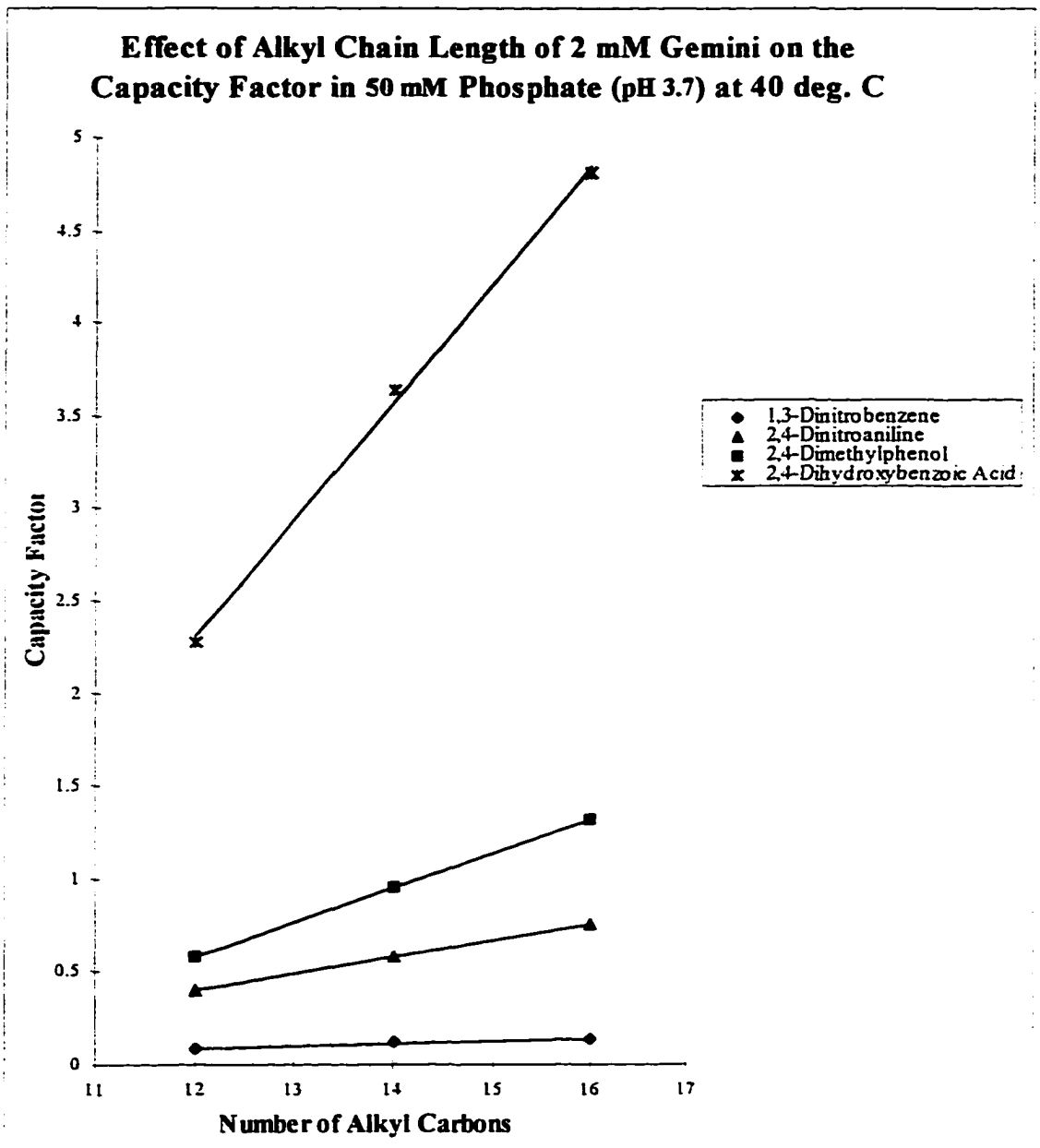

Compounds	*RSQ*
1,3-Dinitrobenzene	0.995
2,4-Dinitroaniline	0.999
2,4-Dimethylphenol	1.000
2,4-Dihydroxybenzoic Acid	0.998

Figure 19 (d)

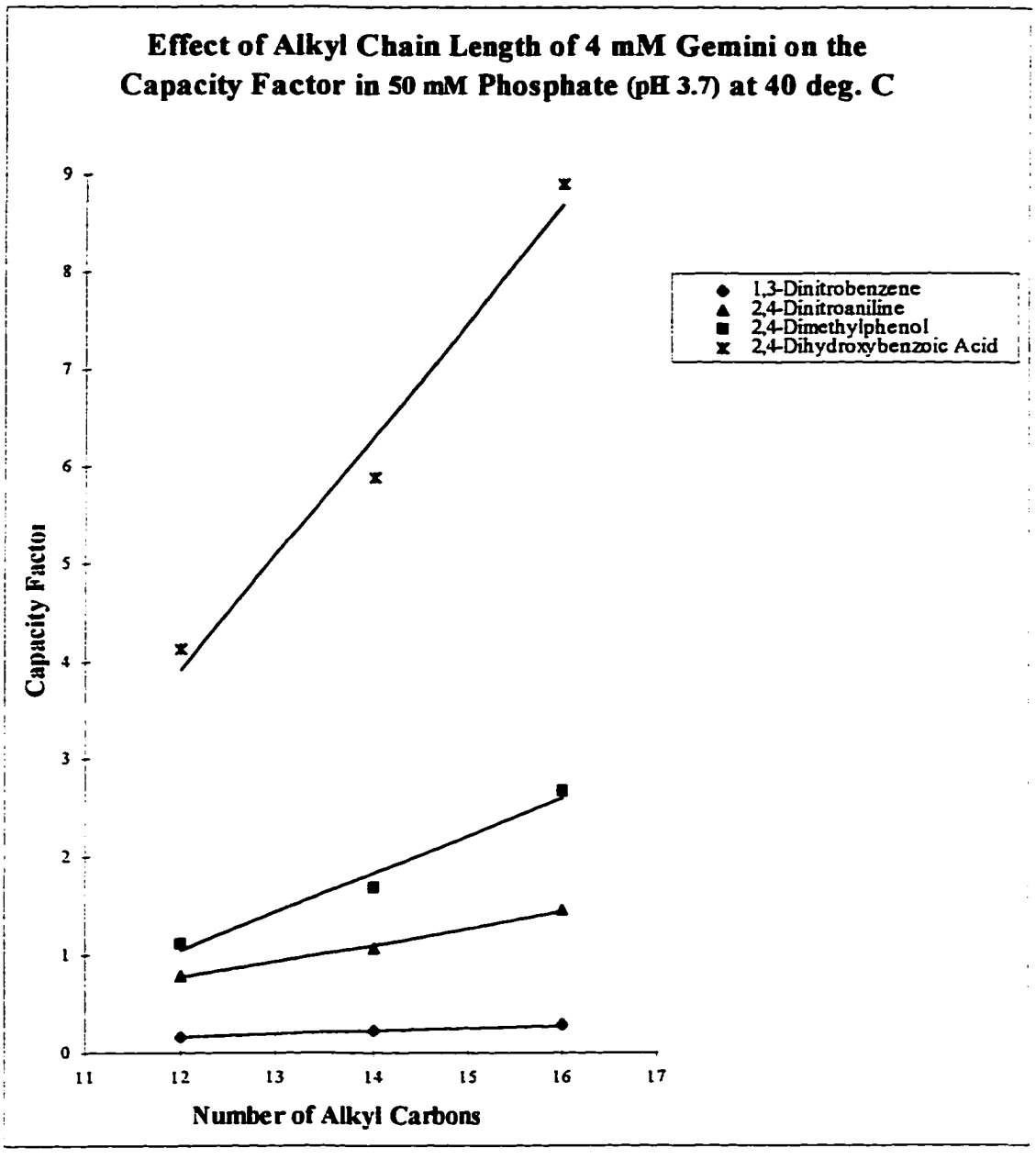

Compounds	*RSQ*
1,3-Dinitrobenzene	0.995
2,4-Dinitroaniline	0.993
2,4-Dimethylphenol	0.978
2,4-Dihydroxybenzoic Acid	0.977

Figure 19 (e)

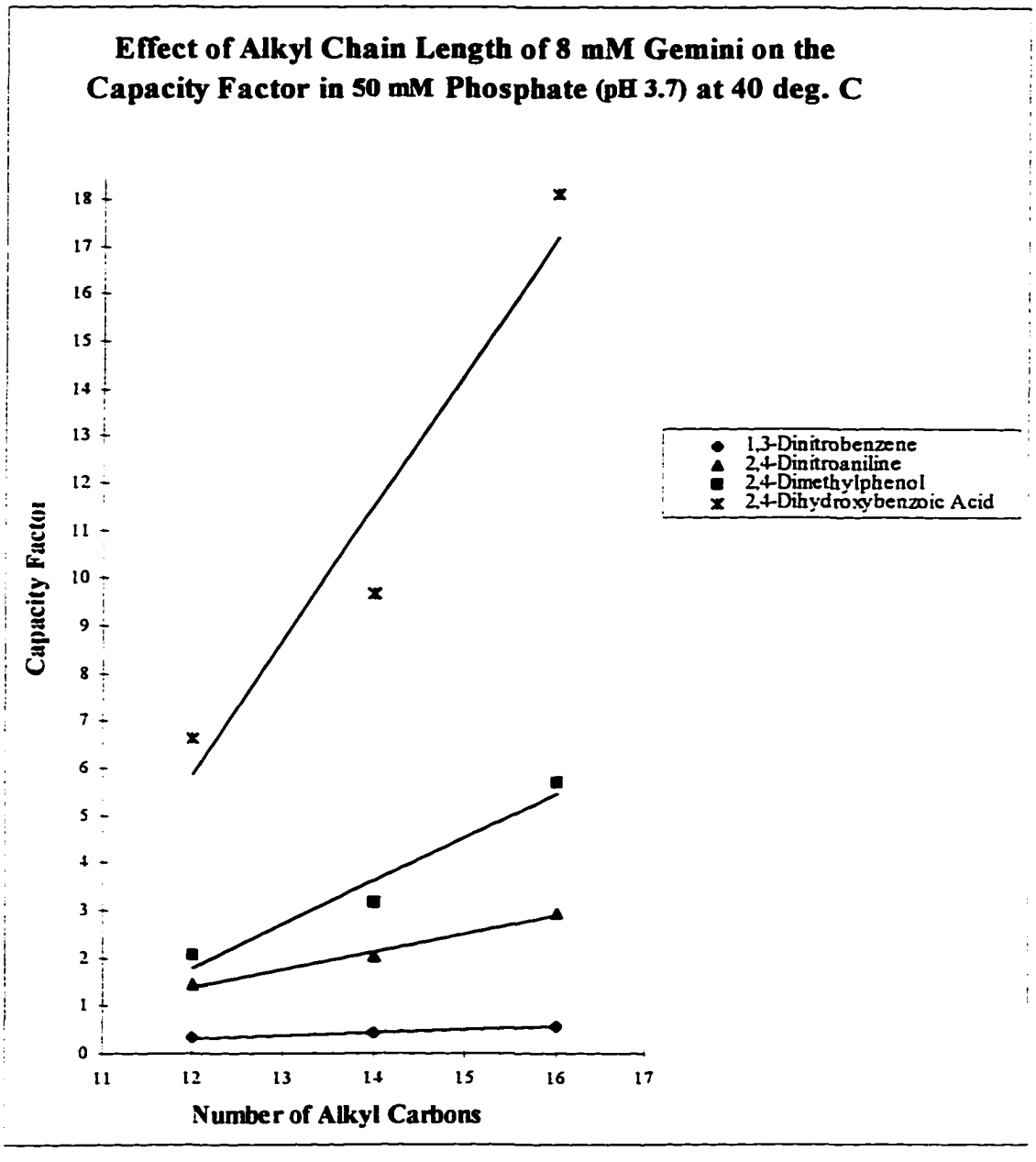

Compounds	*RSQ*
1,3-Dinitrobenzene	1.000
2,4-Dinitroaniline	0.990
2,4-Dimethylphenol	0.955
2,4-Dihydroxybenzoic Acid	0.927

Figure 19 (f)

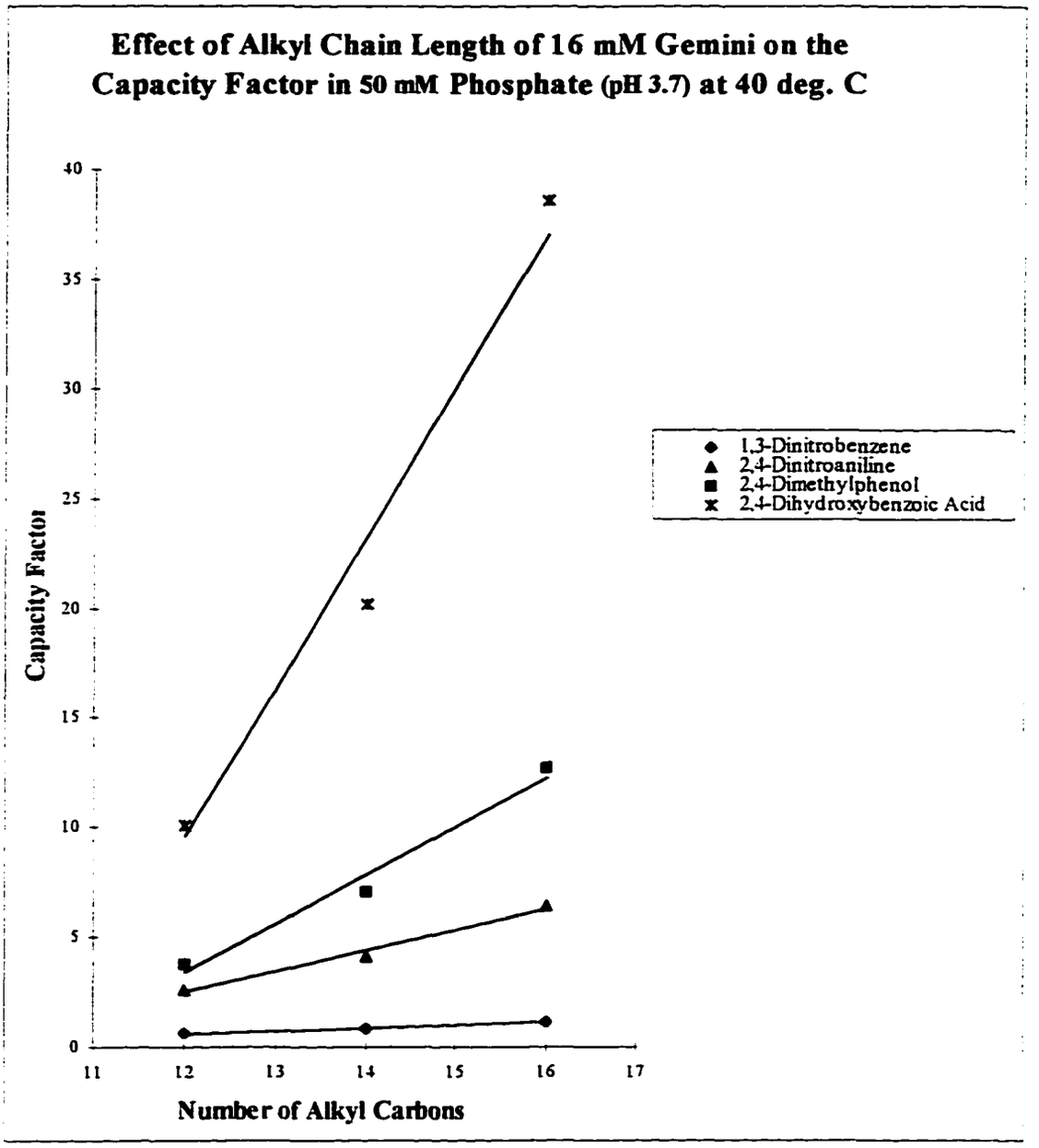

Compounds	*RSQ*
1,3-Dinitrobenzene	1.000
2,4-Dinitroaniline	0.986
2,4-Dimethylphenol	0.973
2,4-Dihydroxybenzoic Acid	0.962

Figure 20 (a)

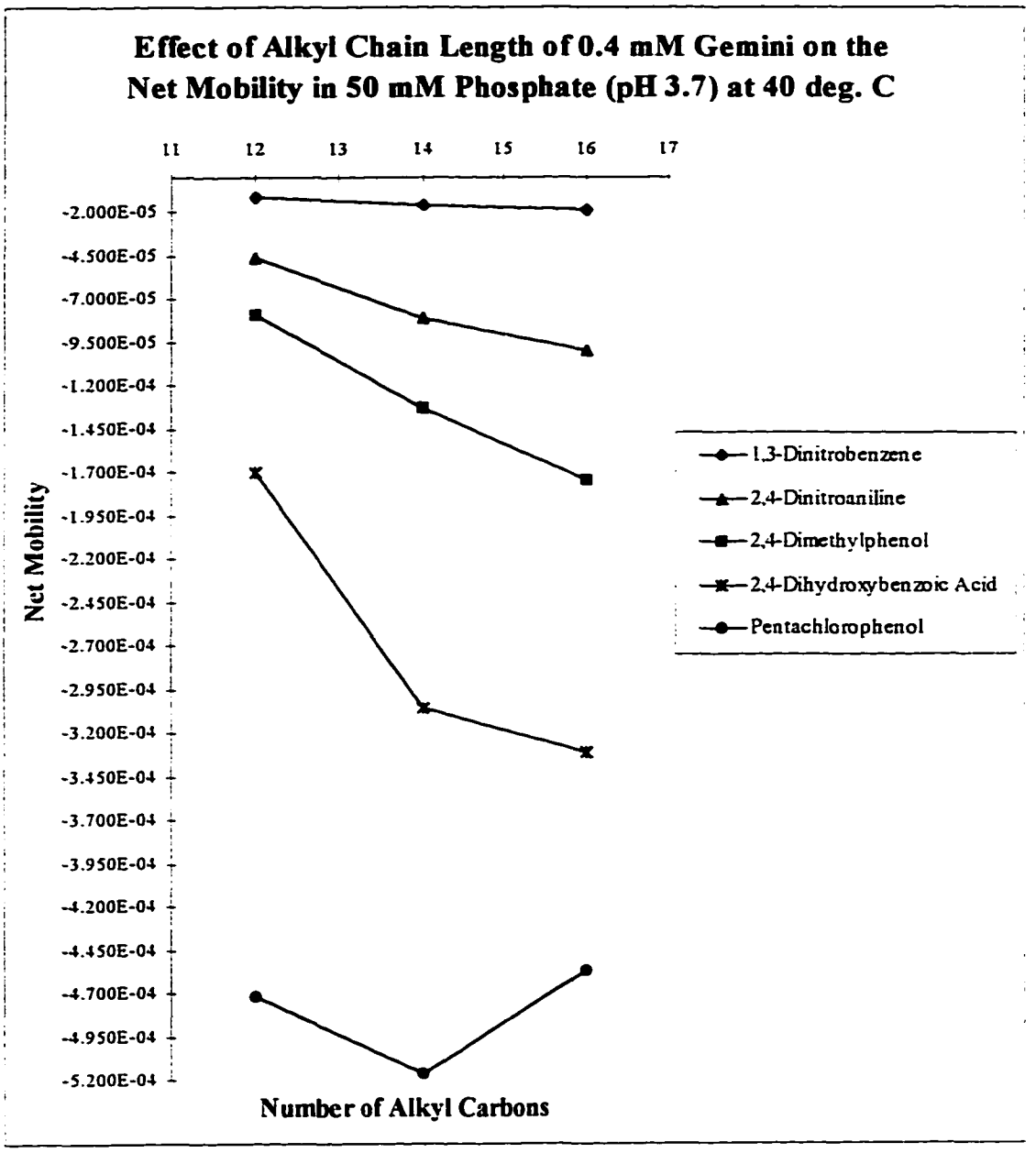

Figure 20 (b)

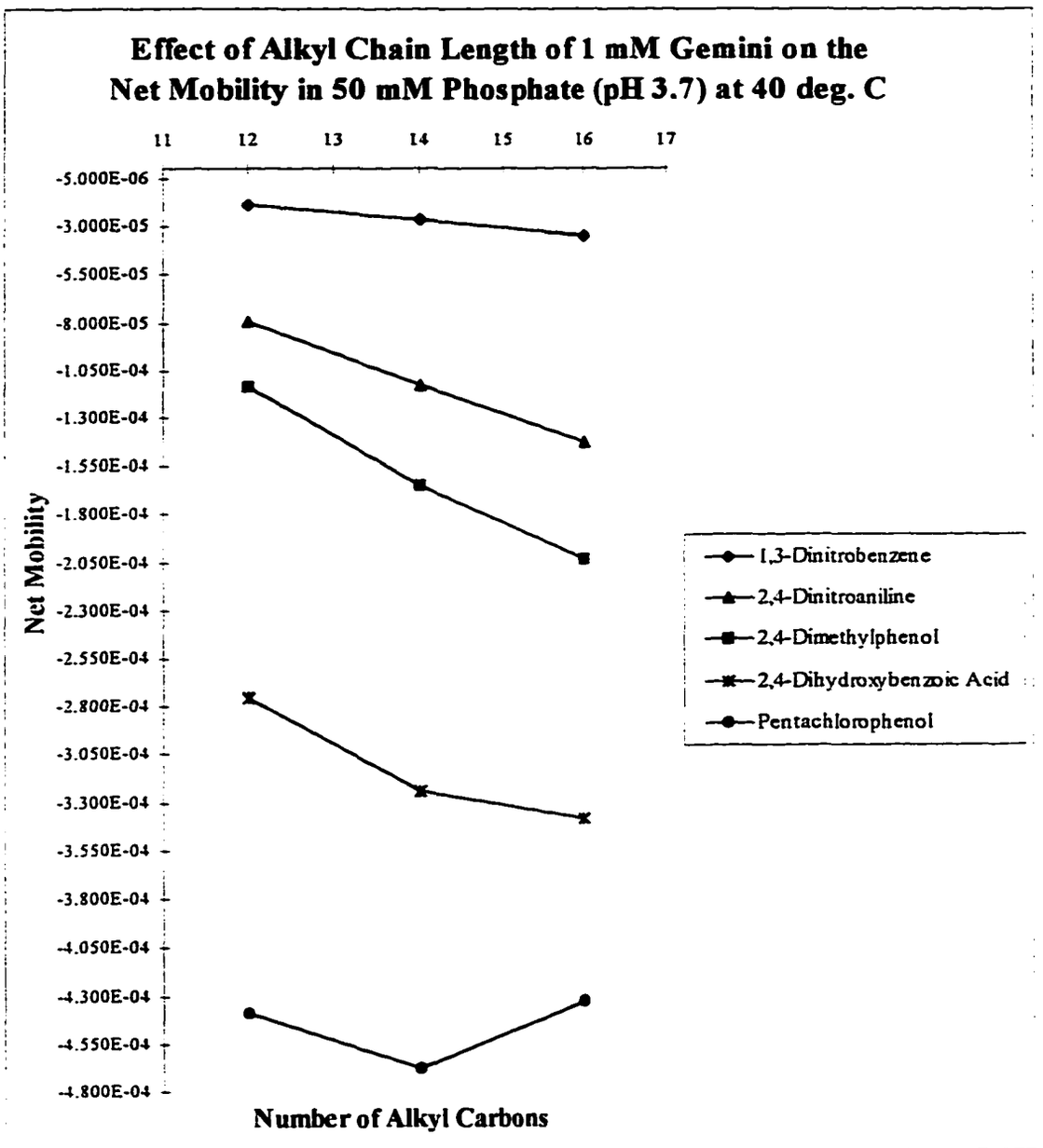

Figure 20 (c)

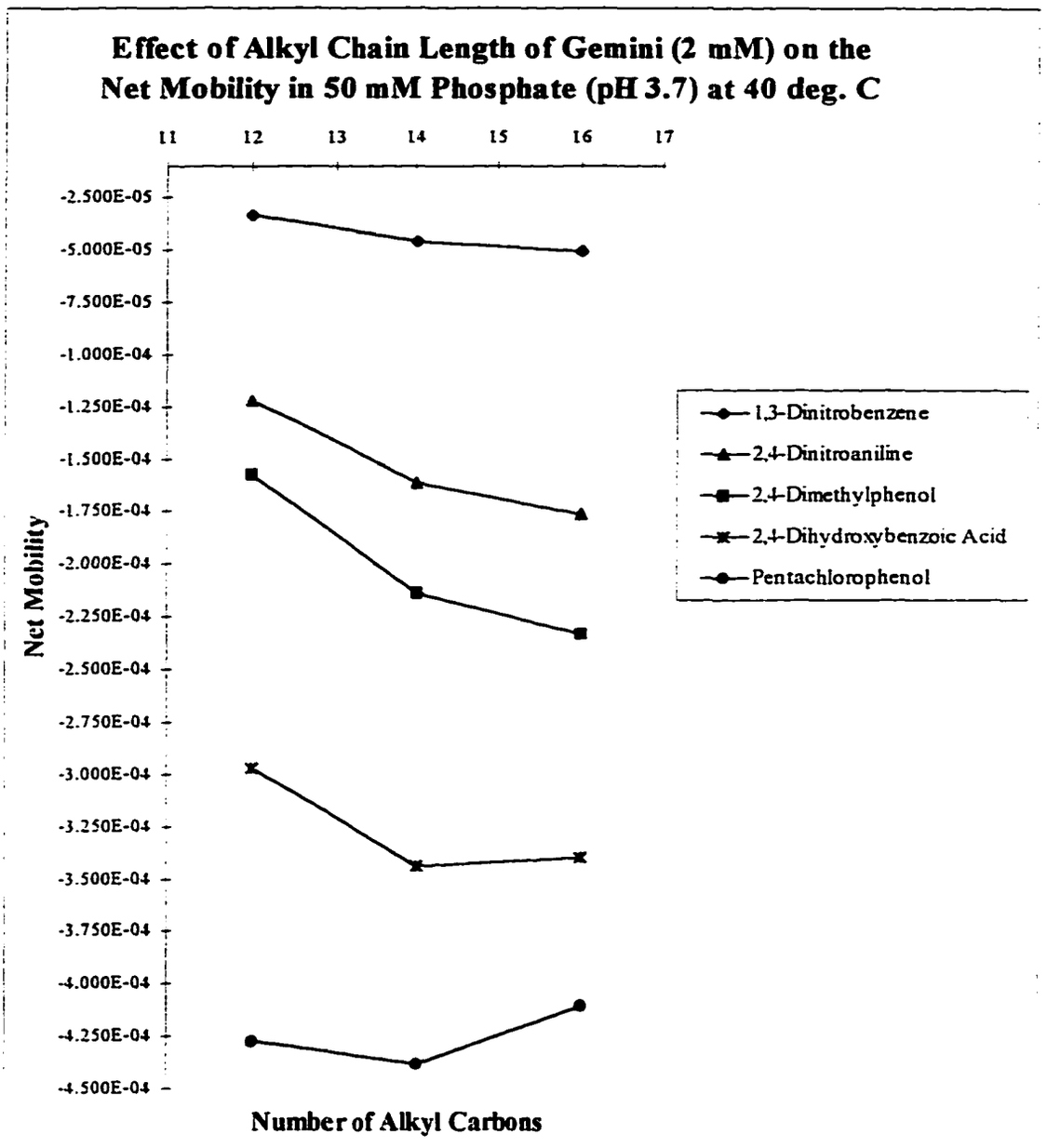

Figure 20 (d)

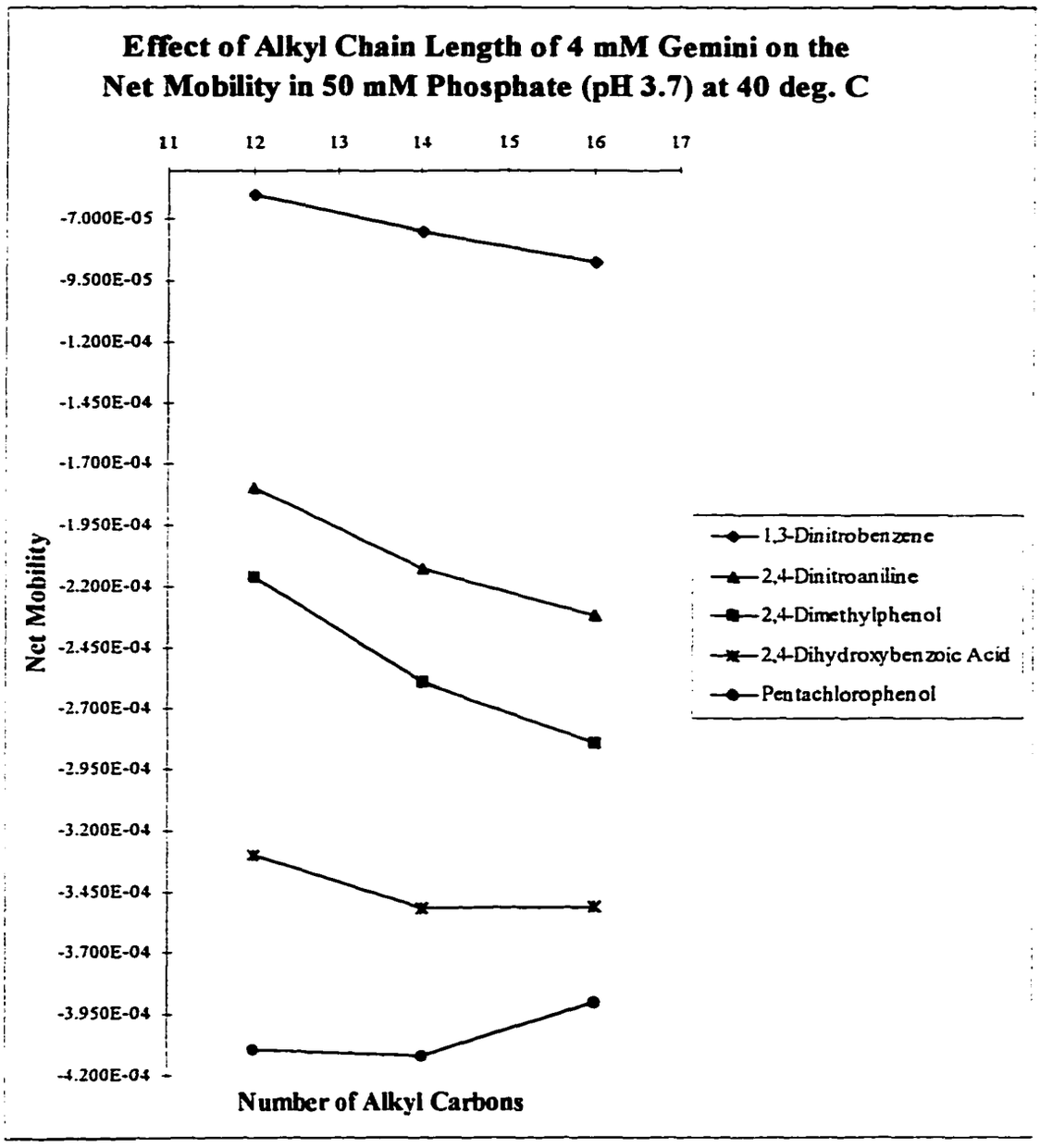

Figure 20 (e)

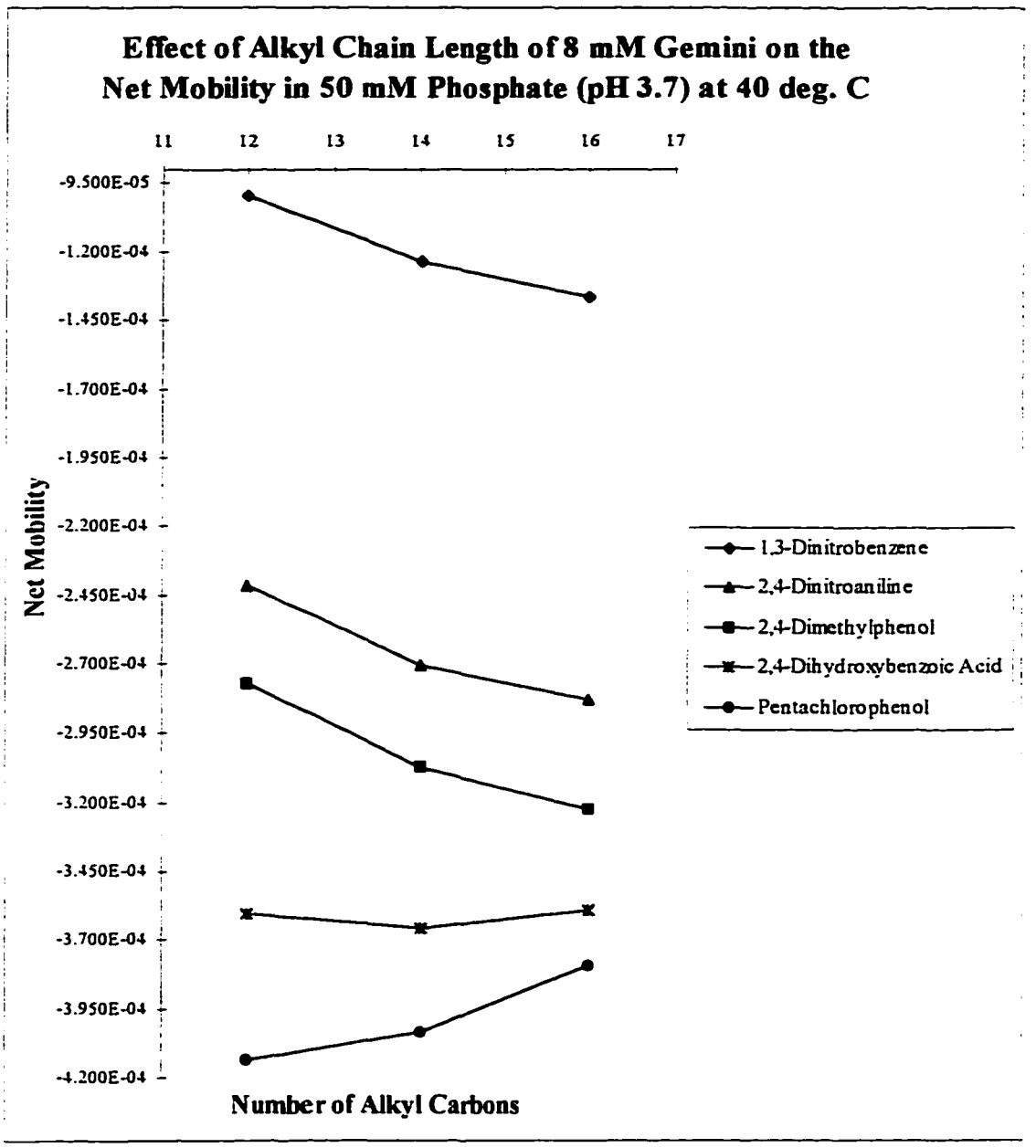

Figure 20 (f)

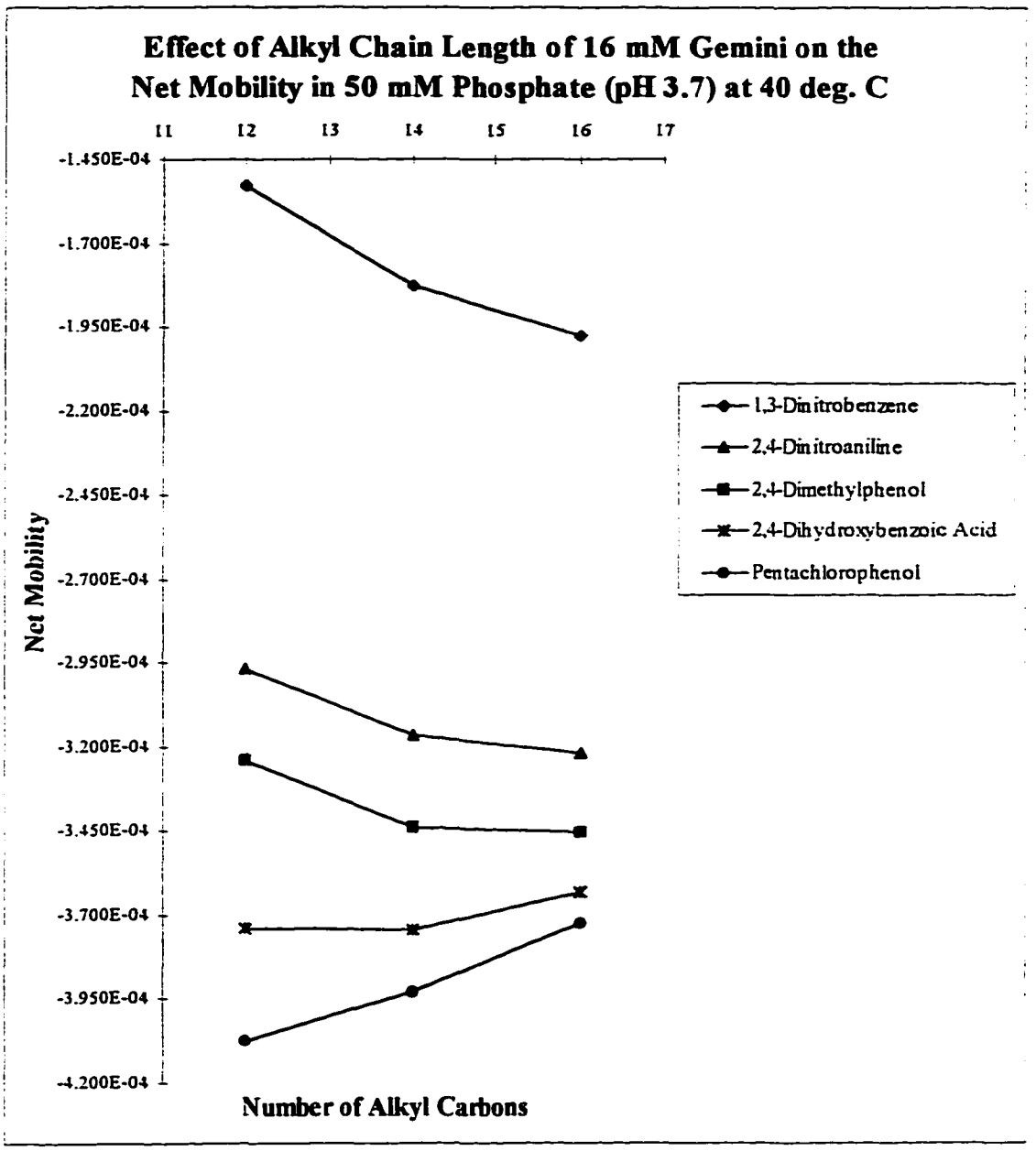

Figure 20 (g)

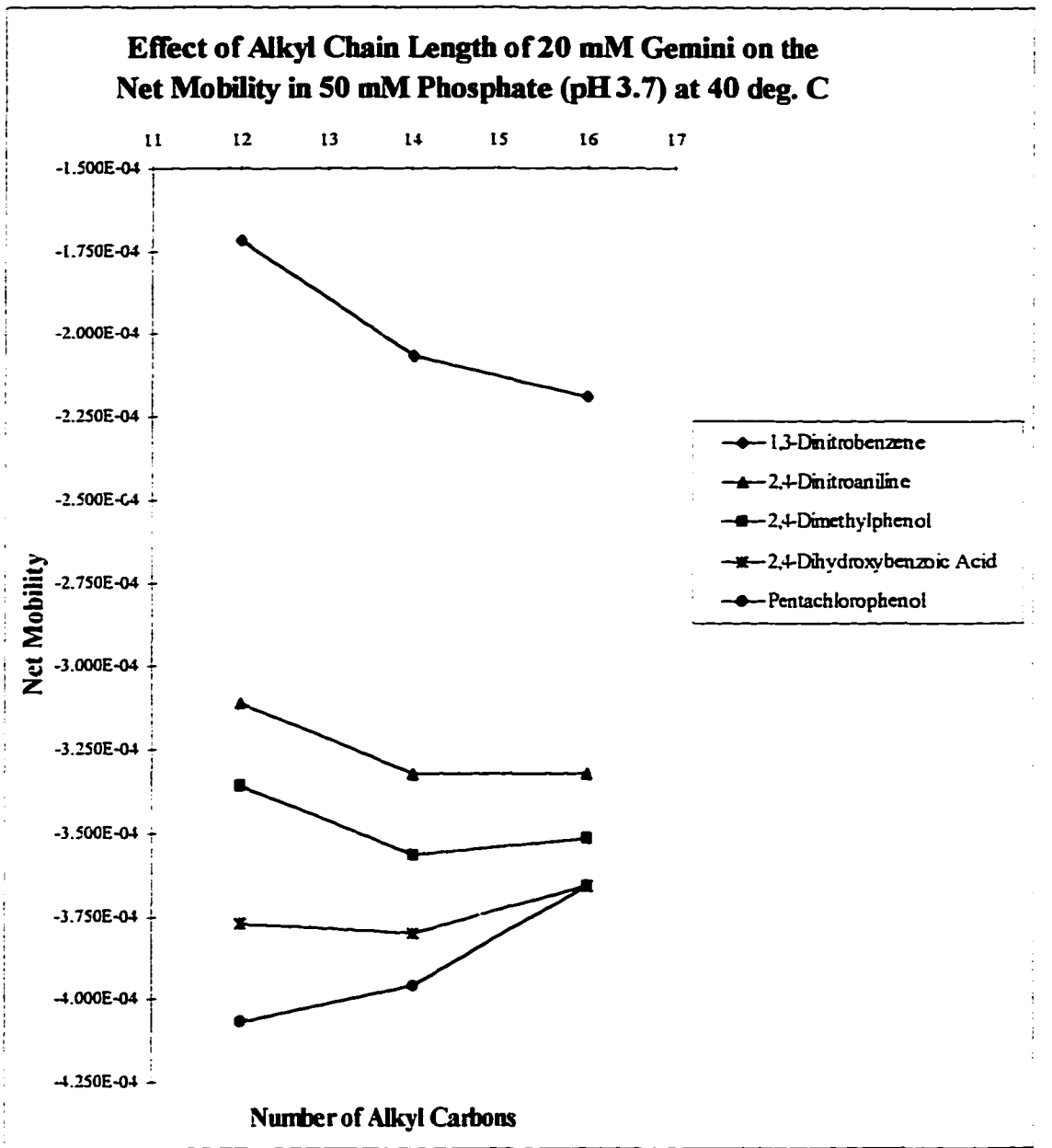

Figure 21 (a)

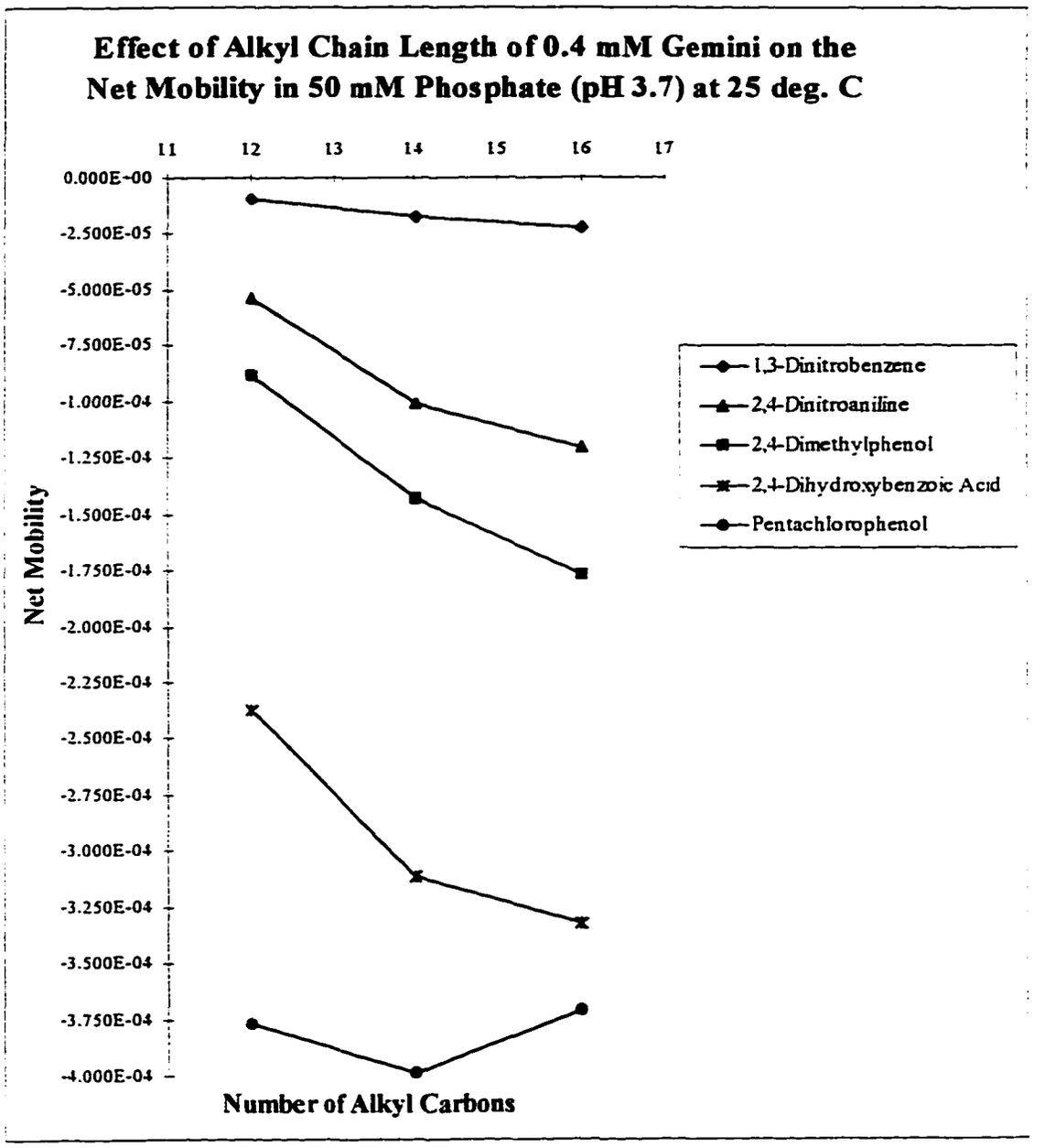

Figure 21 (b)

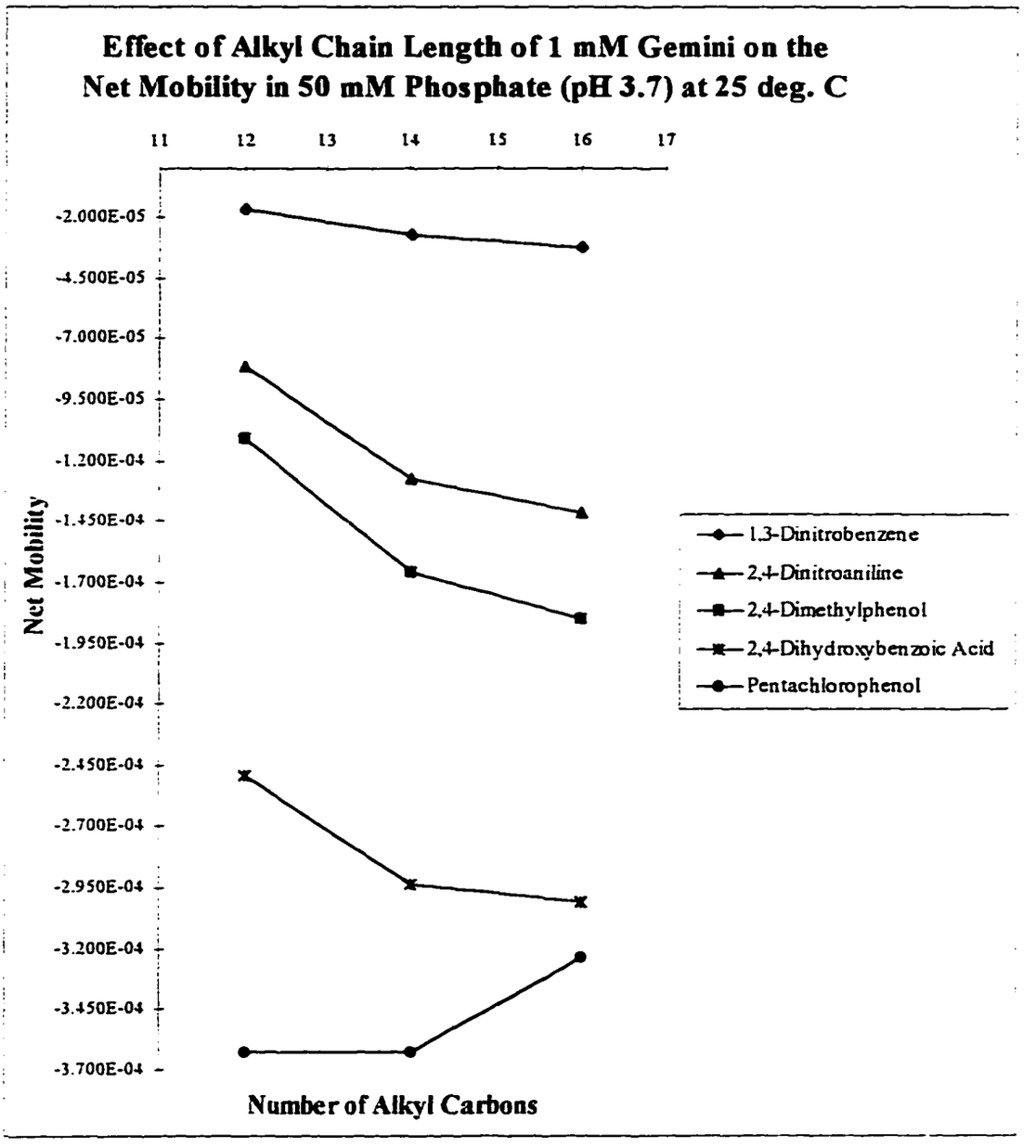

Figure 21 (c)

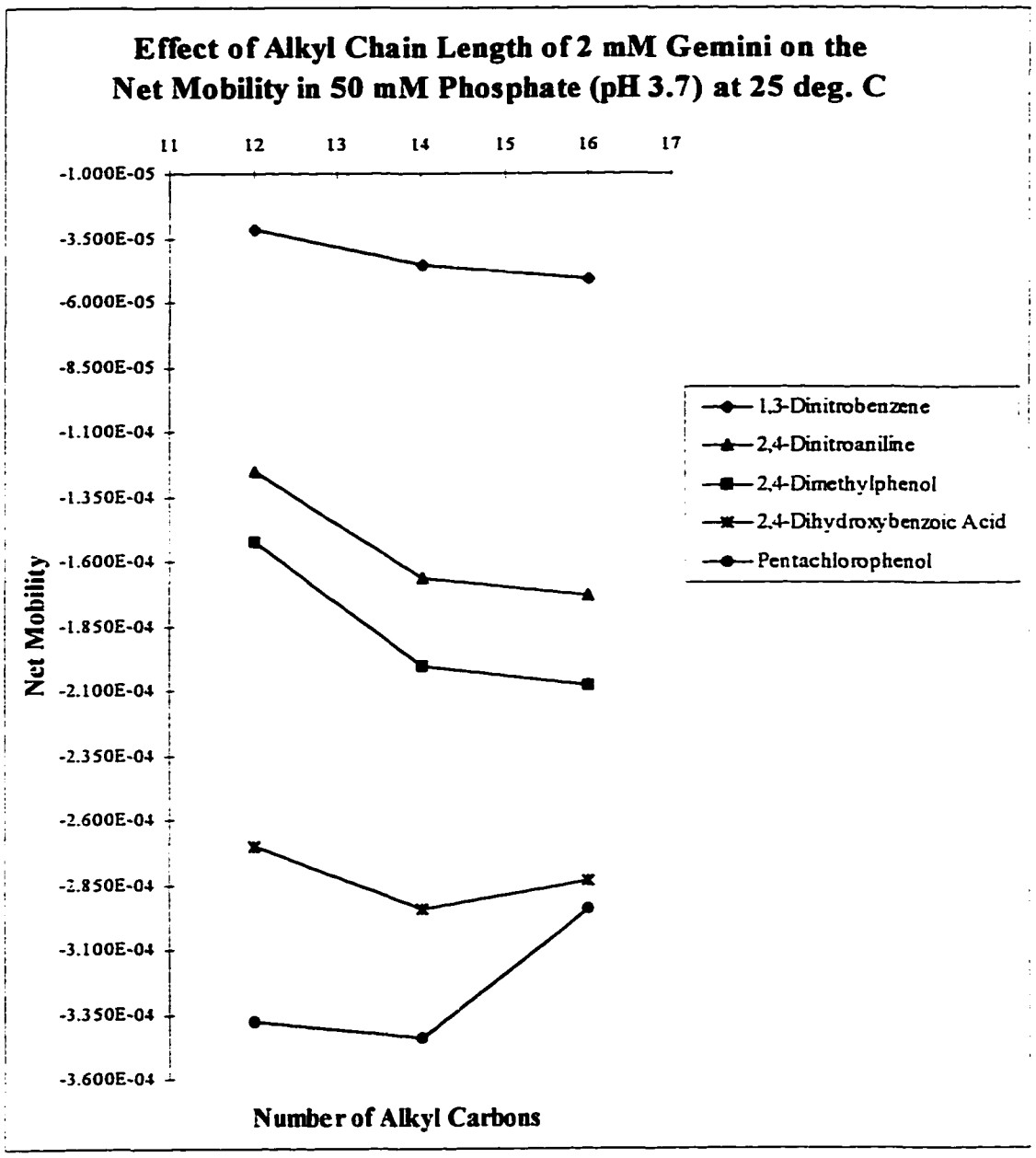

Figure 21 (d)

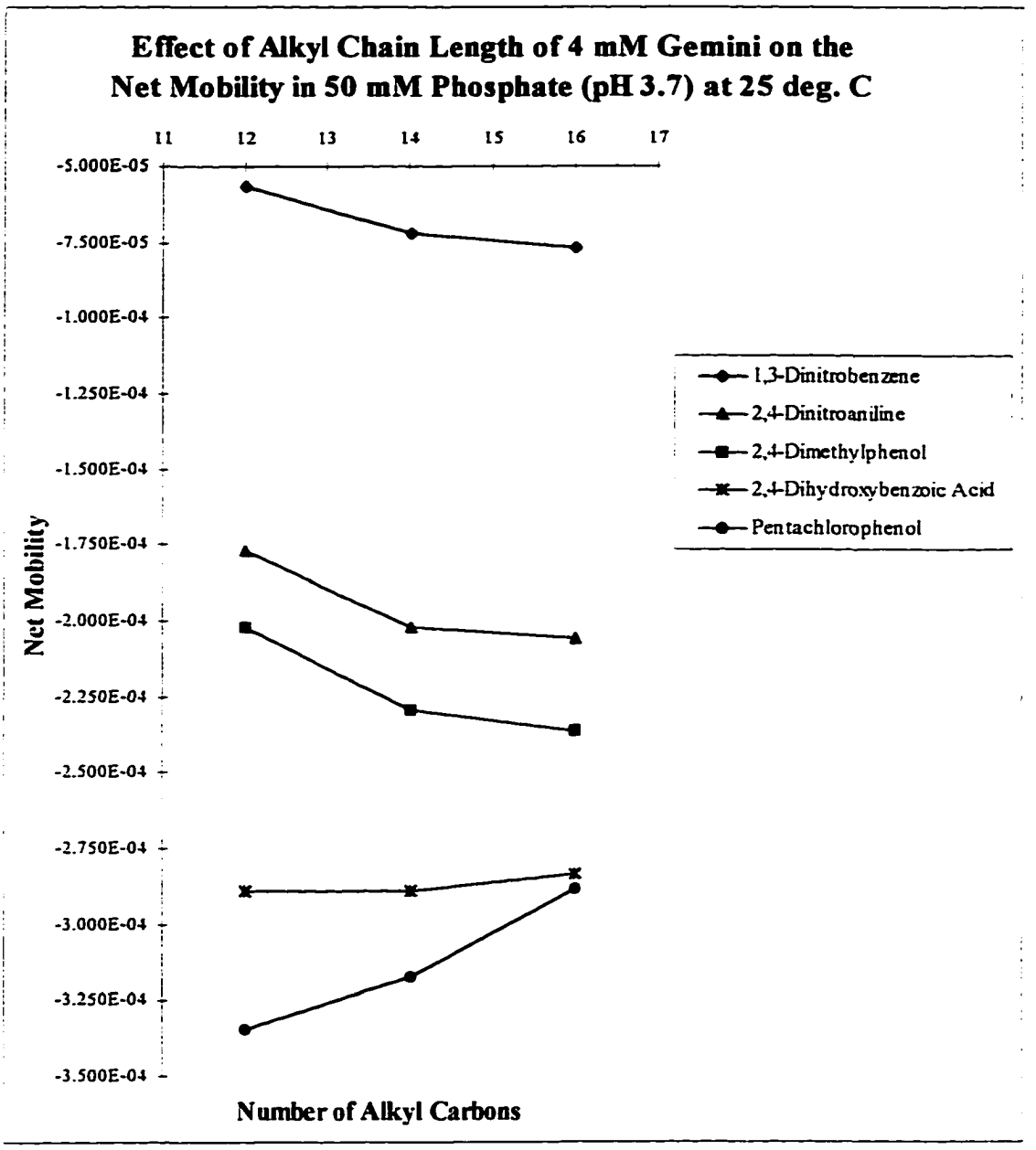

Figure 21 (e)

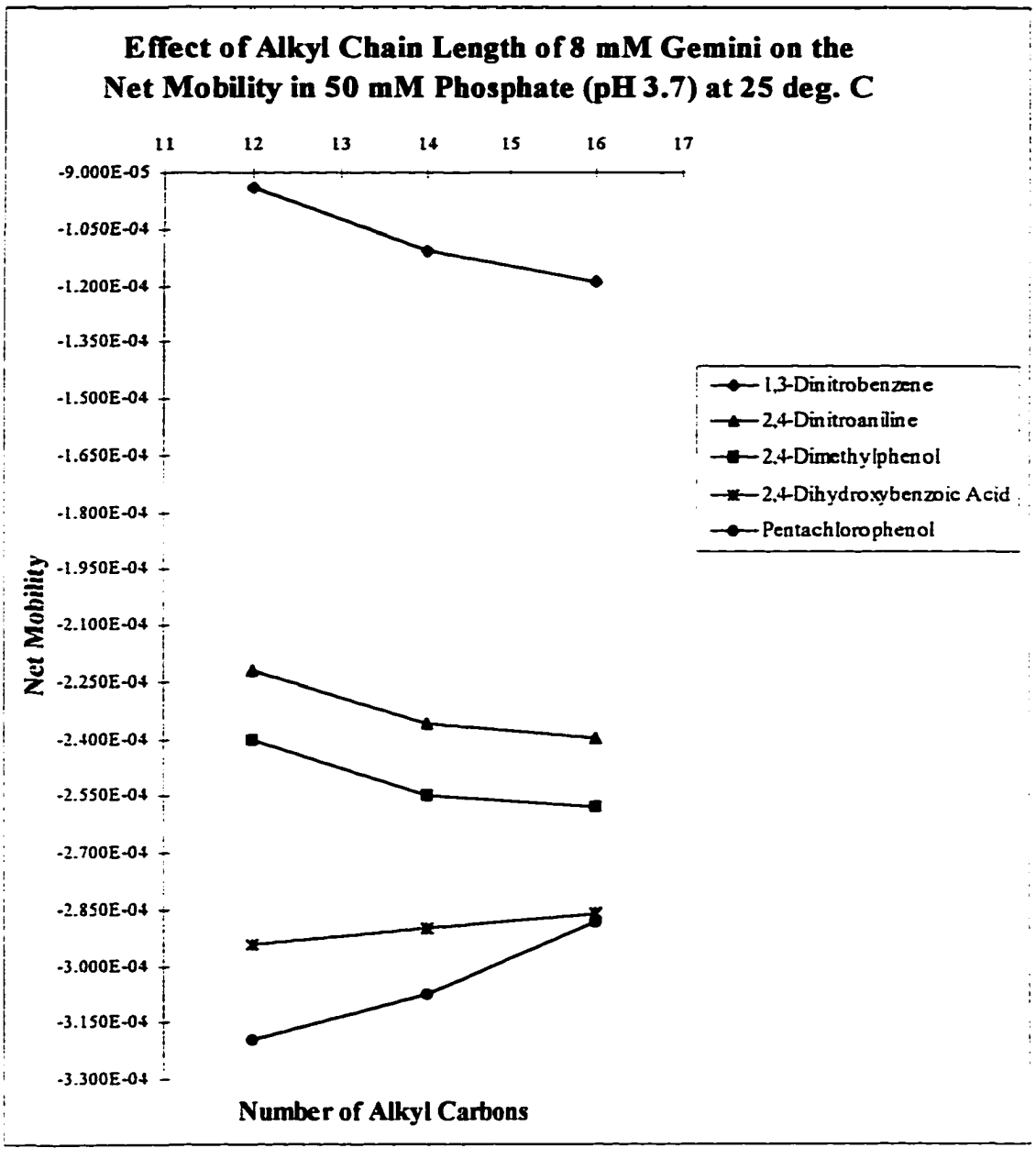

Figure 21 (f)

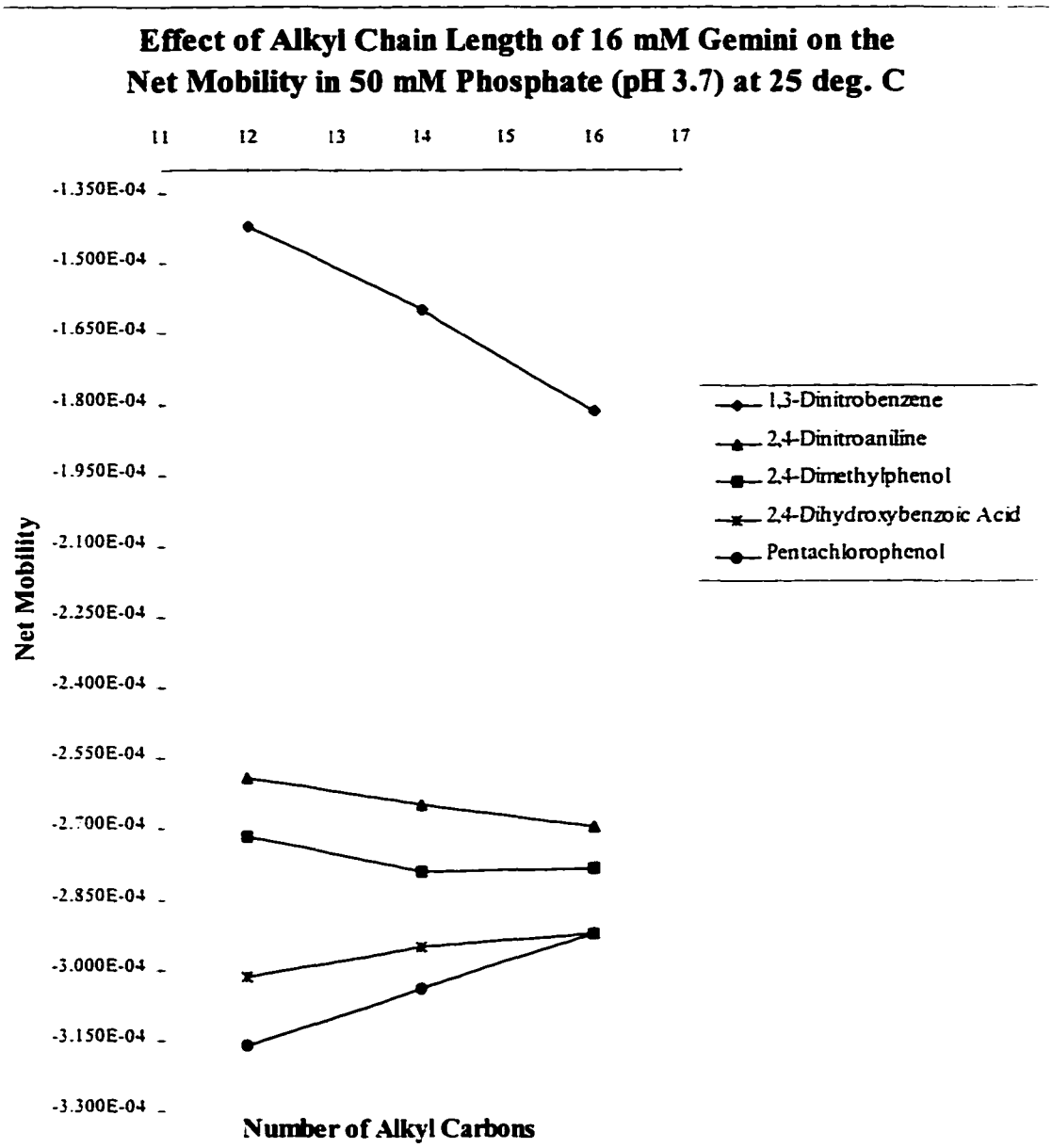

Figure 21 (g)

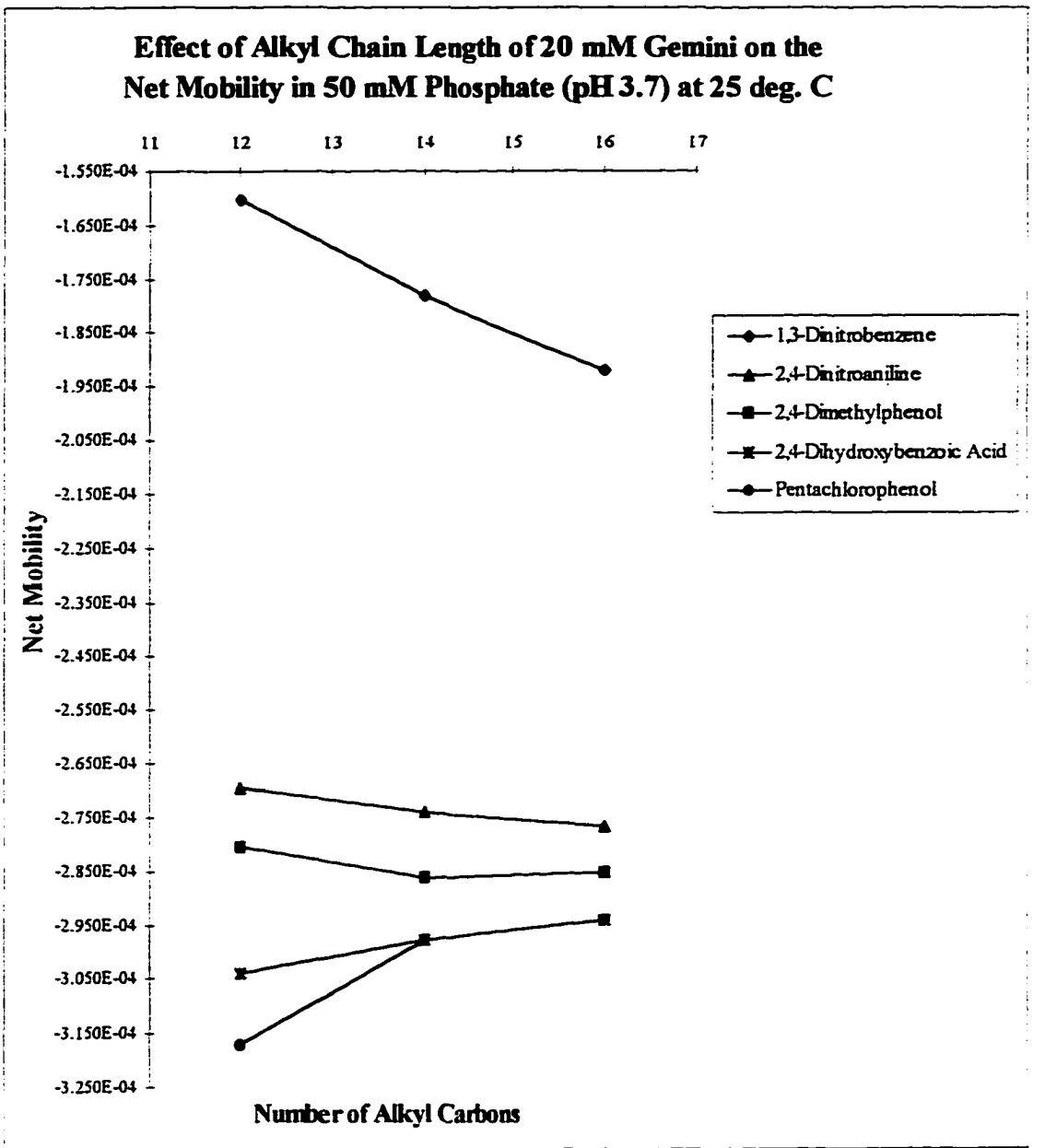

Figure 22

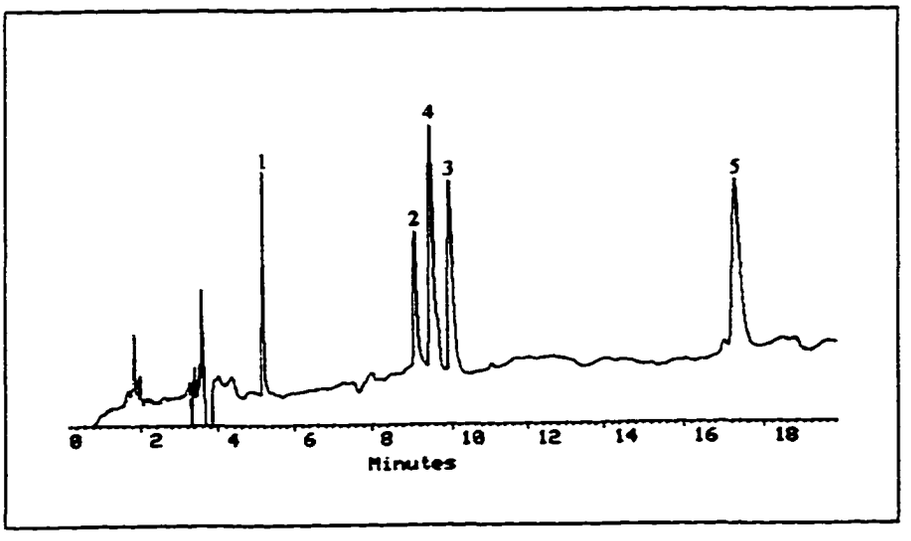

Figure 23

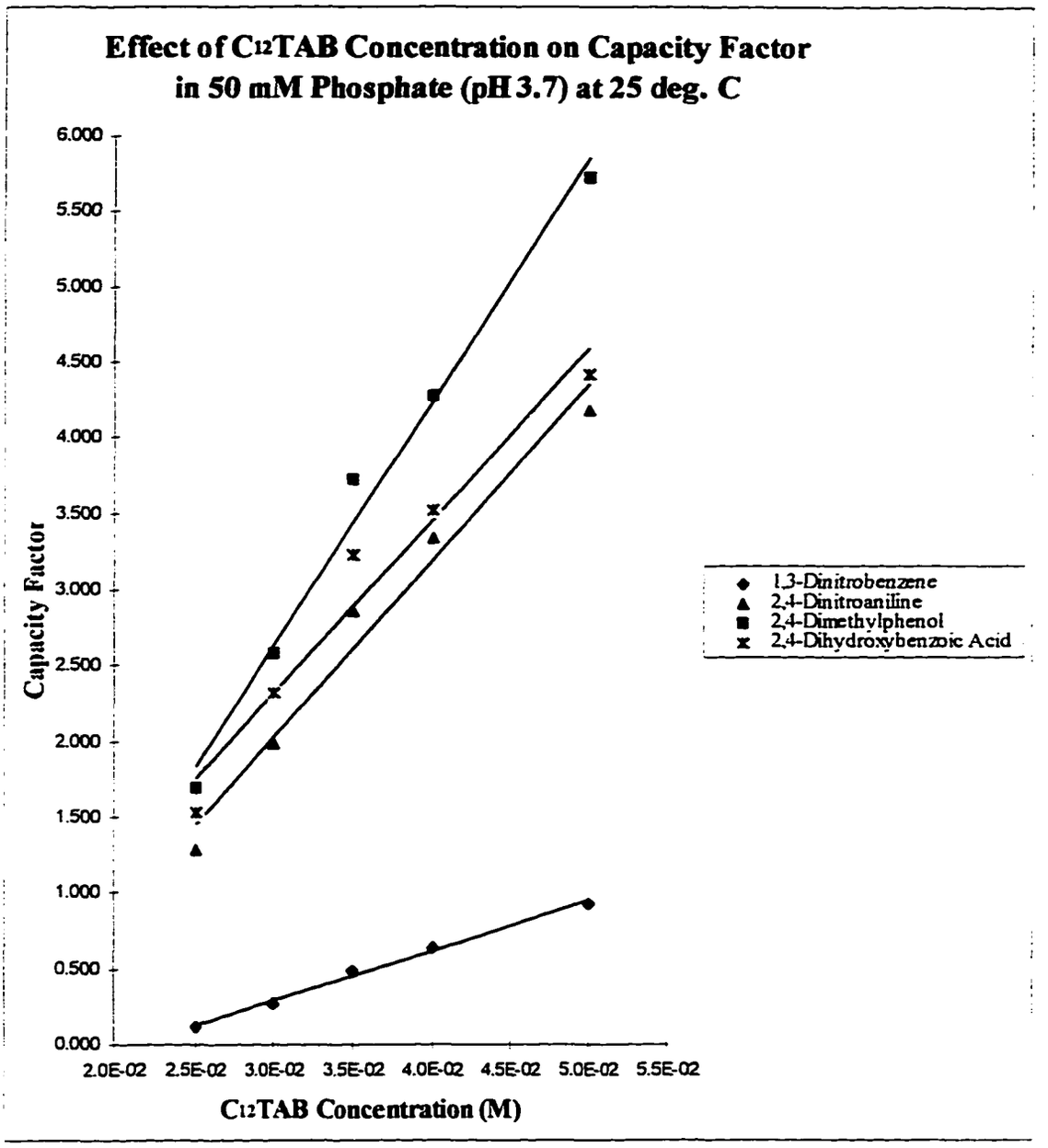

No.	Compounds	*RSQ*	*Slope*	*Intercept*
1	1,3-Dinitrobenzene	0.995	32.628	-0.687
2	2,4-Dinitroaniline	0972	115.897	-1.444
3	2,4-Dimethylphenol	0.987	160.474	-2.178
4	2,4-Dihydroxybenzoic Acid	0.960	113.223	-1.071

Figure 24

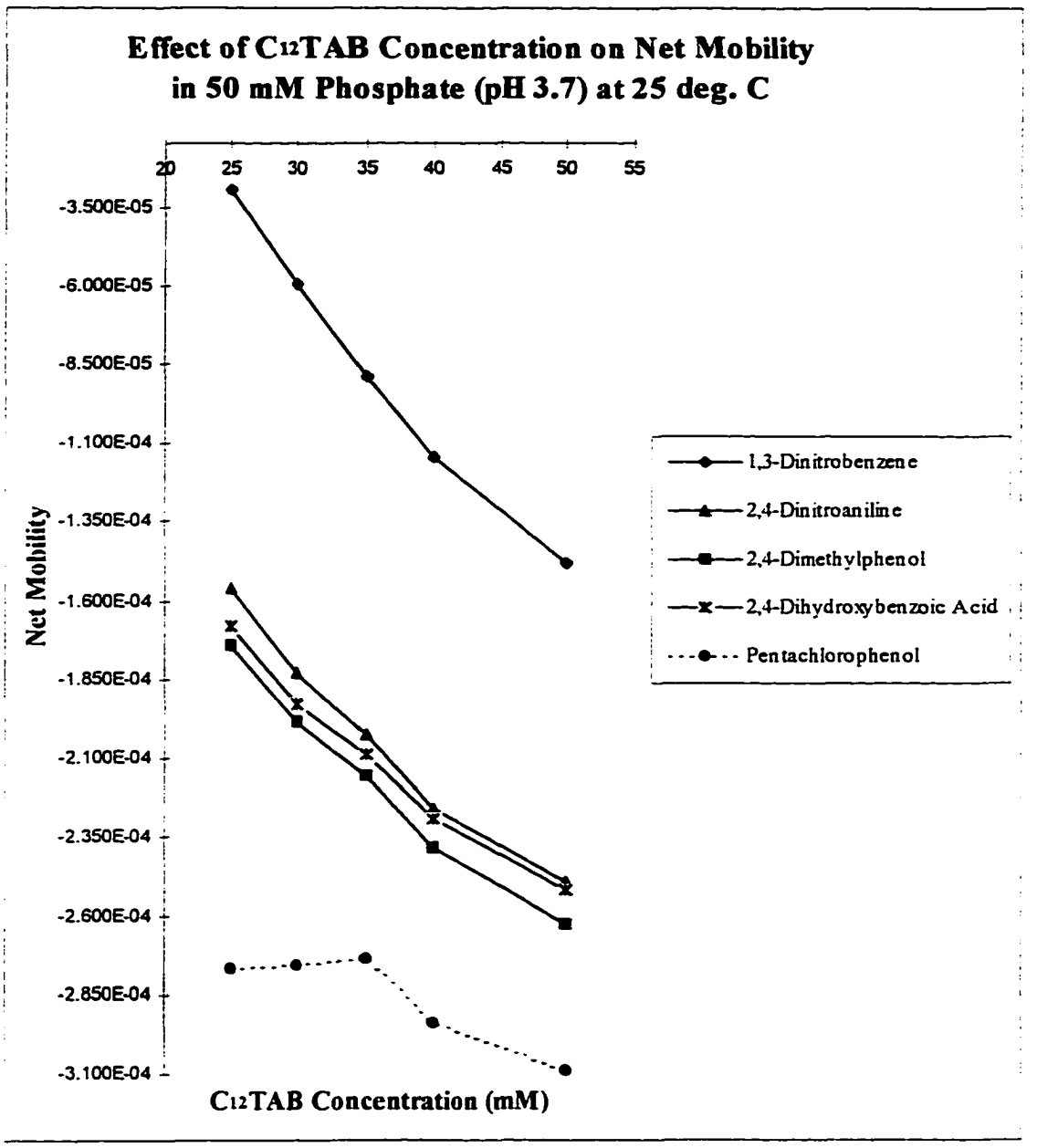

Figure 25

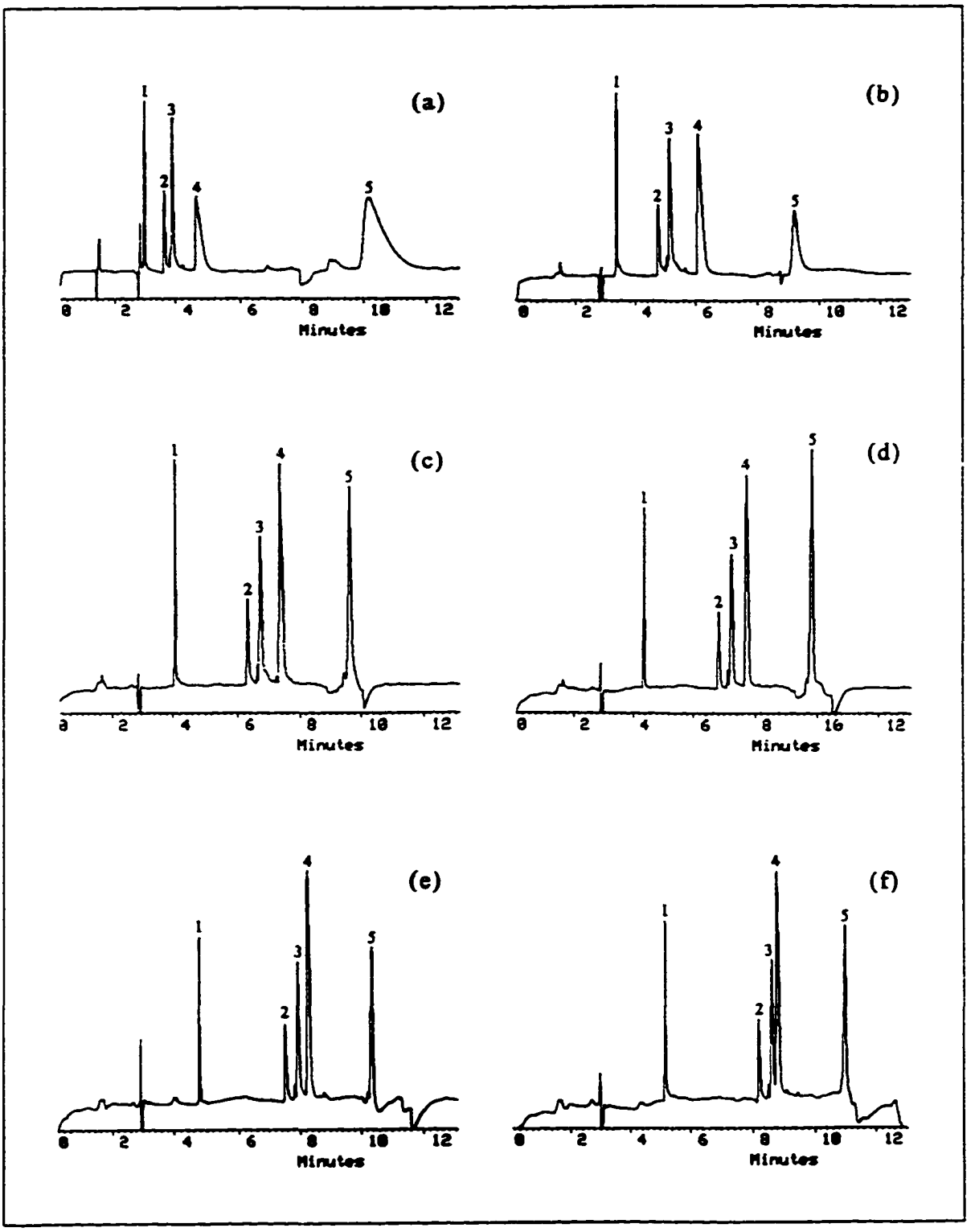

Figure 26

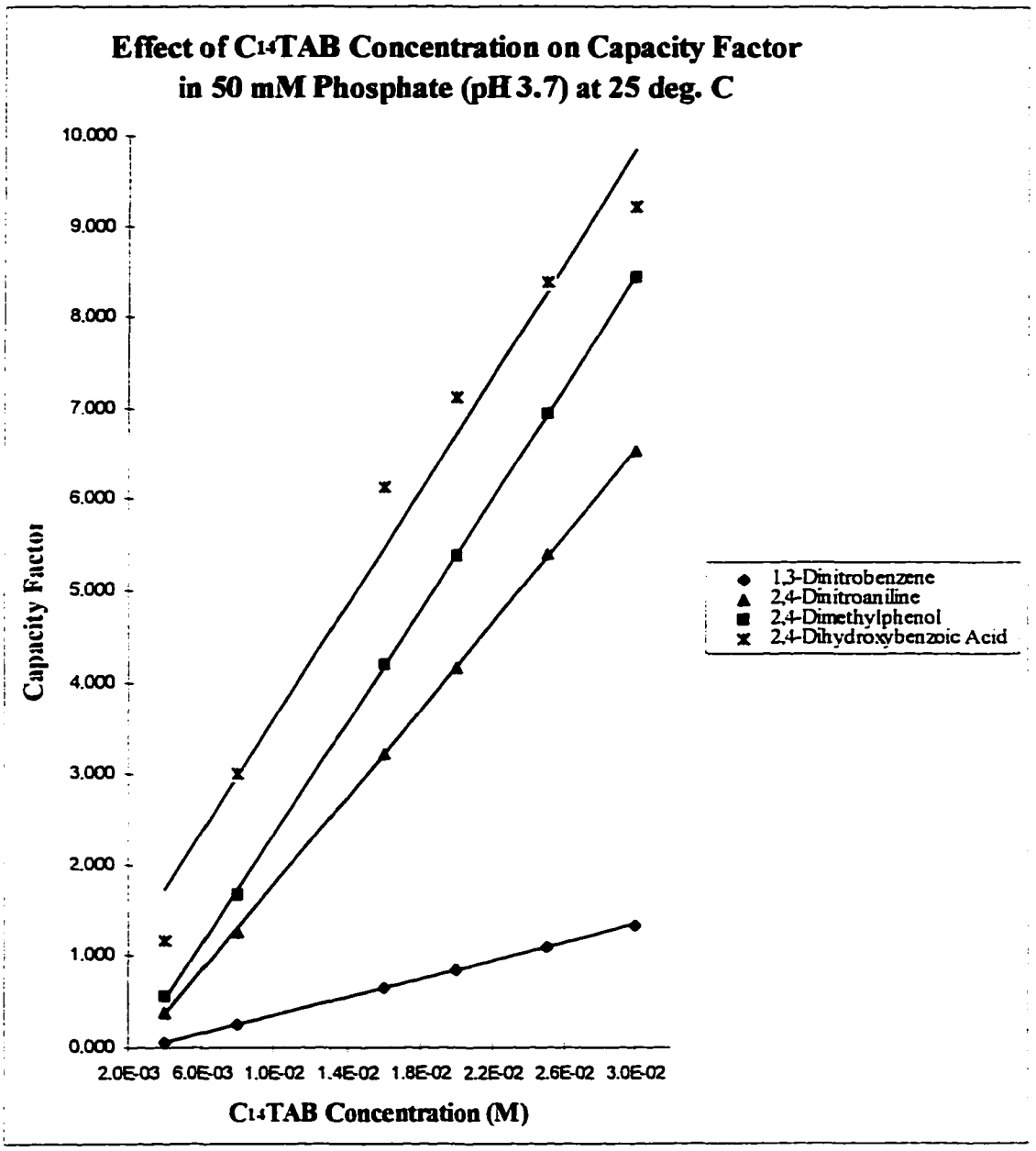

No.	Compounds	*RSQ*	*Slope*	*Intercept*
1	1,3-Dinitrobenzene	1.000	49.691	-0.149
2	2,4-Dinitroaniline	1.000	238.017	-1.596
3	2,4-Dimethylphenol	1.000	305.019	-2.705
4	2,4-Dihydroxybenzoic Acid	0.973	311.893	0.482

Figure 27

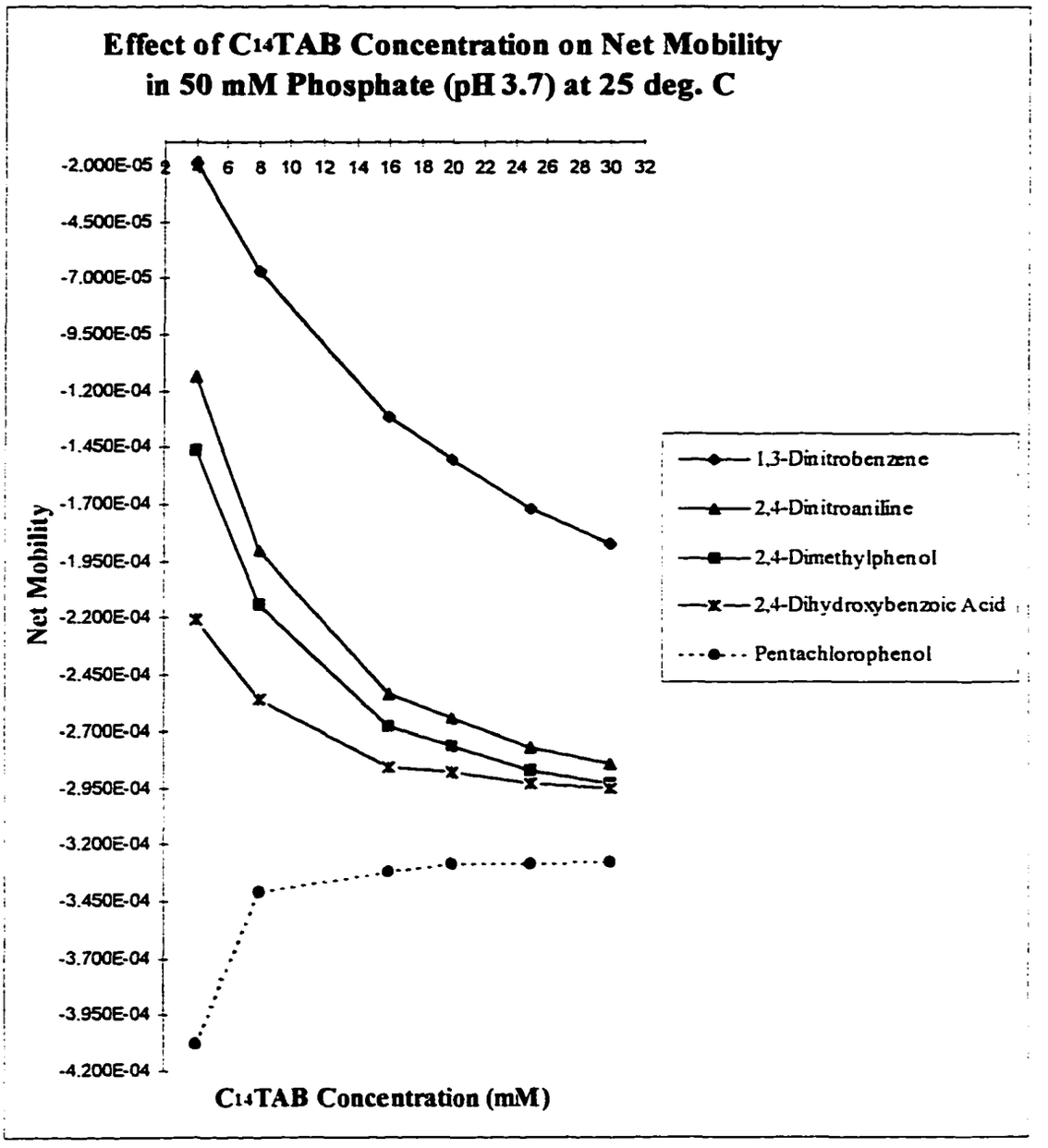

Figure 28

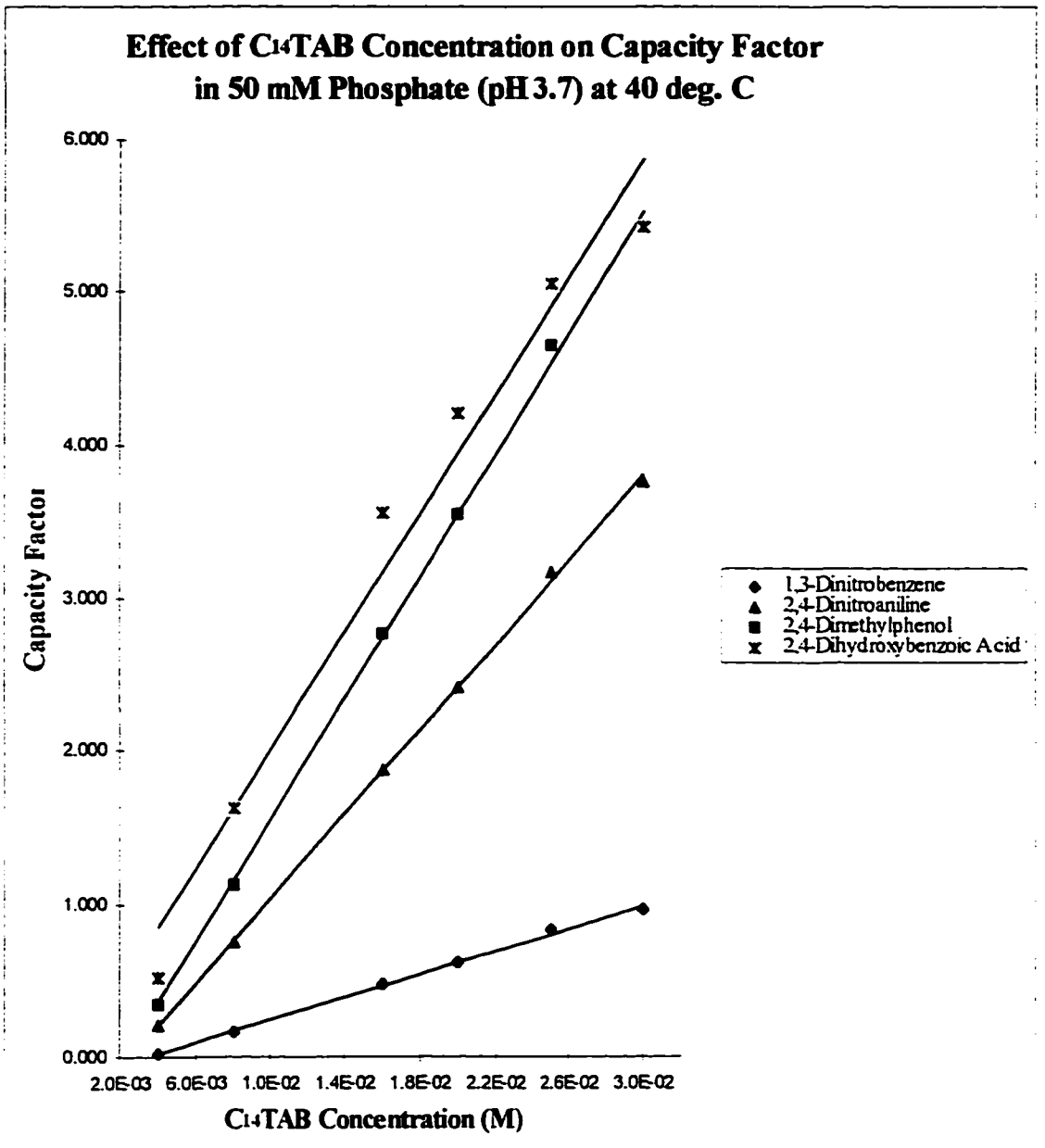

No.	Compounds	*RSQ*	*Slope*	*Intercept*
1	1,3-Dinitrobenzene	0.998	36.901	-0.122
2	2,4-Dinitroaniline	0.999	137.772	-0.337
3	2,4-Dimethylphenol	0.999	198.340	-0.430
4	2,4-Dihydroxybenzoic Acid	0.971	192.906	0.084

Figure 29

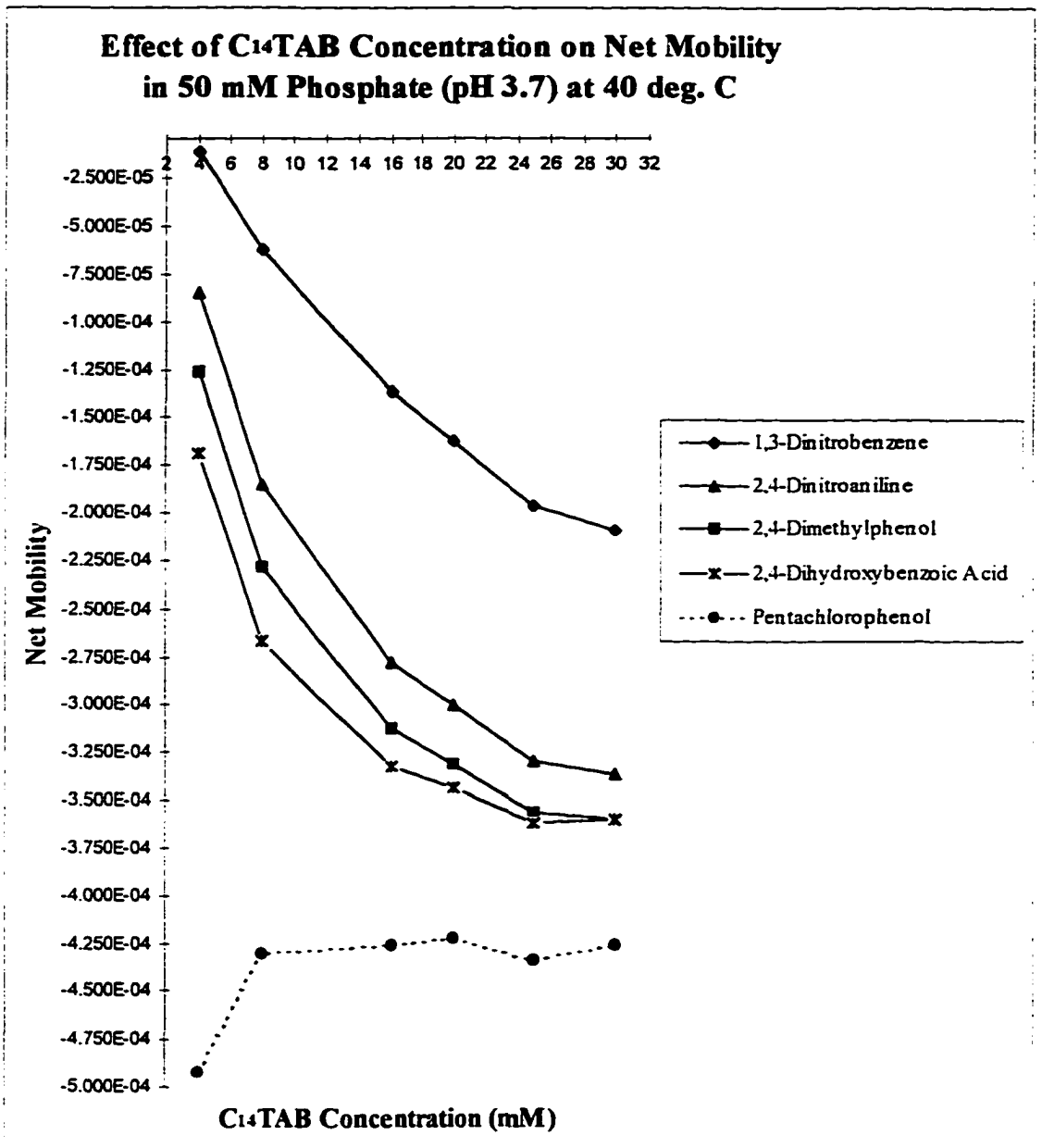

Figure 30

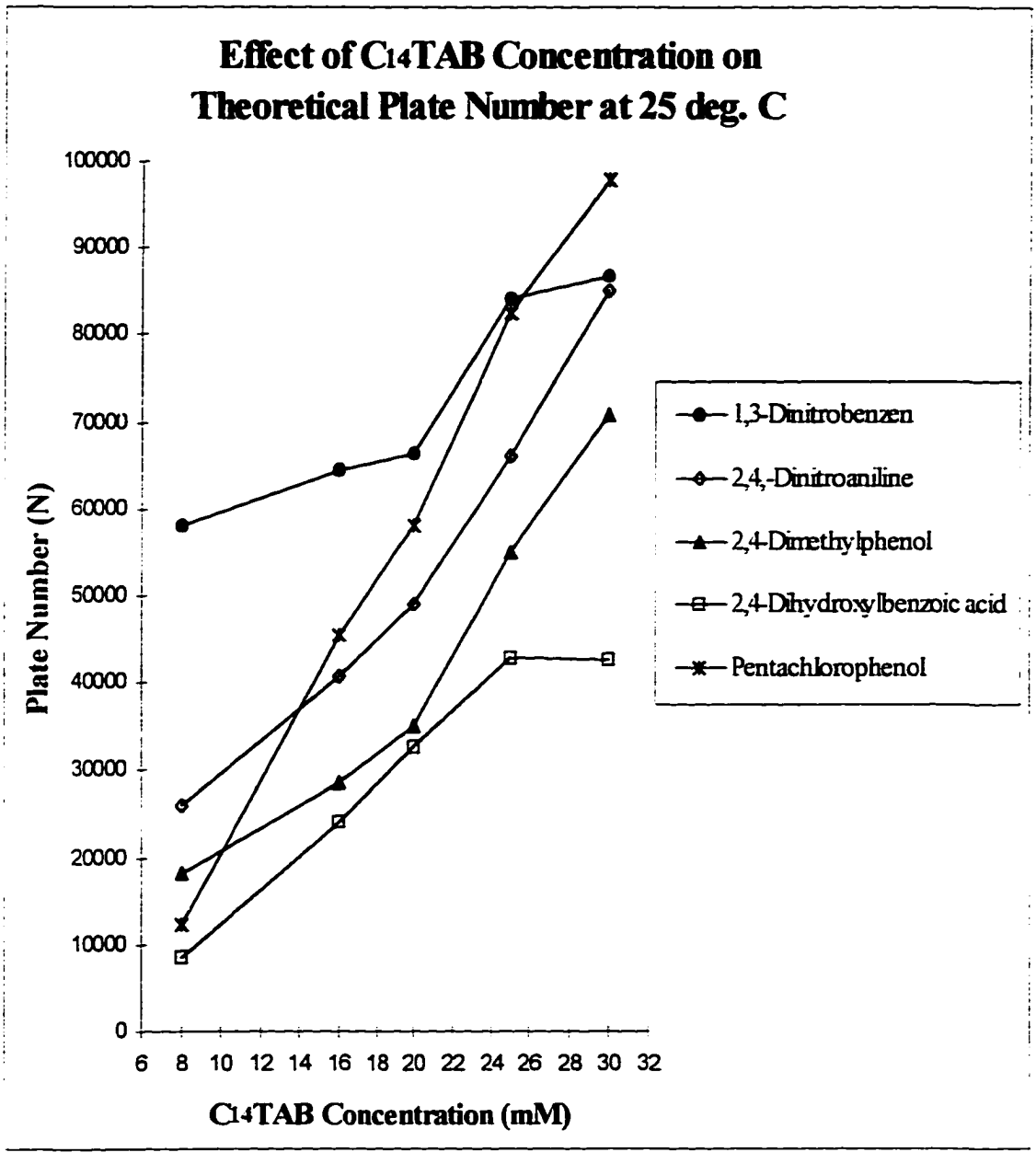

Figure 31

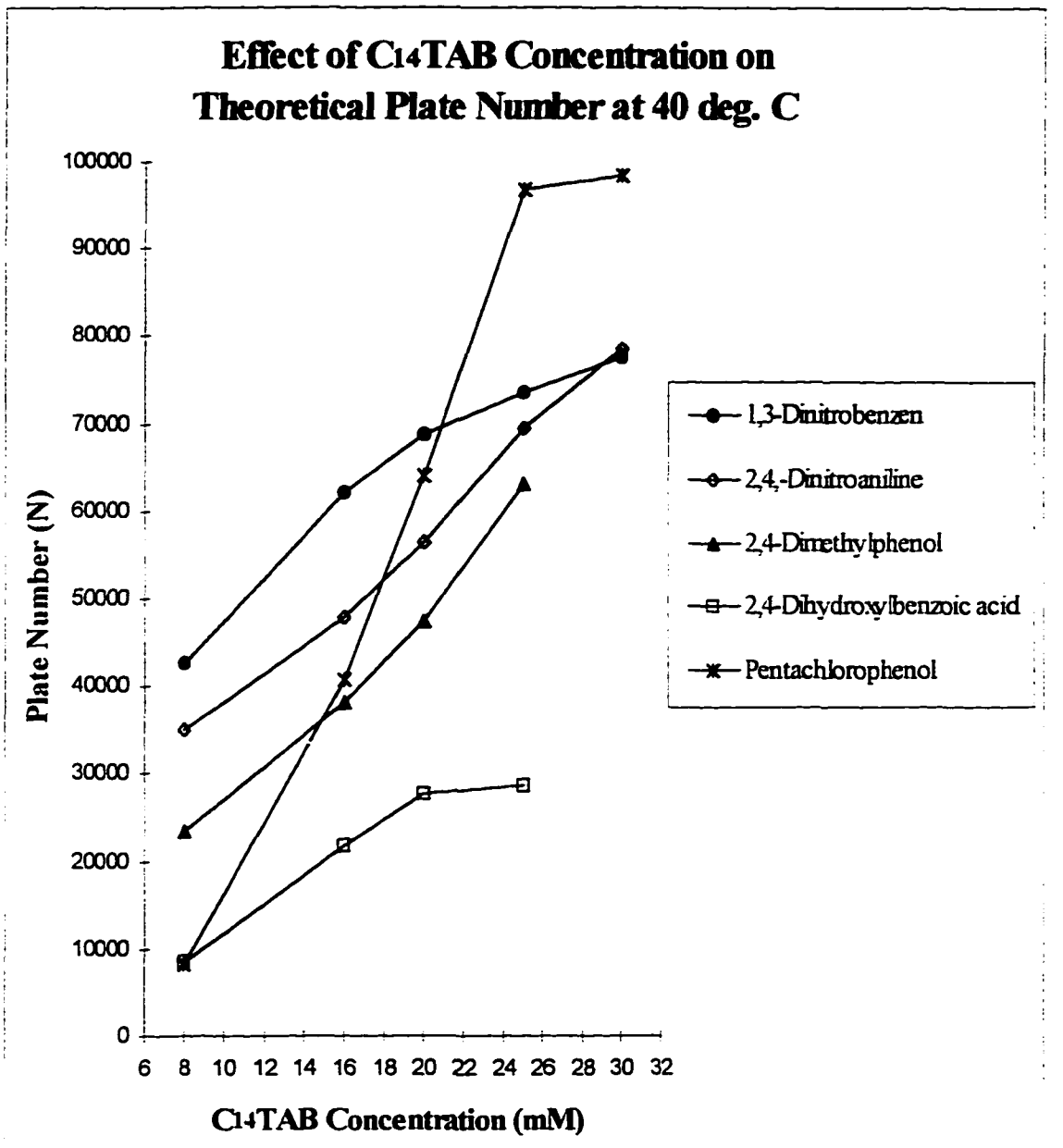

Figure 32

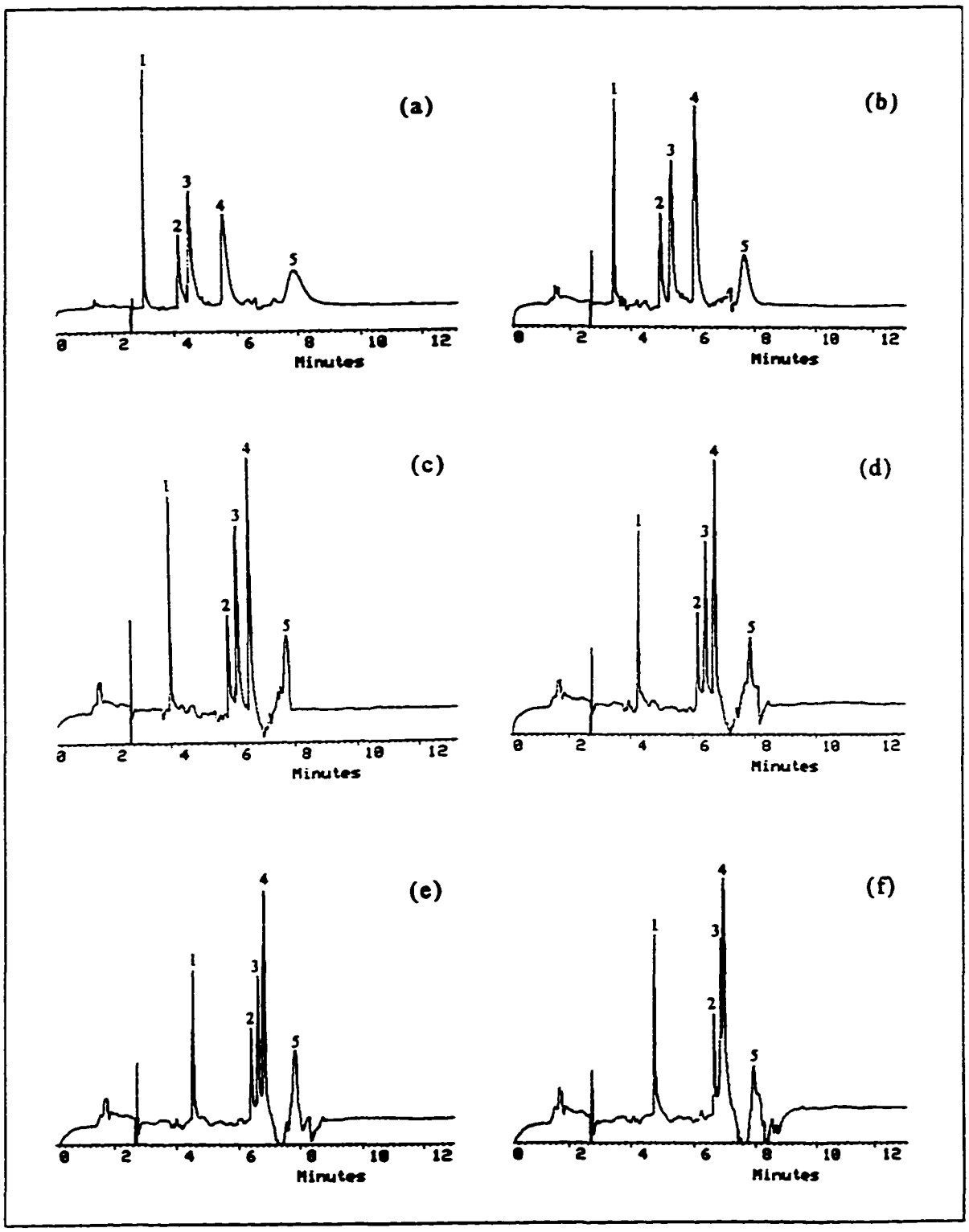

Figure 33

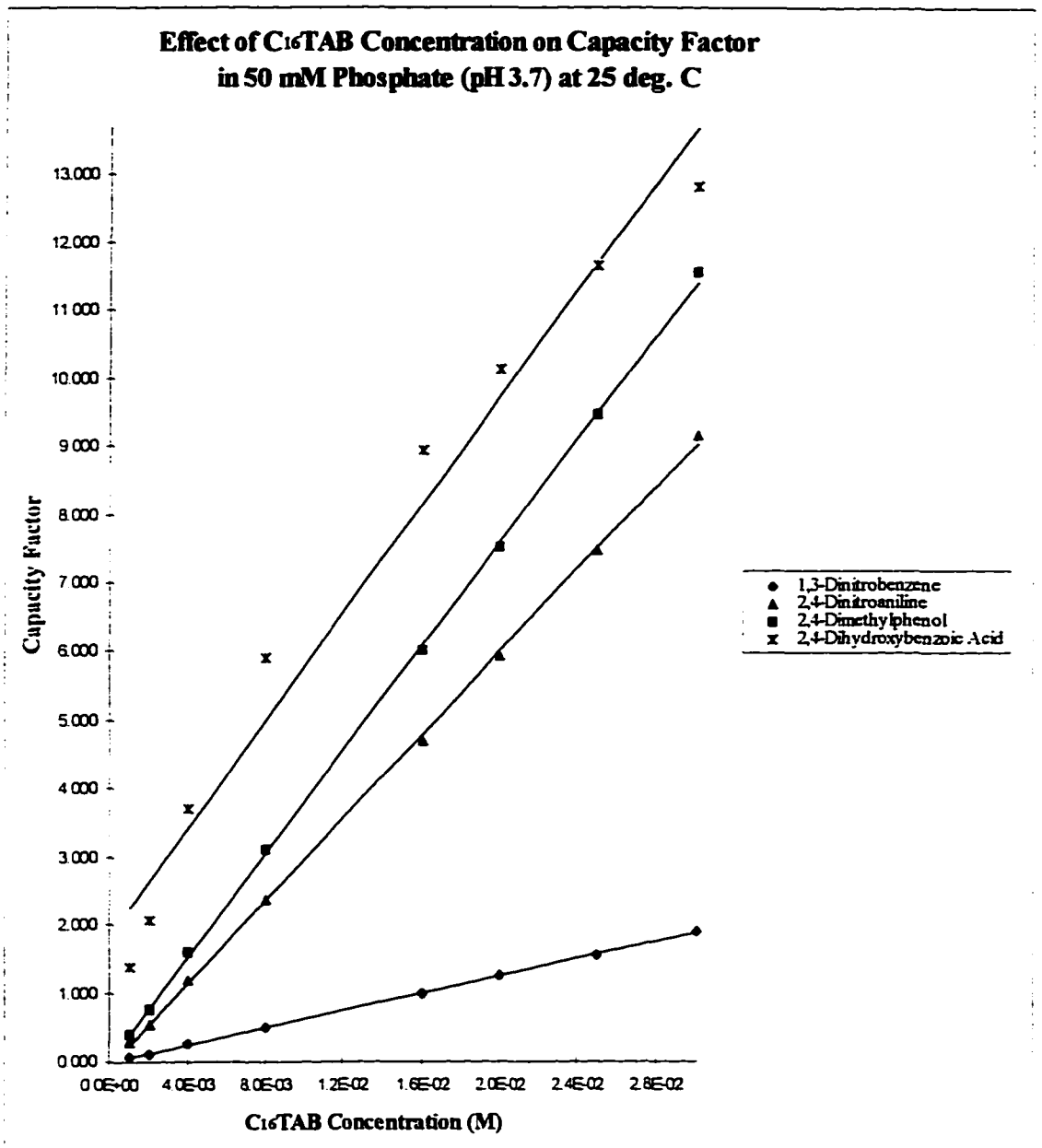

No.	Compounds	*RSQ*	*Slope*	*Intercept*
1	1,3-Dinitrobenzene	1.000	62.964	-0.009
2	2,4-Dinitroaniline	1.000	303.143	-0.063
3	2,4-Dimethylphenol	1.000	379.861	-0.010
4	2,4-Dihydroxybenzoic Acid	0.975	393.848	1.856

Figure 34

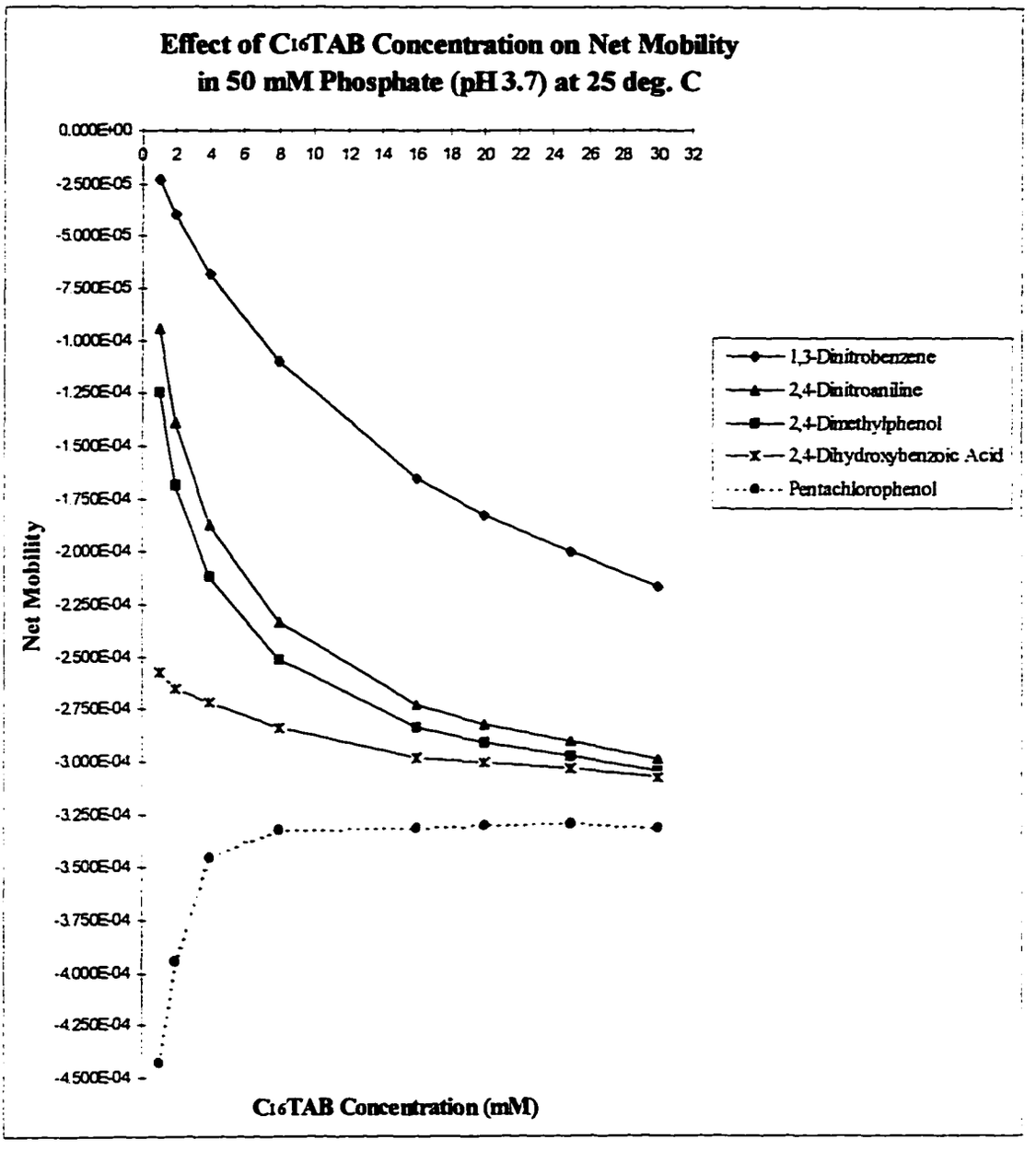

Figure 35

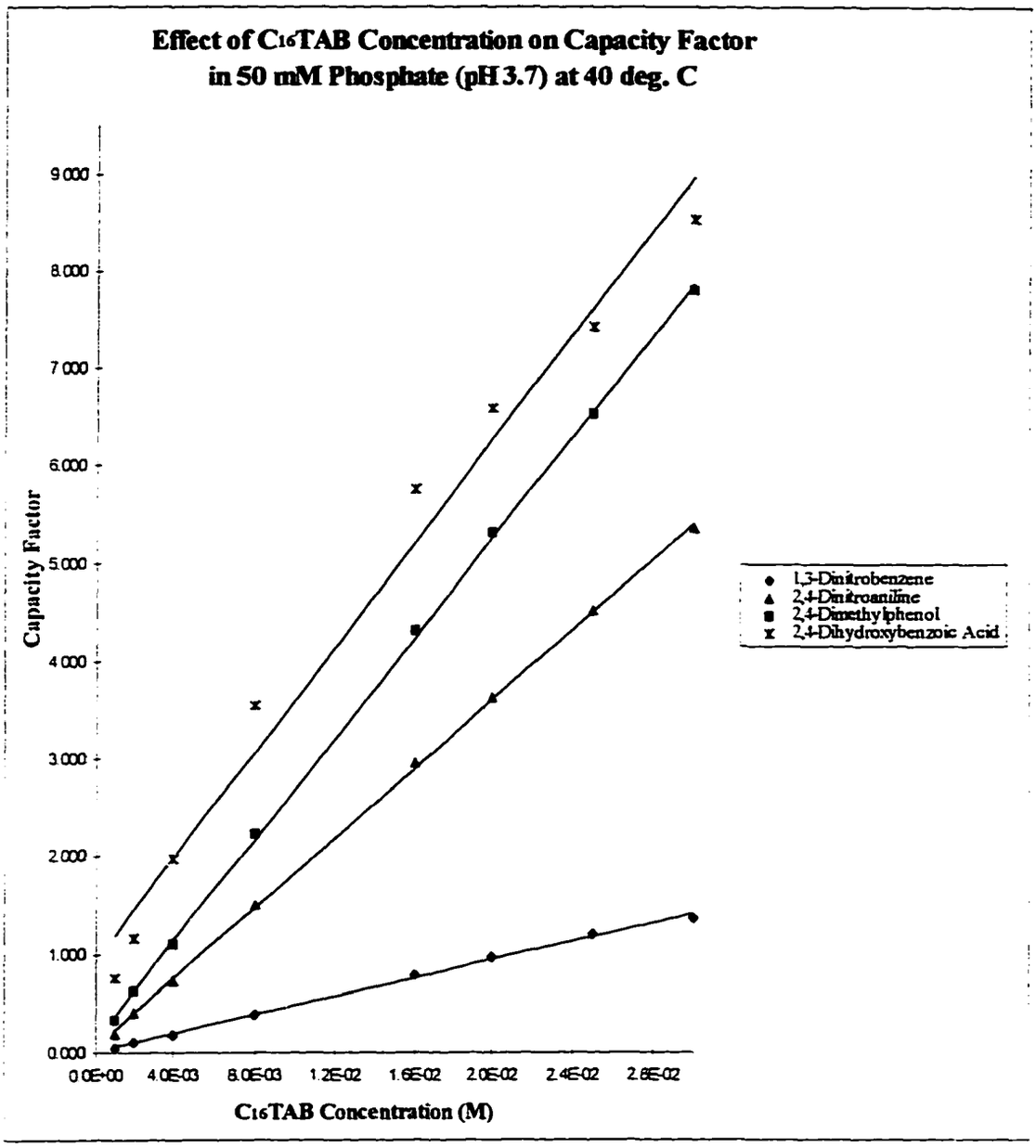

No.	Compounds	*RSQ*	*Slope*	*Intercept*
1	1,3-Dinitrobenzene	0.998	46.713	0.012
2	2,4-Dinitroaniline	1.000	178.677	0.041
3	2,4-Dimethylphenol	1.000	257.825	0.108
4	2,4-Dihydroxybenzoic Acid	0.982	267.989	0.914

Figure 36

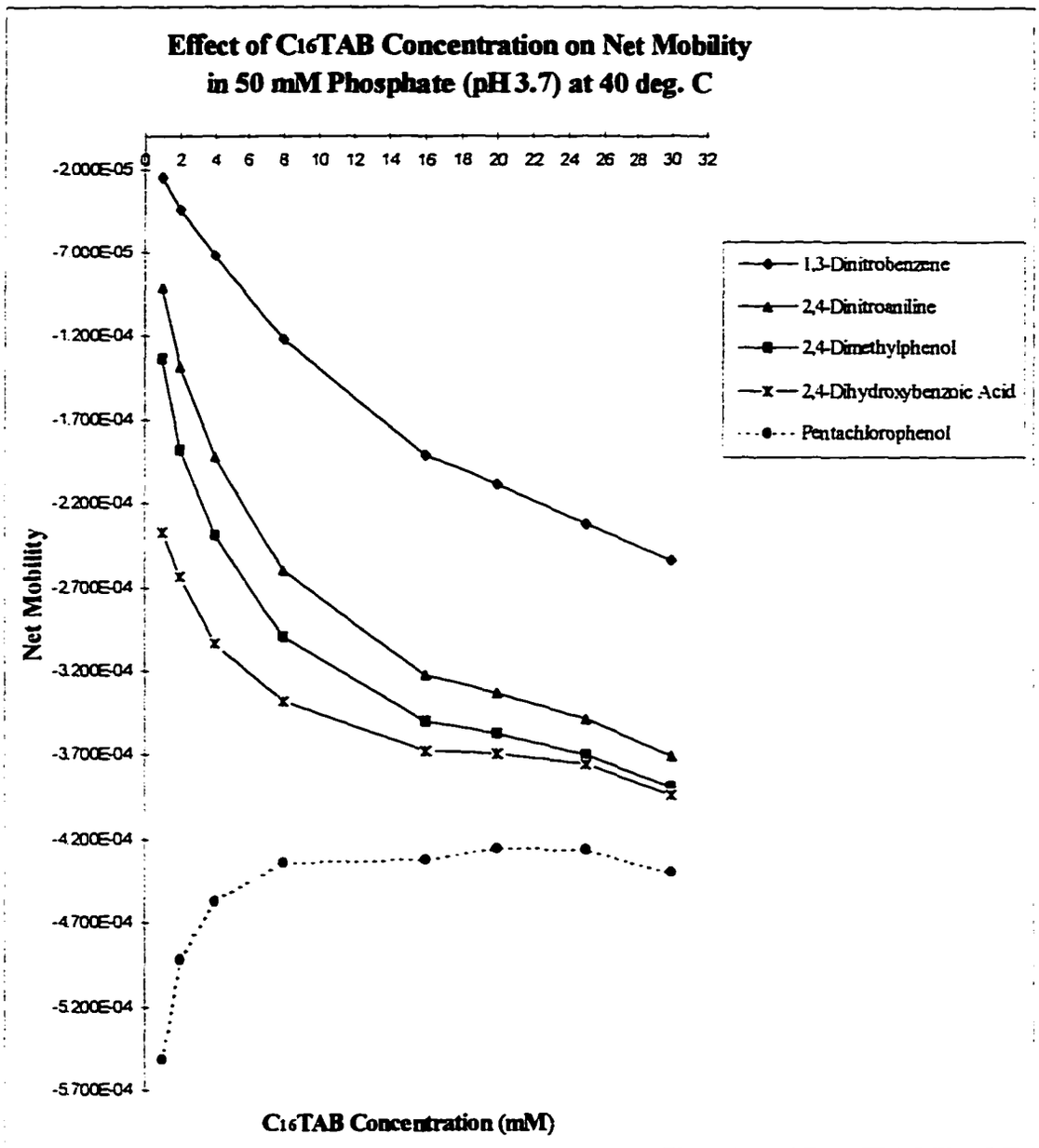

Figure 37 (a)

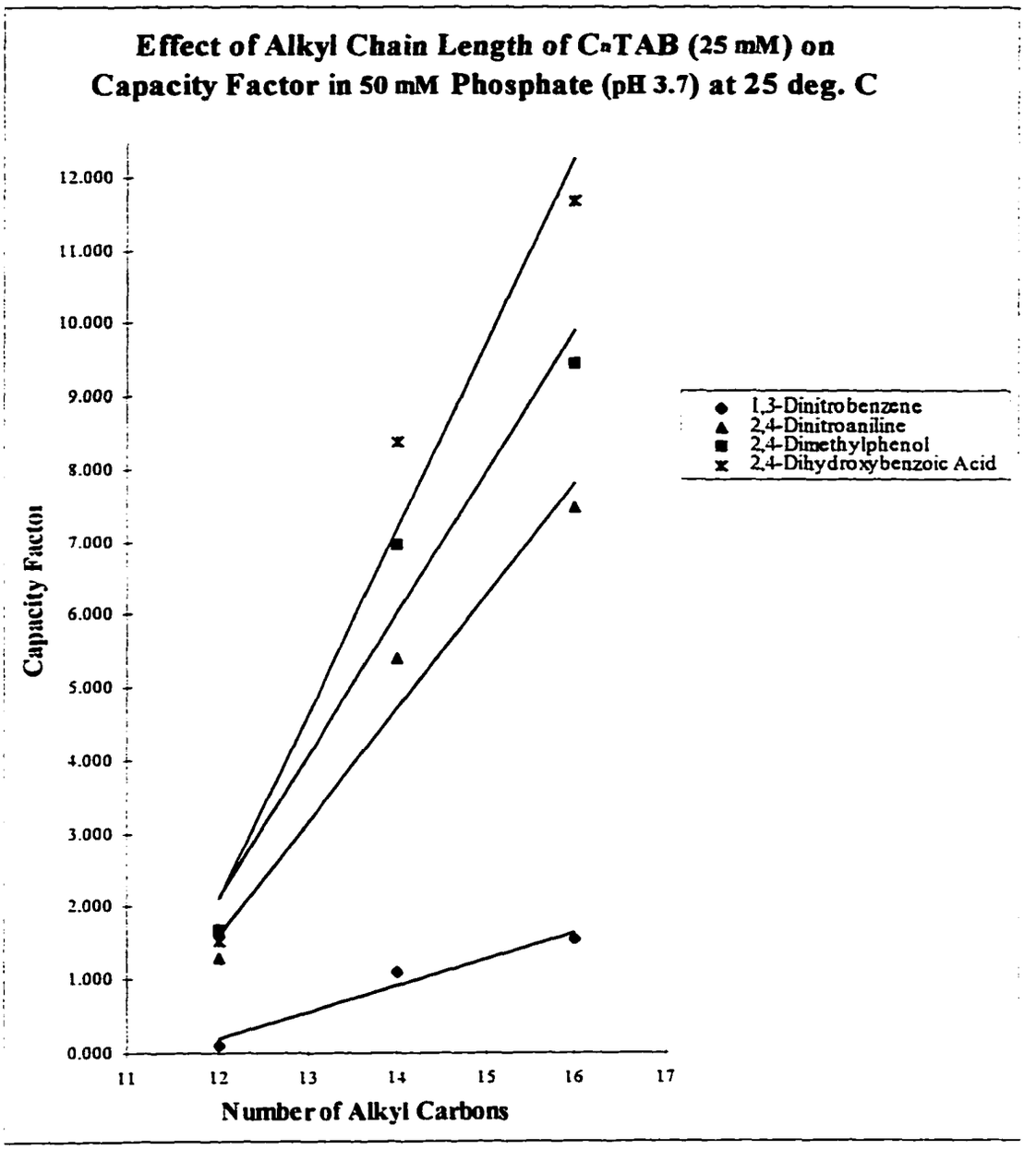

Compounds	*RSQ*
1,3-Dinitrobenzene	0.959
2,4-Dinitroaniline	0.965
2,4-Dimethylphenol	0.960
2,4-Dihydroxybenzoic Acid	0.960

Figure 37 (b)

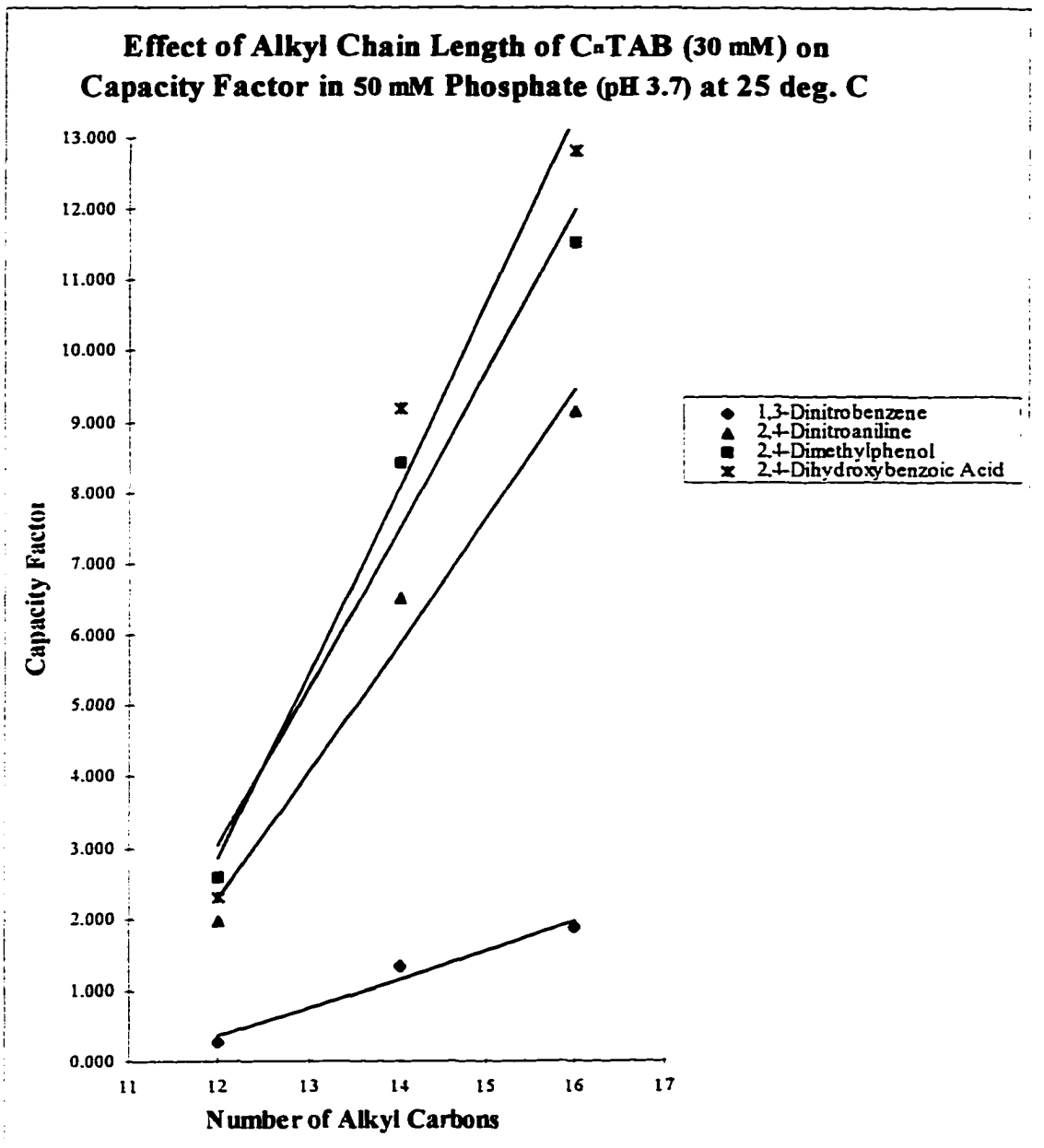

Compounds	*RSQ*
1,3-Dinitrobenzene	0.968
2,4-Dinitroaniline	0.977
2,4-Dimethylphenol	0.969
2,4-Dihydroxybenzoic Acid	0.969

Figure 38 (a)

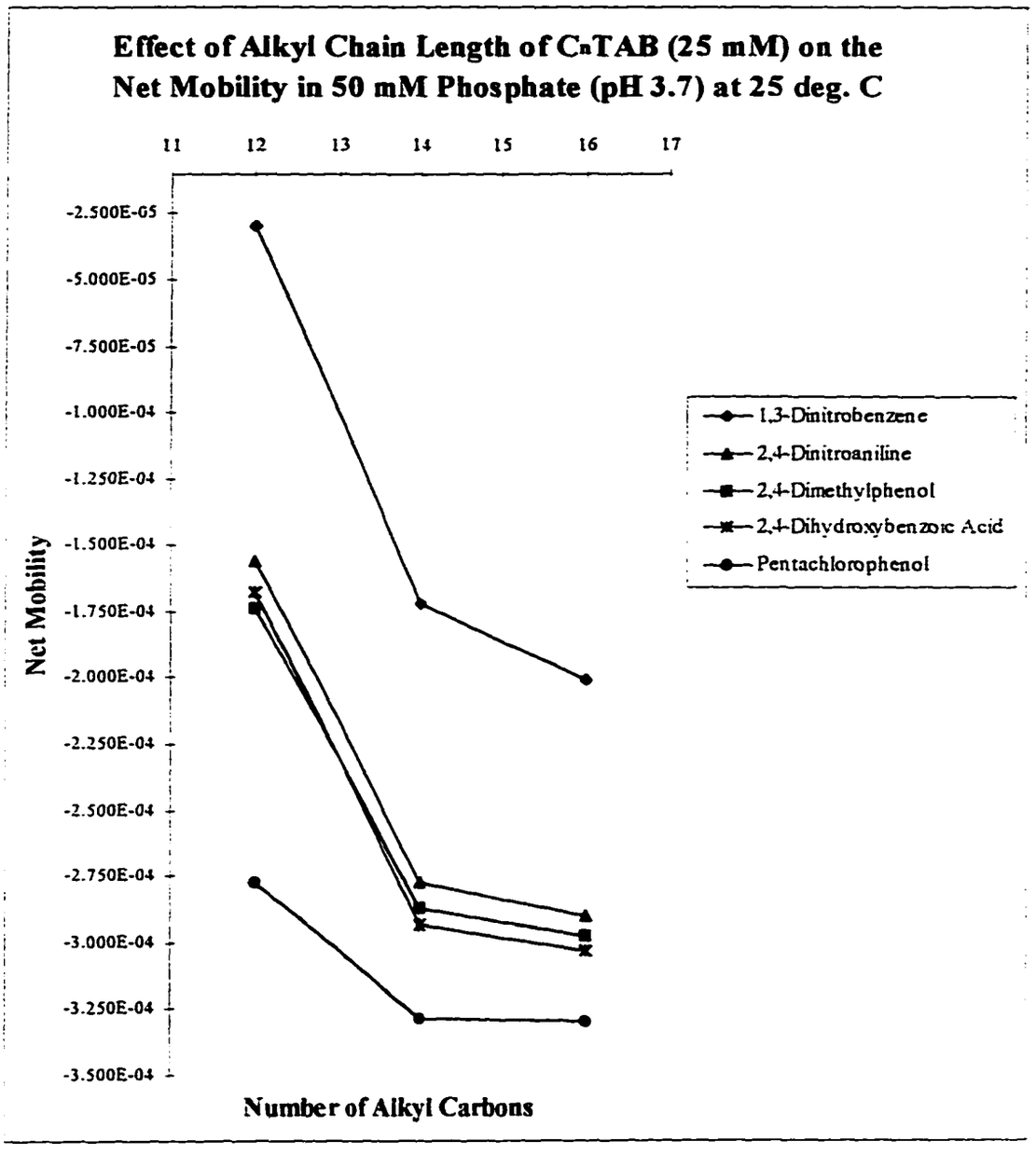

Figure 38 (b)

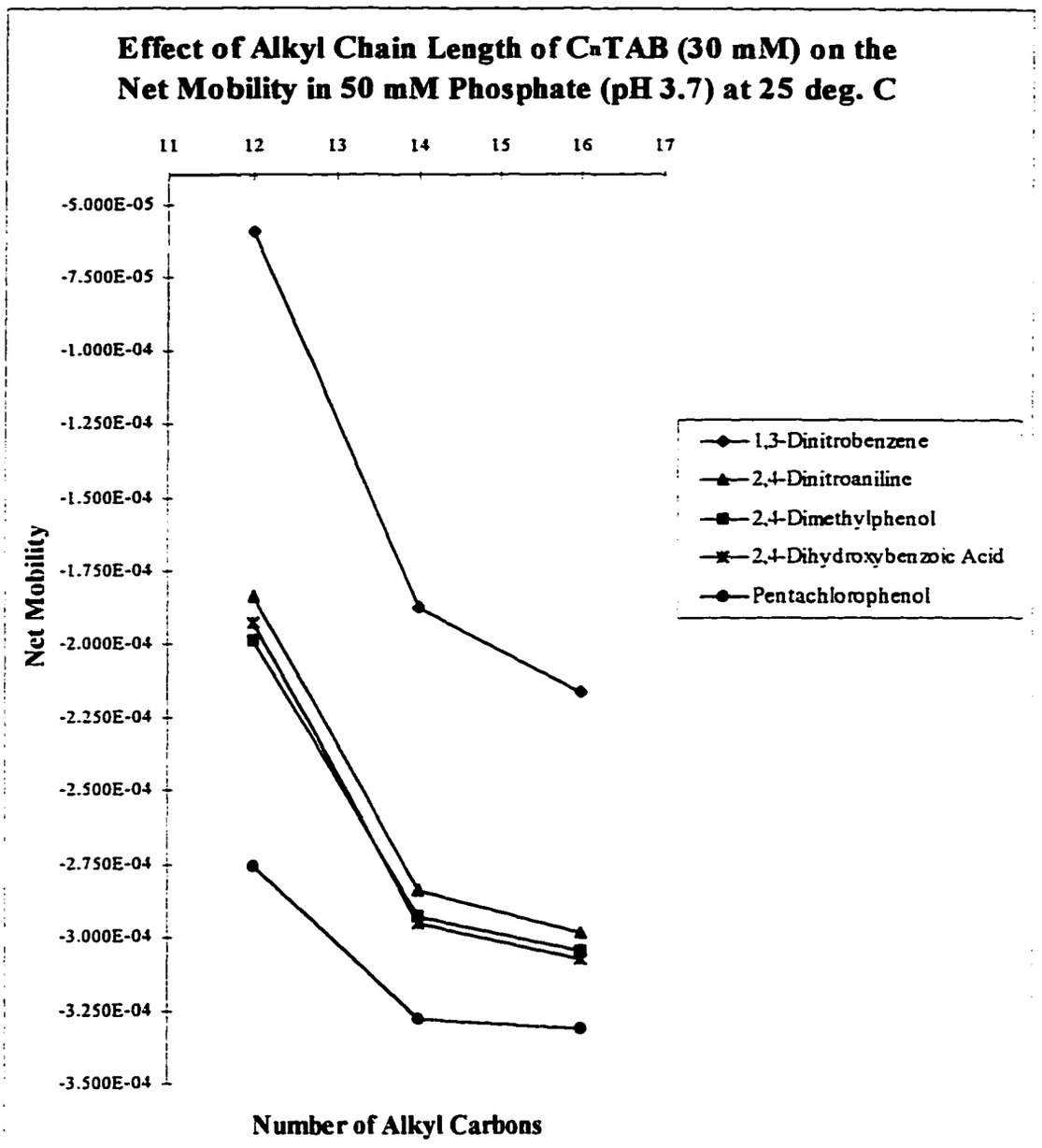

Figure 39

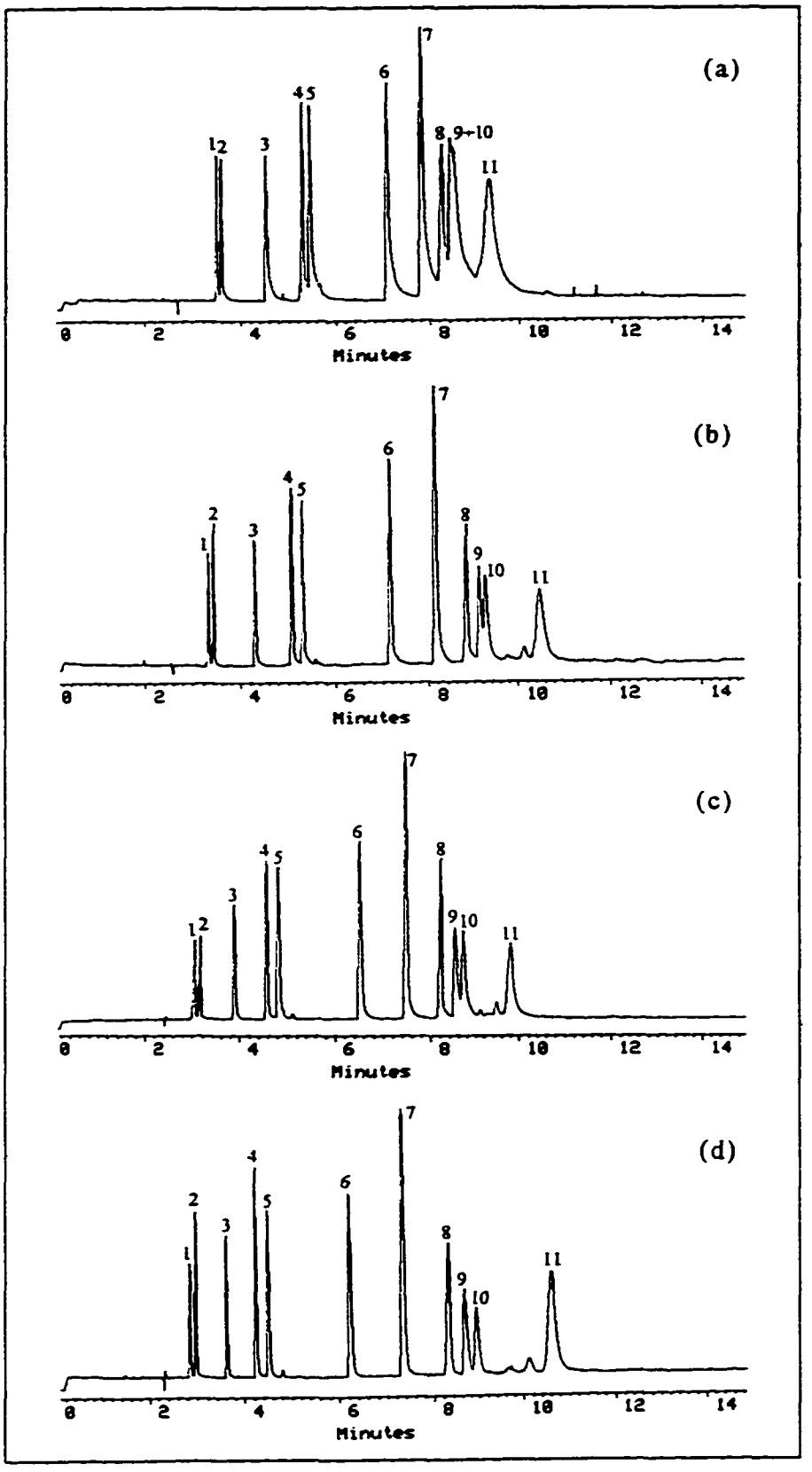

Figure 40

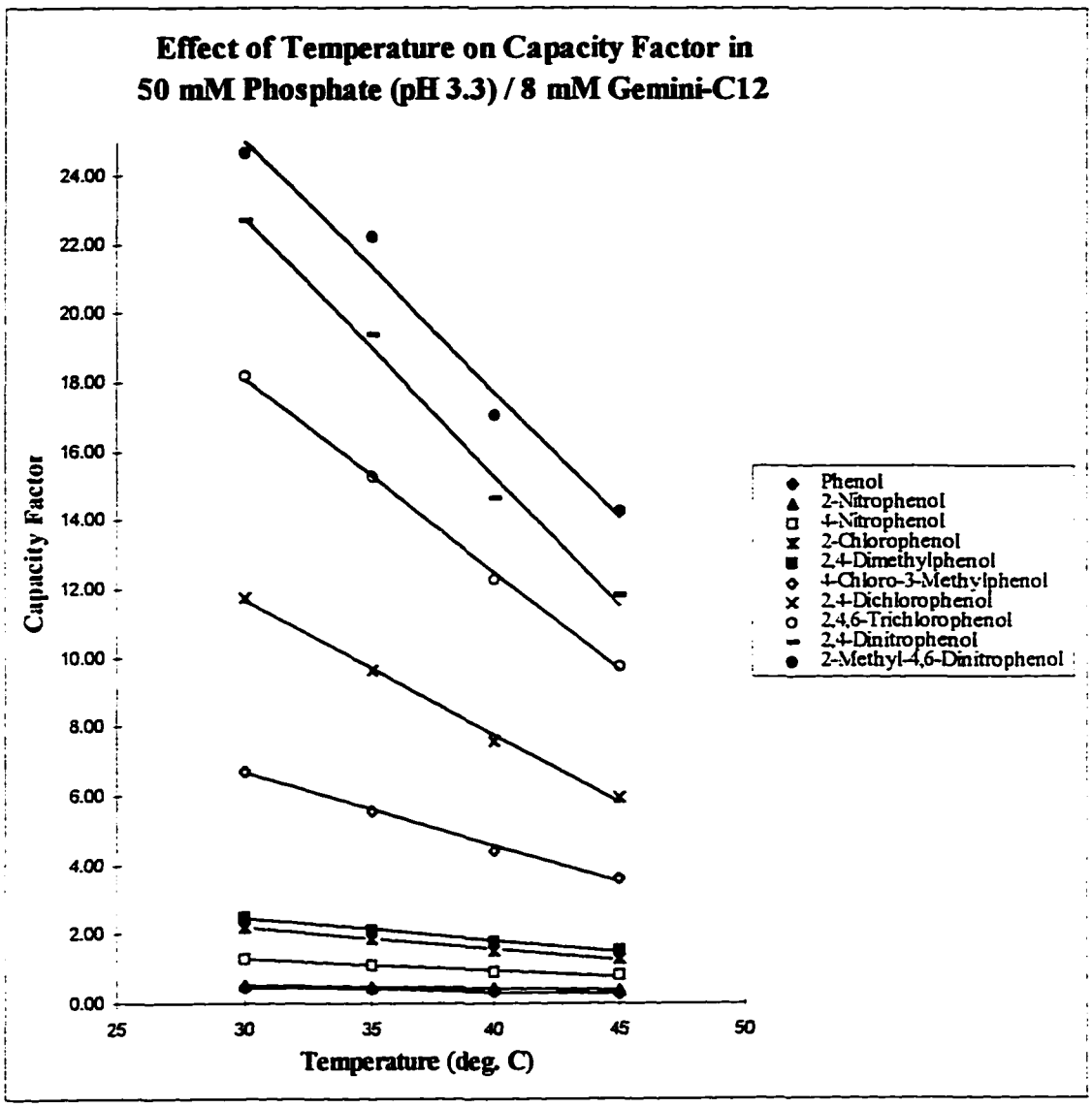

No.	Compounds	*RSQ*	*Slope*	*Intercept*
1	Phenol	0.99	-0.01	0.77
2	2-Nitrophenol	0.99	-0.01	0.84
3	4-Nitrophenol	0.99	-0.03	2.35
4	2-Chlorophenol	0.99	-0.06	4.07
5	2,4-Dimethylphenol	0.99	-0.06	4.39
6	4-Chloro-3-Methylphenol	0.99	-0.21	12.92
7	2,4-Dichlorophenol	1.00	-0.39	23.36
8	2,4,6-Trichlorophenol	1.00	-0.56	35.05
9	2,4-Dinitrophenol	0.99	-0.75	45.22
10	2-Methyl-4,6-Dinitrophenol	0.98	-0.73	46.82

Figure 41

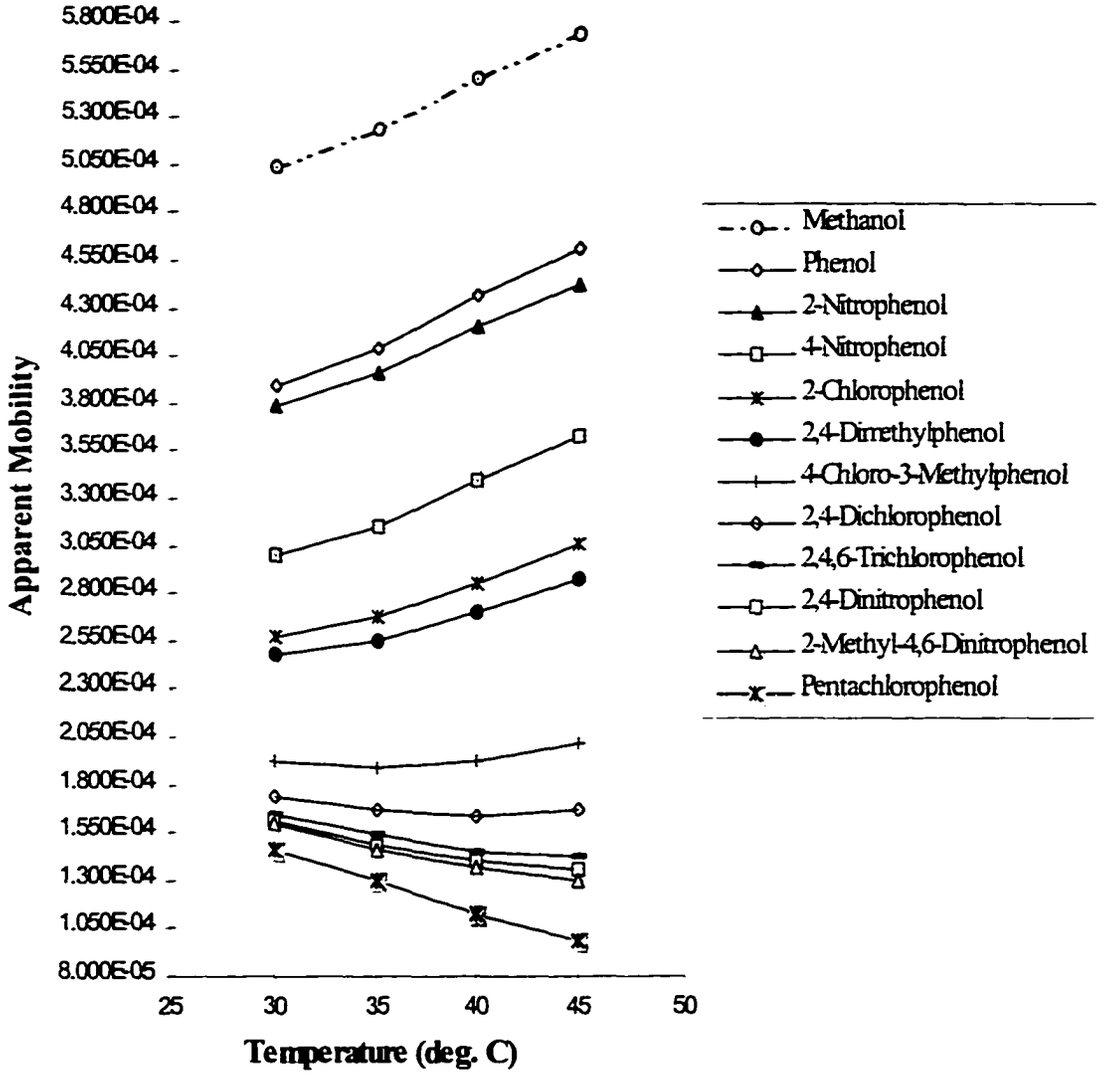

Figure 42

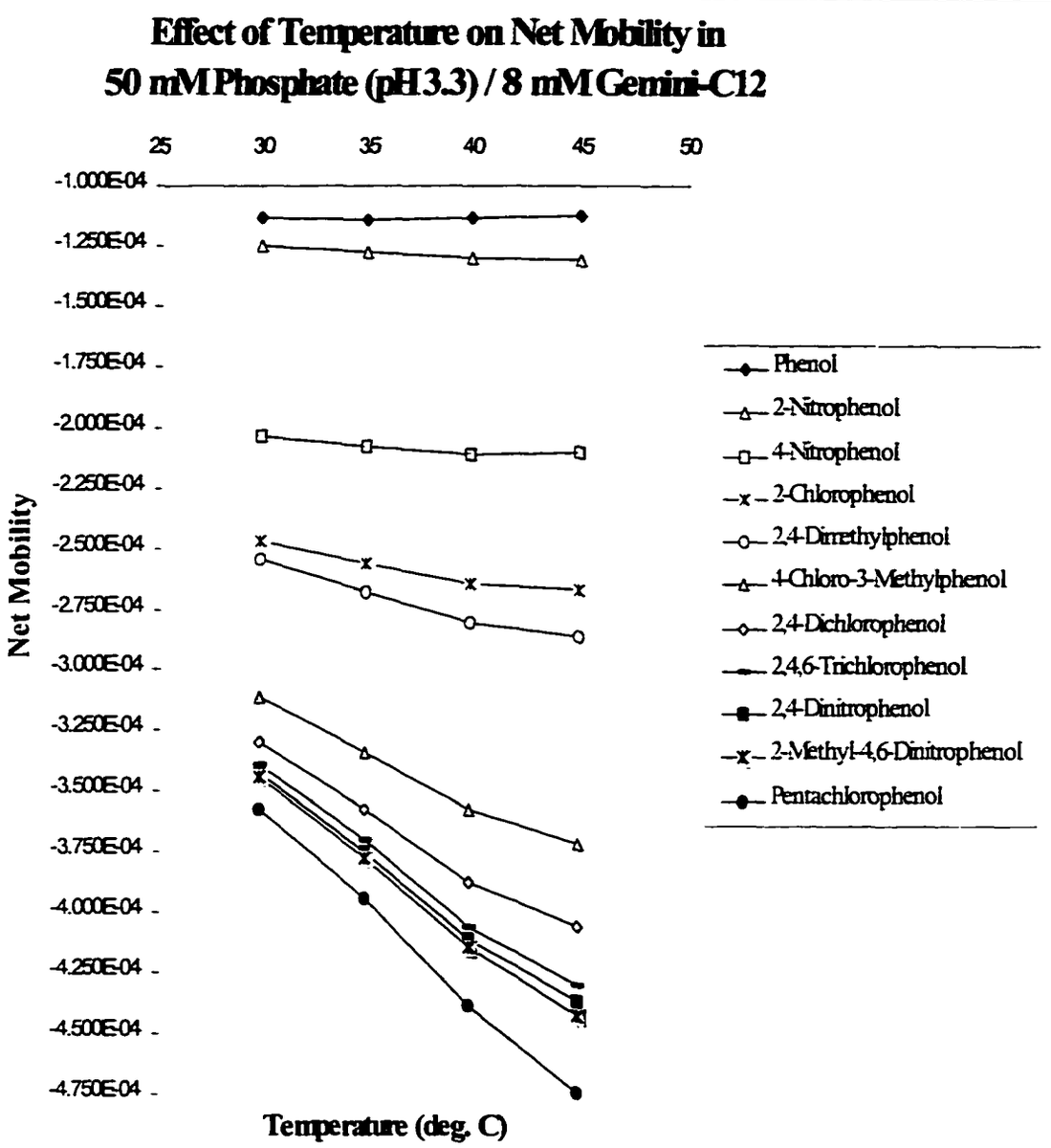

Figure 43

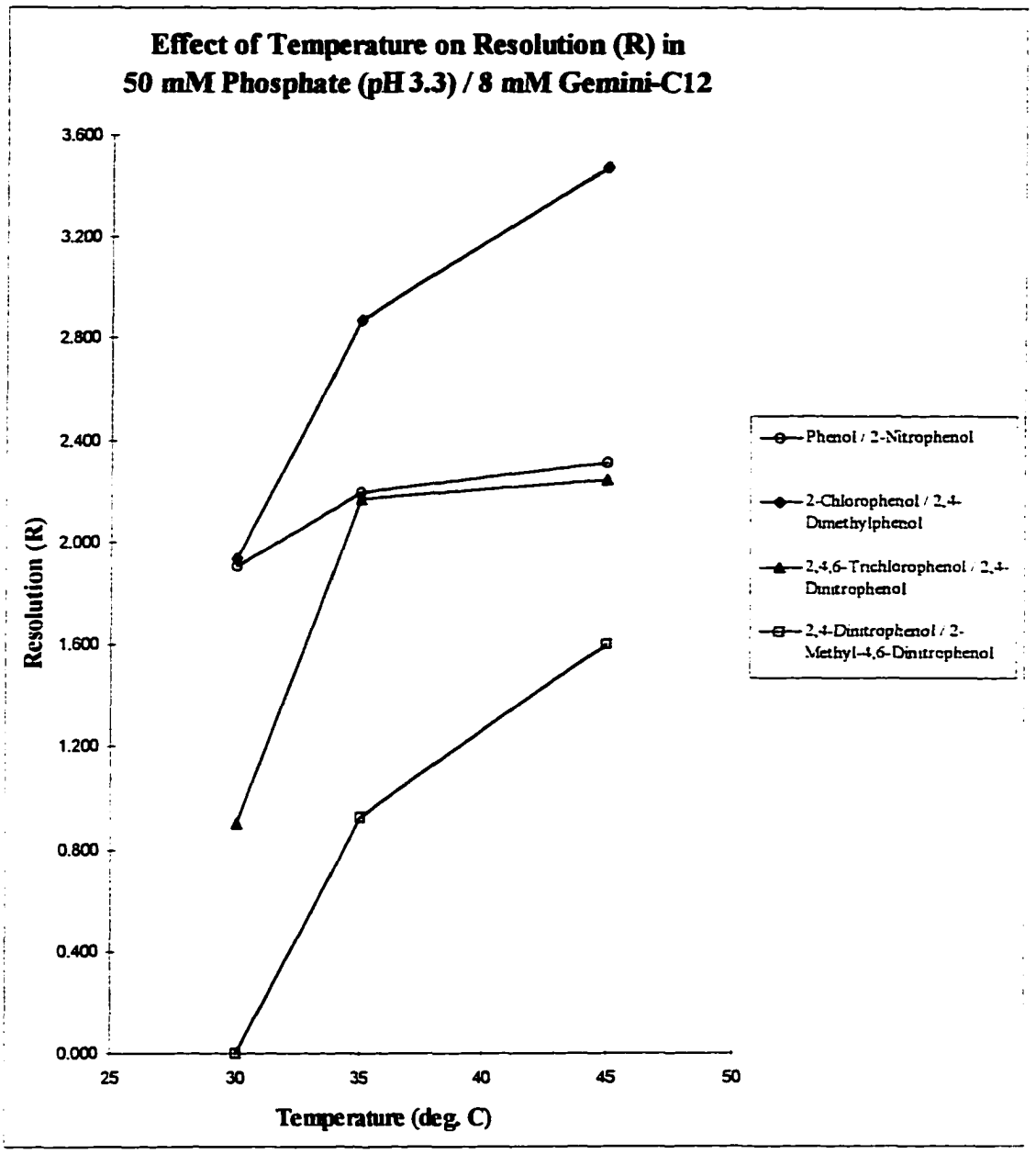

Figure 44

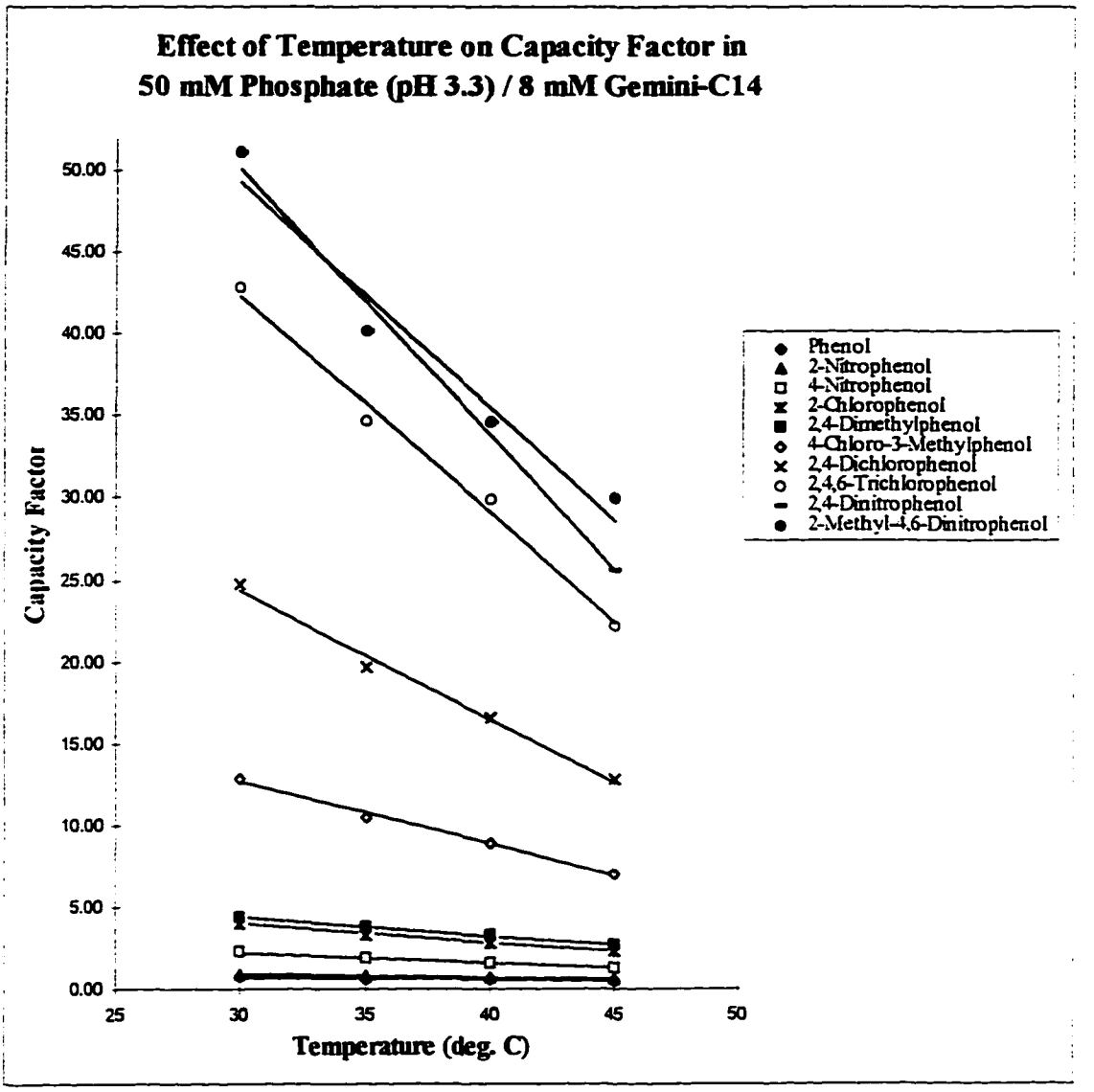

No.	Compounds	*RSQ*	*Slope*	*Intercept*
1	Phenol	1.00	-0.02	1.27
2	2-Nitrophenol	0.99	-0.02	1.45
3	4-Nitrophenol	0.99	-0.06	4.06
4	2-Chlorophenol	1.00	-0.11	7.32
5	2,4-Dimethylphenol	1.00	-0.11	7.80
6	4-Chloro-3-Methylphenol	0.99	-0.38	24.18
7	2,4-Dichlorophenol	1.00	-0.78	47.79
8	2,4,6-Trichlorophenol	1.00	-1.33	82.27
9	2,4-Dinitrophenol	0.99	-1.64	99.36
10	2-Methyl-4,6-Dinitrophenol	0.96	-1.38	90.64

Figure 45

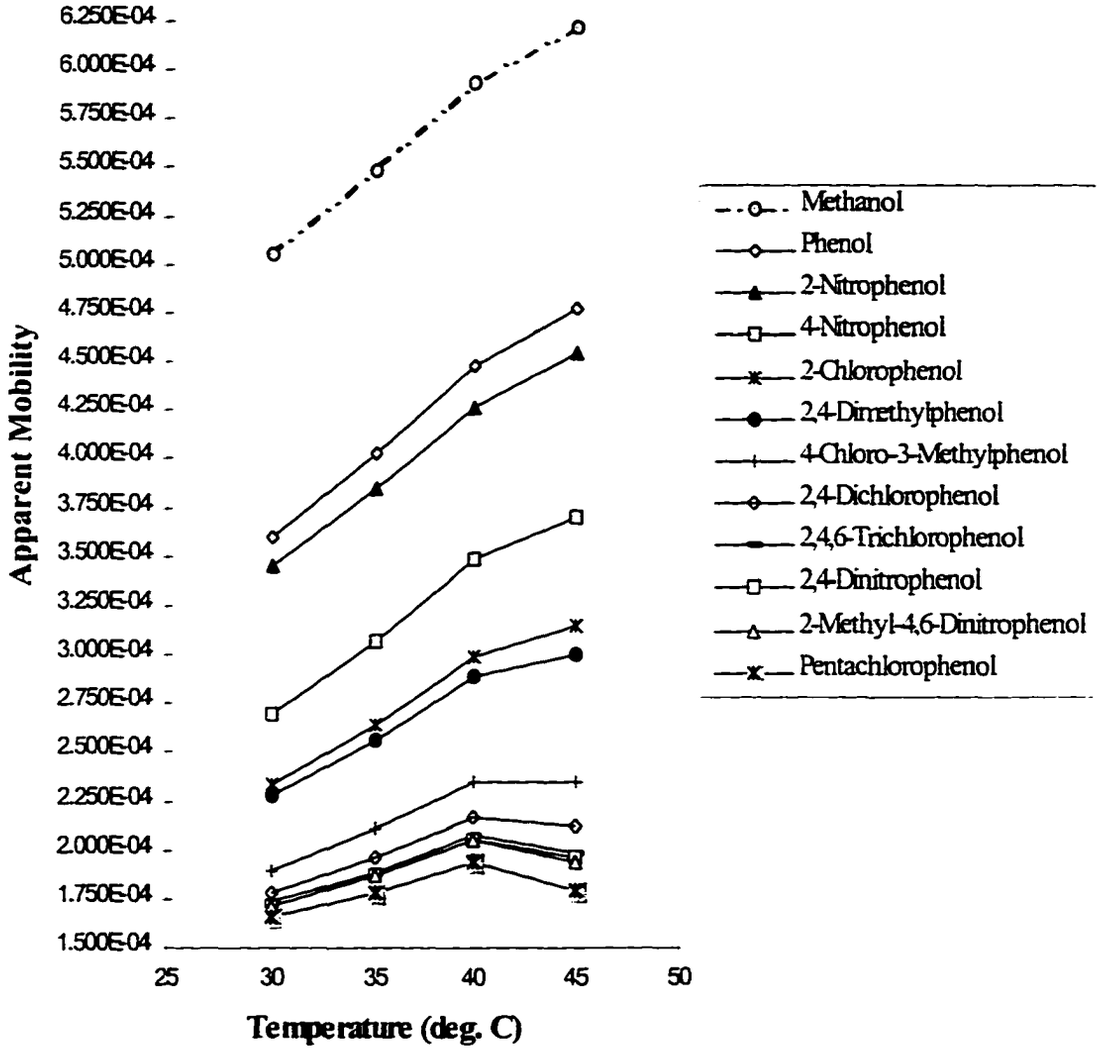

Figure 46

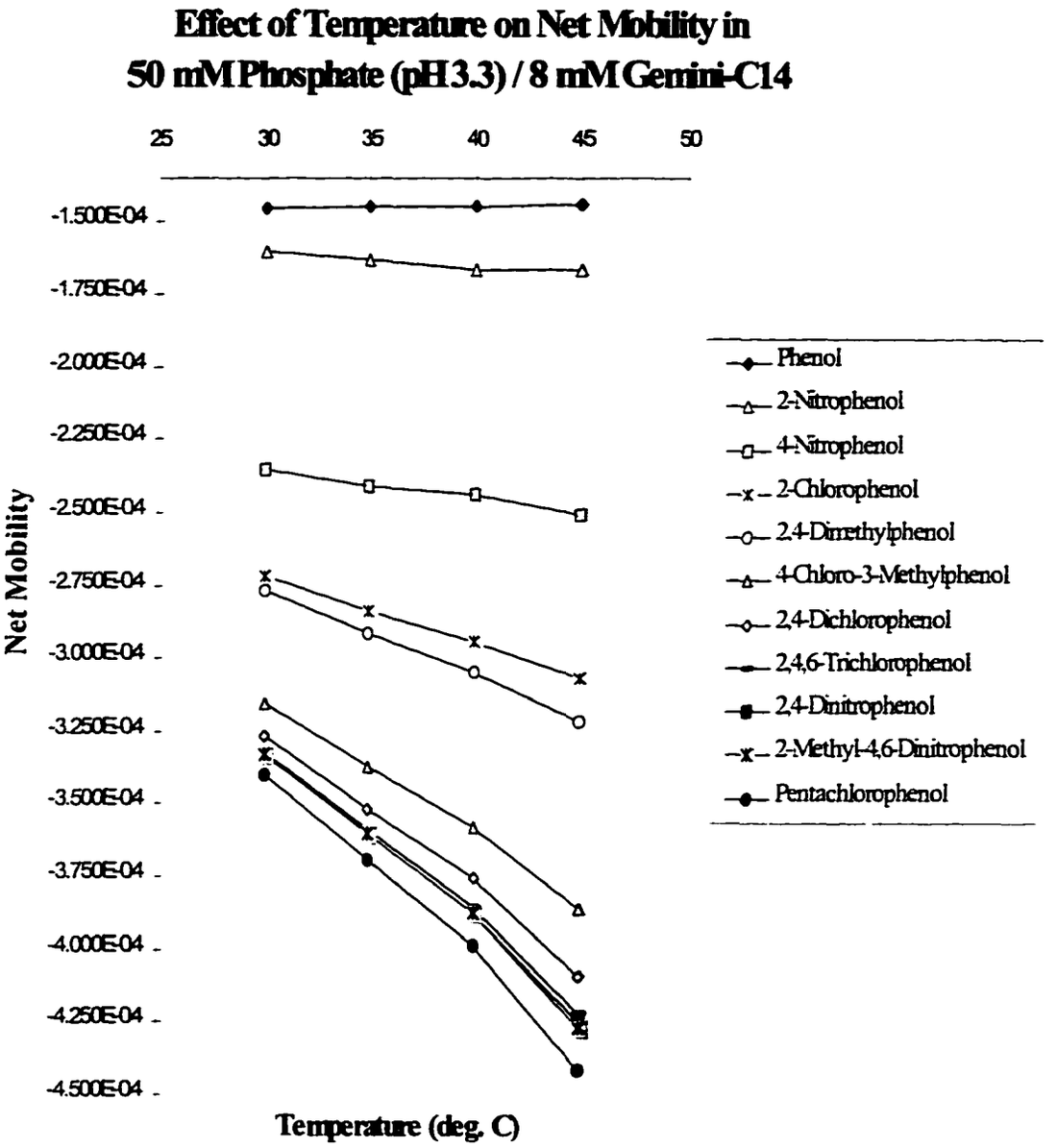

Figure 47

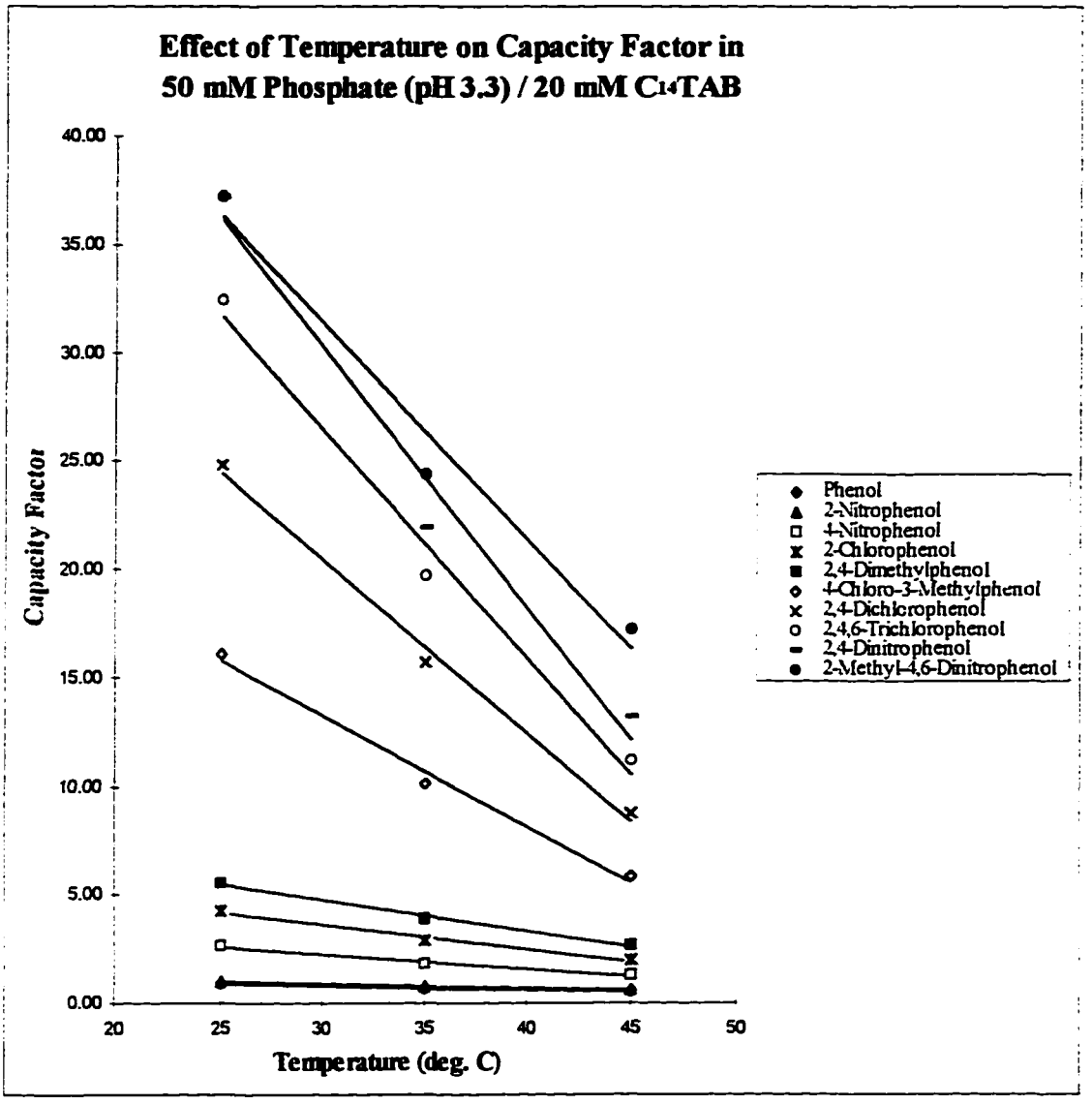

No.	Compounds	*RSQ*	*Slope*	*Intercept*
1	Phenol	0.99	-0.02	1.41
2	2-Nitrophenol	0.99	-0.02	1.47
3	4-Nitrophenol	0.99	-0.07	4.37
4	2-Chlorophenol	0.99	-0.11	7.02
5	2,4-Dimethylphenol	0.99	-0.14	9.09
6	4-Chloro-3-Methylphenol	0.99	-0.51	28.45
7	2,4-Dichlorophenol	0.99	-0.80	44.43
8	2,4,6-Trichlorophenol	0.99	-1.06	58.14
9	2,4-Dinitrophenol	0.98	-1.20	66.14
10	2-Methyl-4,6-Dinitrophenol	0.97	-1.00	61.25

Figure 48

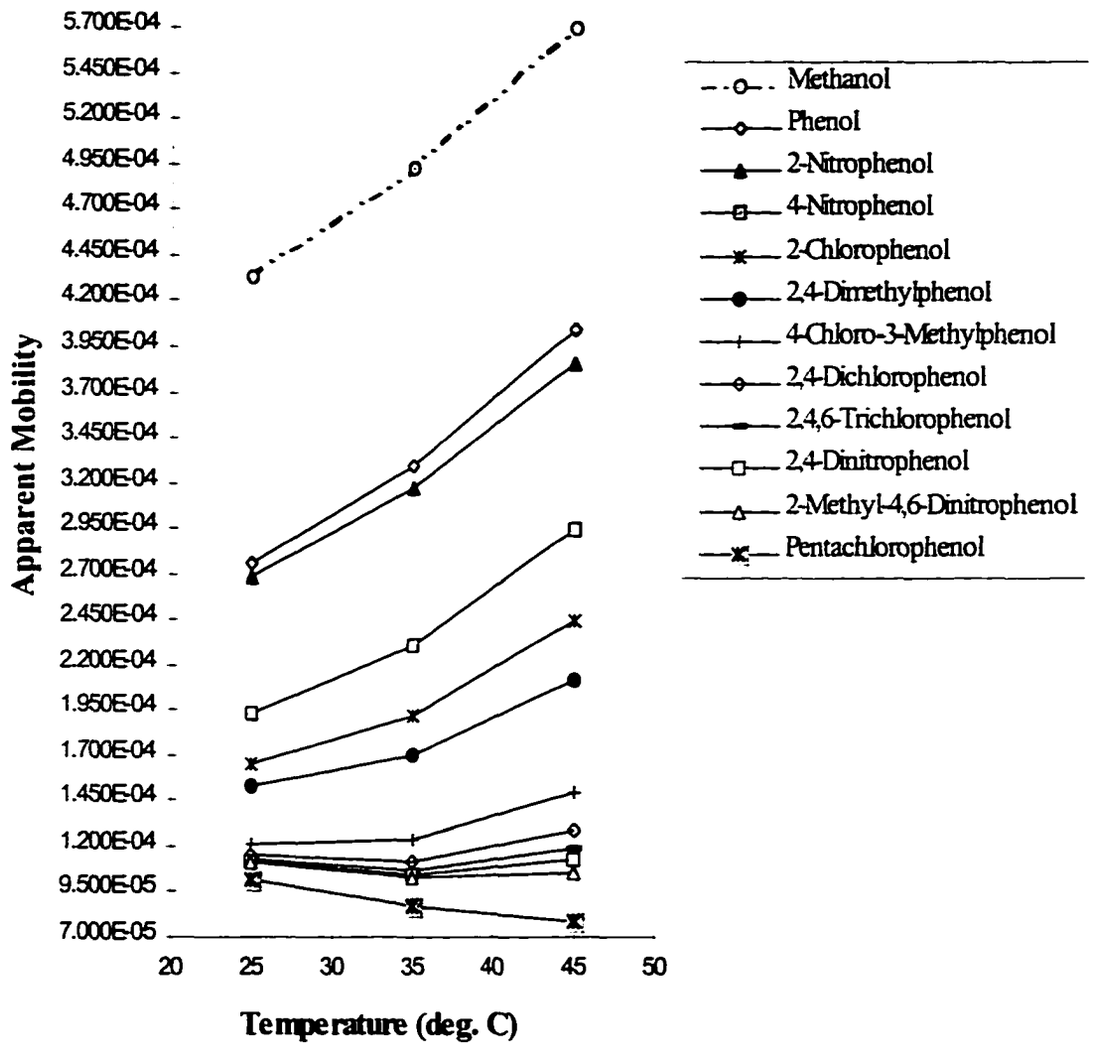

Figure 49

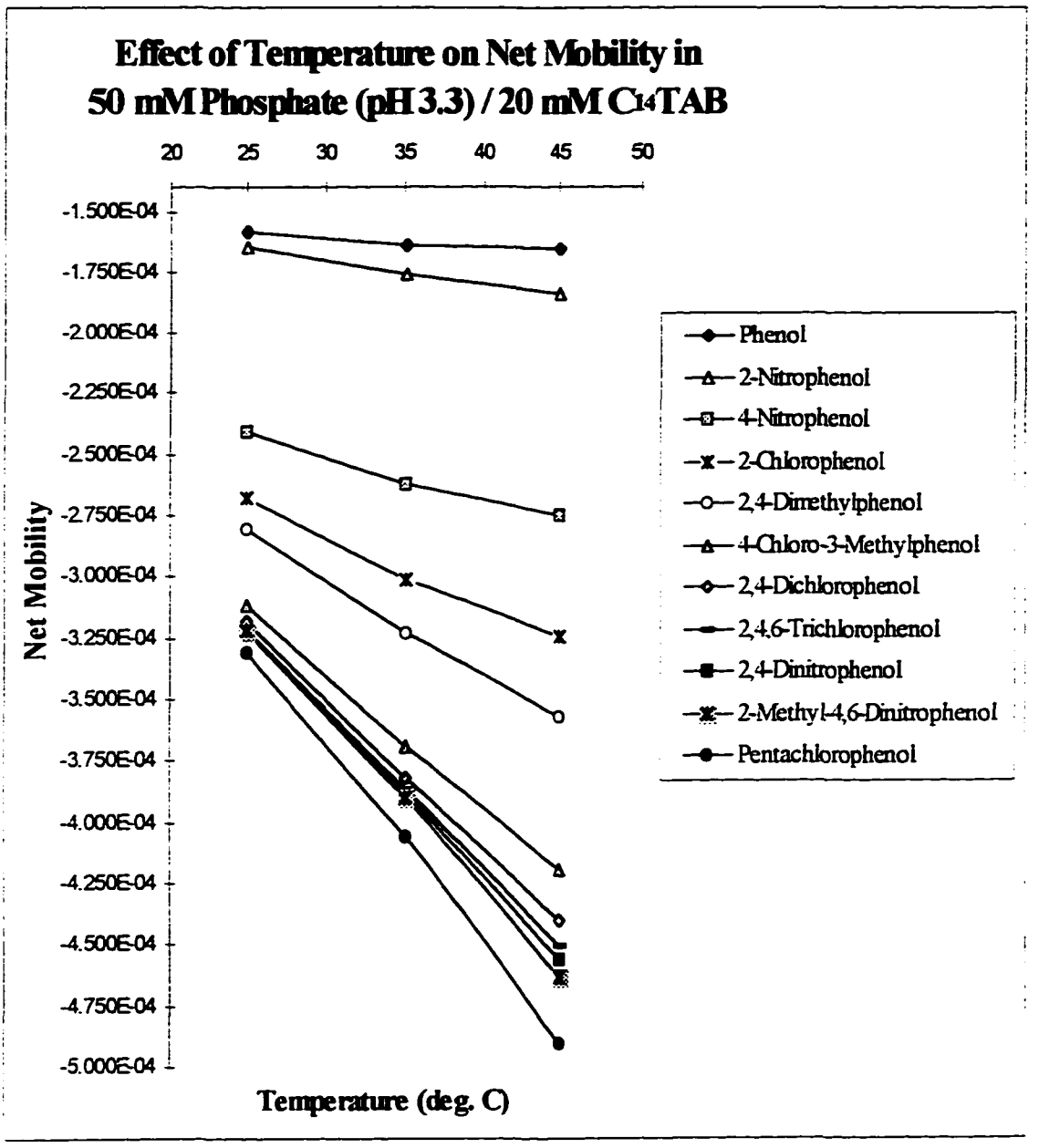

Figure 50

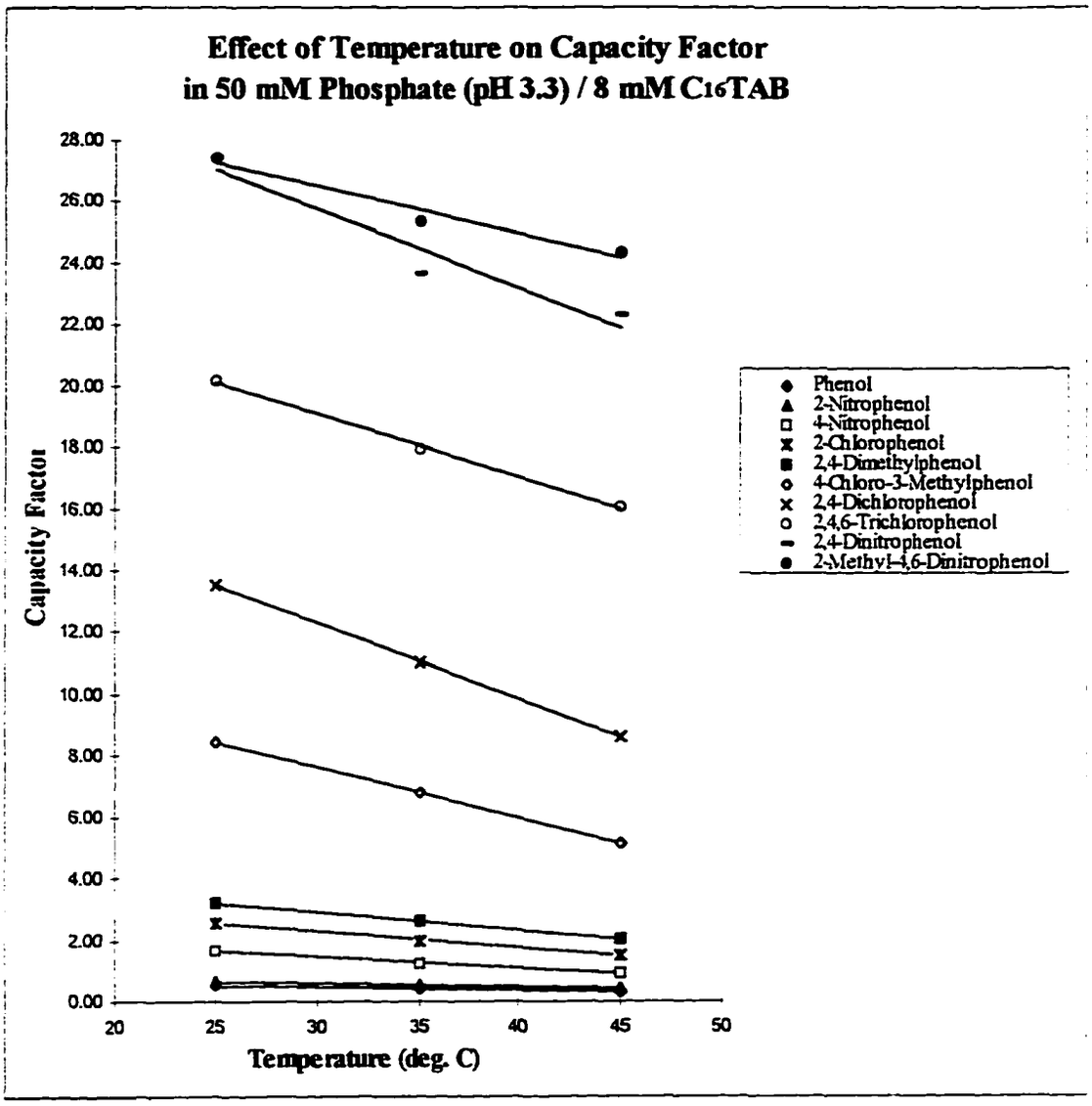

No.	Compounds	*RSQ*	*Slope*	*Intercept*
1	Phenol	1.00	-0.01	0.79
2	2-Nitrophenol	1.00	-0.01	0.86
3	4-Nitrophenol	0.99	-0.04	2.53
4	2-Chlorophenol	1.00	-0.05	3.89
5	2,4-Dimethylphenol	1.00	-0.06	4.69
6	4-Chloro-3-Methylphenol	1.00	-0.17	12.60
7	2,4-Dichlorophenol	1.00	-0.25	19.66
8	2,4,6-Trichlorophenol	1.00	-0.21	25.20
9	2,4-Dinitrophenol	0.93	-0.26	33.47
10	2-Methyl-4,6-Dinitrophenol	0.97	-0.16	31.15

Figure 51

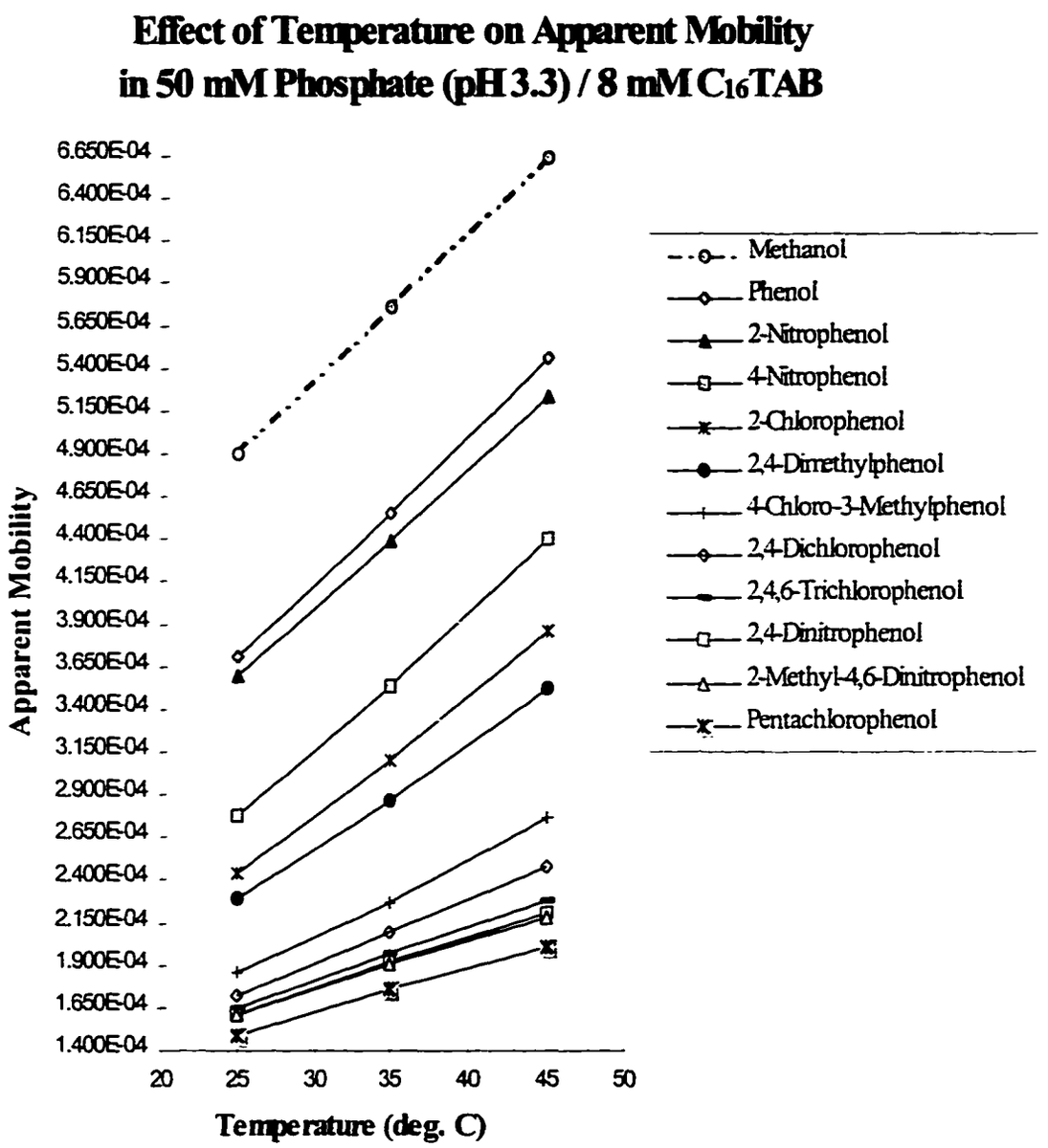

Figure 52

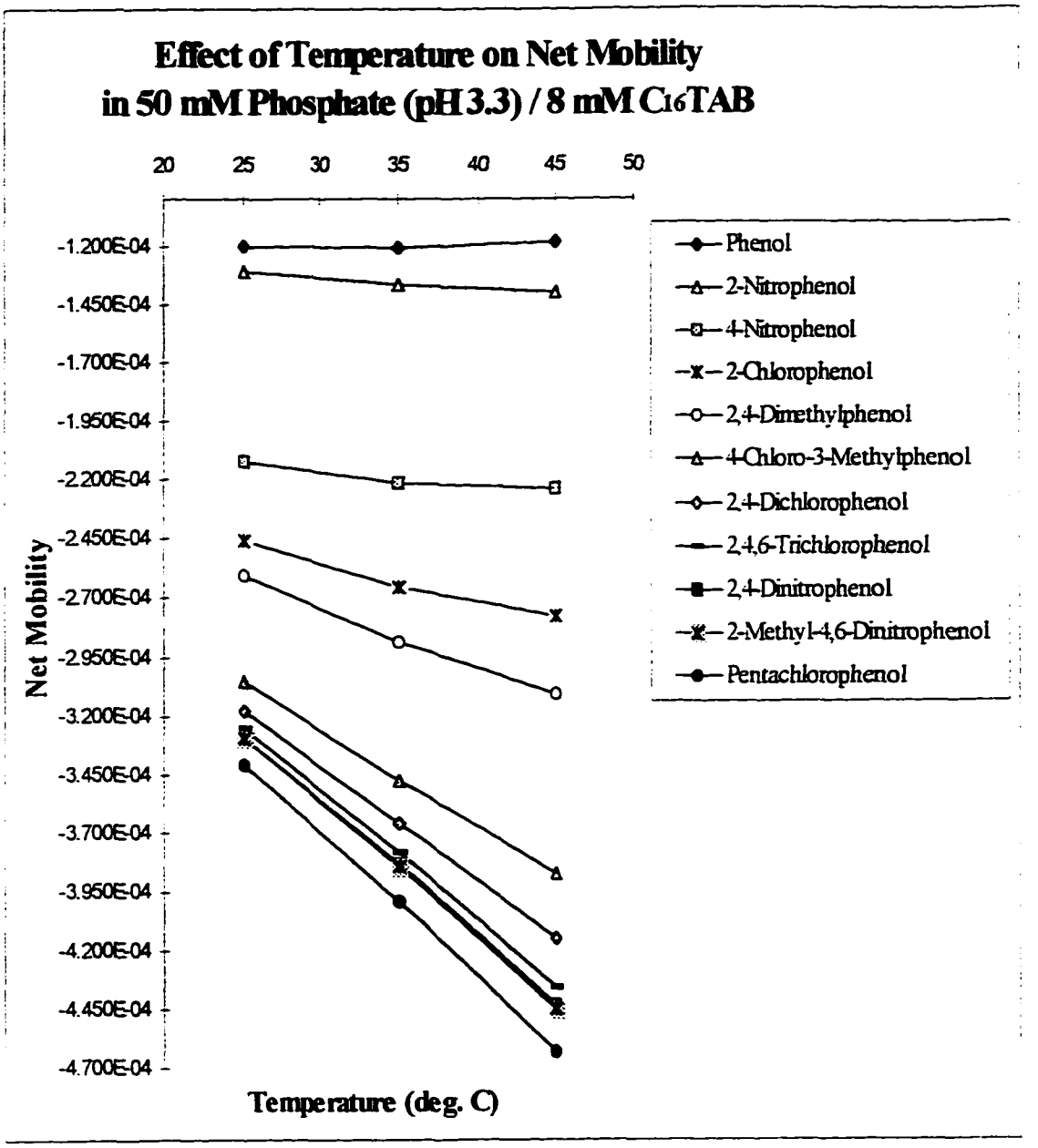

Figure 53

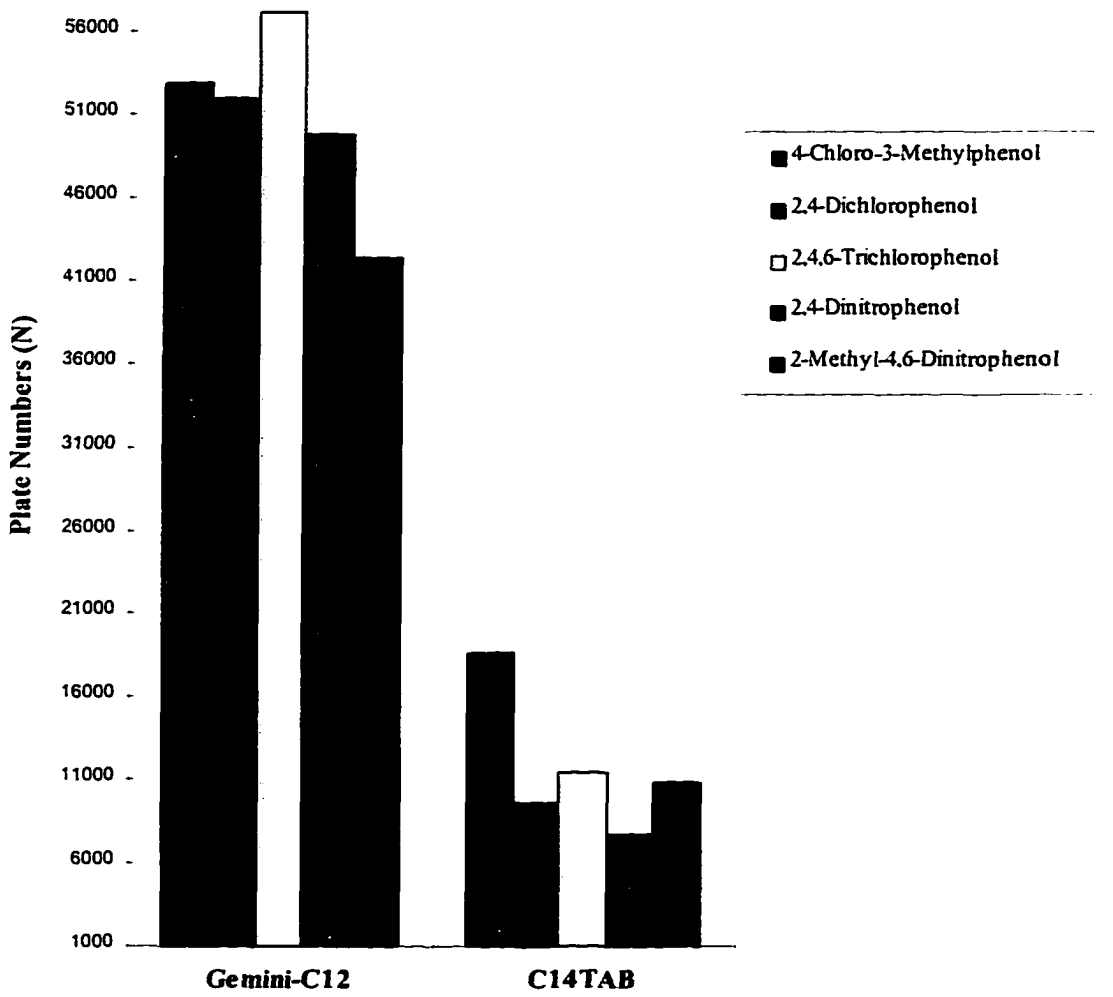

Figure 54

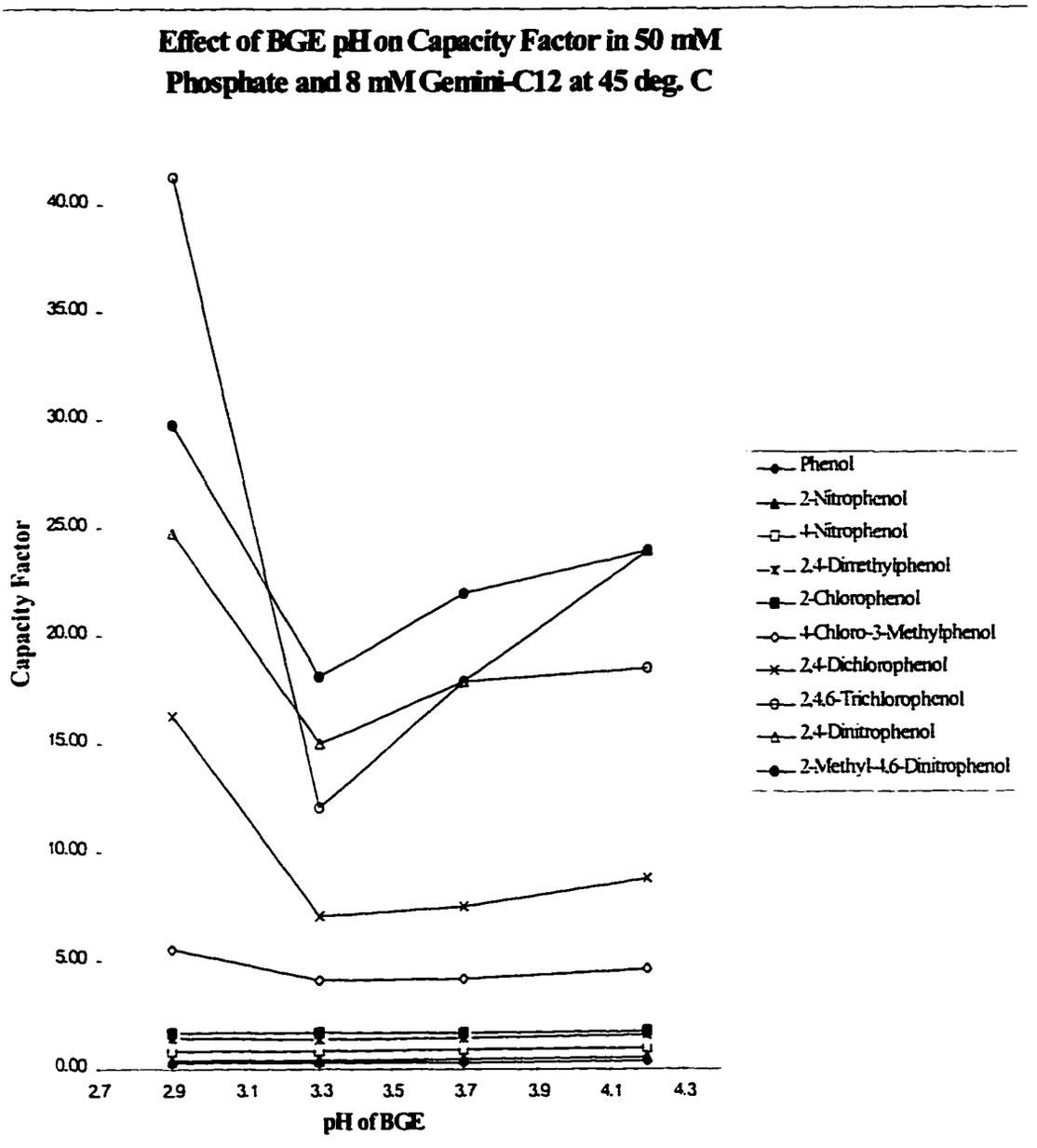

Figure 55

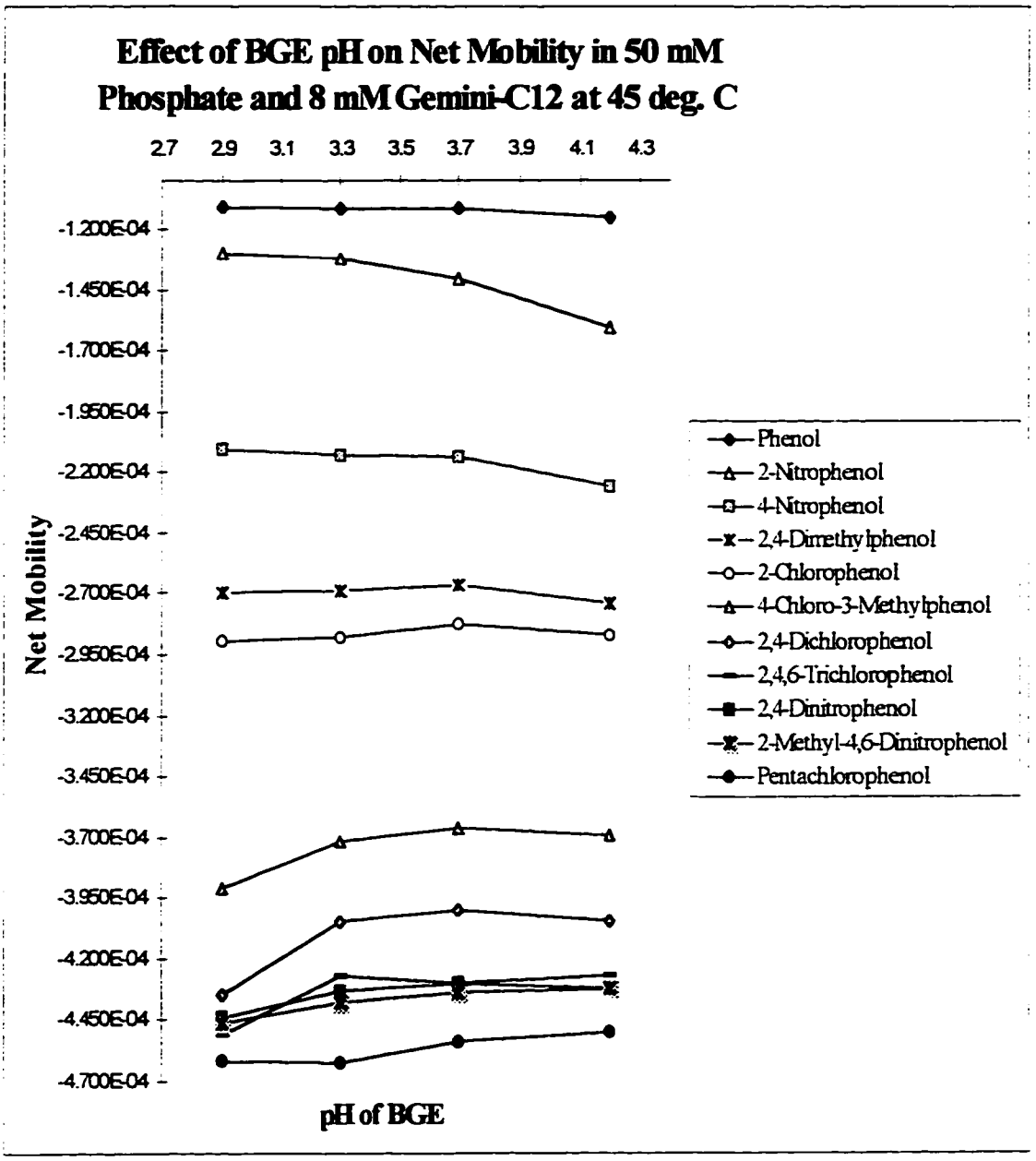

Figure 56

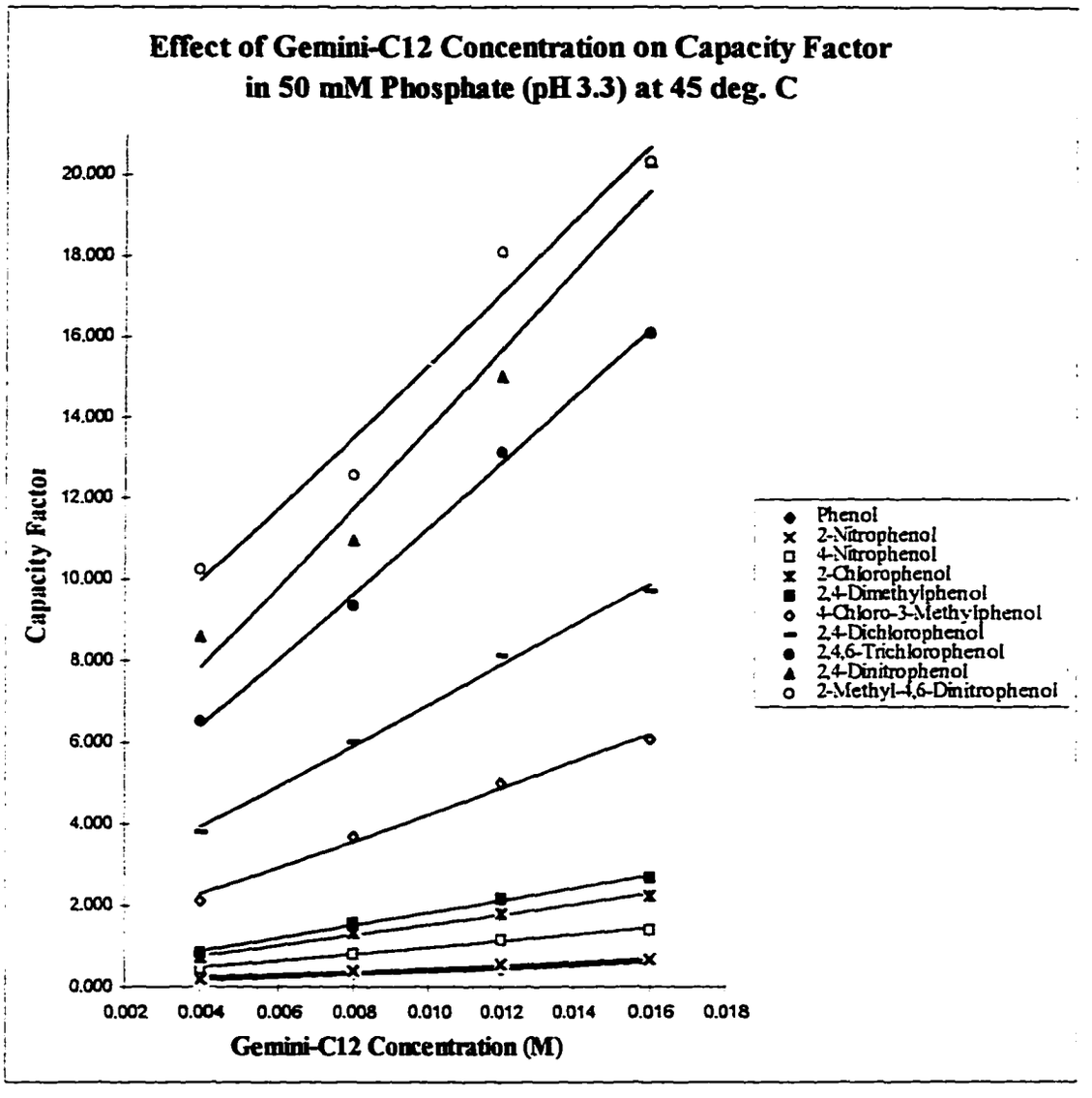

No.	Compounds	*RSQ*	*Slope*	*Intercept*
1	Phenol	0.999	35.078	0.027
2	2-Nitrophenol	0.998	39.419	0.063
3	4-Nitrophenol	0.987	79.296	0.164
4	2-Chlorophenol	0.995	124.532	0.276
5	2,4-Dimethylphenol	0.996	153.851	0.271
6	4-Chloro-3-Methylphenol	0.993	327.960	0.951
7	2,4-Dichlorophenol	0.995	498.120	1.925
8	2,4,6-Trichlorophenol	0.997	812.312	3.147
9	2,4-Dinitrophenol	0.973	979.261	3.929
10	2-Methyl-4,6-Dinitrophenol	0.968	892.970	6.374

Figure 57

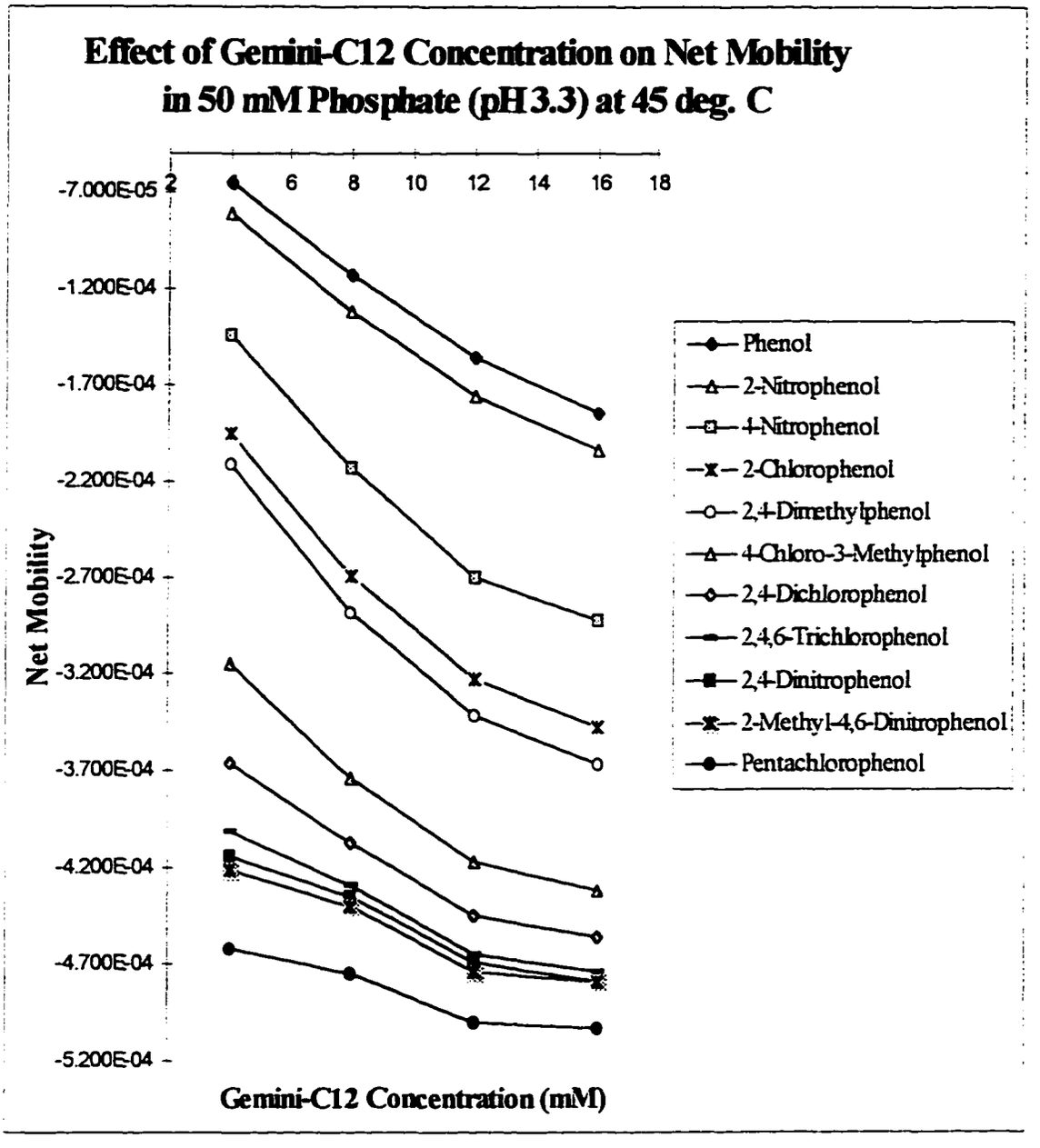

Figure 58

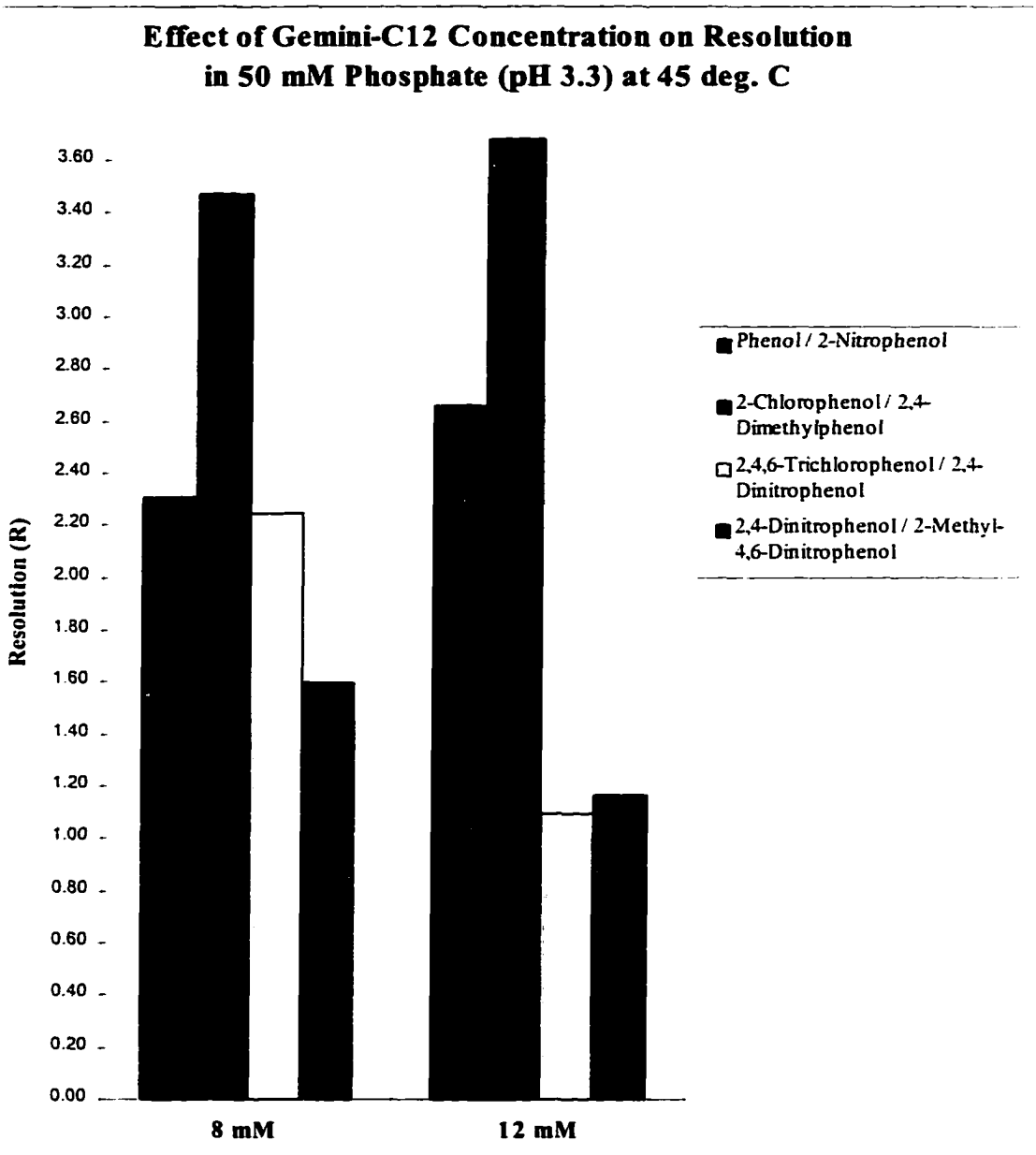

Figure 59

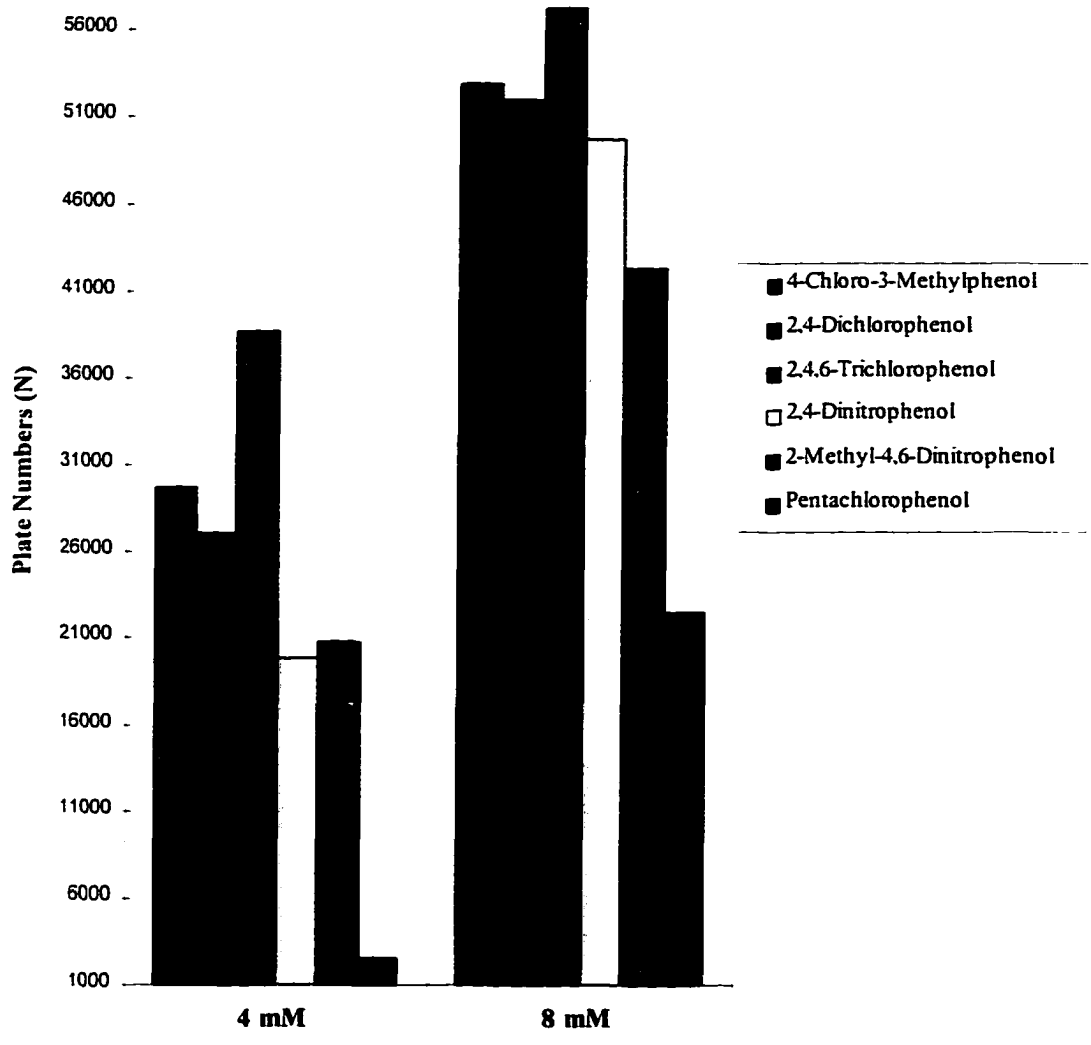

Figure 60

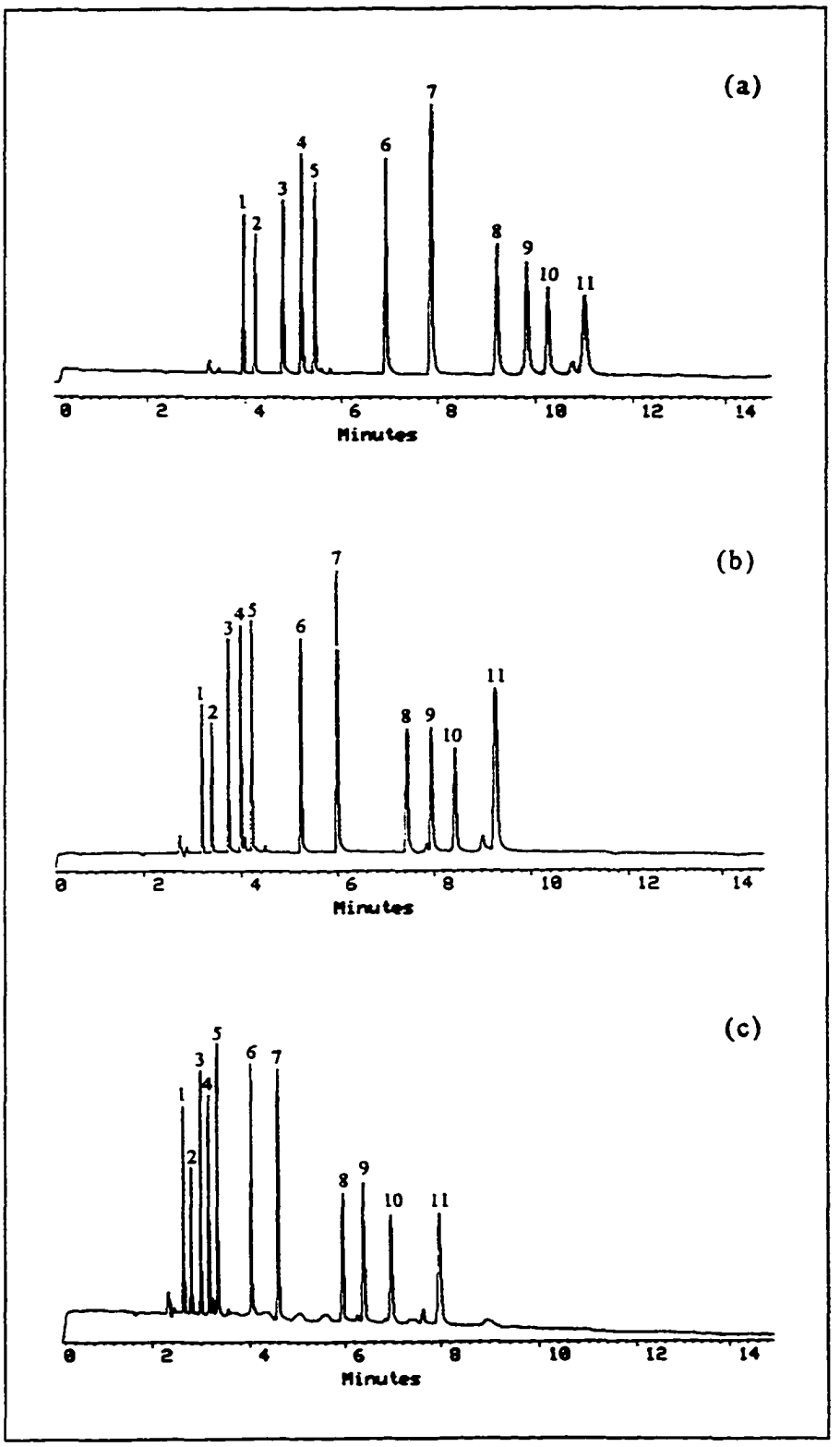

Figure 61

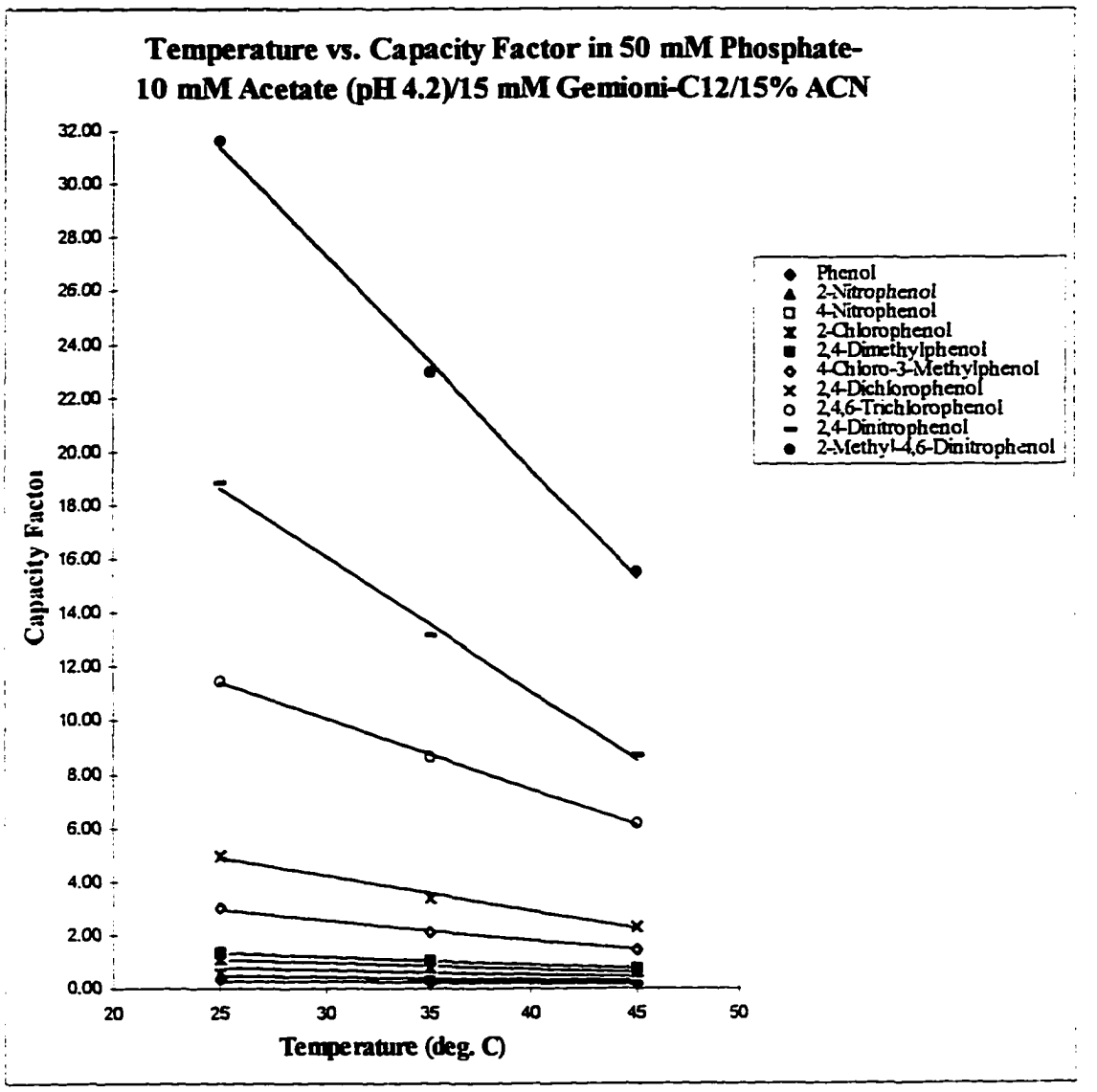

No.	Compounds	*RSQ*	*Slope*	*Intercept*
1	Phenol	1.00	-0.01	0.50
2	2-Nitrophenol	1.00	-0.01	0.66
3	4-Nitrophenol	0.99	-0.02	1.27
4	2-Chlorophenol	0.99	-0.03	1.74
5	2,4-Dimethylphenol	1.00	-0.03	2.07
6	4-Chloro-3-Methylphenol	0.99	-0.08	4.91
7	2,4-Dichlorophenol	0.99	-0.13	8.20
8	2,4,6-Trichlorophenol	1.00	-0.27	18.04
9	2,4-Dinitrophenol	1.00	-0.51	31.30
10	2-Methyl-4,6-Dinitrophenol	1.00	-0.81	51.57

Figure 62

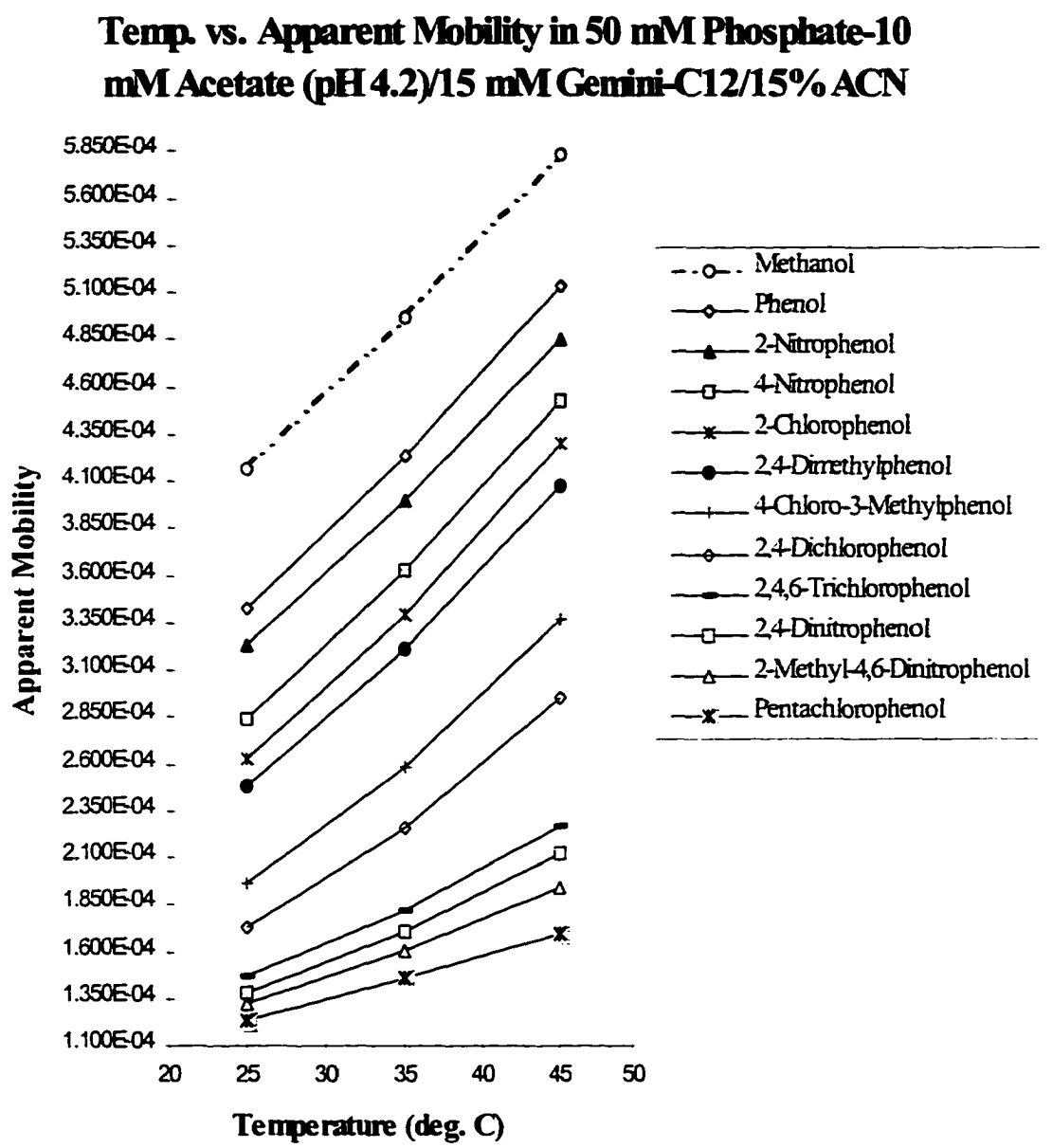

Figure 63

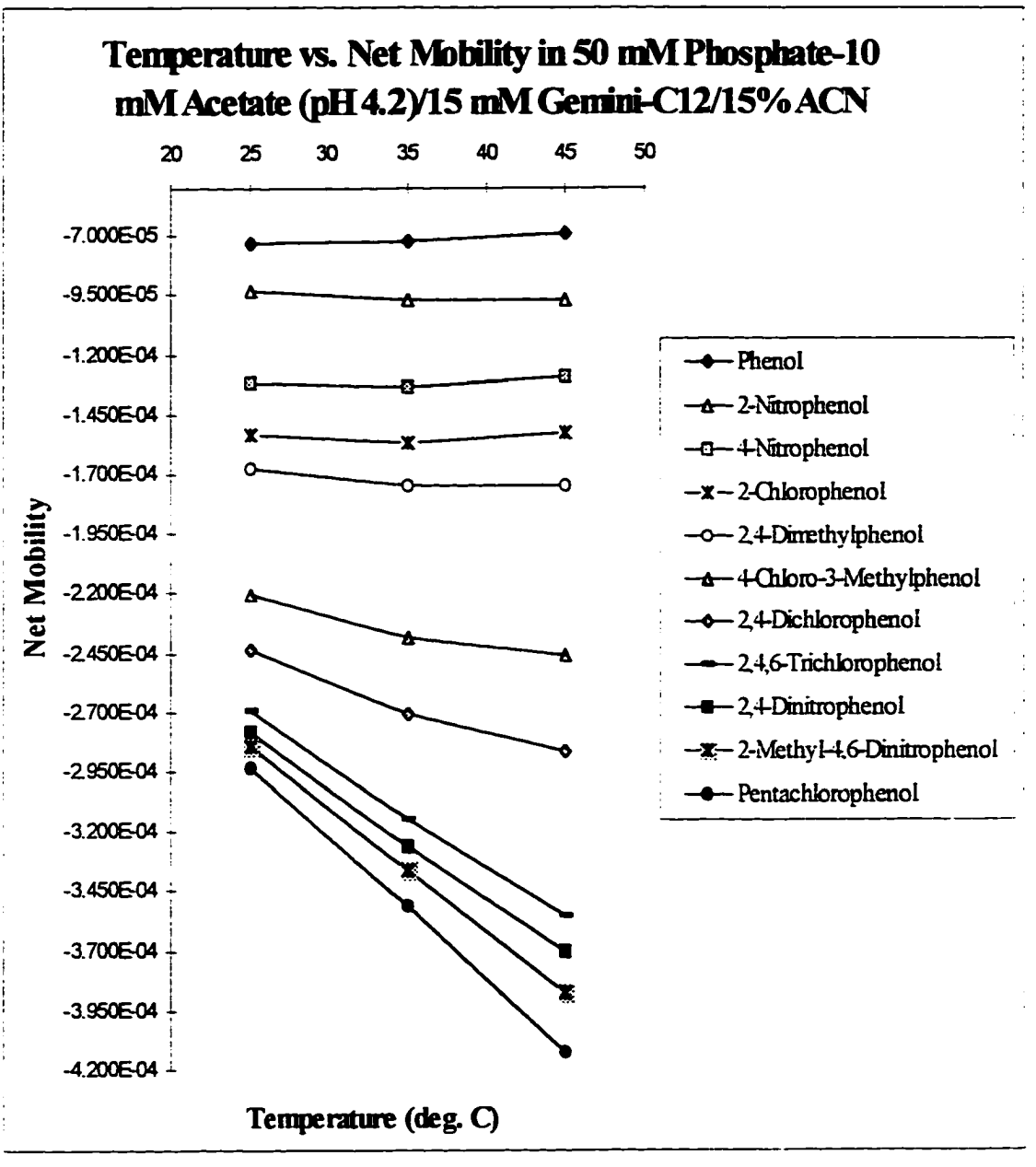

Figure 64

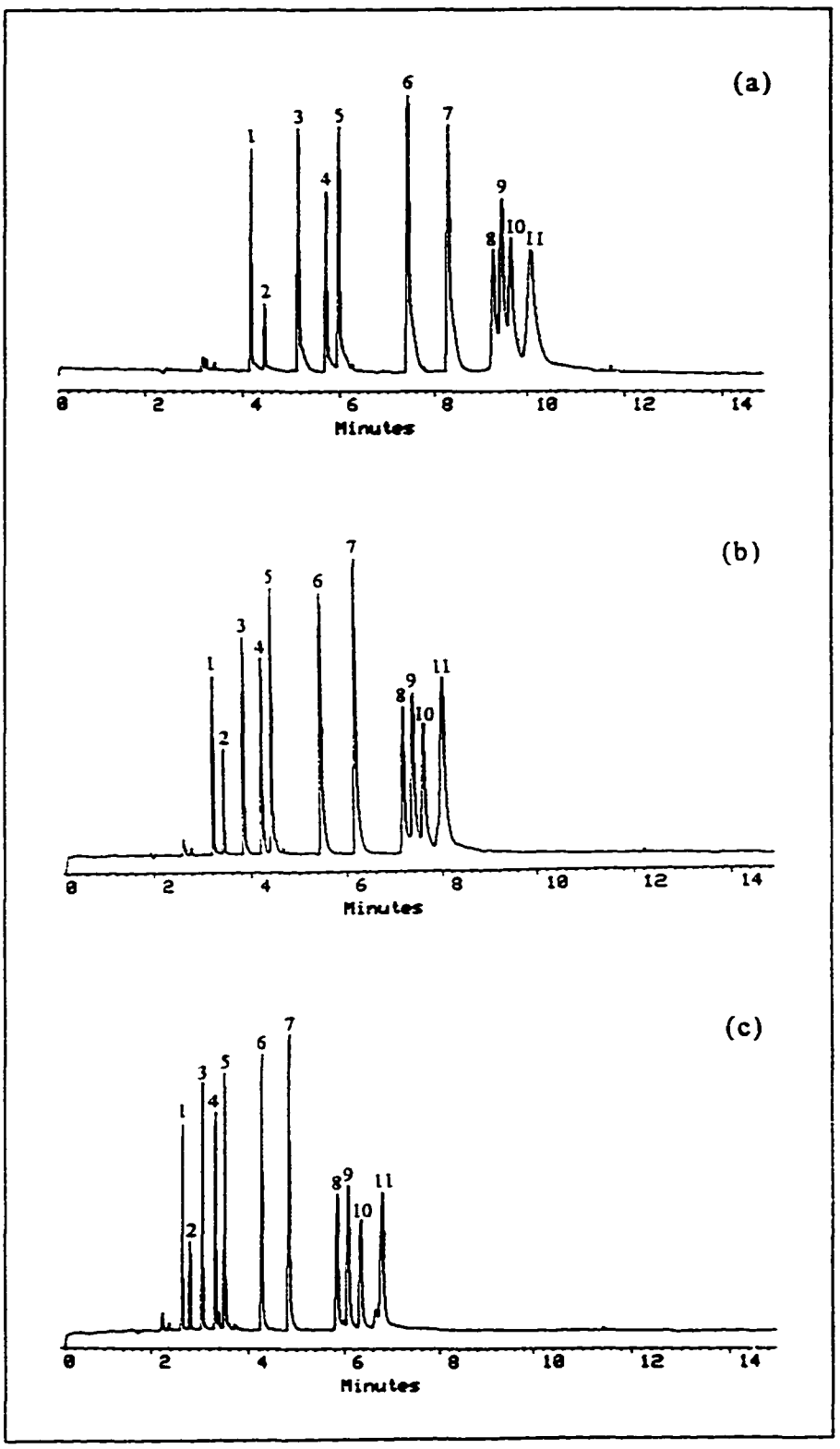

Figure 65

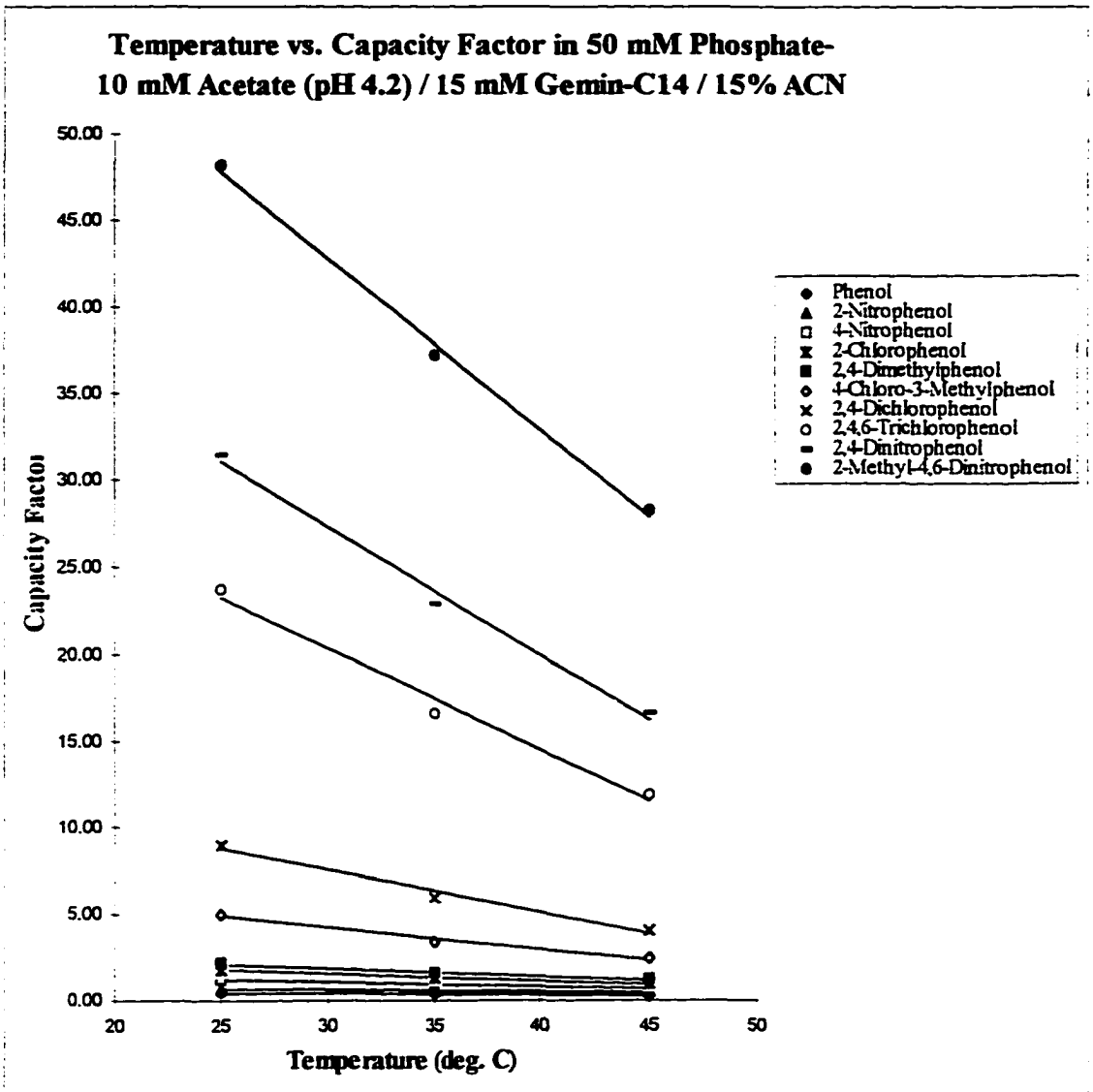

No.	Compounds	*RSQ*	*Slope*	*Intercept*
1	Phenol	0.99	-0.01	0.76
2	2-Nitrophenol	0.99	-0.01	0.99
3	4-Nitrophenol	0.98	-0.03	1.93
4	2-Chlorophenol	0.98	-0.04	2.85
5	2,4-Dimethylphenol	0.99	-0.05	3.30
6	4-Chloro-3-Methylphenol	0.98	-0.13	8.07
7	2,4-Dichlorophenol	0.98	-0.24	14.86
8	2,4,6-Trichlorophenol	0.99	-0.59	38.08
9	2,4-Dinitrophenol	0.99	-0.74	49.61
10	2-Methyl-4,6-Dinitrophenol	1.00	-1.00	72.77

Figure 66

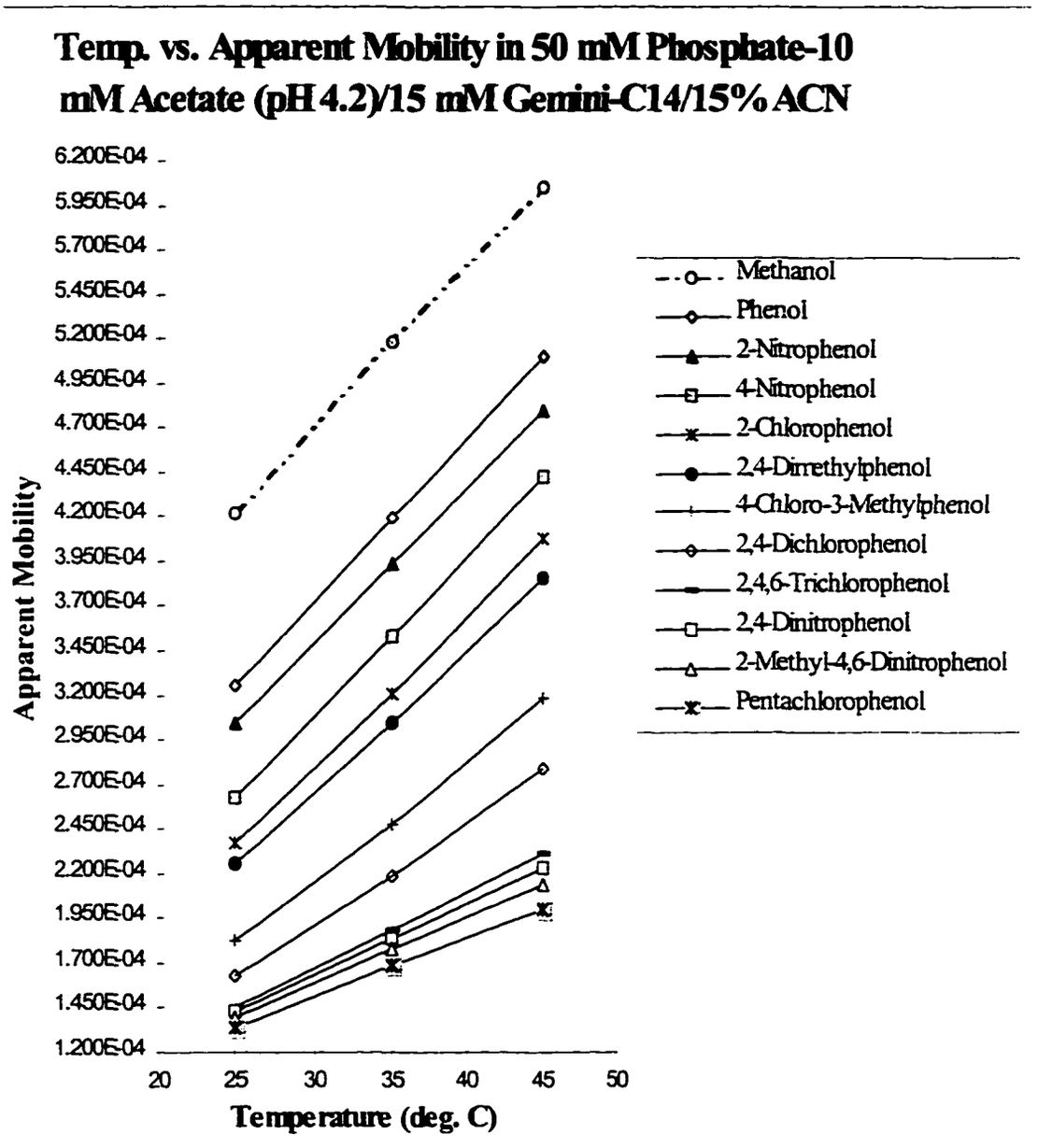

Figure 67

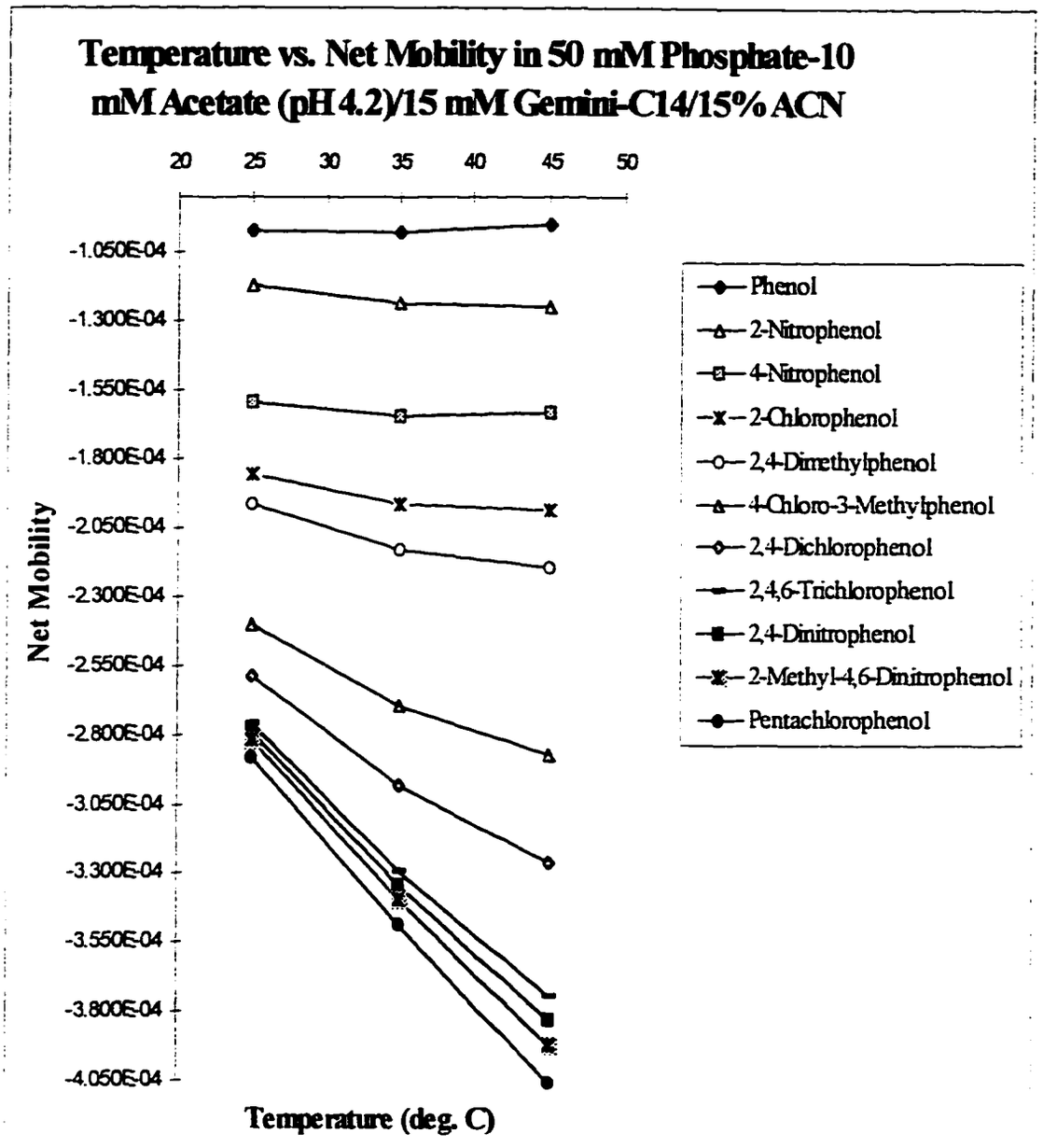

Figure 68

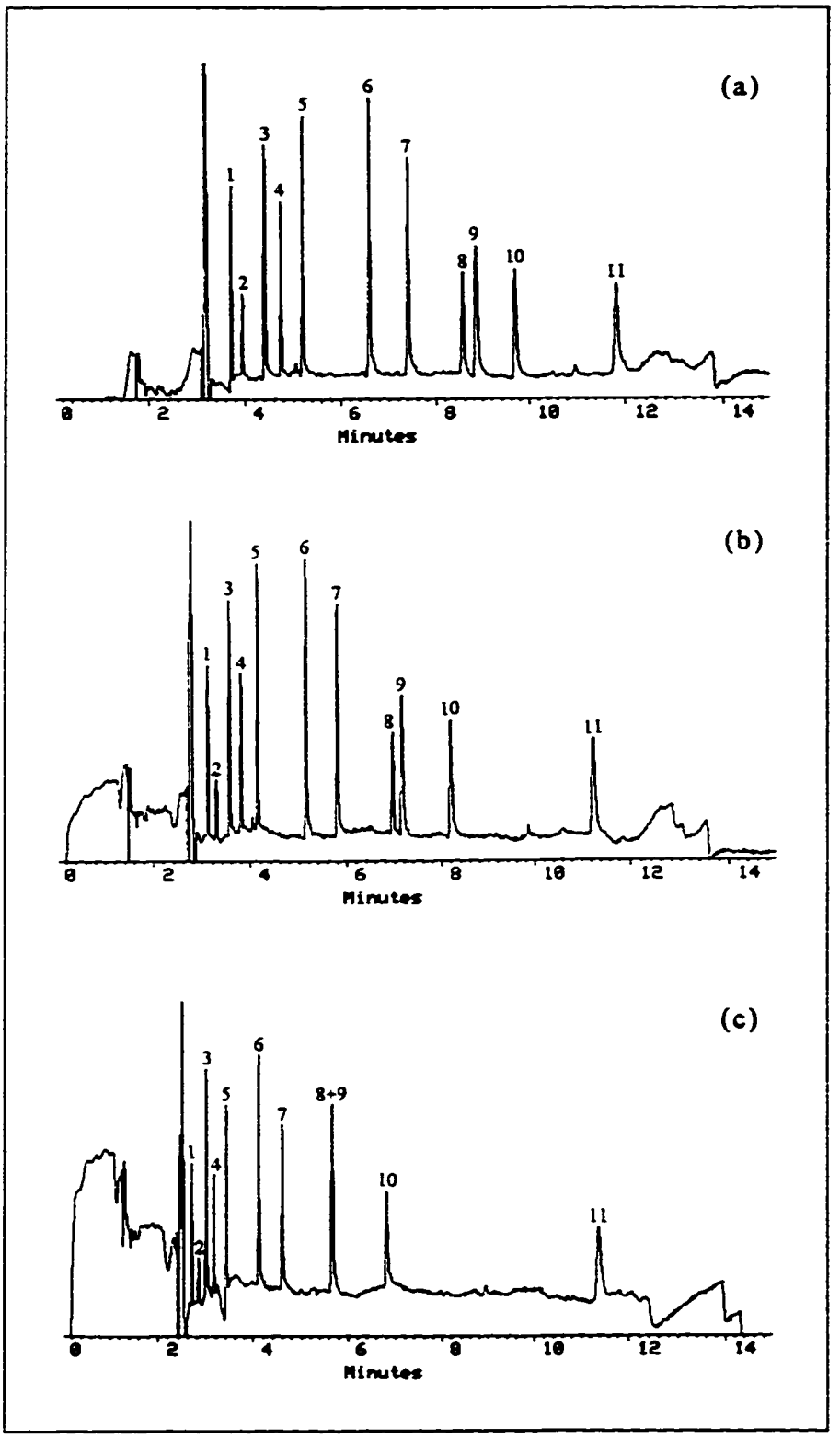

Figure 69

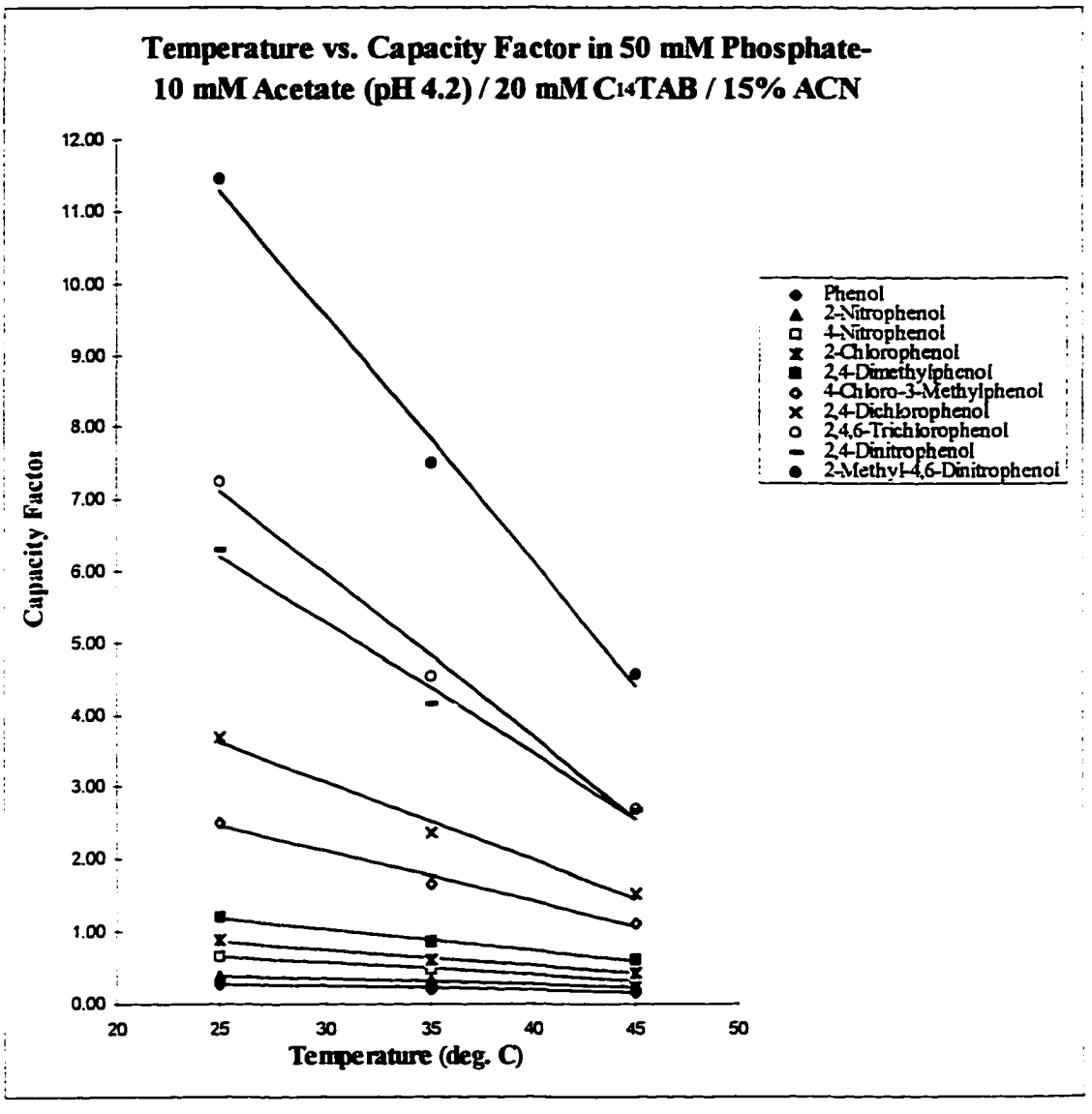

No.	Compounds	*RSQ*	*Slope*	*Intercept*
1	Phenol	0.99	-0.01	0.43
2	2-Nitrophenol	0.99	-0.01	0.59
3	4-Nitrophenol	0.99	-0.02	1.07
4	2-Chlorophenol	0.99	-0.02	1.42
5	2,4-Dimethylphenol	0.99	-0.03	1.92
6	4-Chloro-3-Methylphenol	0.99	-0.07	4.22
7	2,4-Dichlorophenol	0.99	-0.11	6.31
8	2,4,6-Trichlorophenol	0.99	-0.23	12.80
9	2,4-Dinitrophenol	0.99	-0.18	10.75
10	2-Methyl-4,6-Dinitrophenol	0.99	-0.34	19.90

Figure 70

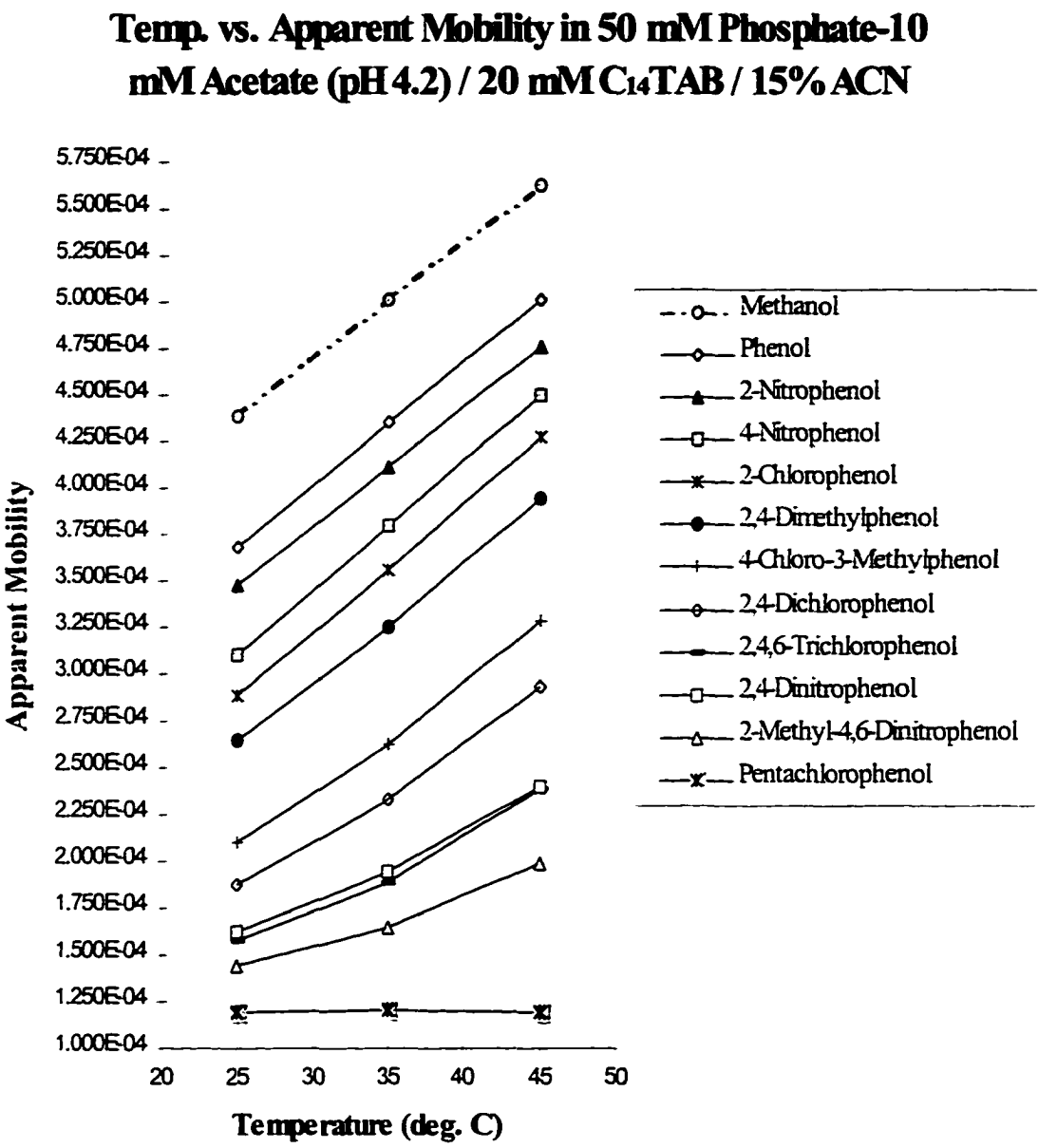

Figure 71

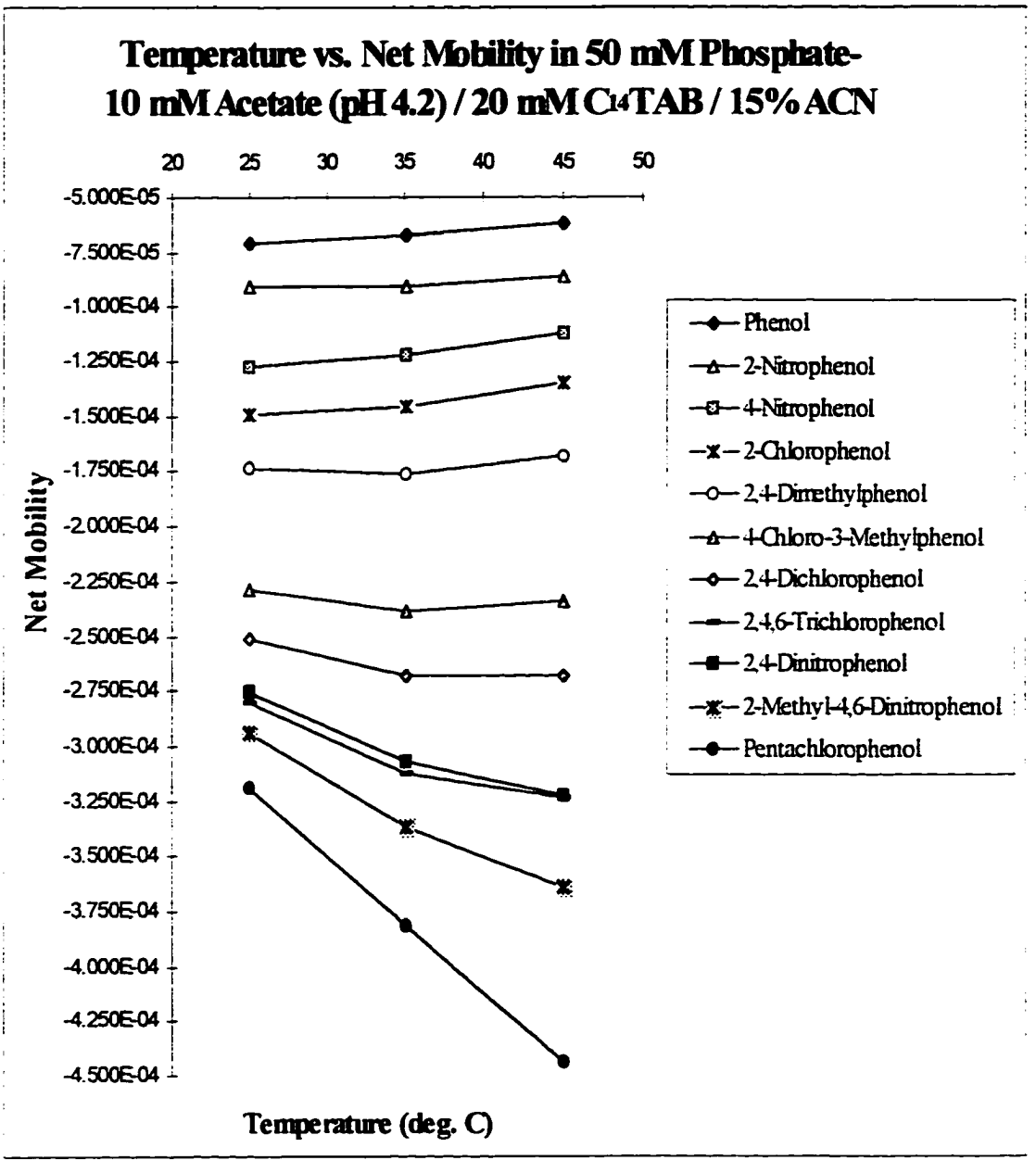

Figure 72

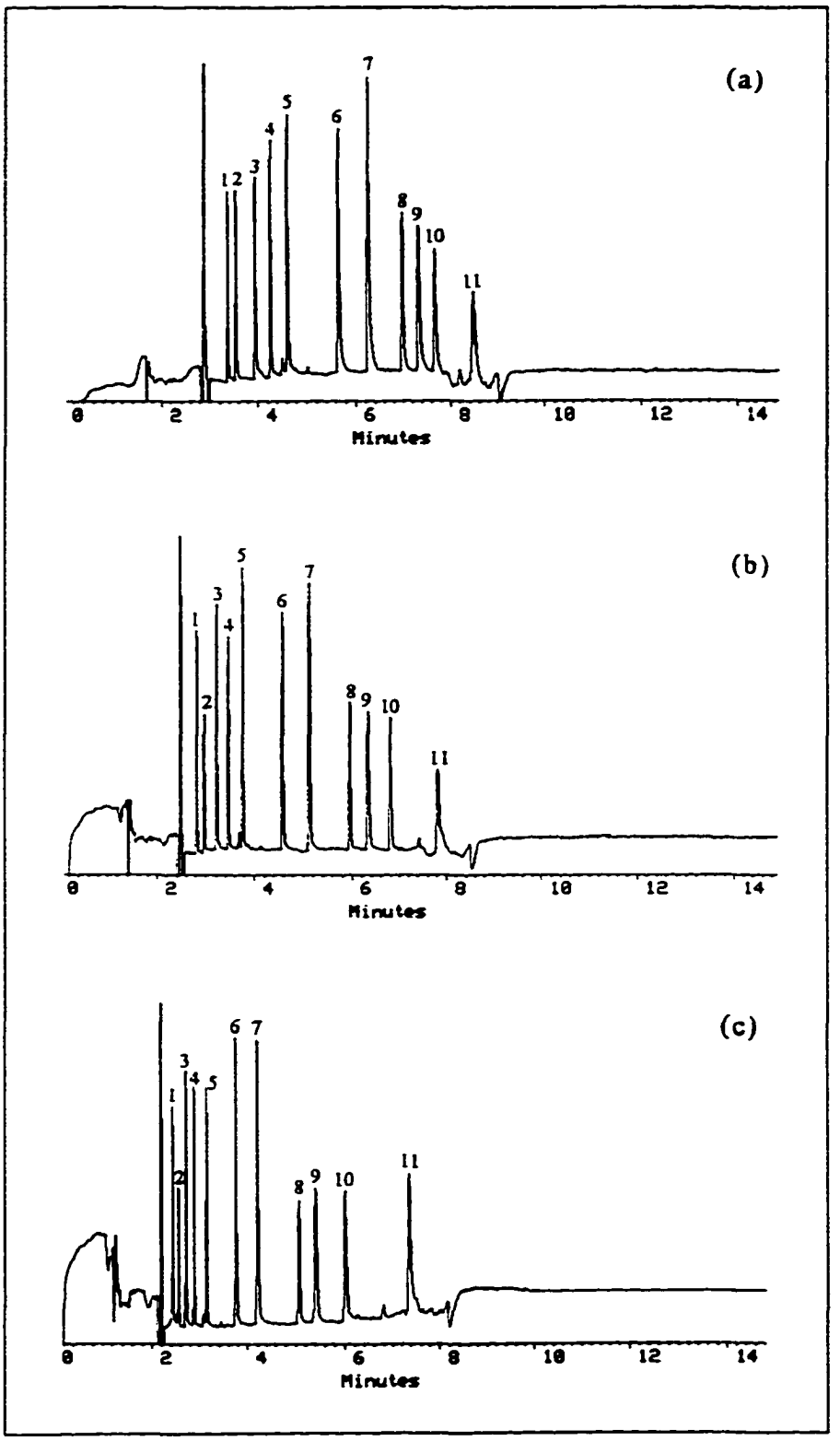

Figure 73

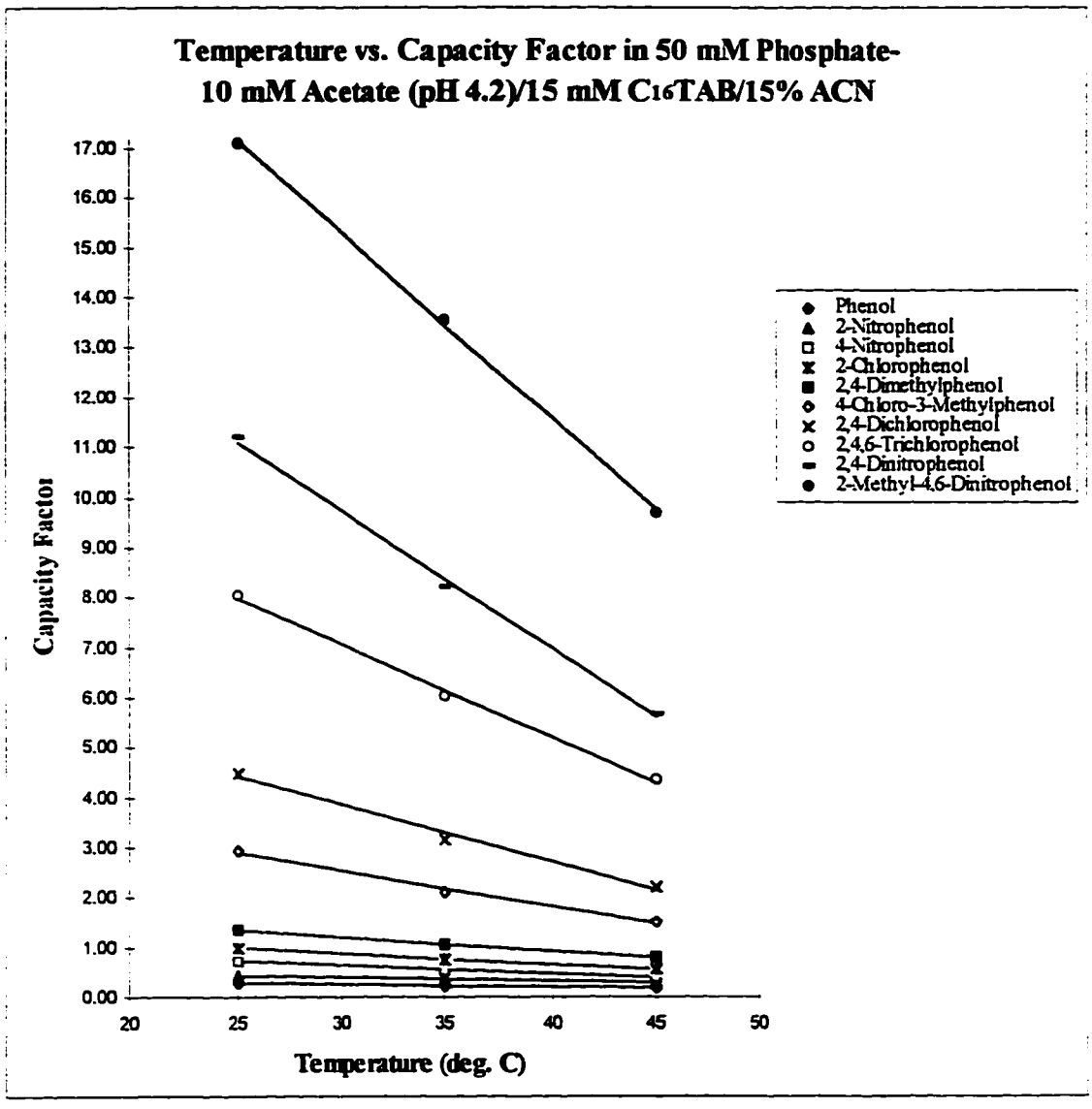

No.	Compounds	*RSQ*	*Slope*	*Intercept*
1	Phenol	1.00	-0.01	0.44
2	2-Nitrophenol	1.00	-0.01	0.66
3	4-Nitrophenol	0.99	-0.02	1.11
4	2-Chlorophenol	0.99	-0.02	1.53
5	2,4-Dimethylphenol	1.00	-0.03	2.05
6	4-Chloro-3-Methylphenol	0.99	-0.07	4.65
7	2,4-Dichlorophenol	0.99	-0.11	7.28
8	2,4,6-Trichlorophenol	1.00	-0.18	12.61
9	2,4-Dinitrophenol	1.00	-0.28	18.04
10	2-Methyl-4,6-Dinitrophenol	1.00	-0.37	26.42

Figure 74

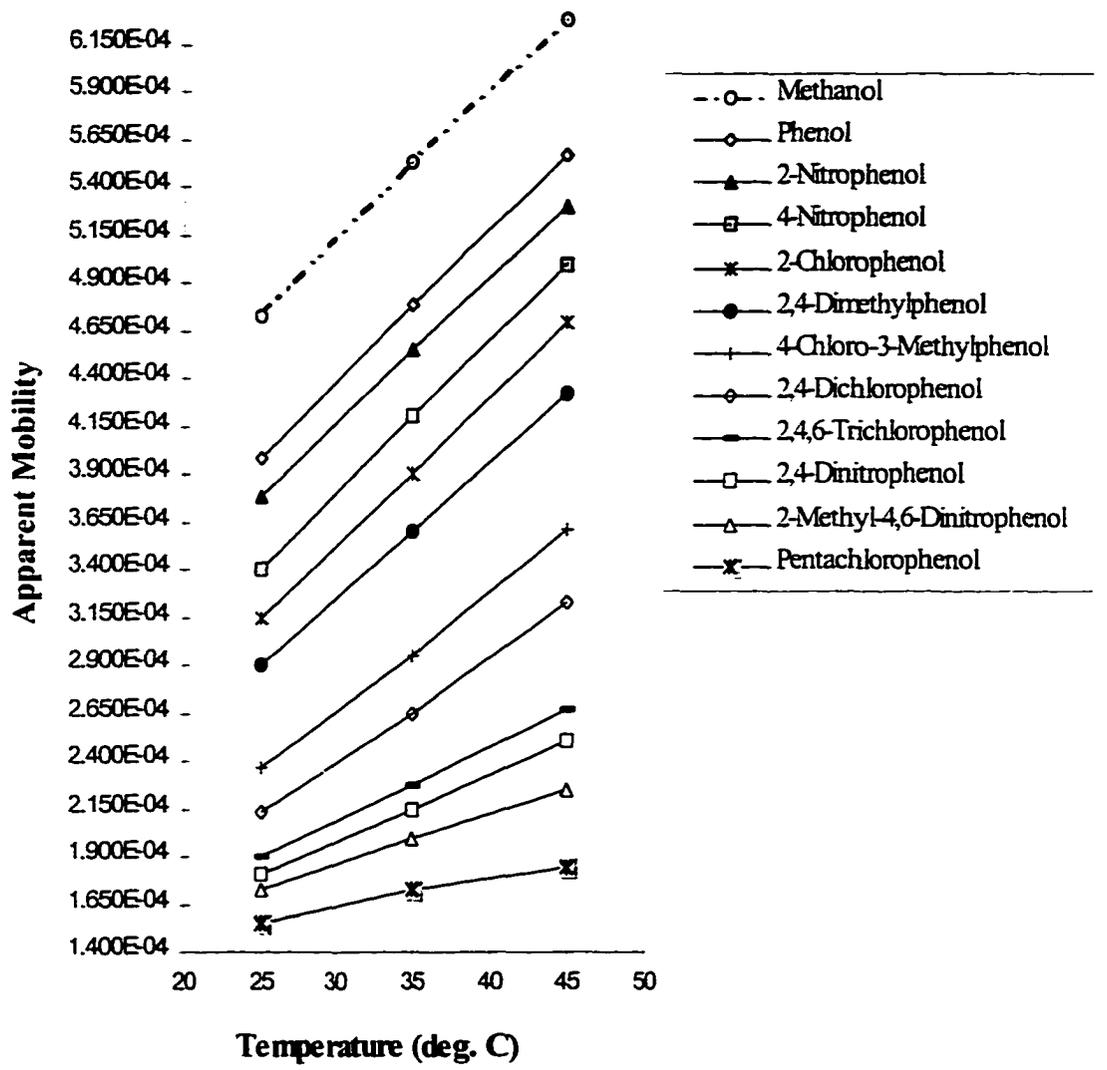

Figure 75

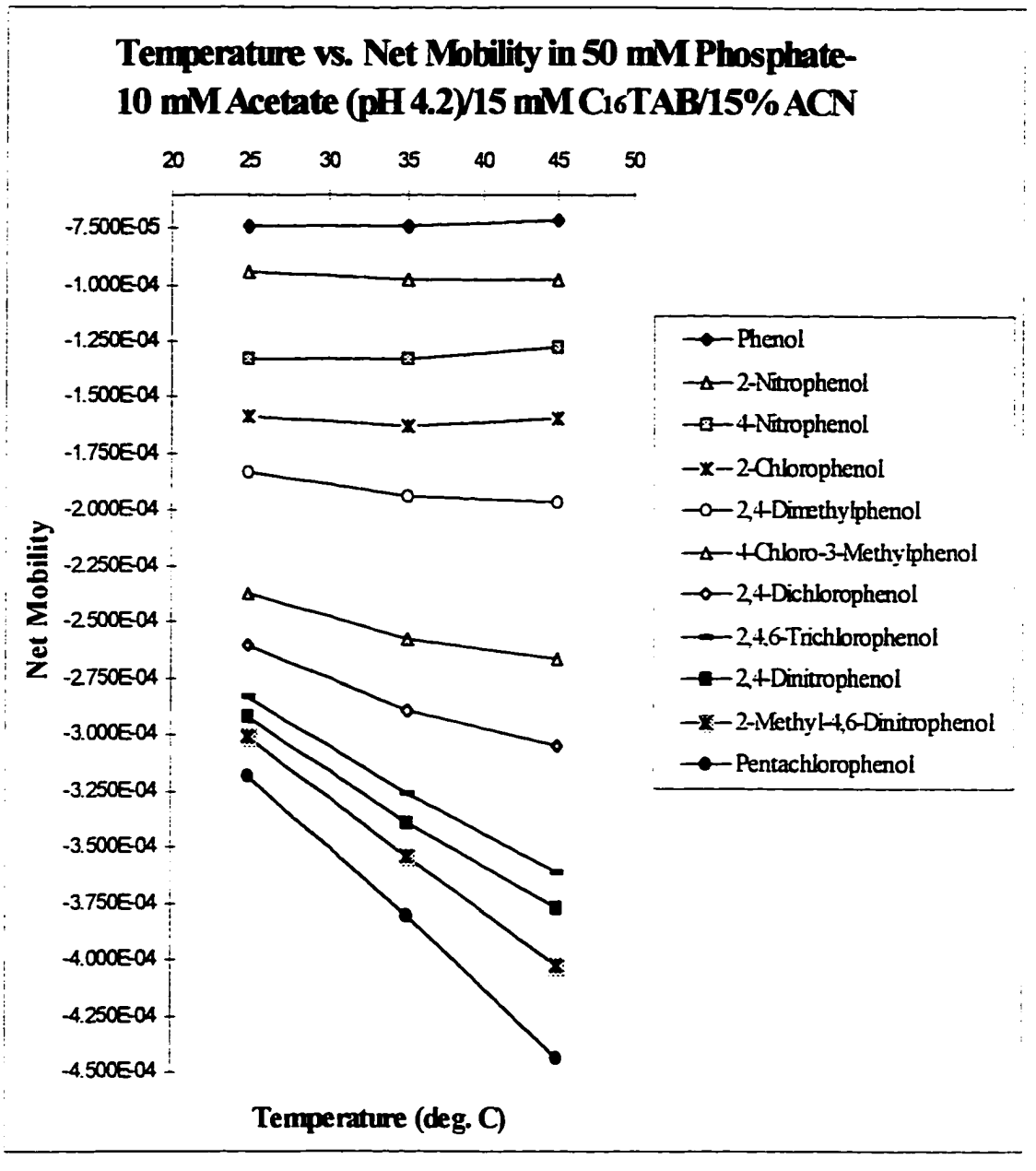

Chapter 5

Synthesis and Use of Novel Gemini Cationic Surfactants in Micellar Electrokinetic Capillary Chromatographic Separation of Ergot Alkaloids

Abstract

Two novel Gemini (double alkyl chain) cationic surfactants (named Gemini-C12 and Gemini-C14) were synthesized and applied to micellar electrokinetic capillary chromatography (MECC) for indicating purity and stability of dihydro-ergotoxines, derivatives of ergotoxine by hydrogenation. Ergotoxine is one group of the natural ergot peptide alkaloids, therapeutic substances which offer indisputable advantages for the treatment of dysregulation of the circulatory system. For comparison, two single alkyl chain cationic surfactants (myristyltrimethylammonium bromide, C_{14}TAB, and cetyltri-methyammonium bromide, C_{16}TAB) were utilized in MECC as well. The separation using the Gemini surfactants was much better than that with the single chain surfactants. Seventeen ergot alkaloids were well resolved in eight minutes using Gemini-C12 as micelle-forming reagent; and Gemini-C14 provided better resolution for all structure isomers in the MECC separation. These separations could not be achieved by MECC using the single chain cationic surfactants.

1. Introduction

Pharmaceutical analysis encompasses a broad range of measurement processes. One of the most challenging parts is the development of methods for indicating purity and stability of bulk drug substances and drug products. This requires that all likely synthetic and degradative impurities be resolved from each other and from the active drug in a sufficiently sensitive level (below 0.1% if possible). Such analytical methods are required to obtain drug approval from the Food and Drug Administration (FDA). Separation methods such as high-performance liquid chromatography (HPLC), gas chromatography (GC), and traditional electrophoresis have long been established in the pharmaceutical industry as means for obtaining required analytical data (1, 2).

In the past few years, capillary zone electrophoresis (CZE) and micellar electrokinetic capillary chromatography (MECC) have been rapidly developing separation techniques with high resolving power and separation speed (3, 4). A number of applications of these novel techniques in the pharmaceutical industry have been reported. For example, the purity of riboflavin-5'-phosphate (vitamin B_2 phosphate) was determined by CZE (5). Quality control of codeine and by-products at the 0.05% level using CZE was reported (6). The separation of tetracycline and its degradation products by CZE was

demonstrated (7). The separation of twelve benzothiozepin analogs for the purity tests of drug substances and tablets was achieved by MECC (8). This chapter describes the first reported MECC separation of dihydroergotoxines, derivatives of natural ergot peptide alkaloids, along with their synthetic and degradative impurities, comparing the Gemini and the single chain cationic surfactants.

The ergot alkaloids are a group of pharmacologically active compounds used as drugs as early as the Middle Ages (9). They are produced primarily by species of *Claviceps*, a fungal parasite of grasses and cereals (10). The ergot alkaloids have multiple actions including effects on uterine and vascular muscles, and have been used as a tool for studying the mechanism of the sympathetic nervous system (10). Nowadays, the ergot alkaloids are highly effective therapeutic substances for the treatment of dysregulation of the circulatory system which offer advantages such as low required dosage, high efficacy and, to a large extent, lack of side effects (11). Within the last few years the newer ergot derivatives have been identified as potential therapeutic agents in many disease states such as parkinsonism, acromegaly, amenorrhea-galactorrhea, suppression of postpartum lactation, treatment of breast cancer, and possibly cancer of the prostate (secondary to inhibition of prolactin secretioin) (10).

The ergot alkaloids can be divided into four main structural groups: clavine alkaloids, lysergic acids, simple lysergic acid amides, and peptide alkaloids (ergopeptines).

Ergopeptines, the "classical" peptide ergot alkaloids, are composed of D-lysergic acid (ergolene with a COOH- group in the C_8 position, see Figure 1) and an L-proline-containing complex tripeptide moiety (a tricyclic ring system). A schematic representation of the sidechains of the known naturally occurring ergot alkaloids is given in Figure 2. The double bond of the 9-ergolene alkaloids can be hydrogenated to form a number of medicinally important compounds. Aci-isomerization, shown in Figure 2, can occur in the peptide alkaloids and the corresponding dihydro derivatives. Since isomerization takes place in acidic solutions (acid catalyzed rearrangement), the alkaloids obtained are designated by the prefix "aci". However, aci-alkaloids are pharmacologically inactive (10). Hydrolysis of the peptide alkaloids can yield D-lysergic acid and proline. Production of lysergic acid and its derivatives is accompanied by formation of isolysergic acid and iso-derivatives, due to stereoisomerism of the H- and COOH-group in the C_8 position (see Figure 1). Isolysergic acid derivatives exhibit only a weak pharmacological action (10).

Dihydro derivatives differ considerably from the natural alkaloids in their pharmacological effects. One of the most

prominent differences was found with respect to the uterine effect (9). The hydrogenated alkaloids are practically devoid of oxytocic action; their main actions are on the autonomic nervous system. However, the dihydro derivatives are indeed able to inhibit both in vitro and in situ the powerful stimulative action of the natural alkaloids (10).

Dihydroergotoxines are the hydrogenation products of ergotoxine, one of the natural ergot peptide alkaloids. Dihydro-ergotoxine is not a single compound, but consists of four alkaloids (9), dihydro-ergocornine, -ergocristine, -α-ergocryptine and -β-ergocryptine. Dihydroergotoxine, in the form of its methanesulfonic acid salt (also called ergoloid mesylates), is now widely used for the treatment of symptoms of mild to moderate impairment of mental function in the elderly (12). The main regions of dihydroergotoxine activity are the central nervous system and the circulation (11). The drug substance contains equal amounts of dihydro-ergocornine, -ergocristine and -ergocryptine, and the ratio of the α- and β-isomers of dihydroergocryptine is approximately 2:1. These proportions correspond to the amounts found in natural ergotoxine isolated from selected and cultivated strains of *Claviceps purourea* (9).

Dihydroergotoxine is prone to light-enhanced oxidative degradation in aqueous solution (12). In the case of

dihydroergocristine, the main oxidation products have been identified (13) as N-formyl-β-seco-dihydroergocristine and its deformylation product, β-seco-dihydroergocristine, the structures of which are given in Figure 3.

Since the supply of naturally grown ergots is not sufficient for commercial production of therapeutically active substances, the classic isolation from ergot has become less advantageous. The syntheses and/or semi-syntheses of the substances have been successful, and many production lines have been approved by FDA (11). HPLC is the predominant separation technique in pharmaceutical analysis. So far, however, an efficient and sensitive method by HPLC for indicating purity and stability of synthesized and/or semi-synthesized dihydroergotoxine has not been developed (14); an HPLC impurity testing method has not been published in the United States Pharmacopoeia (USP).

In this study, an impurity profile of dihydroergotoxine was investigated by MECC using cationic surfactants. Two novel Gemini (double alkyl chain) surfactants, Gemini-C12 and Gemini-C14 (see Figure 4), were synthesized and applied in MECC for indicating purity and stability of dihydroergotoxine. Seventeen alkaloids, listed in Table 1 and whose structures are given in Figure 3, were well resolved within eight minutes using Gemini-C12 as the micelle-forming reagent in MECC; and Gemini-C14 provided better resolution for all the alkaloid

isomers in the MECC separation. For comparison with the Gemini surfactants, myristyltrimethylammonium bromide (C_{14}TAB or TTAB) and cetyltrimethylammonium bromide (C_{16}TAB or CTAB), two single alkyl chain cationic surfactants were examined in MECC as well. However, the separation of the seventeen ergot alkaloids could not be achieved using these single alkyl chain cationic surfactants.

2. Experimental

2.1 Apparatus

MECC experiments were carried out with a Beckman P/ACE 5010 CE system (Beckman Instruments, Palo Alto, CA, USA) equipped with a UV absorbance detector at 214 nm and a liquid cooling circulation for the temperature control. The CE system was connected to a Waters/VAX 4000-50 data system through an LAC/E interface module. The Waters ExpertEase software (version 3.1) was used for data acquisition and processing. A Orion Model 290A pH meter was used to measure pH with a precision of ±0.01 unit.

The separation capillaries were made uncoated fused silica capillary tubes obtained from Polymicro Technologies (Phoenix, AZ, USA) with 50 μm I.D. x 375 μm O.D., and 30 cm effective length and 37 cm total length.

2.2 Chemicals

The seventeen ergot alkaloids in this study were obtained from Sandoz Pharma Ltd. (Basel, Switzerland). They were dissolved in HPLC grade methanol to give a mixed stock sample solution each at a concentration of approximately 5 mg/mL. Pentachlorophenol (used as the micellar marker) was obtained from Aldrich (Milwaukee, WI, USA).

Sodium phosphate, 85% o-phosphoric acid and potassium hydroxide were obtained from Fisher Scientific (Fairlawn, NJ, USA); C_{14}TAB and C_{16}TAB surfactants were obtained from Aldrich; HPLC-grade methanol and acetonitrile were obtained from Burdick & Jackson (Muskegon, MI, USA). Millipore Milli-Q water was used to prepare all aqueous solutions.

2.3 Synthesis of Gemini Cationic Surfactants

The two Gemini cationic surfactants with alkyl chains of C12 and C14 were synthesized according to the procedures of Rosen and Song (15). Gemini-C12 and -C14 were made separately by the reaction of 22.5 mL (30.0 g, 0.235 mole) 1,3-dichloro-2-propanol (Aldrich) with 135.0 mL (105.0 g, 0.488 mole) dodecyl- or tetradecyl-N,N-dimethylamine (Albemarle Corp., Baton Rouge, LA, USA) in 95% ethanol solvent under reflux for four hours. Ethanol and excess dimethylamine were removed in a rotary evaporator under reduced pressure. The

crude Gemini surfactants were dissolved in a minimum amount of acetone, recrystallized from chloroform/acetone three times, and the solvent evaporated under vacuum to give a white solid powder.

The structures of the Gemini surfactants were confirmed using ^{1}H and ^{13}C nuclear magnetic resonance (NMR). Element analysis: (a) theory for Gemini-C12 monohydrate: C, 65.52; H, 12.32; N, 4.83; Cl, 12.36. Found: C, 64.81; H, 12.85; N, 4.82; Cl, 12.37; (b) theory for Gemini-C14 monohydrate: C, 66.74; H, 12.48; N, 4.45; Cl, 11.26. Found: C, 66.85; H, 13.06; N, 4.38; Cl, 11.24. The purity of each Gemini surfactant was determined to be more than 99% by HPLC analysis using a differential refractive index (RI) detector. For the HPLC analysis, a Waters μBondapak CN column (300 x 4 mm, 10 μm particle size) was used at 45 °C with a mobile phase containing 55% acetonitrile / 45% aqueous acetate buffer (pH 5.0) at 2.0 mL/min.

2.4 Procedure

The coating of new capillaries was removed by briefly placing the window area in a flame from a burner and then gently cleaning the burned material with a tissue dampened with methanol. New capillaries were conditioned by purging in order with 1 N potassium hydroxide solution, 0.1 N potassium hydroxide solution, degassed and filtered D.I. water, buffer

without surfactant at a concentration three times greater than running buffer, and finally BGE, each for fifteen minutes.

A stock buffer solution was prepared by mixing equimolar solutions of an acid and its sodium salt and adjusting to the appropriate pH. Final BGE solutions were prepared by mixing the stock buffer solution with the stock aqueous surfactant solution at each concentration studied, and then degassed and filtered through 0.45-μm syringe filters.

A sample solution was prepared by twenty-fold dilution of the mixed stock sample solution in methanol with the ten-fold diluted running buffers without surfactant. The sample solution was injected in the hydrodynamic mode for 2 sec. Experiments were performed at constant negative voltage of 13.5 kV.

3. Results and Discussion

The type and concentration of surfactant; the pH and ionic strength of the BGE; the type and concentration of organic additive; and temperature can influence the MECC separation. Initially, the separation of the seventeen ergot alkaloids was studied with the BGE pH 3.7 at 25 °C, but could not be achieved. Then the effect of organic additive (acetonitrile) on the migration behaviour of the seventeen ergot alkaloids were investigated. As expected, interaction between the micelles and solutes was decreased by adding acetonitrile in the BGEs

because of the increased solute solubility in the aqueous phase. Decreasing the strength of micellar interaction precluded resolution of the seventeen ergot alkaloids. This is in contrast to the separation of the eleven phenols described in Chapters 2 and 4, in which acetonitrile and/or increased temperature were absolutely necessary in order to reduce the strong interactions between the micelles and the eleven phenols, and hence to achieve baseline separation. Because the enhanced micellar interaction was needed for the separation of the seventeen ergot alkaloids, in this part of the study, no organic solvent was added in the BGEs, and the temperature was maintained as low as possible, i.e. 20 °C. The effects of the surfactant type and concentration, the pH and ionic strength of the BGE on the migration behaviour of the seventeen ergot alkaloids were examined in detail.

Pentachlorophenol and methanol were again used as micellar and electroosmotic flow (EOF) markers, respectively. The capacity factor (k') in MECC is calculated by (16, 17)

$$k' = \frac{(t_s - t_{EOF})}{t_{EOF}\left(1 - \frac{t_s}{t_{mc}}\right)} \qquad (1)$$

where t_s, t_{EOF} and t_{mc} are the migration time (sec) of the solute, the EOF marker and the micelle. The net mobility (μ_{net}) is expressed as

$$\mu_{net} = \mu_{app} - \mu_{EOF} = \frac{lL}{Vt_s} - \frac{lL}{Vt_{EOF}} = \frac{lL}{V}\left(\frac{1}{t_s} - \frac{1}{t_{ECF}}\right) \qquad (2)$$

in which μ_{app} and μ_{EOF} are apparent mobility and EOF mobility ($cm^2/V\text{-}sec$); l and L are the length (cm) of the capillary from injection to detection and the total length (cm) of the capillary, respectively; and V is the applied voltage (V). Because the EOF is in the direction opposite to that of the micelles, and is also larger, the net mobility of solute has a value less than zero.

3.1 Effect of Surfactant Type and Concentration

The type of surfactant in MECC has a major effect on the separation of solutes. The interaction between the micelles and solutes is either electrostatic or hydrophobic, or may involve both. For ionic solute, the surfactant head group and sign of the charge on the micellar head group are important. Besides, the partitioning of neutral or ionic solutes between the micelle and aqueous phase is affected by the chain length of the surfactant hydrophobic moiety.

The pK_a and pK_b of 6-methylergoline-8-carboxylic and 6-methylisoergoline-8-carboxylic are approximately 3.4 and 7.7, respectively (18), they can behave as both acids and bases, depending on the pH utilized. In this study using cationic surfactants in MECC, the BGE pH was 3.0, the carboxylic function group was partially ionized and the amine function groups were almost completely ionized, the net charges on the molecules were probably positive. Therefore these two compounds could have ionic repulsion with the positively

charged micellar head. In addition, since β-secodihydroergocristine and N-formyl-β-secodihydroergocristine are two bases and have the same charge as the micelles, they could have ionic repulsion with the micellar head as well. All of the other ergot alkaloids were non-ionic; the interaction between the micelles and the alkaloids was predominantly hydrophobic. On the other hand, the surfactant concentrations have a significant effect on the migration behaviour of the solutes because of the change in the phase ratio. The relationship between the capacity factor (k') and the surfactant concentration (C_{sf}) can be approximated as follows (16):

$$k' = K \Phi_v (C_{sf} - CMC) \qquad (3)$$

in which K is the distribution coefficient and Φ_v is the partial specific volume of the micelle. The capacity factor should be increased linearly with an increase in the surfactant concentration. However, the net mobility is usually decreased with increasing the surfactant concentration in the BGEs.

The experimental results for the seventeen ergot alkaloids are illustrated in Figures 5 to 12. As shown in the figures, for the non-aci-isomerization alkaloids (such as dihydroergocornine, dihydroergocryptine, and dihydroergocristine), the effect of increasing surfactant concentrations on the capacity factors and the net mobilities were as expected. However, the surfactant concentrations were of little and/or slight effects on the capacity factors and the net mobilities of two aci-

isomerization alkaloids (aci-dihydroergocornine and aci-α-dihydroergocryptine), and the relationship between the surfactant concentrations and the capacity factors was not linear for the Gemini surfactants, but was linear for the single chain surfactants. Whereas, for another aci-isomerization compound (aci-dihydroergocristine) the capacity factor was increased and the net mobility was decreased with increasing the surfactant concentrations; and these changes were relatively larger for the single chain surfactants than for the Gemini surfactants. Moreover, unlike the other two aci-isomerization alkaloids, for aci-dihydroergocristine the relationship between the Gemini concentration and the capacity factor was linear (the correlation coefficient, r^2, was 0.99).

The probable explanation for this behaviour lies in the structural difference between the isomers. As shown in Figure 2, the molecules of the aci-isomerization alkaloids are in a "Z"-type configuration whereas the non-aci-isomerization alkaloids are of the "U"-type. For the former conformation, the molecule is more polar, reducing the interaction with the micelles, and causing aci-dihydroergocornine and aci-α-dihydroergocryptine to migrate earlier. For the latter conformation, a strong intramolecular hydrogen bond between the cyclo hydroxyl O and the amide carboxyl oxygen O (10) can be formed to reduce the polarity of the compounds, and increase the hydrophobic interaction with the micelles. Thus the non-aci-isomerization

alkaloids migrated more slowly in a fashion dependent on the surfactant concentration. In addition, as shown in Figure 4, the molecules of the Gemini surfactants are relatively more rigid than the single chain surfactants because of the existence of 2-propanol group between the two micellar heads. This could produce a steric hindrance for the solutes to enter into the core of the micelles and could account for the non-linear relationship between the Gemini surfactant concentration and the capacity factors. The single chain surfactants also interacted weakly with the two aci-isomerization alkaloids, but no steric hindrance interfered, and hence the linear relationship was still observed between the capacity factors and the single chain surfactant concentration.

Aci-dihydroergocristine has a benzene ring in the substituent R (see Figure 3), which does not occur in the other two aci-isomerization alkaloids. Therefore, aci-dihydroergocristine is relatively more hydrophobic which linearly increases the capacity factor and decreases the net mobility with increasing the surfactant concentration. Besides, such changes were higher with the single chain surfactants than by the Gemini surfactants, again because the former had no steric hindrance.

Furthermore, in Figures 5, 7, 9 and 11 can be seen the other unexpected facts that except of the two acid and two aci-isomerization alkaloids (migrated earlier), the capacity factors

of the other ergot alkaloids using the Gemini surfactants were smaller than those using the single chain surfactants; and the capacity factors with Gemini-C12 were close to those with Gemini-C14. Since there are two alkyl chains and two functional groups for each Gemini surfactant molecule, the interactions between the micelles and the ergot alkaloids were predicted to be stronger for the Gemini surfactants than for the single chain surfactants; and the capacity factors by Gemini-C14 were supposed to be higher than those by Gemini-C12 at the same surfactant concentration. Such phenomena were observed in Chapter 4. However, because the sizes of the molecules for the ergot alkaloids are significantly larger than those studied in Chapter 4, the steric hindrance by the Gemini micelles to the ergot alkaloids could be considerably strong in this study, which could be attributed to the unexpected fact that the capacity factors of the ergot alkaloids by the Gemini surfactants were lower than those by the single chain surfactants. The reason for the closeness of the capacity factors (except the two acid and two aci-isomerization alkaloids) by Gemini-C12 and Gemini-C14 was not really clear. What can be suspected is to be addressed in the following. The aggregation number of Gemini-C14 might be larger than that of Gemini-C12 at 20 °C in this study (rather than at or over 25 °C in the previous study), and therefore the micellar numbers of Gemini-C14 could be less than those of Gemini-C12 at the same

concentration in the BGEs, which could reduce the capacity factors by Gemini-C14. However the hydrophobic phase ratio by Gemini-C14 should be larger than that by Gemini-C12 due to the longer alkyl chain, which could give the higher capacity factors by Gemini-C14. As a net result of these two effects, both Gemini-C12 and Gemini-C14 could provide the similar strength of interaction to the ergot alkaloids, which result in the closeness of the capacity factors.

From Figures 6, 8 , 10 and 12 it can be seen that the seventeen ergot alkaloids cannot be separated using the single chain surfactants no matter what the surfactant concentration. However, at 20 mM and 30 mM Gemini-C12, and at 40 mM Gemini-C14, the seventeen ergot alkaloids are resolved; and the best separation is obtained at 20 mM Gemini-C12. Besides, considering that higher surfactant concentrations could result in Joule heating, the separation at 20 mM Gemini-C12 was preferred rather than at 30 mM Gemini-C12 or 40 mM Gemini-C14.

The migration order of the seventeen ergot alkaloids is illustrated in the electropherograms in Figure 13. The fastest migrating compounds are 6-methylergoline-8-carboxylic acid and 6-methylisoergoline-8-carboxylic acid. These two compounds were of the smallest size, and could have ionic repulsion with the positive head of the micelles because they

were positively charged at pH 3.0. Therefore they migrated quickly.

Using the same 20 mM surfactant concentration with the Gemini surfactants, 6-methylergoline-8-carboxyamide and 6-methylisoergoline-8-carboxyamide migrated before aci-dihydro-ergocornine and aci-α-dihydroergocryptine; whereas, if using single chain surfactants, the opposite order was observed.

Lastly, observed were the migration of two compounds (dihydroergostine and dihydroergocristine) with a benzene ring in the substituent R (see Figure 3) due to the highest hydrophobic interaction with the micelles.

Typical values of the theoretical plate numbers using different surfactants at the same 20 mM concentration are listed in Table 2. The overall highest efficiency is found for Gemini-C12. However, if considering only the isomer separation, the slightly higher resolution between 6-Methylergoline-8-carboxamide and 6-Methylisoergoline-8-carboxamide, and between 6-Methylisoergoline-8-carboxamide and aci-dihydro-ergocornine was obtained using Gemini-C14 than Gemini-C12 as shown in Table 3 and Figure 14 of the electropherograms for the separations of the alkaloid isomers. As mentioned above, Gemini-C12 and Gemini-C14 could provide the similar strength of micellar interaction to the ergot alkaloids (except the two

acid and two aci-isomerization alkaloids). However, the individual interaction between each solute and the micelle still could be slightly different for each surfactant, which could cause the slightly different selectivity and hence the resolution.

3.2 Effect of BGE pH with Gemini-C12

The BGE pH is a critical factor in MECC for ionizable solutes. The variation of the EOF mobility with pH is shown in Figure 15. A similar observation was found in the previous study. An explanation was presented in Chapter 2 based on the changes of the net charge density on the capillary surface as a function of the BGE pH. For MECC with a cationic surfactant, a low pH (< 3.0) results in a smaller EOF, and thus the longer analysis time and the lower efficiency. However, the separation might not be successful at relatively high pH (~ 4.5) due to the high EOF and hence the fast migration and possibly the low resolution.

If the solutes are ionizable weak acids or bases, it can be expected that changes in the BGE pH will greatly affect the overall charge of the solute and thus its electrophoretic mobility and its hydrophobicity / hydrophilicity. Consequently, the capacity factors and the net mobilities, as well as the selectivity and the efficiency are affected. Since the changes in pH should affect each ionizable solute differently, the separations could be manipulated by changing the BGE pH. Figures 16 and 17

demonstrate the dependence of the capacity factors and the net mobilities on the BGE pH for the seventeen ergot alkaloids. The best separation could be achieved with the BGEs at pH 3.0.

3.3 Effect of Ionic Strength in BGEs with Gemini-C12

The capacity factors and the net mobilities as a function of ionic strength are plotted in Figures 18 and 19. An increase of ionic strength in the BGE induced a more "polar" aqueous medium because the dielectric constant of the BGE was increased. Therefore the hydrophobic alkaloids (migrated later) preferentially dissolved into the micelles, and then the capacity factors were enhanced. It was also interestingly found that the net mobility of the micelles was significantly increased with increasing the ionic strength, and hence making the net mobilities of the later-eluting alkaloids to be increased due to their micellar dependence by the hydrophobic interaction. With an increase in the ionic strength in BGEs, the CMC would be reduced and the aggregation number could be changed. It was most likely that the aggregation number was increased and therefore the average micellar size was increased, causing the electrophoretic mobility of the micelle to be decreased, and the net mobility to be increased (both have the same absolute values but have the opposite directions). Besides, as the ionic strength of the BGEs was increased there was a decrease in the EOF. The linear dependence of the EOF mobility on the

logarithm of phosphate concentration is demonstrated in Figure 20. As the EOF decreasing, the migration time was increased, the alkaloids were better separated. However, the low EOF at high ionic strength could result in an excessively long run time. Moreover, the high ionic strength and the subsequent high conductivity could result in the high current, and eventually the Joule heat, therefore the separation using 50 mM phosphate (pH 3.0) was preferable. The decrease in the EOF with increasing the BGE ionic strength is well documented (19, 20) and is attributed to a decrease in the zeta potential due to compression of the electrical double-layer. The influence of ionic strength on the current is given in Figure 21. The linear relationship was found with the phosphate concentration changing from 10 mM to 75 mM.

4. Conclusions

Two novel Gemini cationic surfactants (Gemini-C12 and Gemini-C14) were synthesized and the application to MECC for indicating purity and stability of dihydroergotoxine was investigated. For comparison, the single chain surfactants were applied in MECC for the separation as well. The best separation for the seventeen ergot alkaloids was achieved within eight minutes using a 30 cm effective length (37 cm total length) fused-silica capillary with a BGE consisting of 50 mM phosphate (pH 3.0) and 20 mM Gemini-C12 at a negative

voltage of 13.5 kV. However, if only considering the separations of the alkaloid isomers, the separation by Gemini-C14 was preferred rather than by Gemini-C12 due to the overall high resolutions. However, such separations were unable to be obtained by MECC with the single alkyl chain cationic surfactants. There is no any impurity profile method for dihydroergotoxine mesylates (or ergoloid mesylates) in the USP. The method developed here should be successfully validated to be adopted as a USP monograph in the future.

Table 1

Seventeen Ergot Alkaloids for Dihydroergotoxine Impurity Profile

I.D. No.	Compounds
(1)	6-Methylisoergoline-8-carboxylic acid
(2)	6-Methylergoline-8-carboxylic acid
(3)	6-Methylergoline-8-carboxamide
(4)	6-Methylisoergoline-8-carboxamide
(5)	Aci-Dyhydroergocornine
(6)	α-Aci-Dyhydroergocryptine
(7)	Aci-Dihydroergocristine
(8)	β-Secodihydroergocristine
(9)	N-Formyl-β-Secodihydroergocristine
(10)	12-Ethoxydihydroergocornine
(11)	Dihydroergocornine
(12)	12-Ethoxydihydroergocryptine Mixture (α+β)
(13)	Dihydroergoptine
(14)	α-Dihydroergocryptine
(15)	β-Dihydroergocryptine
(16)	Dihydroergostine
(17)	Dihydroergocristine

Table 2

Theoretical Plate Number by 20 mM of Each Surfactant

No.	Compounds	*Gemini-C12*	*Gemini-C14*	*C14TAB*	*C16TAB*
1	6-Methylisoergoline-8-carboxylic Acid	100800	135400	135300	145800
2	6-Methylergoline-8-carboxylic Acid	107800	144000	139300	151400
3	6-Methylergoline-8-carboxamide	176600	147800	132100	152500
4	6-Methylisoergoline-8-carboxamide	181600	151300	128300	162800
5	Aci-Dihydroergocornine	131200	119500	124800	132200
6	α-Aci-Dihydroergocryptine	134400	116800	129400	128200
7	Aci-Dihydroergocristine	181300	163500	122100	180400
8	B-Secodihydroergocristine	183600	131900	93760	114200
9	N-Formyl-B-Secodihydroergocristine	180300	110200	67690	102000
10	12-Ethoxydihydroergocornine	147400	126000	126000	140000
11	Dihydroergocornine	206000	130700	69710	145700
12	12-Ethoxydihydroergocryptine Mix (α+β)	130300	N/A	N/A	173300
13	Dihydroergoptine	176900	N/A	105000	N/A
14	α-Dihydroergocryptine	165900	142500	N/A	N/A
15	β-Dihydroergocryptine	200400	166000	111500	173700
16	Dihydroergostine	209900	148700	111800	165200
17	Dihydroergocristine	202800	154500	110900	164400

Note: N / A is not applicable due to co-eluting.

Table 3

Resolution of the Ergot Alkaloid Isomers by 20 mM of Each Surfactant

No.	Compound Pairs	*Gemini-C12*	*Gemini-C14*	*C14TAB*	*C16TAB*
1	6-Methylergoline- / 6-Methylisoergoline-8-carboxylic Acid	2.69	2.73	1.05	1.39
3	6-Methylergoline- / 6-Methylisoergoline-8-carboxamide	1.98	2.34	4.14	5.10
4	6-Methylisoergoline-8-carboxamide / Aci-Dihydroergocornine	1.86	2.04	N / A	N / A
5	6-Methylergoline-8-carboxamide / α-Aci-Dihydroergocryptine	N / A	N / A	1.25	5.47
6	Aci-Dihydroergocornine / α-Aci-Dihydroergocryptine	2.46	2.61	2.51	2.50
7	α-Aci-Dihydroergocryptine / Aci-Dihydroergocristine	2.20	5.39	N / A	N / A

Note: N / A is not applicable due to non-adjacent pair of compounds.

Figure Captions:

Figure 1: Structures of lysergic acid, isolysergic acid, lysergic acid amide and isolysergic acid amide.

Figure 2: Structures of ergot peptide alkaloids and their aci isomerizations.

Figure 3: Structures of the studied seventeen ergot alkaloids.

Figure 4: Structures of the cationic surfactants.

Figure 5: Effect of Gemini-C12 concentrations on the capacity factors with BGEs containing 50 mM phosphate (pH 3.0).

Figure 6: Effect of Gemini-C12 concentrations on the net mobilities with BGEs containing 50 mM phosphate (pH 3.0).

Figure 7: Effect of Gemini-C14 concentrations on the capacity factors with BGEs containing 50 mM phosphate (pH 3.0).

Figure 8: Effect of Gemini-C14 concentrations on the net mobilities with BGEs containing 50 mM phosphate (pH 3.0).

Figure 9: Effect of C_{14}TAB concentrations on the capacity factors with BGEs containing 50 mM phosphate (pH 3.0).

Figure 10: Effect of C_{14}TAB concentrations on the net mobilities with BGEs containing 50 mM phosphate (pH 3.0).

Figure 11: Effect of C_{16}TAB concentrations on the capacity factors with BGEs containing 50 mM phosphate (pH 3.0).

Figure 12: Effect of C_{16}TAB concentrations on the net mobilities with BGEs containing 50 mM phosphate (pH 3.0).

Figure 13: Electropherograms of the seventeen ergot alkaloids with BGEs containing 50 mM phosphate (pH 3.0) and 20 mM each surfactant. (a) Gemini-C12, (b) Gemini-C14, (c) C_{14}TAB and (d) C_{16}TAB. See Table 1 for the identification.

Figure 14: Electropherograms of the alkaloid isomers with BGEs containing 50 mM phosphate (pH 3.0) and 20 mM each surfactant. (a) Gemini-C12, (b) Gemini-C14, (c) C_{14}TAB and (d) C_{16}TAB. See Table 1 for the identification.

Figure 15: Effect of BGE pH on the EOF mobility with BGEs containing 50 mM phosphate and 20 mM Gemini-C12.

Figure 16: Effect of BGE pH on the capacity factors with BGEs containing 50 mM phosphate and 20 mM Gemini-C12.

Figure 17: Effect of BGE pH on the net mobilities with BGEs containing 50 mM phosphate and 20 mM Gemini-C12.

Figure 18: Effect of the phosphate concentrations on the capacity factors with BGEs containing 50 mM phosphate (pH 3.0) and 20 mM Gemini-C12.

Figure 19: Effect of the phosphate concentrations on the net mobilities with BGEs containing 50 mM phosphate (pH 3.0) and 20 mM Gemini-C12.

Figure 20: Effect of the phosphate concentrations on the EOF mobilities with BGEs containing 50 mM phosphate (pH 3.0) and 20 mM Gemini-C12.

Figure 21: Effect of the phosphate concentrations on the current with BGEs containing 50 mM phosphate (pH 3.0) and 20 mM Gemini-C12.

Figure 1

Lysergic Acid

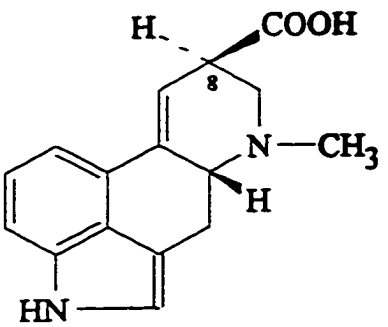

Isolysergic Acid

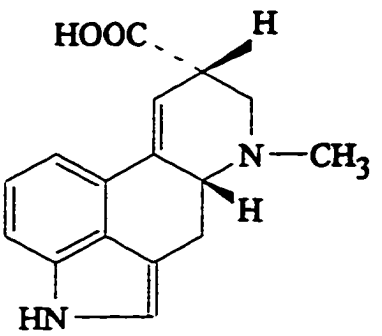

Lysergic Acid Amide

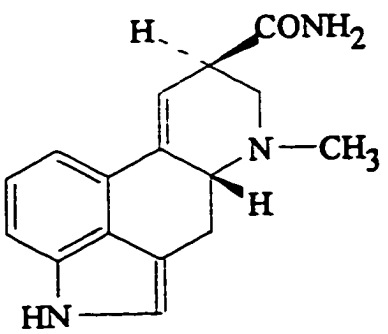

Isolysergic Acid Amide

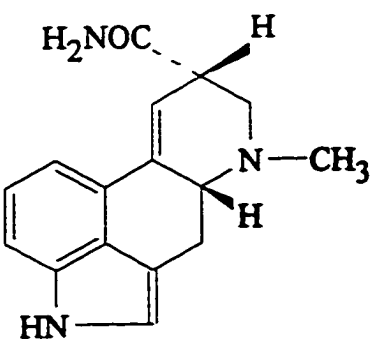

Figure 2

Ergot Peptide Alkaloids

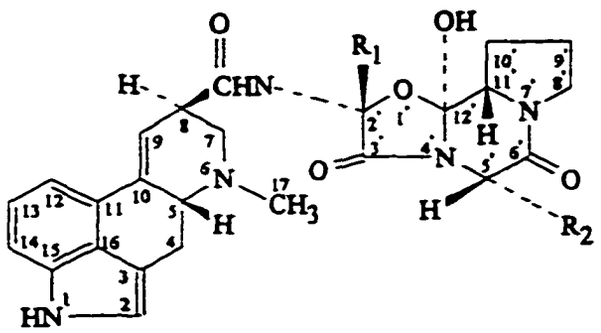

R_1 / R_2	Ergotamine Group	Ergoxine Group	Ergotoxine Group
	CH_3	CH_2CH_3	$CH(CH_3)_2$
$CH(CH_3)_2$	Ergovaline	Ergonine	Ergocornine
$CH_2CH(CH_3)_2$	Ergosine	Ergoptine	Ergocryptine
$CH(CH_3)CH_2CH_3$	β-Ergosine	β-Ergoptine	β-Ergocryptine
$CH_2C_6H_5$	Ergotamine	Ergostine	Ergocristine

Ergot Peptide Alkaloids in Aci-Isomerization

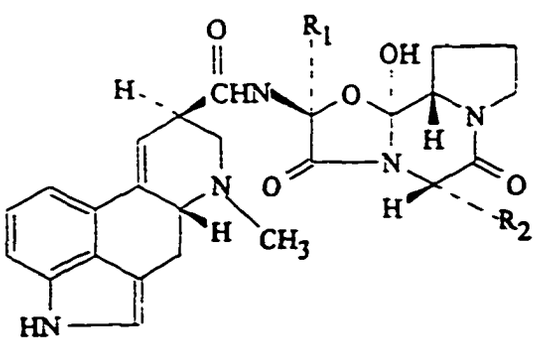

Figure 3

6-Methylergoline-8-carboxylic Acid

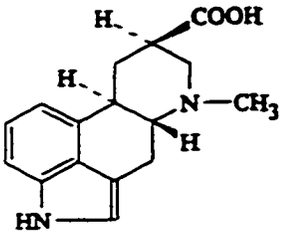

6-Methylisoergoline-8-carboxylic Acid

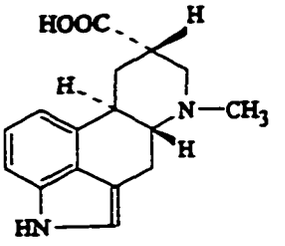

6-Methylergoline-8-carboxamide

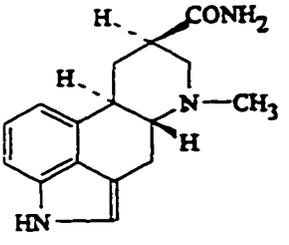

6-Methylisoergoline-8-carboxamide

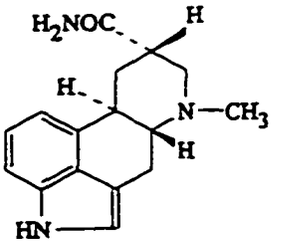

Dihydroergotoxine

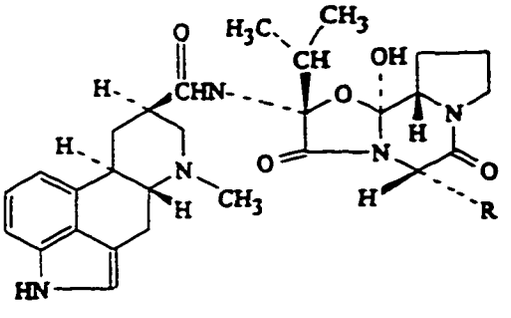

R = $CH(CH_3)_2$,	Dihydroergocornine
$CH_2C_6H_5$,	Dihydroergocristine
$CH_2CH(CH_3)_2$,	Dihydro-α-ergocryptine
$CH(CH_3)CH_2CH_3$,	Dihydro-β-ergocryptine

Aci Dihydroergotoxine

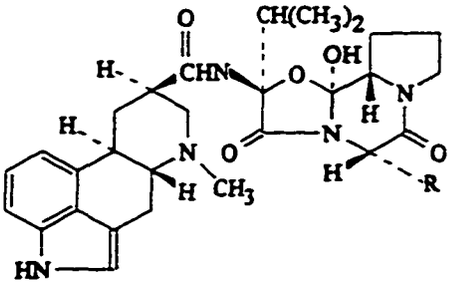

R = $CH(CH_3)_2$,	Aci-Dihydroergocornine
$CH_2C_6H_5$,	Aci-Dihydroergocristine
$CH_2CH(CH_3)_2$,	Aci-Dihydro-α-ergocryptine

Figure 3 (continued)

Dihydroergoxine

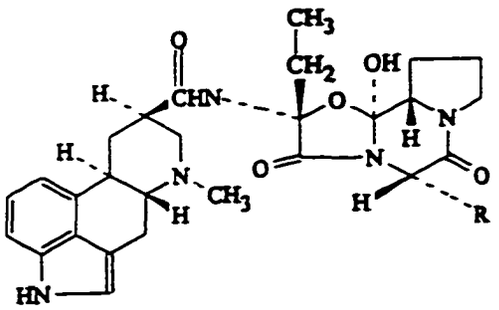

R = $CH_2C_6H_5$, Dihydroergostine
$CH_2CH(CH_3)_2$, Dihydroergoptine

Oxidation Products of Dihydroergocristine

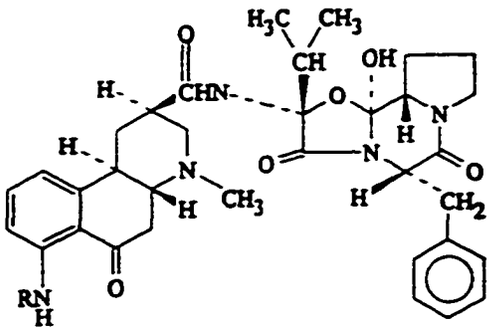

R = CHO, N-Formyl-β-Secodihydroergocristine
H, β-Secodihydroergocristine

12-Ethoxydihydroergocornine

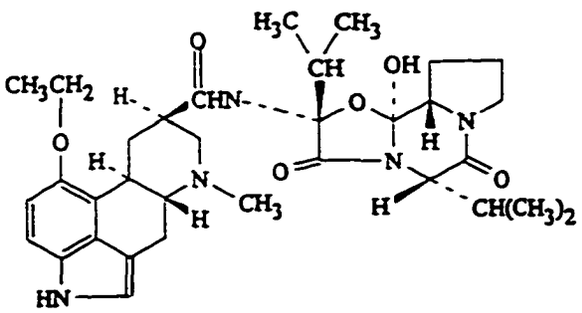

12-Ethoxydihydroergocryptine Mixture (α + β)

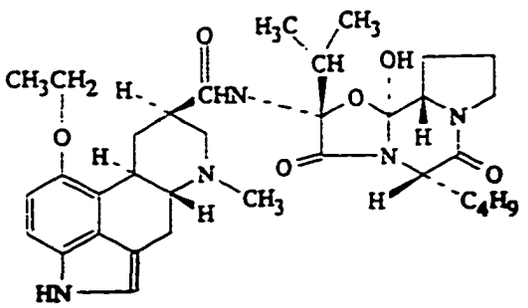

Figure 4

Gemini Surfactants

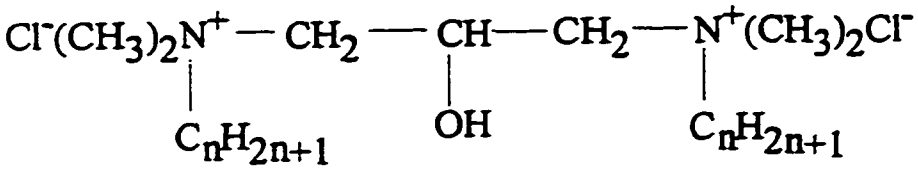

n = 12, Gemini-C_{12}

14, Gemini-C_{14}

Single Chain Surfactants

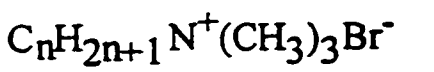

n = 14, C_{14}TAB

= 16, C_{16}TAB

Figure 5

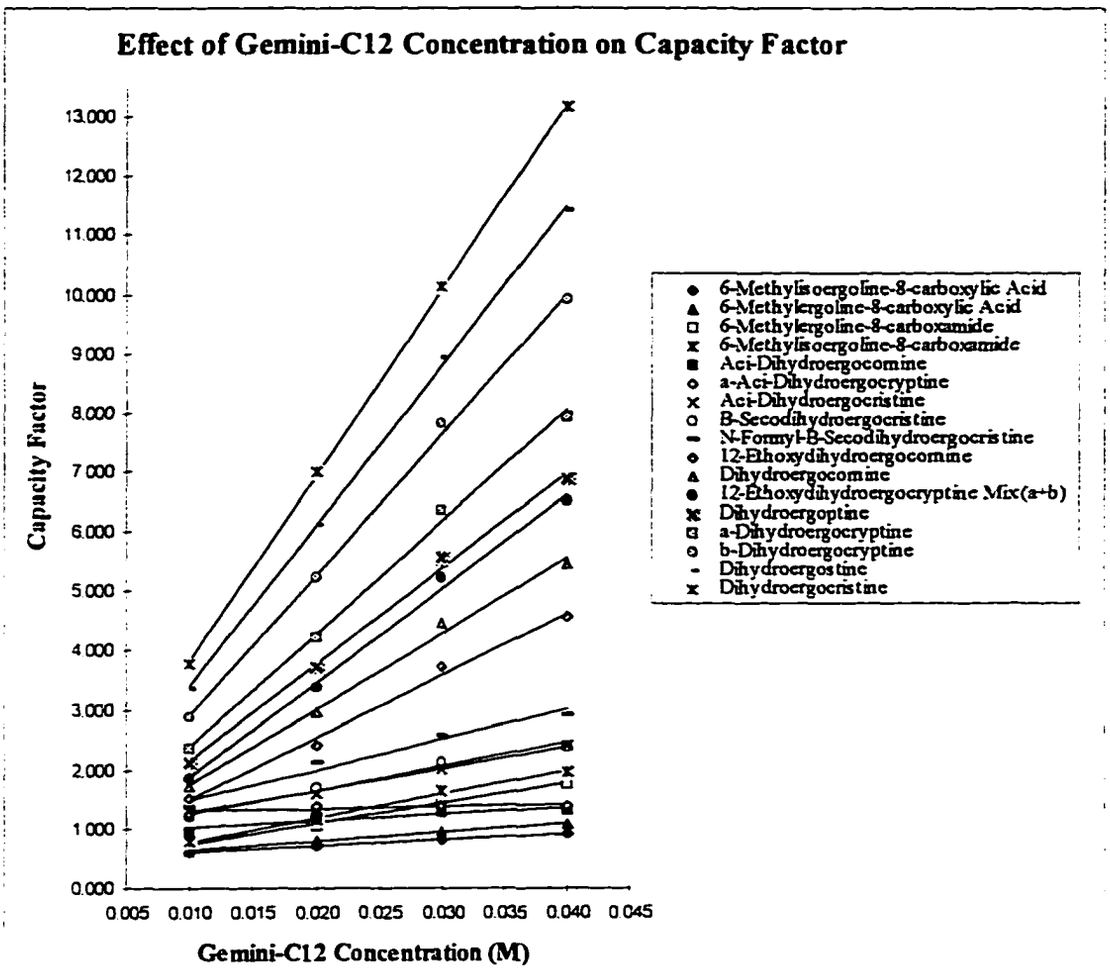

No.	Compounds	*RSQ*	*Slope*	*Intercept*
1	6-Methylisoergoline-8-carboxylic Acid	1.00	10.47	0.50
2	6-Methylergoline-8-carboxylic Acid	1.00	14.98	0.49
3	6-Methylergoline-8-carboxamide	0.99	34.57	0.40
4	6-Methylisoergoline-8-carboxamide	0.99	40.84	0.36
5	Aci-Dihydroergocornine	0.85	11.98	0.89
6	α-Aci-Dihydroergocryptine	0.58	3.86	1.27
7	Aci-Dihydroergocristine	0.99	36.82	0.92
8	β-Secodihydroergocristine	0.98	39.77	0.87
9	N-Formyl-β-Secodihydroergocristine	0.96	51.10	0.97
10	12-Ethoxydihydroergocornine	0.99	103.95	0.46
11	Dihydroergocornine	1.00	126.88	0.48
12	12-Ethoxydihydroergocryptine Mix (α+β)	1.00	157.55	0.31
13	Dihydroergoptine	1.00	160.80	0.55
14	α-Dihydroergocryptine	1.00	187.95	0.52
15	β-Dihydroergocryptine	1.00	236.15	0.55
16	Dihydroergostine	1.00	268.84	0.73
17	Dihydroergocristine	1.00	312.88	0.69

Figure 6

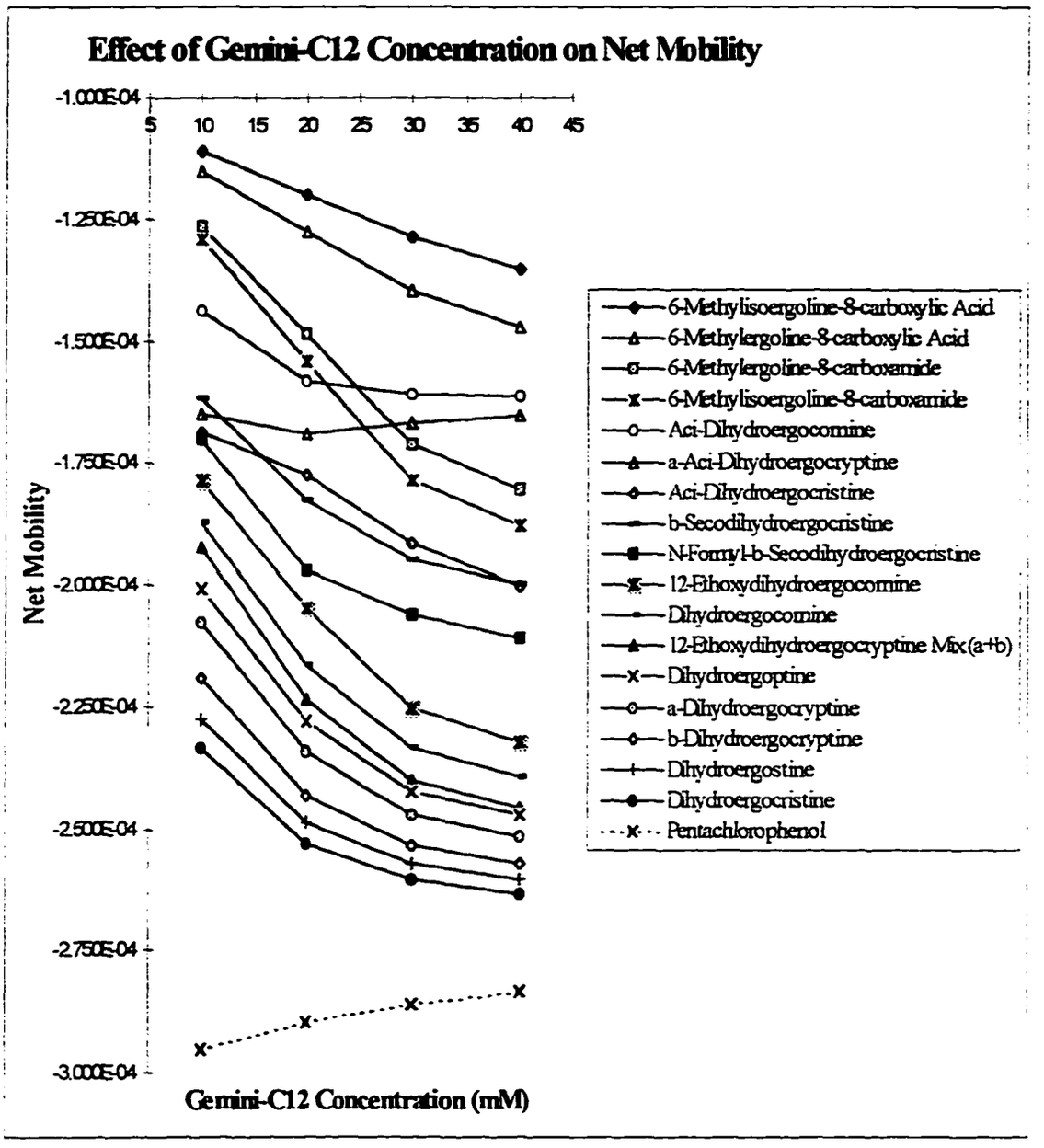

Figure 7

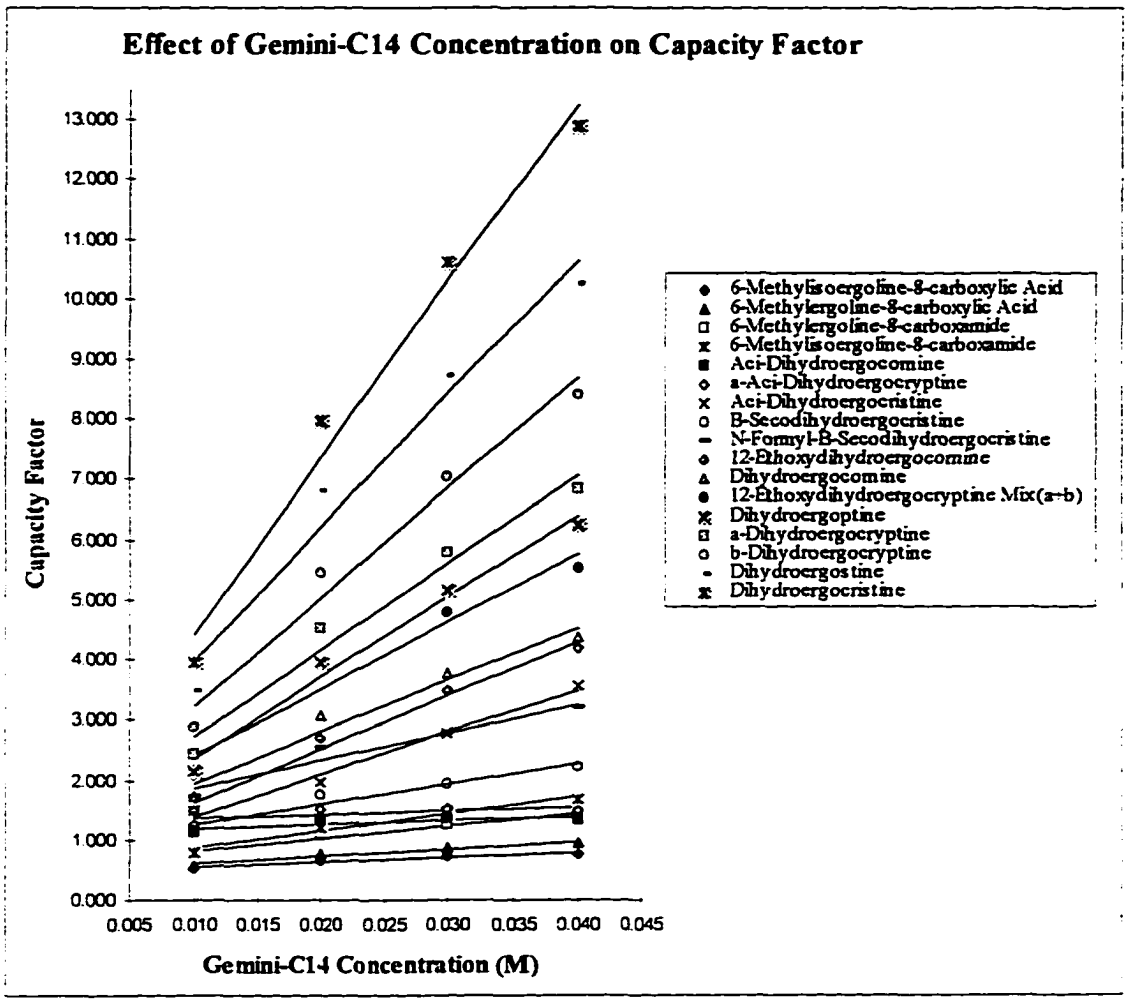

No.	Compounds	*RSQ*	*Slope*	*Intercept*
1	6-Methylisoergoline-8-carboxylic Acid	0.96	8.02	0.47
2	6-Methylergoline-8-carboxylic Acid	0.97	12.27	0.48
3	6-Methylergoline-8-carboxamide	0.96	20.87	0.60
4	6-Methylisoergoline-8-carboxamide	0.98	28.97	0.56
5	Aci-Dihydroergocornine	0.64	7.03	1.11
6	α-Aci-Dihydroergocryptine	0.50	6.61	1.28
7	Aci-Dihydroergocristine	0.99	69.93	0.69
8	β-Secodihydroergocristine	0.94	33.50	0.93
9	N-Formyl-β-Secodihydroergocristine	0.94	46.27	1.39
10	12-Ethoxydihydroergocornine	0.98	88.82	0.74
11	Dihydroergocornine	0.96	86.85	1.06
12	12-Ethoxydihydroergocryptine Mix (α+β)	0.94	112.07	1.28
13	Dihydroergoptine	0.98	133.84	1.03
14	α-Dihydroergocryptine	0.97	144.45	1.27
15	β-Dihydroergocryptine	0.98	182.15	1.39
16	Dihydroergostine	0.97	221.94	1.75
17	Dihydroergocristine	0.98	294.15	1.48

Figure 8

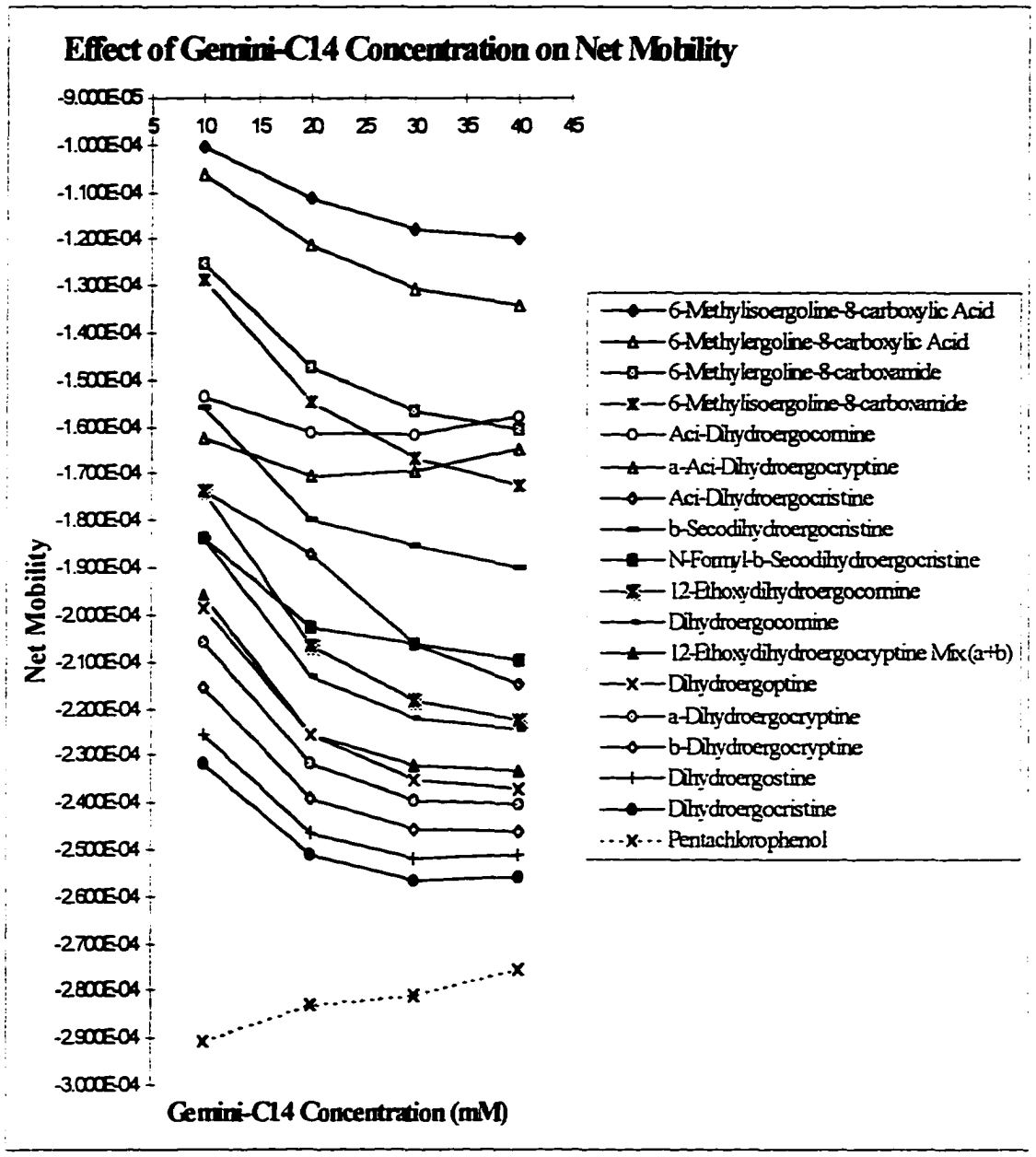

Figure 9

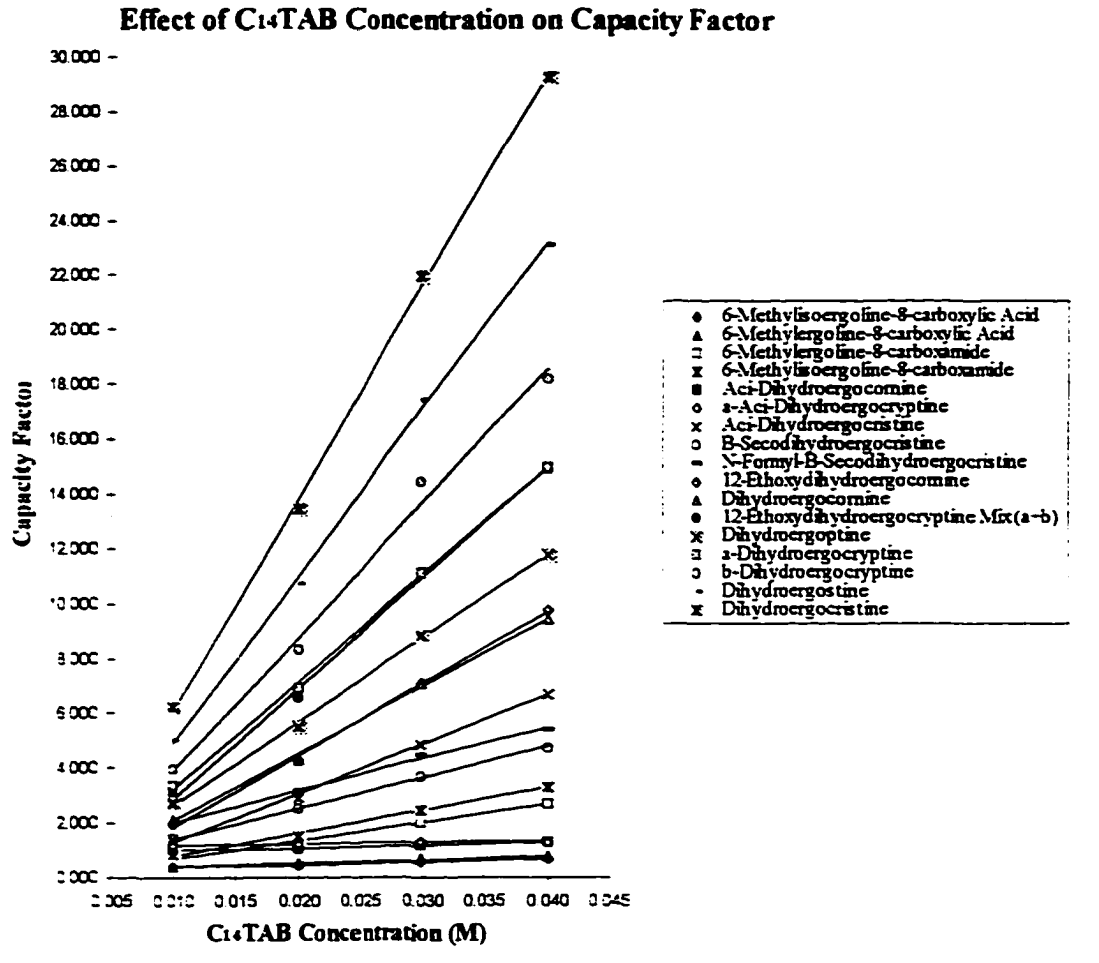

No.	Compounds	*RSQ*	*Slope*	*Intercept*
1	6-Methylisoergoline-8-carboxylic Acid	1.00	10.06	0.27
2	6-Methylergoline-8-carboxylic Acid	1.00	13.49	0.23
3	6-Methylergoline-8-carboxamide	1.00	65.55	0.03
4	6-Methylisoergoline-8-carboxamide	1.00	83.44	-0.07
5	Aci-Dihydroergocornine	0.99	8.93	0.90
6	α-Aci-Dihydroergocryptine	0.98	4.88	1.12
7	Aci-Dihydroergocristine	1.00	179.50	-0.52
8	β-Secodihydroergocristine	1.00	112.88	0.26
9	N-Formyl-β-Secodihydroergocristine	1.00	116.04	0.85
10	12-Ethoxydihydroergocornine	1.00	261.07	-0.75
11	Dihydroergocornine	1.00	246.34	-0.42
12	12-Ethoxydihydroergocryptine Mix (α+β)	1.00	403.93	-1.19
13	Dihydroergoptine	1.00	305.23	-0.42
14	α-Dihydroergocryptine	1.00	391.00	-0.70
15	β-Dihydroergocryptine	0.99	488.23	-0.99
16	Dihydroergostine	1.00	608.71	-1.16
17	Dihydroergocristine	1.00	777.27	-1.71

Figure 10

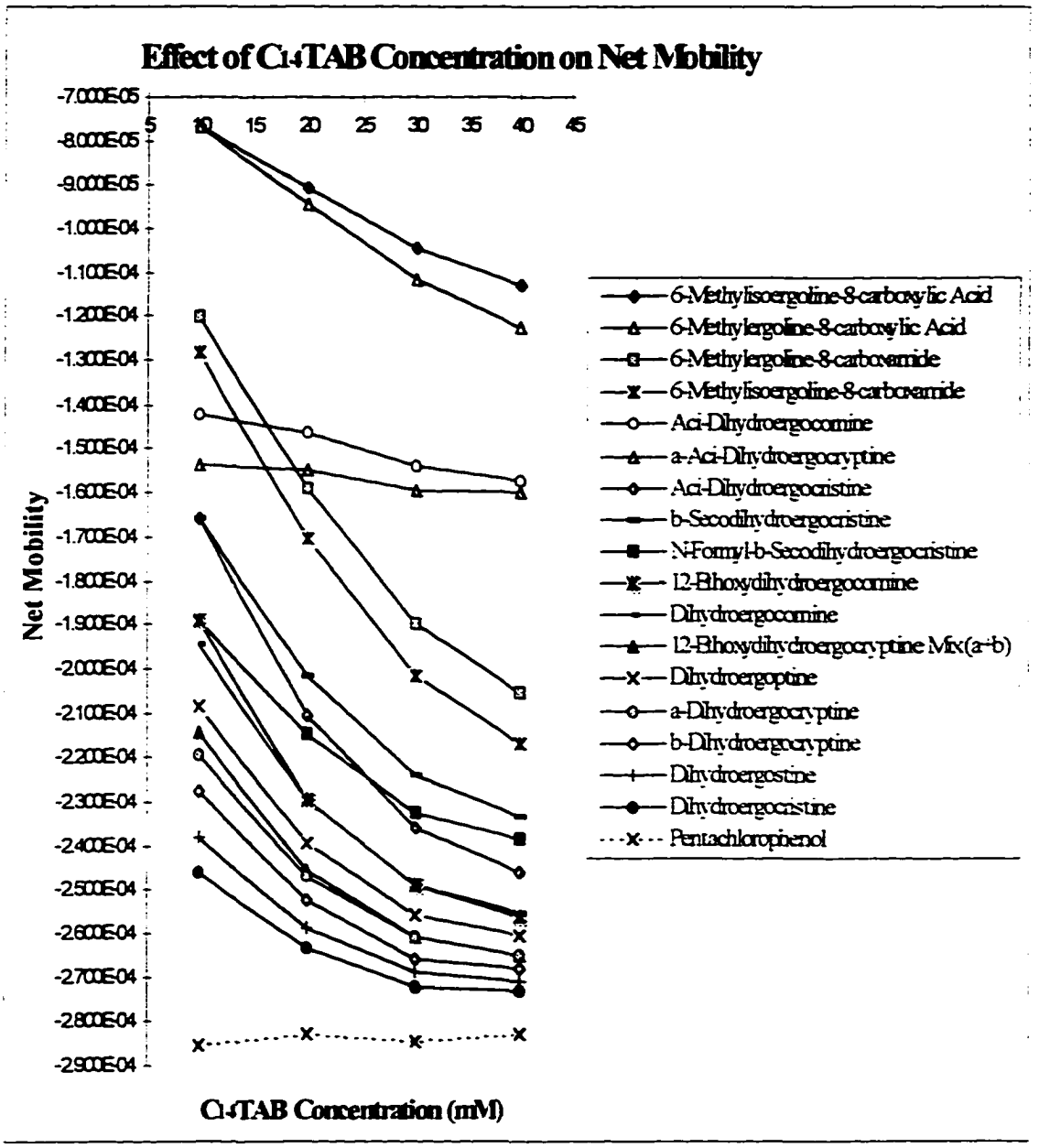

Figure 11

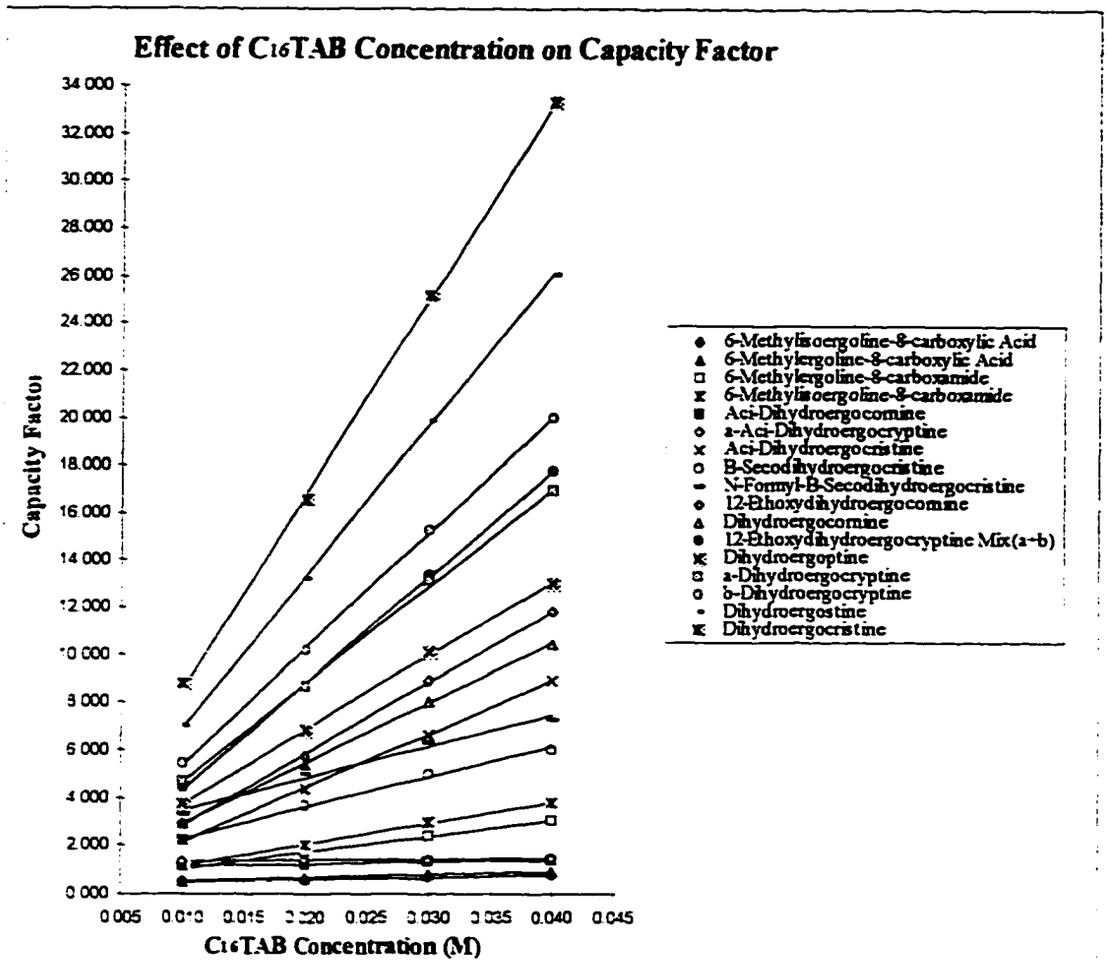

No.	Compounds	*RSQ*	*Slope*	*Intercept*
1	6-Methylisoergoline-8-carboxylic Acid	1.00	8.82	0.40
2	6-Methylergoline-8-carboxylic Acid	1.00	12.48	0.36
3	6-Methylergoline-8-carboxamide	1.00	67.95	0.33
4	6-Methylisoergoline-8-carboxamide	1.00	88.61	0.28
5	Aci-Dihydroergocornine	1.00	7.23	1.08
6	α-Aci-Dihydroergocryptine	0.97	3.03	1.31
7	Aci-Dihydroergocristine	1.00	224.48	-0.08
8	β-Secodihydroergocristine	0.99	127.39	1.03
9	N-Formyl-β-Secodihydroergocristine	0.99	134.32	2.11
10	12-Ethoxydihydroergocornine	1.00	300.12	-0.16
11	Dihydroergocornine	1.00	252.76	0.36
12	12-Ethoxydihydroergocryptine Mix (α+β)	1.00	447.10	-0.14
13	Dihydroergoptine	1.00	311.70	0.62
14	α-Dihydroergocryptine	1.00	412.22	0.54
15	β-Dihydroergocryptine	0.99	487.80	0.52
16	Dihydroergostine	1.00	636.58	0.61
17	Dihydroergocristine	1.00	821.25	0.41

Figure 12

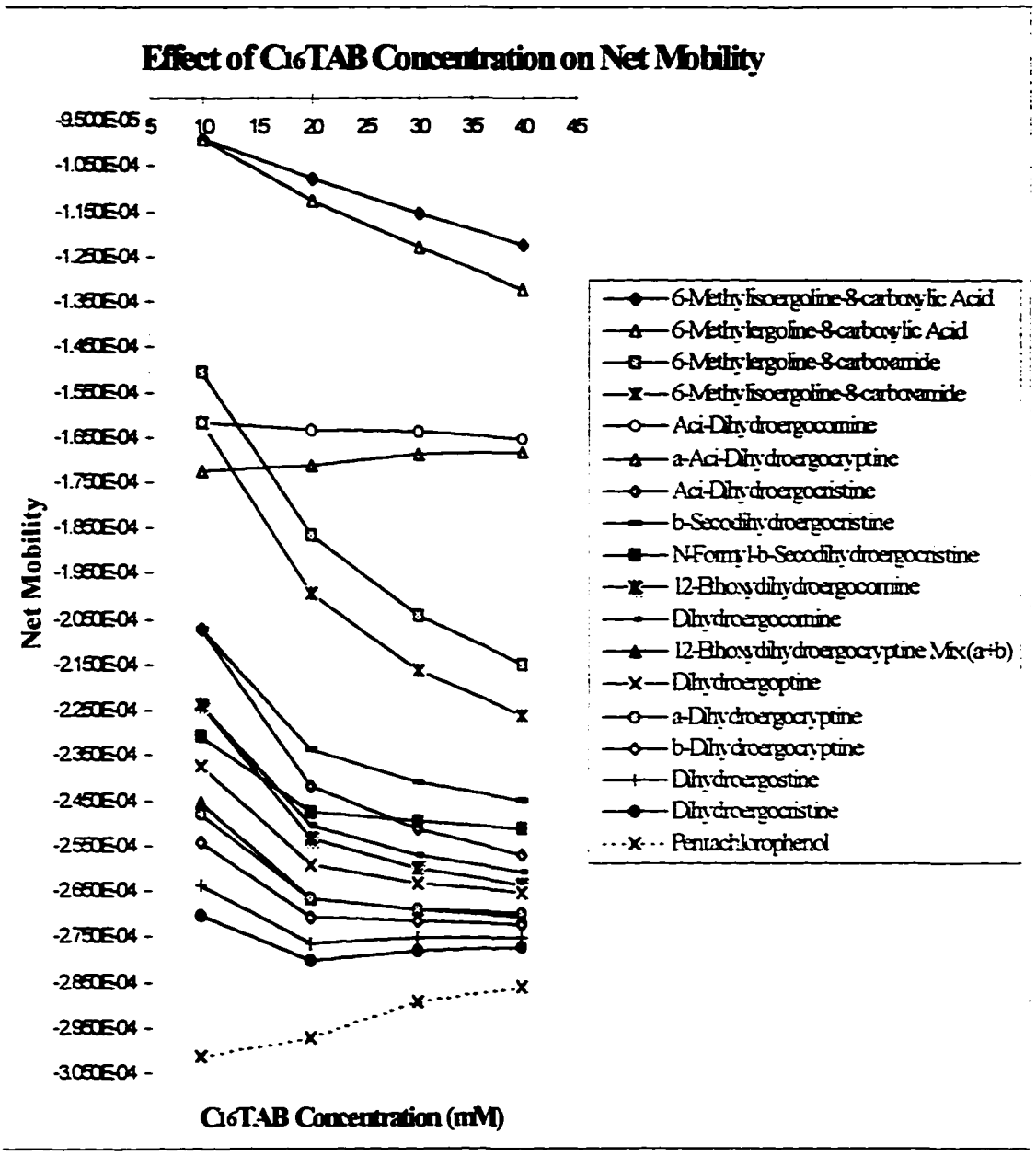

Figure 13

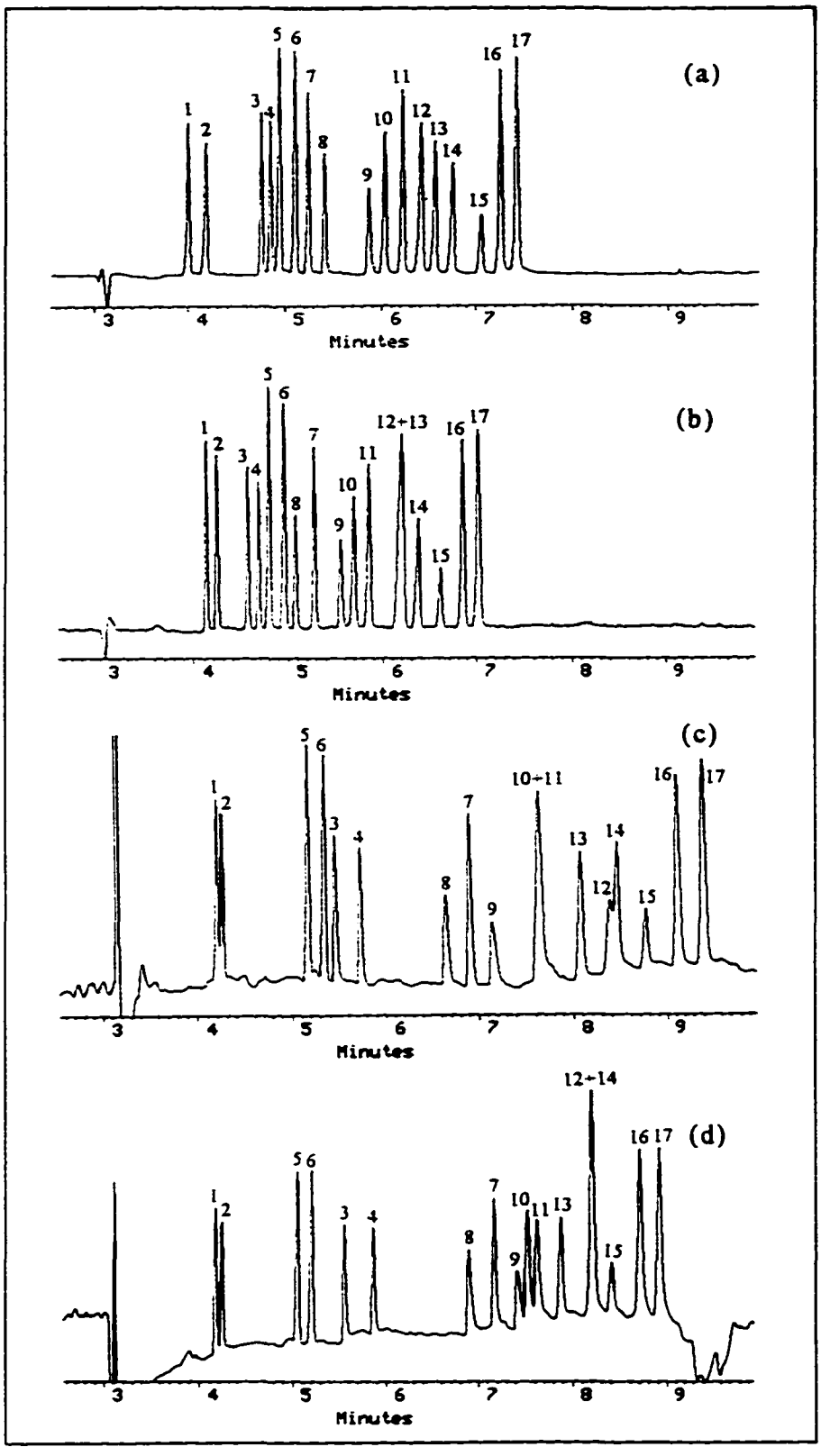

Figure 14

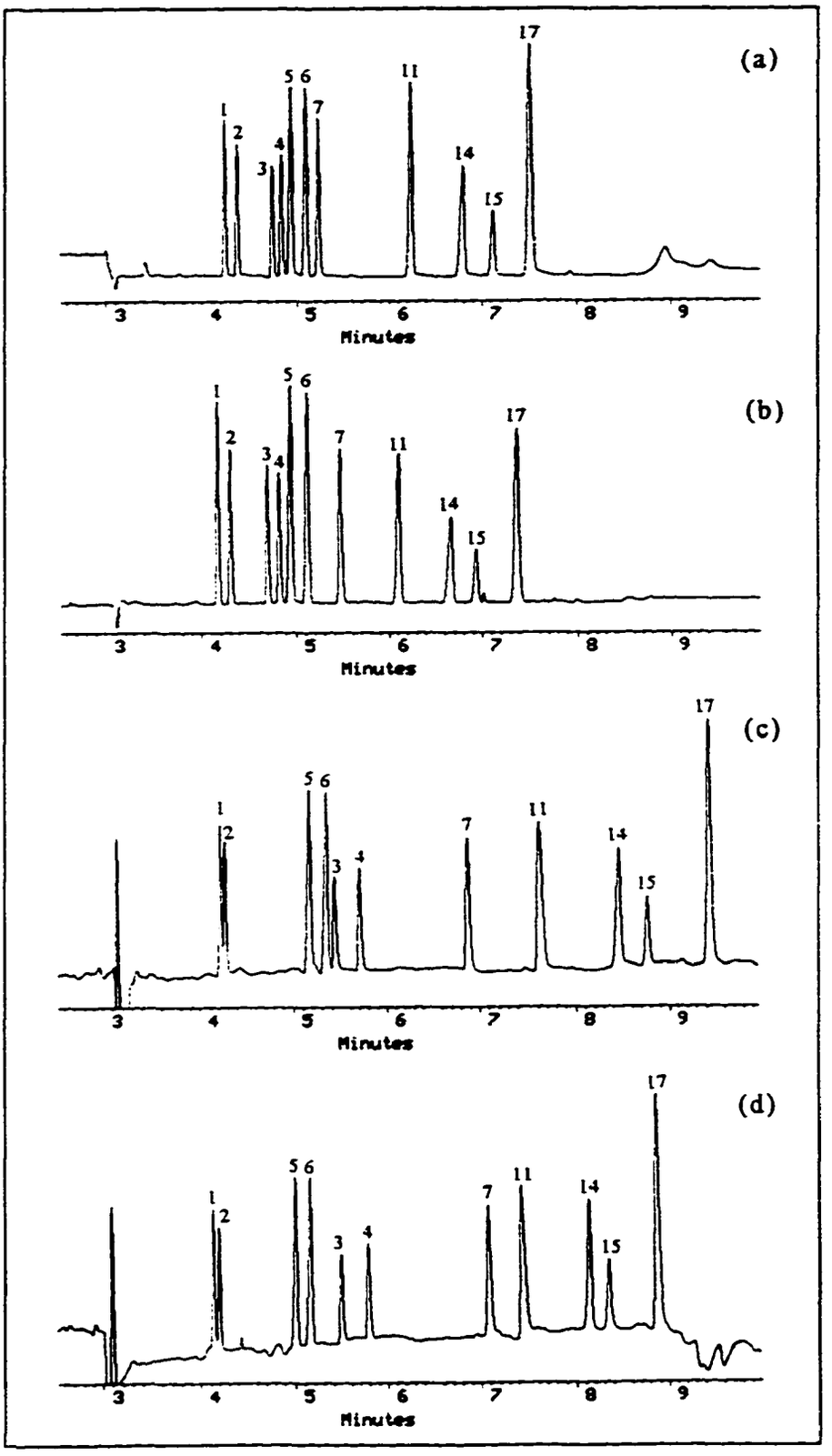

Figure 15

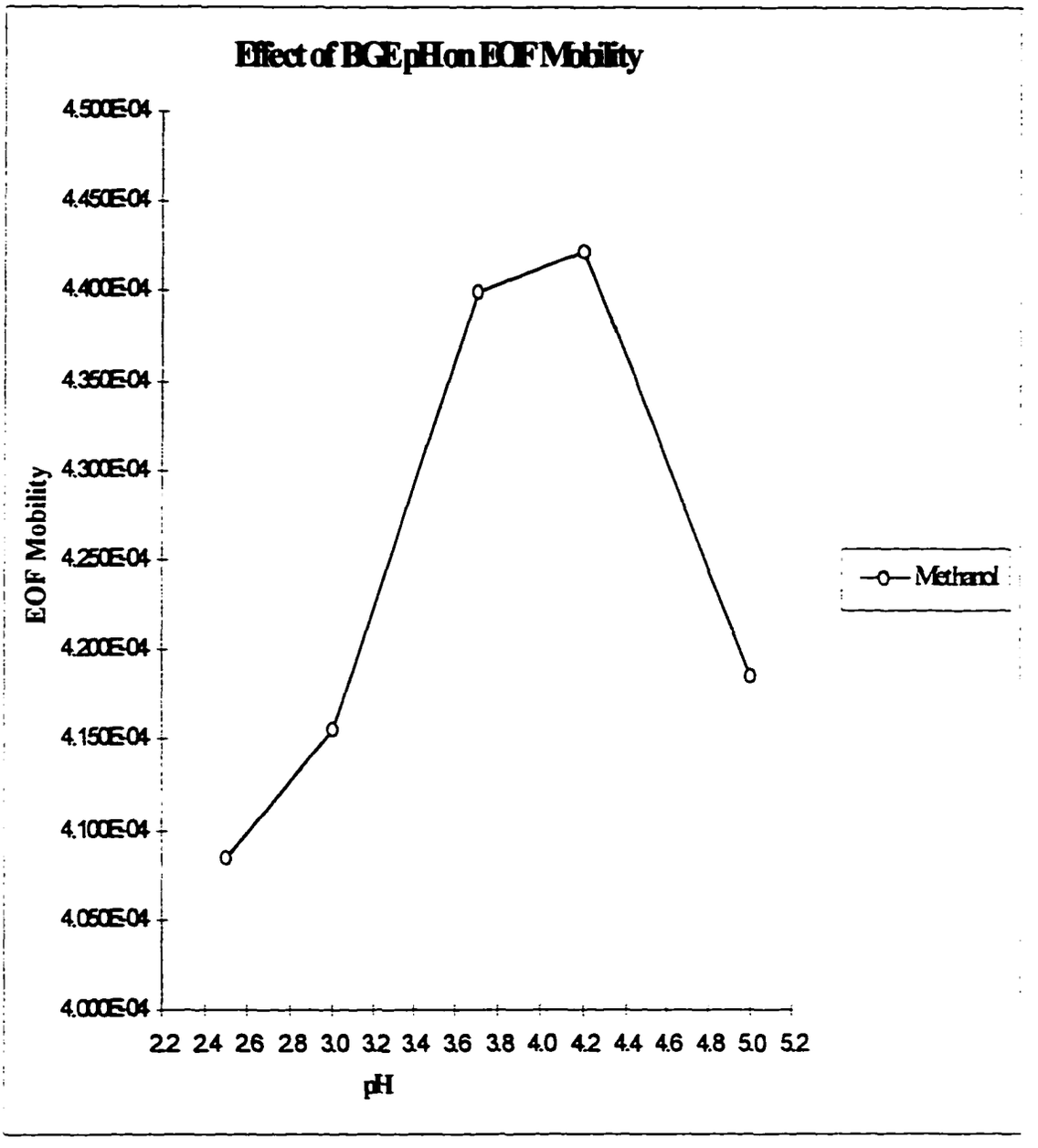

Figure 16

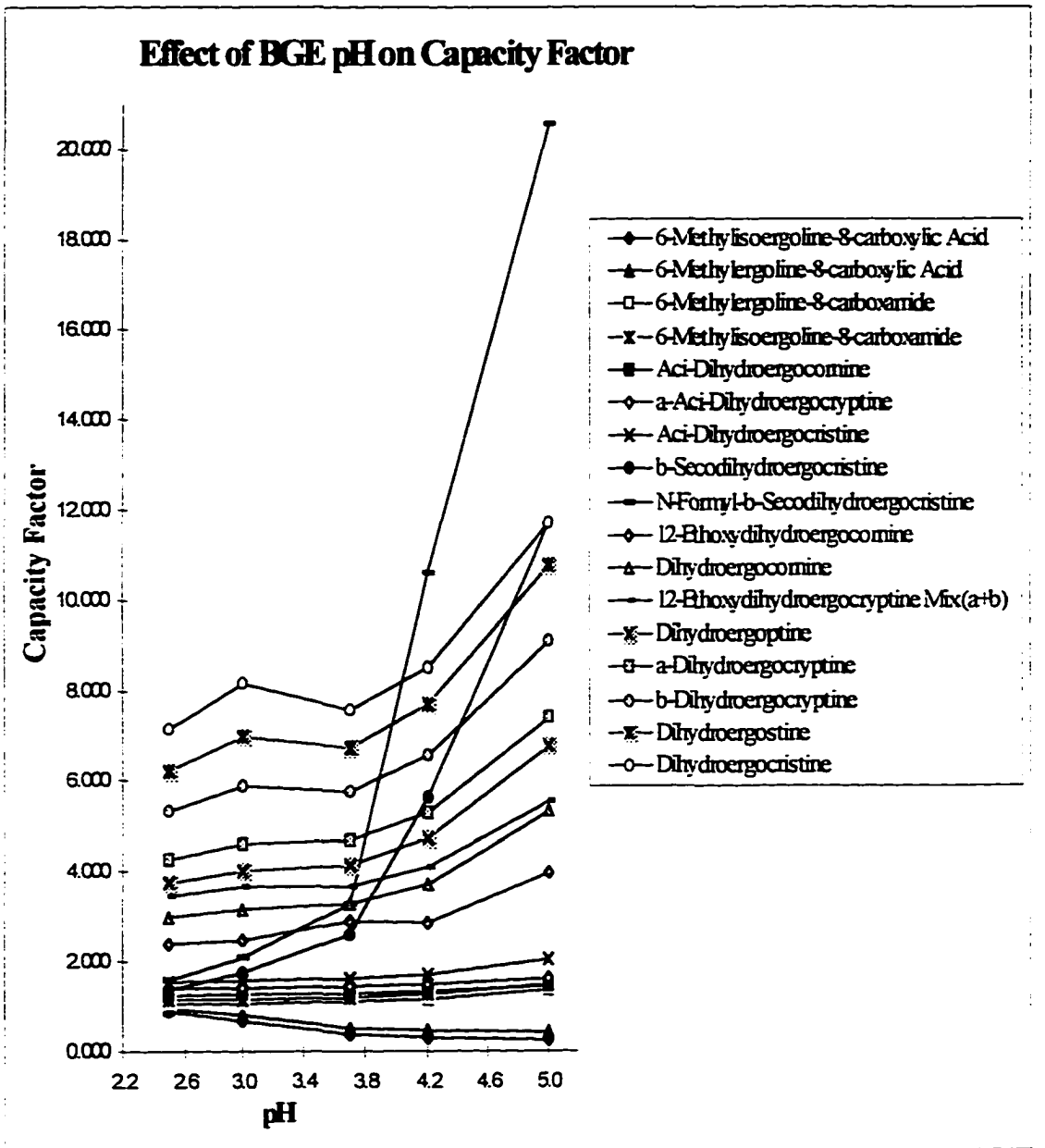

Figure 17

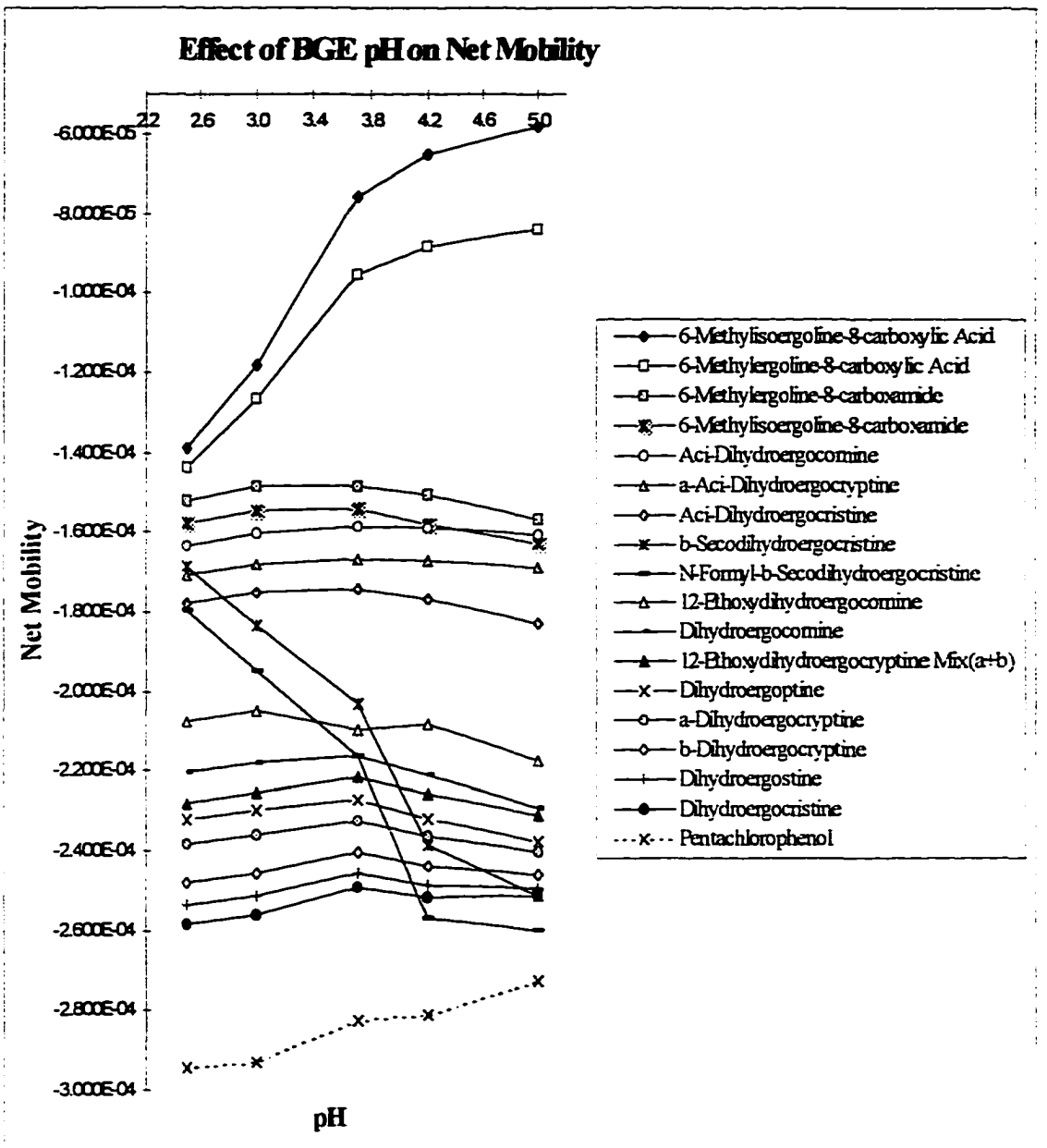

Figure 18

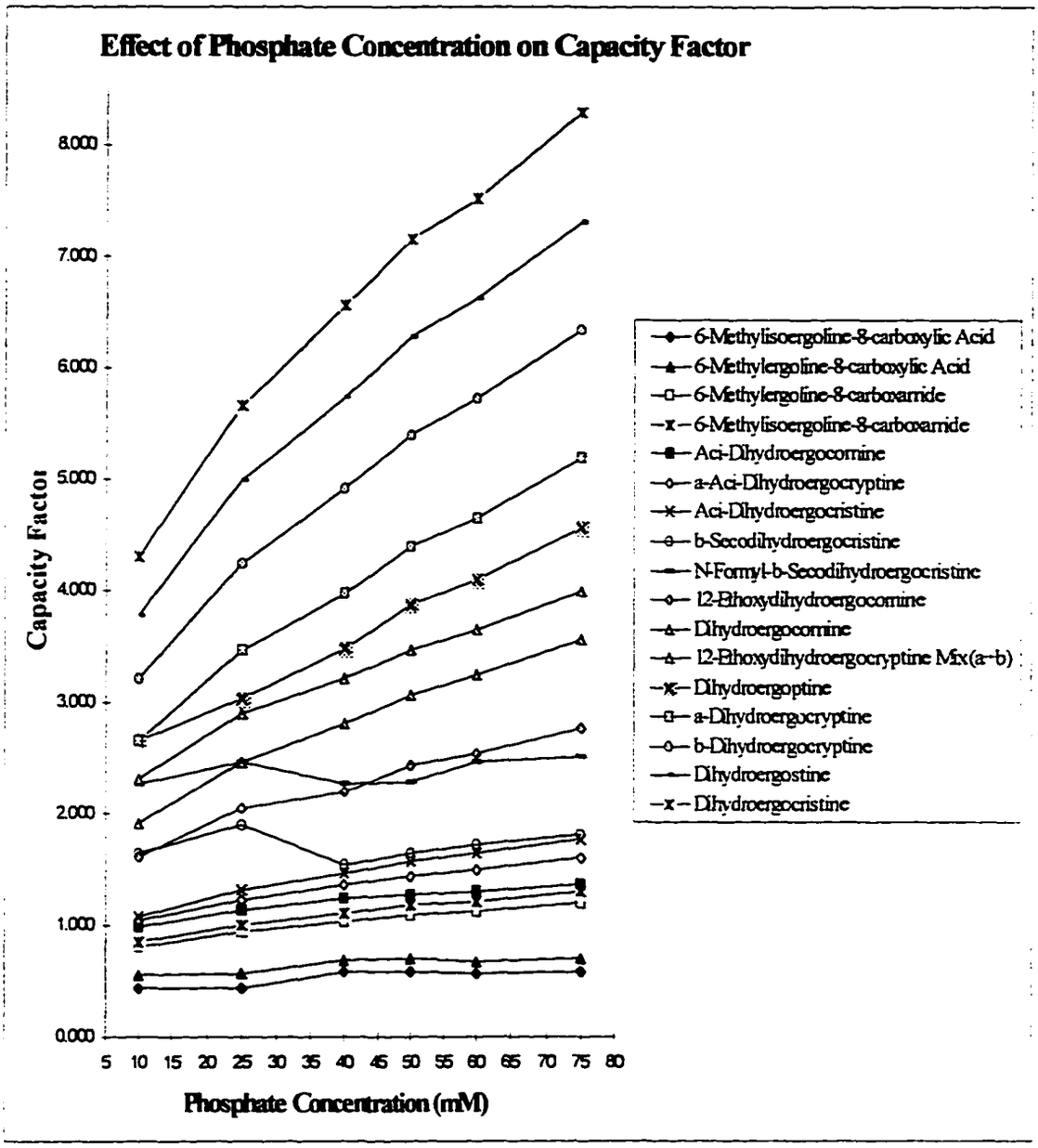

Figure 19

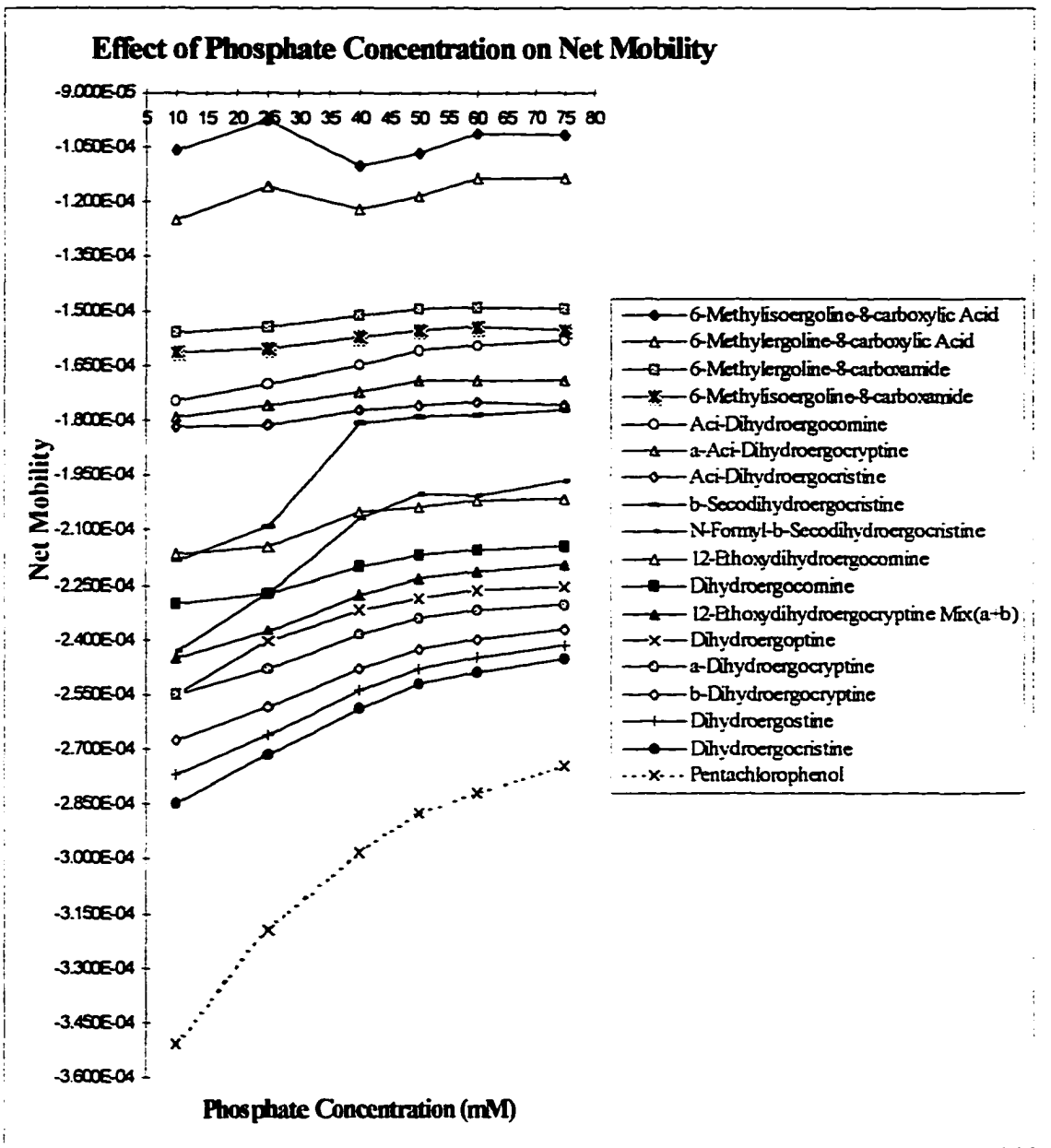

Figure 20

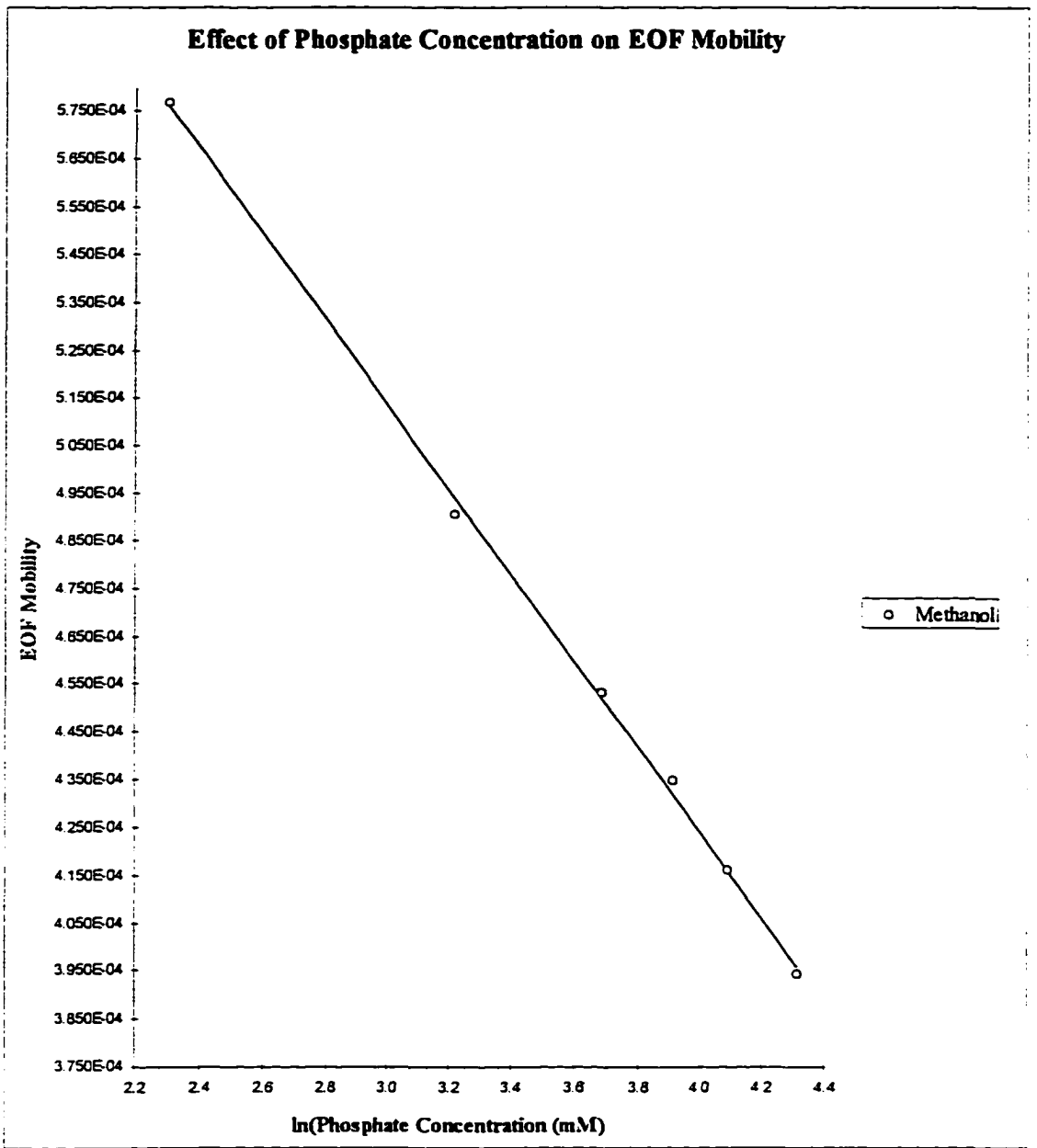

RSQ:	**0.999**
Slope:	**-8.954E-05**
Intercept:	**7.819E-04**

Figure 21

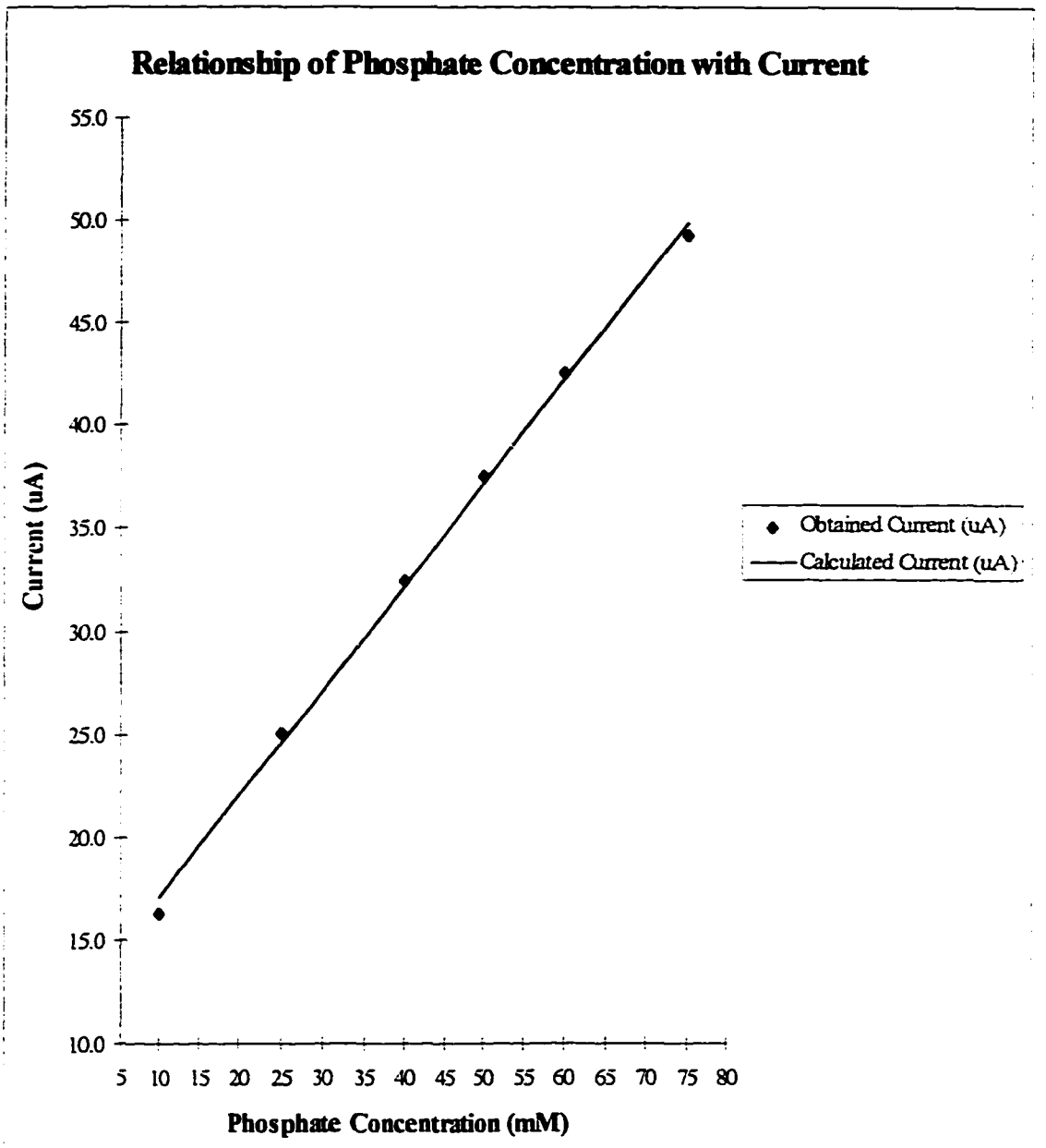

RSQ:	**0.998**
Slope:	**0.505**
Intercept:	**11.984**

References:

Chapter 1.

1) S. Terabe, *Micellar Electrokinetic Chromatography* 1993, Beckman Instruments, Inc., Palo Alto, CA, USA

2) S. Terabe, K. Otsuka, K. Ichikawa, A. Tsuchiya and T. Ando, *Anal. Chem.*, 56 (1984) 111

3) L.J. Cline-Love, J.G. Habarta, J.G. Dorsey, *Anal. Chem.*, 56 (1984) 1133A

4) J.H. Fendler, *Membrane Micetic Chemistry*, John Wiley & Sons, New York, 1982

5) D.A. Armstrong, *Sep. Purif. Methods*, 14 (1985) 213

6) B. Lindman and H. Wennerstrom, *Topics in Current Chemistry*, 87 (1980) 3

7) D.E. Burton and M.J. Sepaniak, *J. Chromatogr. Sci.*, 25 (1987) 514

8) M.J. Rosen, *Surfactants and Interfacial Phenomena*, 2nd Ed., John Wiley, 1989

9) M.J. Sepaniak, A.C. Powell, D.F. Swaile and R.O. Cole in *Capillary Electrophoresis - Theory and Practice*, Ed. by P.D. Grossman and J.C. Colburn, Academic Press, 1992

10) H.T. Chang and E.S. Yeung, *Anal. Chem.*, 65 (1993) 650

11) B.B. Vanorman and G.L. McIntire, *J. Microcolumn Sep.*, 1 (1989) 289

12) T.J. Kasper, M. Melera, P. Gozel and R.G. Brownlee, *J. Chromatogr.*, 458 (1988) 303

13) J. Liu, K.A. Cobb and M. Novotny, *J. Chromatogr.*, 519 (1990) 189

14) X. Huang, J.A. Luckey, M.J. Gordon and R.N. Zare, *Anal. Chem.*, 61 (1989) 766

15) J. Varghese and R.B. Cole, *J. Chromatogr. A*, 652 (1993) 369

16) T. Kaneta, S. Tanaka, M. Taka and H. Yoshida, *Anal. Chem.*, 64 (1992) 798

17) P. Morin, F. Villard, A. Quinsac and M. Dreux, *J. High Resolut. Chromatogr. Chromatogr. Commun.*, 15 (1992) 271

18) M.G. Khaledi, S.C. Smith and J.K. Strasters, *Anal. Chem.*, 63 (1991) 1820

19) C. Quang, J.K. Strasters and M.G. Khaledi, *Anal. Chem.*, 66 (1991) 1646

20) M.A. Abubaker, J.R. Petersen and M.G. Bissell, *J. Chromatogr. B*, 674 (1995) 31

21) M.J. Rosen, *Chem. Tech.*, 23 (1993) 30

22) H. Harino, M. Tanaka, T. Araki, Y. Yasaka, A. Masujama, Y. Nakatsuji, I. Ikeda, K. Funazo and S. Terabe *J. Chromatogr. A*, 715 (1995) 135

23) M. Tanaka, T. Ishida, T. Araki, A. Masujama, Y. Nakatsuji and M. Okahara, *J. Chromatogr. A*, 715 (1995) 135

24) D.N. Heiger, *High Performance Capillary Electrophoresis - An Introduction*, 1992, Hewlett-Packard GmbH, Germany

Chapter 2.

1) Toxic Substance Control Act, U. S. Environmental Protection Agency, Washington, D.C., 1979

2) G. Lamprecht and J. Huber, *J. Chromatogr.*, 667 (1994) 47

3) H. K. Lee, S.F.Y. Li and Y.H Tay, *J. Chromatogr.*. 438 (1988) 429

4) D.N. Armentrout, J.D. McLean and M.W. Long, *Anal. Chem.*, 51 (1979) 1039

5) C.P. Ong, C.L. Ng, N.C. Chong, H.K. Lee and S.F.Y. Li, *J. Chromatogr.*, 516 (1990) 263

6) Y. Chao and C. Whang, *J. Chromatogr. A*, 663 (1994) 229

7) G. Li and D.C. Locke, *J. Chromatogr. B*, 669 (1995) 93

8) G. Li and D.C. Locke, *J. Chromatogr. A*, 734 (1996) 357

9) T. Tsuda, *J. High Resolut. Chromatogr. Commun.*, 10 (1987) 622

10) S. Terabe, K. Otsuka, K. Ichikawa, A. Tsuchiya and T. Ando, *Anal. Chem.*, 56 (1984) 111

11) S. Terabe, K. Otsuka and T. Ando, *Anal. Chem.*, 57 (1985) 834

12) G.M. Janini, K.C. Chan, J.A. Barnes, G.M. Muschik and H.J. Issaq, *J. Chromatogr. A*, 653 (1993) 321

13) G.J.M. Bruin, J.P. Chang, R.H. Kuhlman, K. Zegers, J.C. Kraak and H. Poppe, *J. Chromatogr.*, 471 (1989) 429

14) M.J. Sepaniak, A.C. Powell, D.F. Swaile and R.O. Cole in *Capillary Electrophoresis - Theory and Practice*, P.D. Grossman and J.C. Colburn (eds.), Academic Press, 1992

15) A.T. Balchunas and M.J. Sepaniak, *Anal. Chem.*, 59 (1987) 1466

16) W. Nashabeh and Z.E. Rassi, *J. Chromatogr.*, 514 (1990) 57

Chapter 3.

1) K. Ghowsi, J.P. Foley and R.J. Gale, *Anal. Chem.*, 62 (1990) 2714

2) K. Otsuka, S. Terabe and T. Ando, *J. Chromatogr.*, 332 (1985) 219

3) K. Otsuka, S. Terabe and T. Ando, *J. Chromatogr.*, 348 (1985) 39

4) T. Kaneta, S. Tanaka, M. Taka and H. Yoshida, *Anal. Chem.*, 64 (1992) 798

5) M.G. Khaledi, S.C. Smith and J.K. Strasters, *Anal. Chem.*, 63 (1991) 1820

6) C. Quang, J.K. Strasters and M.G. Khaledi, *Anal. Chem.*, 66 (1991) 1646

7) Chapter 2 of this Thesis

8) S. Terabe, K. Otsuka and T. Ando, *Anal. Chem.*, 57 (1985) 834

9) L.V. Dearden and E.M. Woolley, *J. Phys. Chem.*, 91 (1987) 4123

10) H.T. Chang and E.S. Yeung, *Anal. Chem.*, 65 (1993) 650

11) S. Terabe, K. Otsuka, K.Ichikawa, A. Tsuchiya and T. Ando, *Anal. Chem.*, 56 (1984)

12) P.R. Haddad and P.E. Jackson, Chapter 2, *Ion Chromatography - Principles and Applications*, Ed. by P.R. Haddad and P.E. Jackson, J. Chromatogra. Lib., Vol 46 , Elsevier, 1990

Chapter 4.

1) D.E. Burton and M.J. Sepaniak, *J. Chromatogr. Sci.* 25 (1987) 514

2) J.R. Mazzeo, E.R. Grove, M.E. Swartz and J.S. Petersen *J. Chromatogr.*, 680 (1994) 125

3) D.D. Dalton, D.R. Taylor and D.G. Waters, *J. Chromatogr.*, 712 (1995) 365

4) M.J. Rosen, *Chem. Tech.*, 23 (1993) 30

5) H. Harino, M. Tanaka, T. Araki, Y. Yasaka, A. Masujama, Y. Nakatsuji, I. Ikeda, K. Funazo and S. Terabe *J. Chromatogr. A*, 715 (1995) 135

6) M. Tanaka, T. Ishida, T. Araki, A. Masujama, Y. Nakatsuji and M. Okahara, *J. Chromatogr. A*, 715 (1995) 135

7) M.J. Rosen and L.D. Song, *J. Colloid Interface Sci.*, 179 (1996) 261

8) S. Terabe, *Micellar Electrokinetic Chromatography* 1993, Beckman Instruments, Inc., Palo Alto, CA, USA

9) S. Terabe, K. Otsuka, K. Ichikawa, A. Tsuchiya and T. Ando, *Anal. Chem.*, 56 (1984) 111

10) S. Terabe, K. Otsuka and T. Ando, *Anal. Chem.*, 57 (1985) 834

11) H.T. Chang and E.S. Yeung, *Anal. Chem.*, 65 (1993) 650

12) M.J. Sepaniak, A.C. Powell, D.F. Swaile and R.O. Cole in *Capillary Electrophoresis - Theory and Practice*, Ed. by P.D. Grossman and J.C. Colburn, Academic Press, 1992

13) N.M. van Os, J.R. Haak, andL.A.M. Rupert *Physico-chemical Properties of Selected Anionic, Cationic and Nonionic Surfactants*, Elsevier,1993

Chapter 5.

1) *Chromatographic Analysis of Pharmaceuticals*, Ed. by John A. Adamovics, Chromatographic Science Series, Vol. 49, Marcel Dekker, 1990

2) C. Silverman and C. Shaw, *Capillary Electrophoresis in the Evaluation of Pharmaceuticals*, Ch. 10, Handbook of Capillary electrophoresis, Ed. by James P. Landers, CRC Press, 1994

3) *Capillary Electrophoresis - Principles, Practices and Applications*, S.F.Y. Li, J. Chromatogr. Lib. Vol. 52, Elsevier, 1992

4) C.A. Morning and R.T. Keanedy, *Anal. Chem.*, 66 (1994) 280R

5) E. Kenndler, C. Schwer and D. Kaniansky, *J. Chromatogr.*, 508 (1990) 203

6) M. Korman, J. Vindevogel and P. Sandra, *J. Chromatogr.*, 645 (1993) 366

7) C.X. Zhang, Z.P. Sun, D.K. Ling and Y.J. Zhang *J. Chromatogr.*, 627 (1992) 281

8) H. Nishi, T. Fukugama, M. Matsuo and S. Terabe, *J. Chromatogr.*, 513 (1990) 279

9) *The Ergot Alkaloids - Chemistry, Pharmacology and Clinical Application*, Sandoz Ltd., Basel, Switzerland

10) Z. Rehacek and P. Sajdl, *Ergot Alkaloids - Chemistry, Biological Effects, Biotechnology*, Elsevier, 1990

11) *Ergot Alkaloids - Basic Information*, Chemapol U.S. Chemical Corp., Piscataway, N.J. 08854, USA

12) W.D. Schoenleber, A.L. Jacobs and A. Brewer, Jr., *Analytical Profiles of Drug Substances*, Vol. 7, 1978

13) P.A. Stadler, *J. Pharm. Sci.* (1978)

14) Unpublished data, Novartis Pharmaceuticals Corp., East Hanover, N.J., 07936, USA

15) M.J. Rosen and L.D. Song, *J. Colloid Interface Sci.*, 179 (1996) 261

16) S. Terabe, K. Otsuka, K. Ichikawa, A. Tsuchiya and T. Ando, *Anal. Chem.*, 56 (1984) 113

17) S. Terabe, K. Otsuka and T. Ando, *Anal. Chem.*, 57 (1985) 834

18) Estimated values from lysergic acid listed in *The Merck Index*, Tenth Ed. Merck & Co., Inc., Rahway, N.J., USA

19) W. Nashabeh and Z.E. Rassi, *J. Chromatogr.*, 514 (1990) 57

20) G.J.M. Bruin, J.P. Chang, R.H. Kuhlman, K. Zegers, J.C. Kraak and H. Poppe, *J. Chromatogr.*, 471 (1989) 429